



Durham E-Theses

Approaches to Novel B-N Chemistry at the Boundary of Frustrated Lewis Pairs and Bifunctional Catalysis

ARKHIPENKO, SERGEY, YURIEVICH

How to cite:

ARKHIPENKO, SERGEY, YURIEVICH (2017) *Approaches to Novel B-N Chemistry at the Boundary of Frustrated Lewis Pairs and Bifunctional Catalysis*, Durham theses, Durham University. Available at Durham E-Theses Online: <http://etheses.dur.ac.uk/12213/>

Use policy

The full-text may be used and/or reproduced, and given to third parties in any format or medium, without prior permission or charge, for personal research or study, educational, or not-for-profit purposes provided that:

- a full bibliographic reference is made to the original source
- a [link](#) is made to the metadata record in Durham E-Theses
- the full-text is not changed in any way

The full-text must not be sold in any format or medium without the formal permission of the copyright holders.

Please consult the [full Durham E-Theses policy](#) for further details.



**Approaches to Novel B-N Chemistry at the
Boundary of Frustrated Lewis Pairs and
Bifunctional Catalysis**

Sergey Arkhipenko

*A thesis submitted in partial fulfilment of the requirements for the degree of
Doctor of Philosophy*

Department of Chemistry, Durham University, UK

2016

Declaration

The work described in this thesis was carried out in the Department of Chemistry at Durham University between October 2013 and December 2016, under the supervision of Prof. Andy Whiting. The material contained has not been previously submitted for a degree at this or any other university. The research reported within this thesis has been conducted by the author unless indicated otherwise.

Statement of Copyright

The copyright of this thesis rests with the author. No quotations from it should be published without prior consent and information derived from it should be acknowledged.

Contents

I. Abstract.....	5
II. Acknowledgements	6
III. Abbreviations.....	8
1. Introduction.....	10
1.1. Frustrated Lewis Pairs	11
1.1.1. The FLP concept.....	11
1.1.2. Hydrogenations.....	12
1.1.3. Other applications	18
1.2. The Boundary between FLP and bifunctional catalysis.....	22
1.2.1. Separate Lewis acids and bases in comparison with FLP chemistry	22
1.2.2. “Frustration” and reactivity of Lewis pairs.....	25
1.2.3. Reactivity of classic Lewis adducts (CLAs).....	26
1.2.4. Benefits of reducing Lewis acidity and basicity.....	29
1.2.5. Other approaches to avoid Lewis adduct formation.....	30
1.2.6. Importance of link between LA and LB centres.....	32
1.3. Conclusion	33
2. Results and discussion	34
2.1. Aims of the project.....	34
2.2. Part I. New bifunctional B-N catalysts.....	34
2.2.1. Design and retrosynthetic analysis of new catalysts.....	34
2.2.2. Path A. Diaryl α -chloromethyl borane 110 approach.....	36
2.2.2.1. Borinate synthesis.....	36
2.2.2.2. Borinate approach. Further steps.....	43
2.2.2.3. Boron halides approach.....	47
2.2.2.4. Other approaches	52
2.2.3. Paths B-C and hydroboration attempt	54
2.2.4. Path D. Borylation with B ₂ pin ₂	56
2.2.4.1. Homoboroproline 114 synthesis.....	56
2.2.4.2. Attempted derivatisation of homoboroproline 114.....	61
2.2.4.3. Attempted catalysis with homoboroproline derivative 176.....	65

2.2.5.	NMR analysis of proline derivatives.....	66
2.2.5.1.	Analysis of diastereotopic protons and rotamers.....	67
2.2.5.2.	¹ H NMR resolution in prolinol 159 spectra	71
2.3.	Part II. Direct amide formation.....	74
2.3.1.	Non-catalysed, background thermal direct amide formation	74
2.3.1.1.	Amide formation: Flow reactor	75
2.3.1.2.	Amide formation: Microwave reactor.....	78
2.3.2.	Boron-catalysed direct amide formation.....	86
2.3.2.1.	Interactions of borinic and boronic acids with amines.....	86
2.3.2.2.	Interactions of borinic and boronic acids with carboxylic acids	90
2.3.2.3.	Interactions of borinic and boronic acids with carboxylic acids and amines.....	98
2.3.2.4.	Borinic and boronic acids in direct amide formation	103
2.3.2.5.	Boronic diamides	107
2.3.2.6.	Mechanistic conclusions on boronic acid catalysed direct amide formation	111
2.4.	Conclusions and future work.....	117
3.	Experimental	119
3.1.	General Information.....	119
3.2.	Synthetic procedures	120
4.	Appendix 1.....	142
5.	Appendix 2.....	148
6.	References.....	149

I. Abstract

This project is devoted to boron chemistry in two ways. Firstly, the development of the boron – nitrogen “Frustrated” Lewis Pairs (FLPs) was investigated by combining the principles of this approach with known bifunctional catalytic methods. This also included design and synthetic efforts towards new bifunctional catalysts **108** and **157** on the basis of *L*-proline connected to Lewis acidic borane or borinic derivatives, which revealed multiple peculiarities of boron chemistry. Catalyst **176** was successfully utilised in nitro-Michael addition reaction.

Secondly, boronic acids are promising catalysts for the important process of direct amide formation, which is a much more atom efficient and sustainable alternative to the current industrial approaches to amide synthesis. However, the mechanism of action of boronic acids in this process is not yet well understood, while this is crucial for effective design and future application of catalysts for direct amide formation. Thus the roles of both borinic and boronic acids in direct amide formation reactions were investigated. This included isolation of multiple Lewis adducts formed as intermediates or byproducts in different reaction mixtures between amines, carboxylic acids and boron-containing compounds. These results have helped to better understand the reactivity of boron-based catalysts and allowed development of the new mechanistic understanding of boronic acids in direct amide formation.

These findings underlined the complexity of boron-containing systems, the importance of boron-nitrogen Lewis adduct interactions and the high possibility of multiple boron atoms orchestrating the investigated processes.

The non-catalytic thermal direct amide formation reaction was also studied both in flow and microwave reactors in order to better understand these complex multicomponent systems.

II. Acknowledgements

First of all, I would like to thank my supervisor, Prof. Andy Whiting, who gave me a brilliant opportunity to work in his group in UK. Apart from owning outstanding knowledge of chemistry and passion for research, Andy showed kindness and patience and proved to be a very caring leader, whose support, advice and encouragement constantly guided me on the long road of this project.

I acknowledge Dr Andrei Batsanov of X-ray Crystallography Services in Durham, as his help and co-operation were invaluable for this work, and discussions with him always inspired a home-like comforting feeling. I thank Prof. Ian Baxendale, Prof. Graham Sandford and Dr AnnMarie O'Donoghue, whose support made possible Flow, Microwave and Kinetic parts of this project. I also thank Dr Tom Sheppard and Marco Sabatini from UCL as well as Prof. Henry Rzepa from ICL for a great collaborative experience around boron-catalysed direct amide formation.

I also express my gratitude to everyone who formed the Whiting group, past and present. Not only colleagues, but also friends, these people always supported me and shared both tough and bright moments of this journey: Dr Wade Leu, Dr Farhana Ferdousi, Dr Alex Gehre, Dr Mona Al-Batal, Dr Adam Calow, Dr Ludovic Eberlin, Dr Hesham Hafez, Hannah Wilson, Kate Madden, David Chisholm, Alba Pujol-Santiago, Sylvain David, Enrico La Cascia, and everyone else all made my life interesting and fun during these years. My special thanks goes to my good friend Dr Garr-Layy Zhou, who helped me to integrate into this scientific community initially and also opened links to many outstanding people outside the Chemistry Department in Durham.

I am thankful for the help and support of technical staff in Durham University (NMR, Crystallography, Mass Spec, Elemental Analysis and general technical personnel), without which none of this research would have been possible. I am forever grateful to Dr Alan M. Kenwright and Dr Juan A. Aguilar Malavia, whose amazing advice has guided me in the NMR world over 3 years.

Moreover, I would like to acknowledge Chemistry Department of Durham University for funding this entire project.

During my life in Durham I met many other interesting people, who became my good (best?) friends here and who were always ready to discuss major questions

and goals in life. Thus I thank my philosophical (and sociological?) partners and members of our small “Imagine” Club – Chaoqun, Ruxi, Jay, Ruoyu, Iman, Raminder and Jo. I also thank my friend and colleague Sergey Shuvaev.

During the course of this work I became a husband and a father, and I thank my beloved wife Olga for her absolute patience, encouragement and for all the beautiful evenings we spent in Durham.

Finally, I thank my beloved parents Yury and Tatyana, my super brother Alex and my dear granny Valentina, who supported me even from over the sea, and whose high expectations were the most important motivation through my whole life.

III. Abbreviations

Å	Angström
Ac	Acyl
aq.	Aqueous
ASAP	Atmospheric Solids Analysis Probe
B-N	Boron-Nitrogen
Boc	<i>N-tert</i> -Butoxycarbonyl
br s	Broad singlet
BuLi	<i>n</i> -Butyllithium
^t Bu	<i>tert</i> -butyl
CBS	Corey, Bakshi and Shibata
COSY	Homonuclear COrrrelation SpectroscopY
d	Doublet
dd	Doublet of doublets
ddd	Doublet of doublets of doublets
DCM	Dichloromethane
DEAD	Diethyl azodicarboxylate
DFT	Density Functional Theory
dm	Doublet of multiplets
DMAD	Dimethyl acetylenedicarboxylate
DMS	Dimethyl sulphide
DMSO	Dimethylsulfoxide
dt	Doublet of triplets
<i>ee</i>	Enantiomeric excess
Et	Ethyl
ESI	Electrospray ionization
EXSY	EXchange SpectroscopY
FLP	Frustrated Lewis Pairs
HOMO	Highest Occupied Molecular Orbital
HRMS	High Resolution Mass Spectrometry
HSQC	Heteronuclear Single Quantum Correlation
IPA	Isopropanol
IR	Infra-Red
J	Coupling constant

LA	Lewis Acid
LB	Lewis Base
LRMS	Low Resolution Mass Spectrometry
LUMO	Lowest Unoccupied Molecular Orbital
m	Multiplet
<i>m</i>	<i>meta-</i>
Mp	Melting point
MS	Molecular sieves
Me	Methyl
Mes	Mesityl
Neop	Neopentyl
NMR	Nuclear magnetic resonance
NOESY	Nuclear Overhauser Effect Spectroscopy
<i>o-</i>	<i>ortho-</i>
<i>p</i>	<i>para-</i>
pent	Pentet
pin	Pinacolato
Ph	Phenyl
ⁱ Pr	<i>iso</i> -propyl
PSYCHE	Pure Shift Yielded by CHirp Excitation
r.t.	Room temperature
s	Singlet
sept	Septet
t	Triplet
Tf	trifluoromethanesulfonyl
THF	Tetrahydrofuran
TMP	2,2,6,6,-Tetramethylpiperidine
TMSCl	Trimethylsilyl chloride
Tol	Tolyl
Ts	Tosyl
TLC	Thin-layer chromatography
VT	Varying temperature

1. Introduction

Scientists are always inspired by Nature. In the field of organic chemistry one of the most thrilling examples of how efficient natural systems can be is enzyme catalysis. Enzymes are big organic molecules, which allow effective stereo- and regio-selective molecular transformations thanks to special orientation of functional groups and steric peculiarities of the enzyme configuration. Thus, organic chemists try to mimic this remarkable catalytic activity, which includes the design of smaller molecules with catalytic properties close to those of natural enzymes.

The development of small molecules as organic catalysts has a long history and numbers many discovered principles and approaches. However, apart from developing already existing catalytic ideas and widening the field of their applications, it is also important to investigate new strategies in catalysis that open opportunities to use chemical reactivity in novel ways.

The bifunctional approach to catalysis emerged as early as 1925¹ and developed ever after. However, the significant increase in attention towards this concept happened after 1987, when Corey, Bakshi and Shibata introduced the CBS catalyst for reductions.² Nowadays, bifunctional catalysis is a popular and well-developed field in organic chemistry.

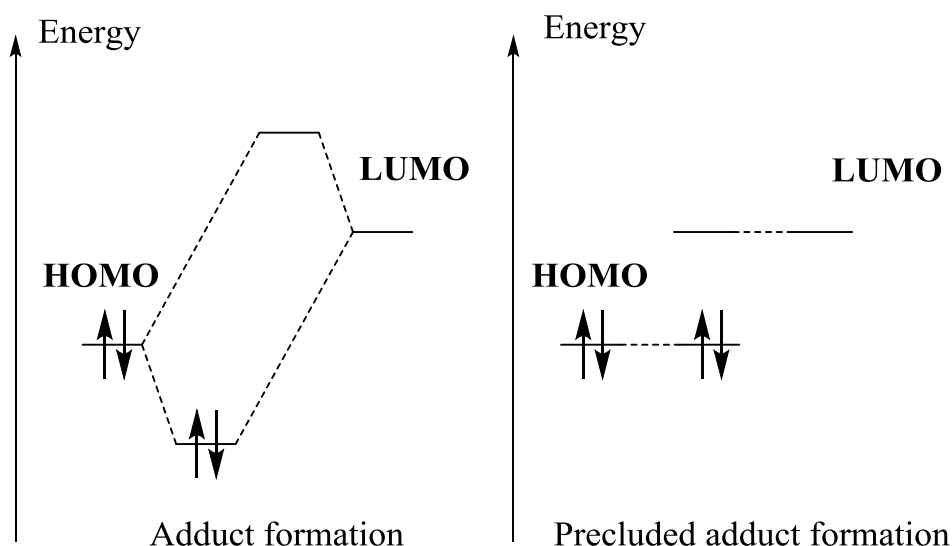
In 2006 Stephan *et al.*³ made an important discovery of novel chemical reactivity which was developed into the concept of “Frustrated Lewis Pairs” (FLP).⁴ It was shown that coexistence of bulky Lewis acid and Lewis base in the same reaction mixture without them forming the Lewis adduct is possible. This approach was used for hydrogen activation, and later was extended to reactions of other small molecules. However, this remarkable discovery still has very limited applications and was never commercialized,⁵ because of fairly narrow range of catalysts used and generally because of philosophical isolation of FLP reactivity from other catalytic concepts, despite efforts of chemists to broaden the scope of FLP possibilities.

One goal of this work is to bring together the principles of bifunctional catalysis and Frustrated Lewis Pairs chemistry both theoretically and practically. The design, synthesis and applications of new catalysts on the basis of these ideas, represent an effort to investigate the catalytic activity at the “boundary” of principles used, which contributes to the fundamental understanding of chemical reactivity. The boronic acids role in direct amide formation is also touching on B-N interactions, expanding the topic and discussion.

1.1. Frustrated Lewis Pairs

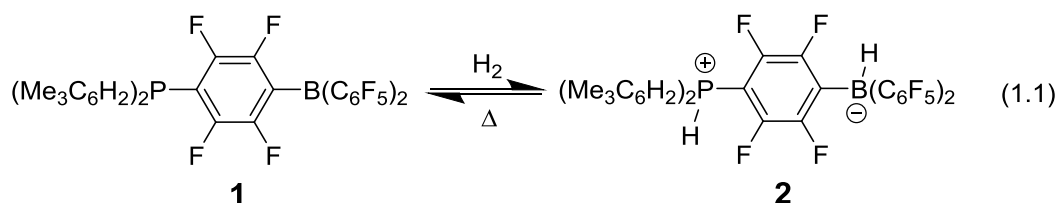
Categorization of molecules as electron acceptors (Lewis acids, LA) and donors (Lewis bases, LB) was introduced by Lewis⁶ in 1923 and now plays a huge role in our understanding of chemistry. It is also well-known, that when mixed, LA and LB form adducts (Figure 1). Later,^{7a} it was found that the formation of Lewis adduct is impossible for some sterically hindered LA and LB, such as trimethylboron and 2,6-lutidine, and it was shown that certain Lewis adducts can activate small molecules, such as butadiene^{7b}. However, the activity of unquenched coexisting Lewis acids and bases was only shown in the 21st century and was named “frustrated” Lewis pair reactivity⁴.

Figure 1 Formation of a LA-LB adduct and prevention of orbital interaction due to steric hindrance



1.1.1. The FLP concept

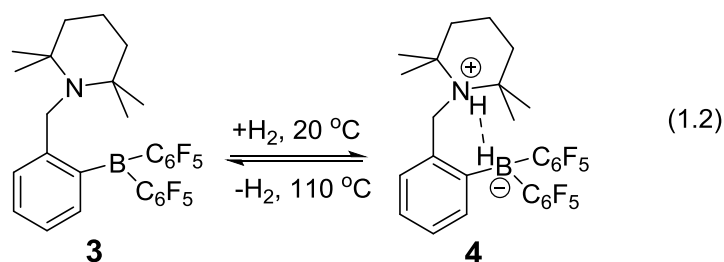
The concept of Frustrated Lewis pairs (FLP) emerged when Stephan *et al.*³ synthesized a bifunctional compound **1** and reacted it with 1 atmosphere of H₂ at 25 °C to form adduct **2**, which remarkably was found to lose H₂ at temperatures above 100 °C (eqn. 1.1).



This result was very important because the metal-free systems for H₂ activation are considered to be rare and promising in terms of cost and waste remediation, compared to transition-metal catalysed processes.⁸ Later this approach was developed for activation of other small molecules (see Section 1.1.3 Other Applications), but hydrogenations remain the dominant field of FLP research.

1.1.2. Hydrogenations

Since 2006, many FLP systems able to initiate heterolytic cleavage of dihydrogen have been developed.⁹ Some of them bind hydrogen to form zwitterion complexes immune to H₂ liberation,¹⁰ whereas others, such as **3**,¹¹ are capable of reversible activation (eqn. 1.2). This type of reactivity was used for development of FLP catalysts **5-17** (Figure 2) which were used for hydrogenation of different unsaturated compounds.



From a literature survey it is clear that reduction of imines is the most well-studied application of FLP, and these substrates were the first to be tested in hydrogenations with newly developed catalysts. Reactions of imines with H₂ at 5 atm in the presence of 5 mol.% of catalyst **1**¹² proceed well only for bulky and strongly basic substrates (Table 1, entries 1-3). Hydrogenation of less hindered imines (Table 1, entry 4) as well as nitriles is limited to the formation of strongly bound adducts, but the catalyst turnover can be achieved by sequestering nitrogen lone pair of such substrates with B(C₆F₅)₃ (Table 1, entries 5-7). The same catalyst, as well as Lewis acid **5** is active in reductive hindered azyridine ring-openings (Table 1, entries 8, 14)⁸. Repo and Rieger¹³ used catalyst **3** to partially decrease the steric requirements of imines in FLP hydrogenations (Table 1, entries 9-11). However, most of the above imine hydrogenations require rather harsh reaction conditions (H₂ pressure 5-15 bar, T 65-120 °C). Erker group developed FLP system **6**, which worked well for catalytic reduction of both imines (Table 1, entry 12) and enamines (Table 2, entries 1-2) with H₂ (2.5 bar) at r.t.¹⁴ The same system **6** was used to achieve formal 1,4-hydrogenation

of conjugated metallocene dienamines (Table 2, entry 3),¹⁵ and was applied in non-hydrogenation reactions as well (see below).

Reduction of hindered imines can also be catalysed by using $\text{B}(\text{C}_6\text{F}_5)_3$ **5** without a Lewis base,¹⁶ as the nitrogen of the substrate forms an FLP with **5** and acts as a catalyst⁸ (Table 1, entries 13-14). The same approach can be used for hydrogenation of sensitive organometallic imines.¹⁷

The same semi-autocatalytic explanation is given to $\text{B}(\text{C}_6\text{F}_5)_3$ **5** induced hydrogenation of amine-substituted benzenes, yielding cyclohexyl-amine derivatives,¹⁸ as well as reduction of *N*-heterocycles, such as acrydine and substituted quinolones.¹⁹ It was shown that when mixed with **5**, some heterocycles form equilibria between the Lewis adduct and uncoordinated LA and LB. Despite this fact, these systems often experience quantitative hydrogenation with H_2 in presence of **5** at ambient temperatures. Hydrogenation of pyridine derivatives to piperidine salts was also possible using 1 equivalent of **5**,²⁰ and this approach was extended to 2,6-substituted pyridines, which yielded specifically *cis*-adducts in good yields when catalytic amount of Lewis acid **7** was generated *in situ* by reaction of $\text{HB}(\text{C}_6\text{F}_5)_2$ with alkene.²¹

Figure 2 FLP catalysts used for hydrogenations.

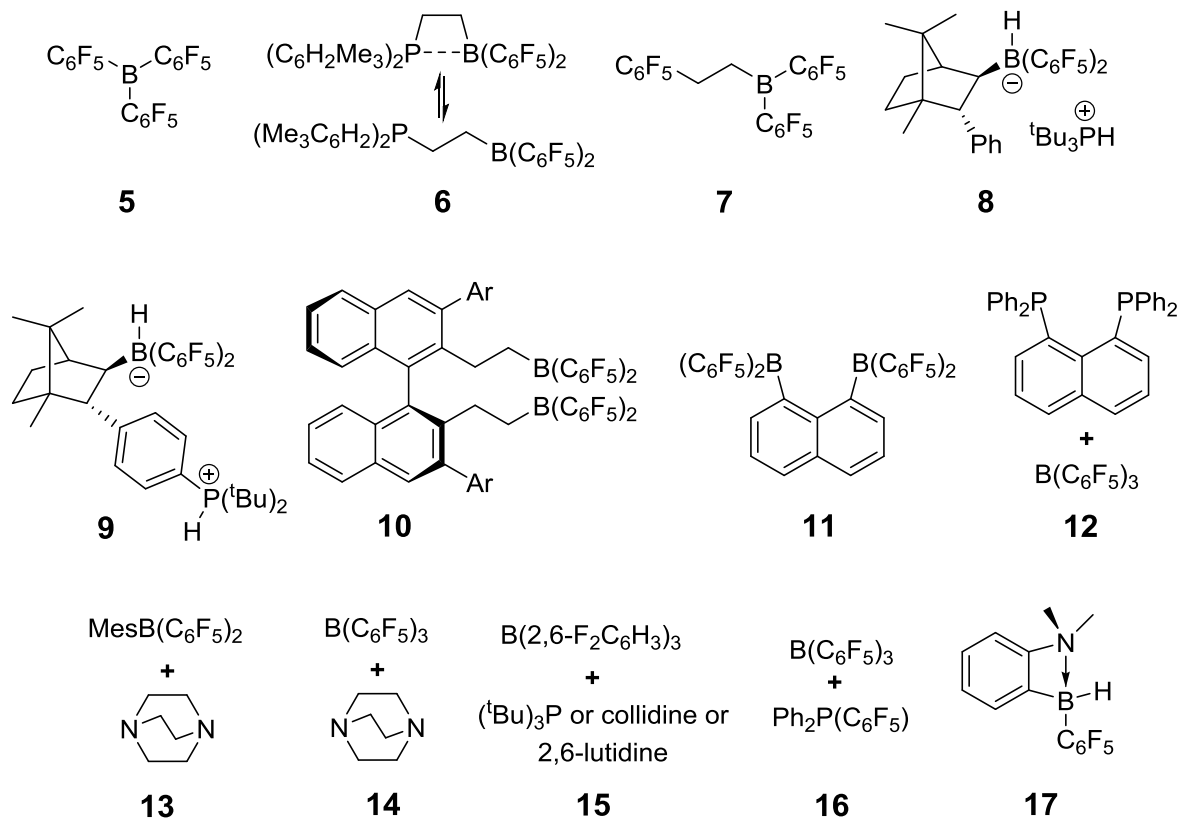


Table 1 Hydrogenation of imines, protected nitriles, azyridines and silylenol ethers using FLP catalysts.

Entry	Substrate	Catalyst	Yield, %	Product	Reference
1	Ph(H)C=N ^t Bu	1	79	PhCH ₂ NH ^t Bu	12
2	Ph(H)C=NSO ₂ Ph	1	97	PhCH ₂ NHSO ₂ Ph	12
3	Ph(H)C=NCHPh ₂	1	88	PhCH ₂ NHCHPh ₂	12
4	Ph(H)C=NCH ₂ Ph	1	5	PhCH ₂ NHCH ₂ Ph	12
5	Ph(H)C=NCH ₂ Ph(B(C ₆ F ₅) ₃)	1	57	PhCH ₂ NHCH ₂ Ph(B(C ₆ F ₅) ₃)	12
6	MeCNB(C ₆ F ₅) ₃	1	75	MeCH ₂ NH ₂ B(C ₆ F ₅) ₃	12
7	PhCNB(C ₆ F ₅) ₃	1	84	PhCH ₂ NH ₂ B(C ₆ F ₅) ₃	12
8	PhCH(NPh)CHPh	1	98	PhCH ₂ CH(NHPh)Ph	12
9	Ph(H)C=NCH ₂ Ph	3	99	PhCH ₂ NHCH ₂ Ph	13
10	Ph(Me)C=NMe	3	99	Ph(Me)CHNH ₂ Me	13
11	Ph(H)C=NMe	3	4	Ph(H)CHNH ₂ Me	13
12	Ph(H)C=N ^t Bu, mild conditions	6	87	PhCH ₂ NH ^t Bu	14
13	Ph(H)C=NCHPh ₂	5	99	PhCH ₂ NHCHPh ₂	8
14	PhCH(NPh)CHPh	5	95	PhCH ₂ CH(NHPh)Ph	8
15		8	95, <i>ee</i> 79% (R)		22
16		8	37, <i>ee</i> 74% (-)		22
17		8	93, <i>ee</i> 80% (-)		22
18		8	96, <i>ee</i> 83% (+)		22
19		10	98, <i>ee</i> 78%		24
20		10	91, <i>ee</i> 89%		24
21	PhCH=NCHPh ₂	11	99	PhCH ₂ NHCHPh ₂	25
22		12	99		26
23		12	99		26
24	Ph(H)C=N ^t Bu	13	100	PhCH ₂ NH ^t Bu	28

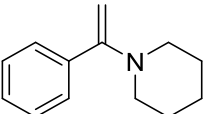
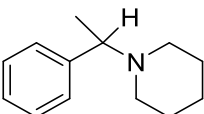
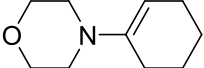
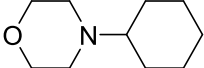
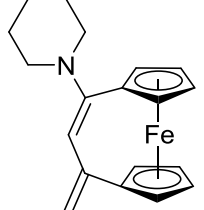
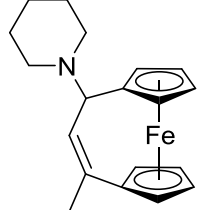
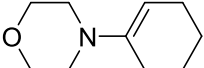
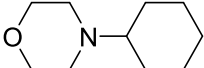
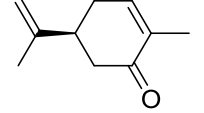
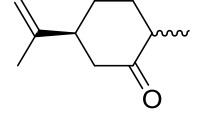
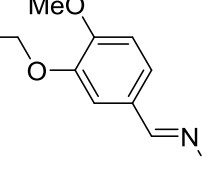
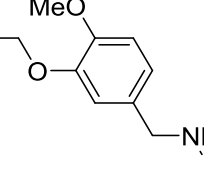
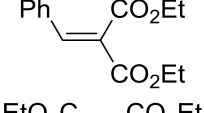
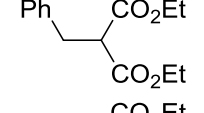
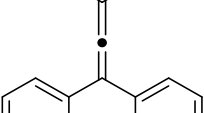
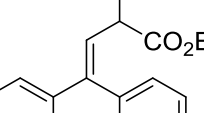
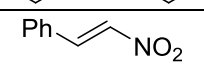
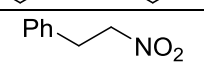
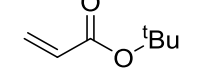
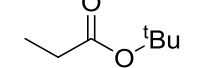
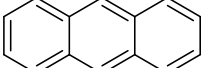
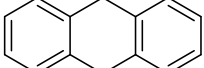
FLP-catalysed reductions of prochiral imines can be used to obtain enantiomeric products.¹⁶ This concept was developed with a camphor-derived borane, which activated H₂ when in mixture with ^tBu₃P to form salt **8**²² that catalysed hydrogenation of imines in up to 97% yield and up to 83% *ee*. It was also noticed, that increasing the steric hindrance around the nitrogen led to a decrease of both yield and *ee* in these reactions (Table 1, entries 15-16), whereas introducing electron-donating substituents at nitrogen led to better conversion and selectivity (Table 1, entries 17-18). A camphor core was also used for the design of an intramolecular FLP catalyst **9**,²³ which allowed chiral imine conversion with good yields and 70-76% *ee*. Applying the semi-autocatalytic approach, described above, the *in situ* generation of Lewis acid catalysts **10** from chiral binaphthyl-derived dienes allowed quantitative asymmetric imine hydrogenation with *ee* up to 89% (Table 1, entries 19-20).²⁴

The catalyst on the basis of bifunctional Lewis acid **11** was also used in imine reduction (Table 1, entry 21).²⁵ Bifunctional Lewis bases were tried in FLP catalysis as well: Erker *et al.* showed the possibility of silylenol ethers hydrogenation catalysed by FLP **12** (Table 1, entries 22-23).²⁶ This type of reduction was later used for domino hydrosilylation/hydrogenation of enones catalysed by [2.2]paracyclophane-derived bisphosphines.²⁷

The intermolecular FLP catalyst **13**,²⁸ having a relatively small amine as its LB part was designed to be more selective and apart from showing imine reducing capabilities at r.t. (Table 1, entry 24), allowed hydrogenation of enamines and enones in the presence of terminal olefin (Table 2, entries 4-6). Electron-poor alkenes and allenes were successfully hydrogenated using analogous catalyst **14** (Table 2, entries 7-8).²⁹ Selective catalytic reduction of C=C double bond in conjugated nitroolefins and acrylates (Table 2, entries 9-10) became possible with FLP systems **15** having lower Lewis acidity of boron-containing component, presumably due to increased nucleophilicity of the [(C₆H₃F₂)₃BH]⁻ ion, compared to [(C₆F₅)₃BH]⁻.³⁰

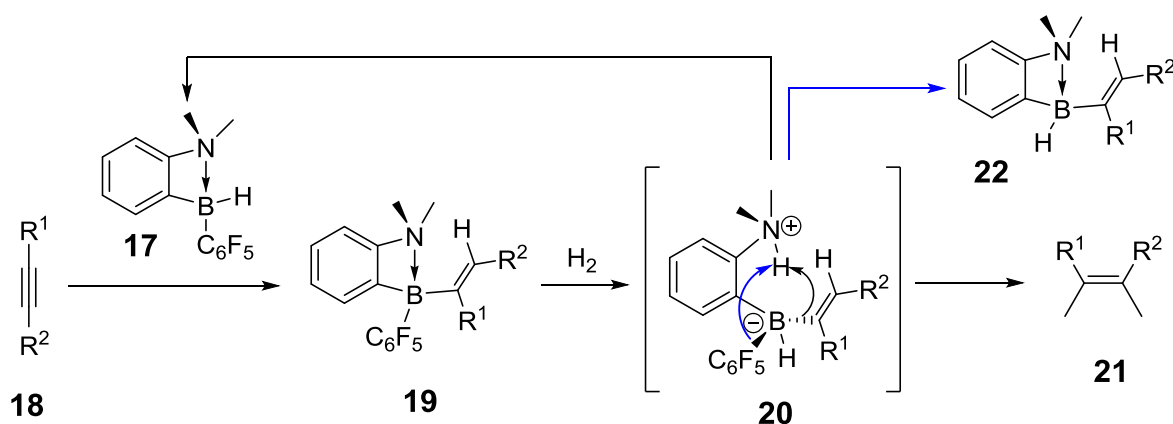
FLP system **16**,³¹ can be used at high H₂ pressures (100 bar) and at 80 °C for reduction of polycyclic aromatic hydrocarbons (Table 2, entry 11). The same catalyst was used for H₂ activation (5 bar) at -80 °C³² and for electron-rich olefin hydrogenation at r.t., but optimizing the balance between protonation and efficient nucleophilic attack was needed. A range of other P-bases gave better results for different olefins.

Table 2 Hydrogenation of enamines, conjugated olefins and other unsaturated compounds.

Entry	Substrate	Catalyst	Yield, %	Product	Reference
1		6	100		14
2		6	88		14
3		6	90		15
4		13	92		28
5		13	87		28
6		13	100		28
7		14	92		29
8		14	93		29
9		15	>95		30
10		15	>95		30
11		16	97		31

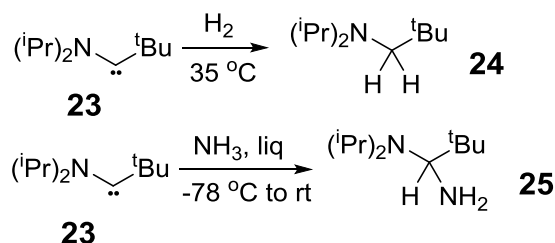
An important example of FLP reactivity application is hydrogenation of internal alkynes to *cis*-alkenes.³³ First, hydroboration of alkynes **18** by catalyst **17** (which is generated *in situ*) occurs (Scheme 1), and obtained compound **19** activates H₂ by FLP-mediated mechanism to yield intermediate **20**. This then goes through intramolecular protonation, which gives the product alkene **21** and regenerated catalyst (Scheme 1, black arrows), however, an alternative route *via* protonolysis of

the B-C₆F₅ bond is also possible (Scheme 1, blue arrows), and leads to degradation of the catalyst. Both experimental and computational studies provided support for this mechanism.



Scheme 1 Hydrogenation of alkynes to *cis*-alkenes³³

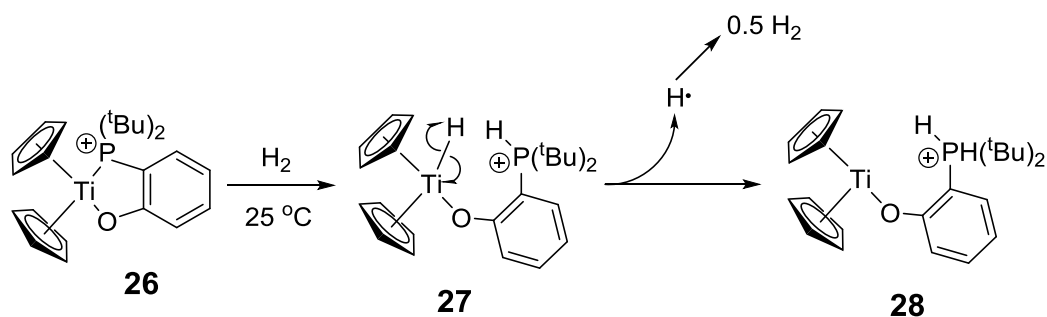
Apart from B-N and B-P FLP systems, some carbenes, such as **23**, have been shown to activate both H₂ and NH₃³⁴ (Scheme 2), and thus they can be viewed as a specific form of FLP.³⁵ In these systems both Lewis acid and Lewis base exist at the same atom, yet the orthogonality of their orbitals prevents them from interacting. Hindered *N*-heterocyclic carbenes do not form adducts with B(C₆F₅)₃, and these FLP systems were found to activate hydrogen H-H and amine N-H bonds,³⁶ as well as initiate THF ring-opening.³⁷



Scheme 2 Carbenes as FLP³⁴

B←O systems containing combinations of ethers (Et₂O, crown ethers) with B(C₆F₅)₃,³⁸ were also shown to catalyse hydrogenations of 1,1-diphenylethylene and anthracene in good yields.

The FLP approach was extended to organometallic systems as well. The Ti^{IV} complex **26** (Scheme 3) activates H₂ at low pressures (1-3 bar) at r.t. and the Zr-analogue catalyses dehydrogenation of amine-borane Me₂NBH₃.³⁹



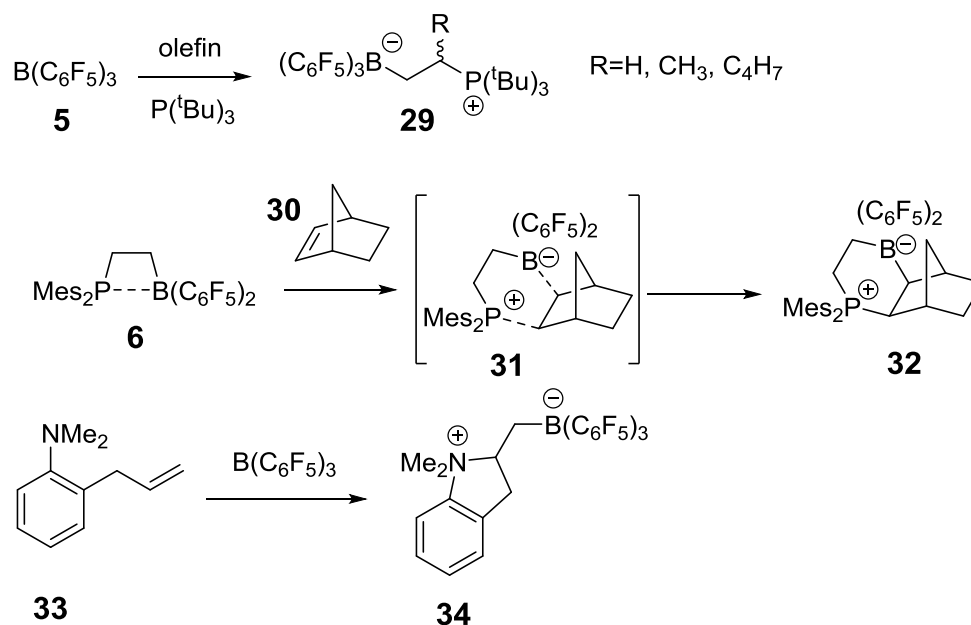
Scheme 3 Activation of H₂ by Ti^{IV} complex³⁹

Efforts were made to study the mechanism of FLP-mediated H₂ activation. Computational studies showed that the system (tBu)₃P/B(C₆F₅)₃ reacts with H₂ through formation of a loosely bound “frustrated complex”, in which the H₂ molecule is nearly aligned with the P···B axis.⁴⁰ Later a different quantum calculated explanation to FLP activation on the basis of electron field generated by donor/acceptor atoms was suggested,⁴¹ and these two approaches were compared.⁴² Kinetic studies of FLP-catalysed imine reductions⁴³ showed that hydrogen activation is the rate-determining step in most cases, and that Lewis base component is important not only for H₂ activation, but also for proton transfer to the substrate, as well as that phosphine bases with higher pK_a values are more efficient in these processes.

1.1.3. Other applications

The discovery of FLP catalysis led not only to the development of H₂ activation and hydrogenations, but to investigations into many other applications in catalysis.⁴⁴

Stephan *et al.*⁴⁵ found that the combination of the hindered phosphine P^tBu₃ and borane B(C₆F₅)₃ **5** undergoes addition to olefins, such as ethylene, propylene and 1-hexene (Scheme 4). This is remarkable because these phosphines or boranes do not individually react with olefins. The same FLP system also undergoes 1,4-addition to conjugated dienes.⁴⁶ The already discussed system **6** reacts in an asynchronously concerted way with norbornene **30** to form cyclised zwitterionic phosphonium borate **32** (Scheme 4).⁴⁷ Intramolecular cyclizations, leading to heterocyclic derivatives can be achieved by reacting 1 equivalent of B(C₆F₅)₃ with amines, containing olefinic or acetylenic residues (Scheme 4).⁴⁸



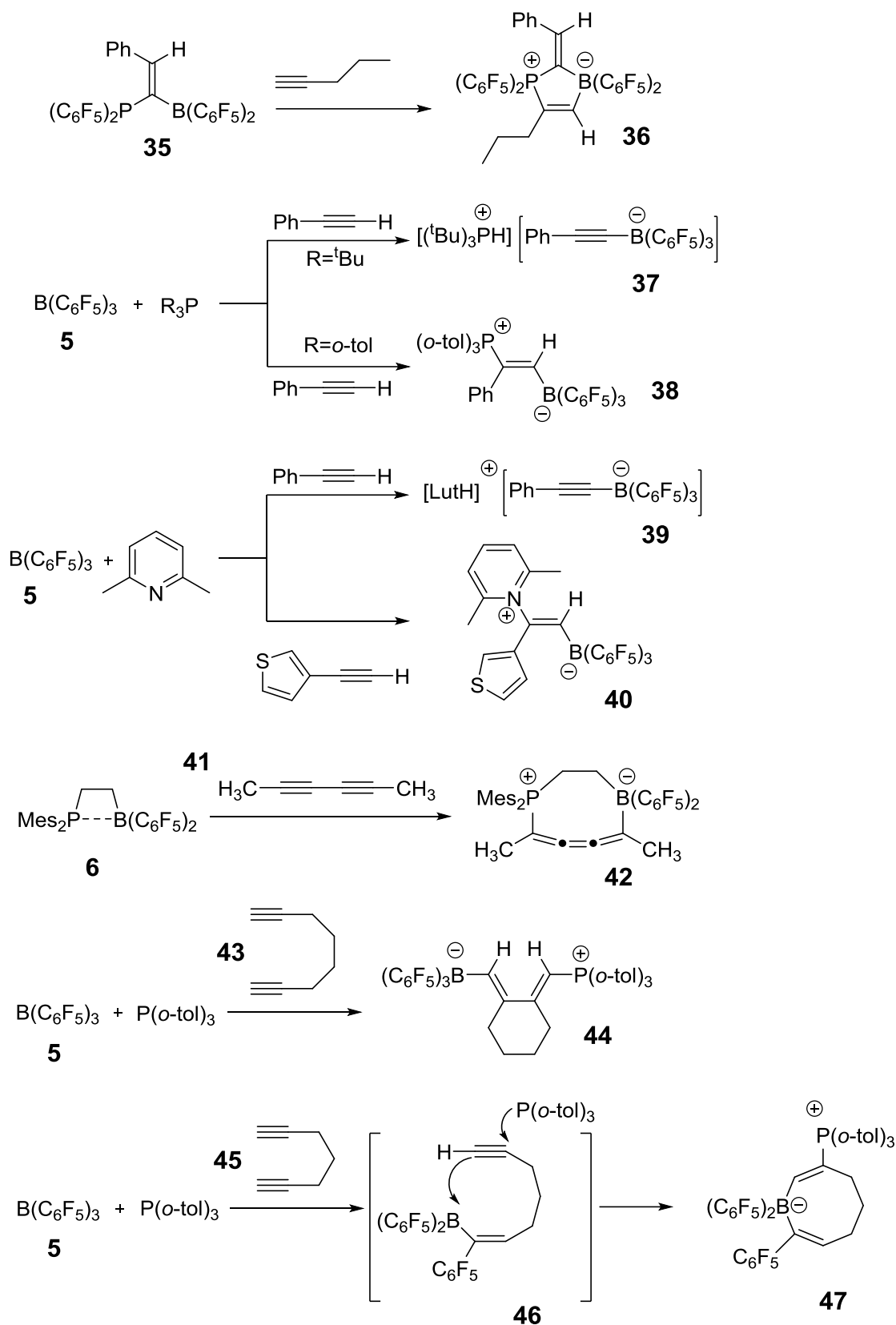
Scheme 4 Reactions of FLP with alkenes^{45, 47, 48}

FLP systems were also shown to react with alkynes. In most cases either C-H activation or *cis*-⁴⁹ or *trans*-1,2-addition occurs, depending on the base⁵⁰ and alkyne⁵¹ used (Scheme 5). Sulfur-based LB was also shown to be a suitable nucleophile for FLP addition to alkynes.^{52a} Carbon-based LB^{52b} also showed FLP activity. System **6** underwent 1,4-addition to butenyne and conjugated dialkynes, such as **41**, thus showing a convenient route to cyclic cummulenes (Scheme 5).⁵³ Reacting a mixture of B(C₆F₅)₃ and P(^tBu)₃ with 4,6-decadiyne yielded linear cummulenes.⁵⁴ At the same time, reacting a mixture of B(C₆F₅)₃ and P(*o*-tolyl)₃ with non-conjugated 1,7-octadiyne **43** resulted in the cooperative addition to both acetylenes, together with formation of a new C(sp²)-C(sp²) bond as in product **44** (Scheme 5).⁵⁵ It is worth mentioning, that the reaction of the same FLP system with 1,6-heptadiyne **45** took a different course, which involved 1,1-hydroboration and led to formation of a doubly unsaturated zwitterionic eight membered heterocycle **47** (Scheme 5).

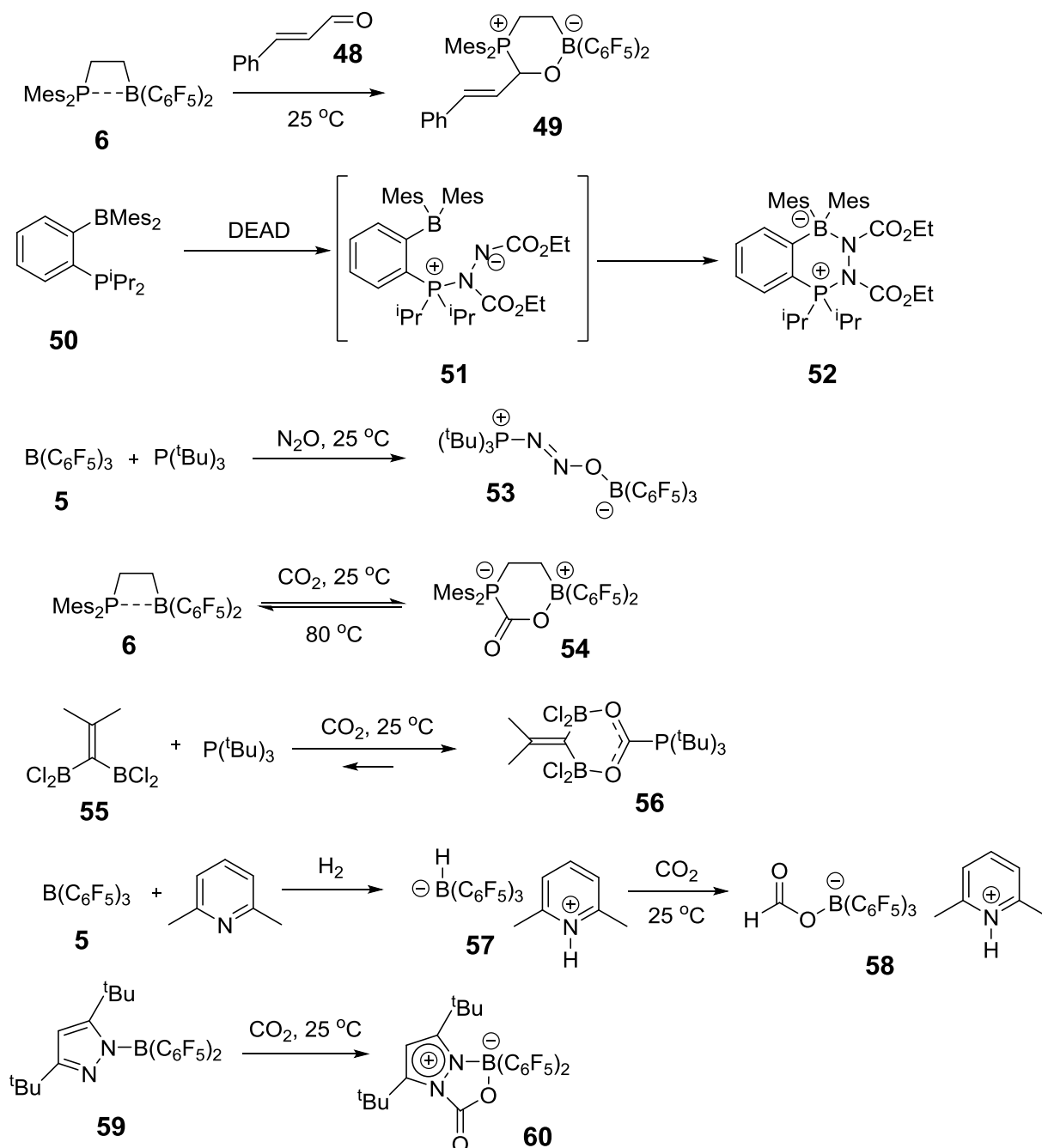
FLP also added to C=O bonds, sometimes leaving the alkene moiety untouched, as in reaction of **6** with *trans*-cinnamic aldehyde (Scheme 6).⁴⁷ Compound **6** was also shown to add azides, isocyanates and nitroso-compounds.⁵⁶ Another system **50** was shown to add isocyanates and N=N bond from DEAD (Scheme 6).⁵⁷

The mixture of P^tBu₃ with B(C₆F₅)₃, is capable of binding greenhouse gases, such as N₂O⁵⁸ and CO₂,⁵⁹ the latter can also be bound by system **6** (Scheme 6). Al-based FLP bind CO₂ irreversibly and allow its subsequent reduction to MeOH using

BH₃-NH₃ as a source of hydrogen.^{60a} Reduction of CO₂ could also be achieved using Zn/P FLP.^{60b} TMP-based FLP system allows CO₂ transformation to MeOH by



Scheme 5 Reactions of FLP with alkynes^{49-51, 53, 55}



Scheme 6 Reactions of FLP with C=O, N=O and N=N bonds^{47, 57-59, 63-65}

using H_2 ,⁶¹ and if Et_3SiH is used as a source of hydrogen it is possible to convert CO_2 to CH_4 .⁶² Chelate binding of CO_2 was also achieved with chlorinated bis-borane **55** in mixture with P^tBu_3 (Scheme 6),⁶³ despite the existence of weak interactions between bis-borane and the phosphine. It was also reported, that CO_2 can be reduced to a boronate derivative **58** by the zwitterionic product **57** of H_2 activation prepared from $\text{B}(\text{C}_6\text{F}_5)_3$ and 2,6-lutidine (Scheme 6).⁶⁴

The importance of tether length between frustrated Lewis acid and base components in intramolecular FLP systems was shown with pyrazolylborane **59** (Scheme 6). This catalyst not only activated hydrogen being the first example of

intramolecular B-N FLP system capable of binding CO₂, but also activated formaldehyde, isocyanates, isothiocyanates, nitriles, isonitriles and alkynes.⁶⁵ The authors highlight that B and N atoms are “ideally oriented” or “preorganised”.

Among other FLP applications are the ring-opening of THF⁶⁶ and lactones.⁶⁷

1.2. The Boundary between FLP and bifunctional catalysis

The discovery of new principles and concepts in science can be viewed from two different perspectives: 1) how the new finding is different and separate from already existing data; and 2) how it is connected, and which place it occupies, in the established system of knowledge. In this light, any new discovery, to a certain extent, abstracts itself from the known by simply being novel. Unfortunately, this frequently leads to a degree of isolation of new research areas from previously discovered fields. However, progress often occurs through uniting principles, thus multiplying their potential.

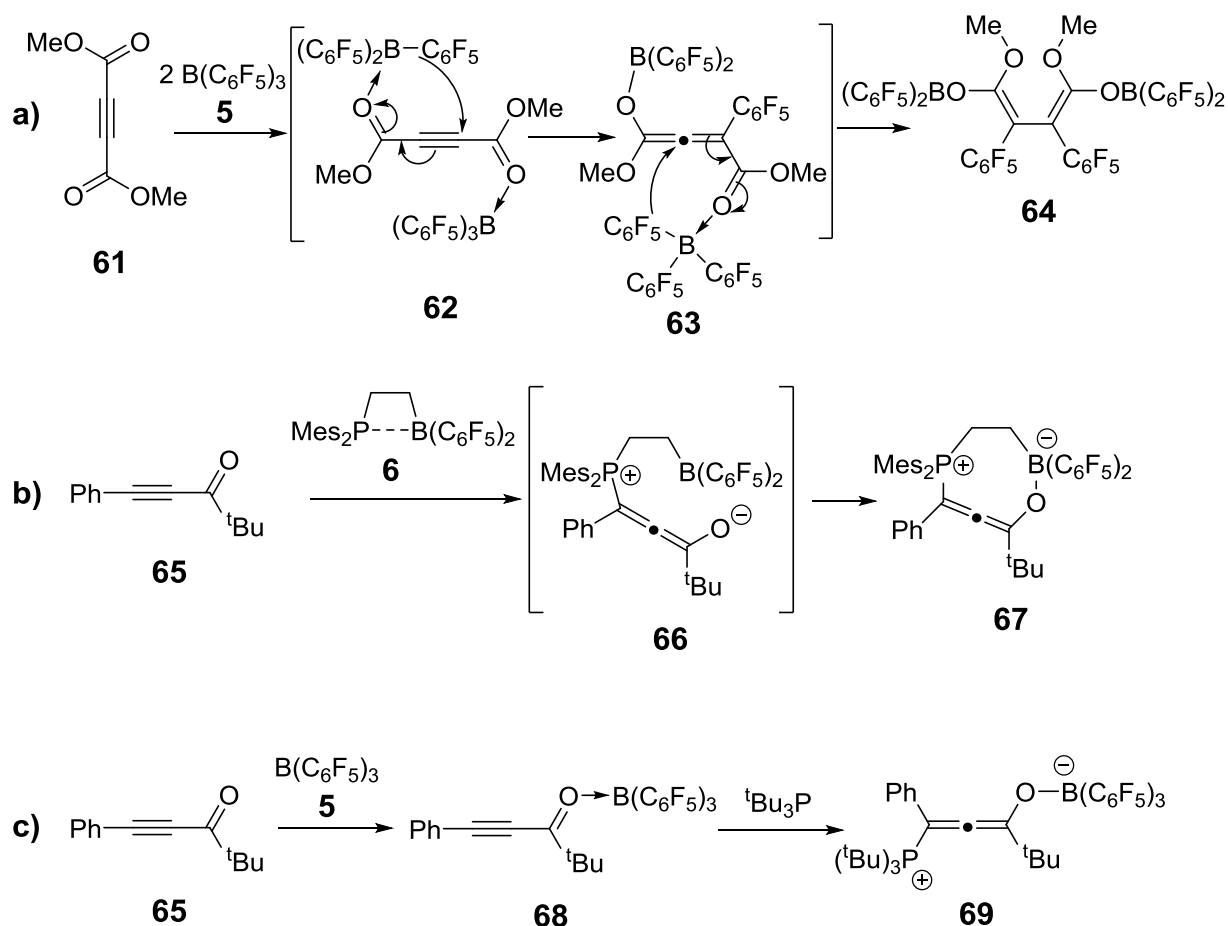
Even though the FLP concept is beginning to be usefully viewed in context with previous research in the areas of bifunctional catalysis and organometallic chemistry,⁶⁸ it is important to analyse how the scope of FLP applications could be increased by widening that context even further. Indeed, it can be suggested that softening Lewis acidity, basicity, steric requirements and tuning tether length between the components, is likely to lead to improved performance and hence, wider applications in organic chemical reactions.

1.2.1. Separate Lewis acids and bases in comparison with FLP chemistry

As shown above, the majority of the existing FLP examples incorporate B(C₆F₅)₃ or its derivatives as the Lewis acid component. This borane has been intensely used⁶⁹ in organic synthesis as a strong Lewis acid since its discovery,⁷⁰ and it is important to investigate the parallels between FLP reactivity and reactions, occurring with B(C₆F₅)₃ and its derivatives alone.

Reaction of dimethyl acetylenedicarboxylate (DMAD) **61** with 2 equivalents of B(C₆F₅)₃ **5** proceeds *via* an unusual rearrangement through a cummulene intermediate **63**, leading to product **64** (Scheme 7a).⁷¹ The intermediate, and the way it is formed, are reminiscent of a “traditional” FLP example of cyclic cummulene **67** formation from FLP **6** and ynone **65** (Scheme 7b).⁷² Similar 1,4-additions are shown

as proceeding by two different pathways: 1) through initial coordination of the B species to the carbonyl oxygen with subsequent nucleophilic attack of the C₆F₅ group onto the alkyne; or 2) the nucleophilic attack of the P lone-pair onto the alkyne with the following stabilization of product to give cyclic compound **67**. However, it is also known,⁷² that ynone **65** reacts with B(C₆F₅)₃ **5** to yield the stable, chelated species **68** (Scheme 7c), and subsequent treatment with ^tBu₃P leads to the zwitterionic product **69**. It seems, that the more electron-withdrawing carboxy substituent in intermediate **62** makes the nucleophilic attack of C₆F₅ group on *sp*-carbon possible. In the case of a phenyl group, the chelated boron adduct **68** is stable unless a stronger nucleophile, i.e. ^tBu₃P is introduced. These examples show the similarities in mechanisms of both free LA and FLP action.

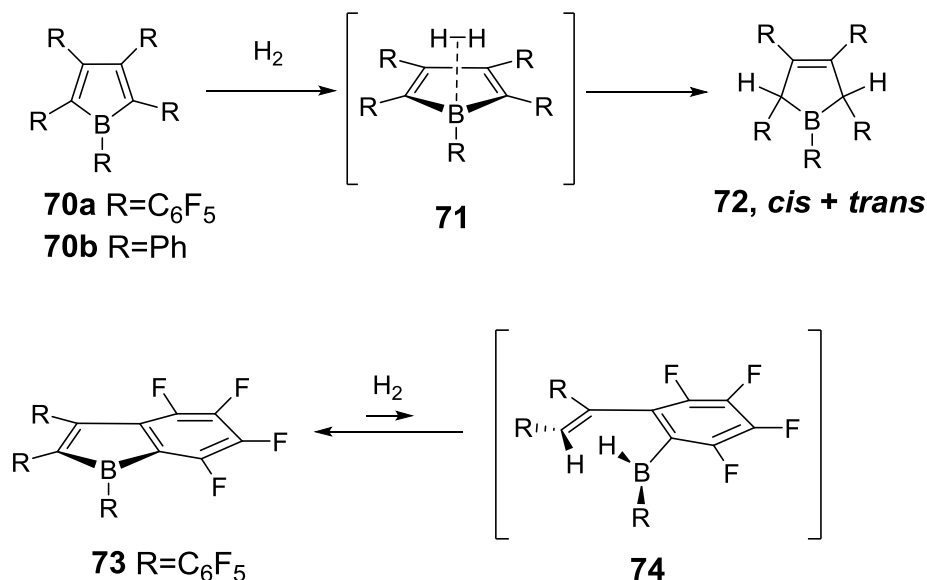


Scheme 7 Comparison of FLP and B(C₆F₅)₃ reactivity^{71, 72}

FLPs are known to activate terminal C-H bonds in alkynes, however, B(C₆F₅)₃ alone is known to show similar reactivity with some alkynes.⁷³

Another important example that brings FLP chemistry to the boundary with other catalytic mechanisms is the metal-free hydrogen activation by antiaromatic organoboranes. Both **70a** and **70b** (Scheme 8), were shown to bind H₂.⁷⁴ The initial

formation of H₂ adduct **71**⁷⁵ is most likely followed by B-C bond cleavage and subsequent rapid cyclization. This approach was extended further to make the process reversible with catalyst **73**.⁷⁶ In these examples the energetic destabilisation of 4- π -electron systems provides additional driving force for H₂ activation.



Scheme 8 H₂ activation by antiaromatic ⁶ boranes⁷⁴⁻⁷⁶

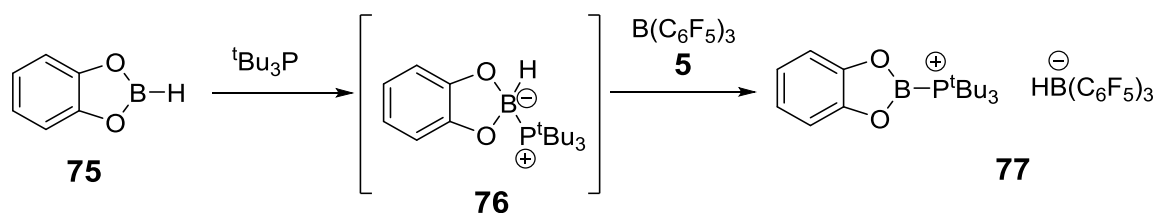
Hydrogen activation can also be achieved by a simple borane HB(C₆F₅)₂, which undergoes direct [2+2] σ -bond metathesis by H₂.⁷⁷ This borane also catalyzes hydrogenation of olefins *via* hydroboration of the substrate, followed by hydrogenolysis of the B-H bond.⁷⁸

It has also been shown that in FLP-mediated CO₂ reductions, the main role of activating substrates belongs to the LA component,⁷⁹ though the LB plays a role in stabilizing the FLP•CO₂ complex. At the same time, the LB actually hinders hydride transfer by donating its lone pair to the LUMO of CO₂, making it less electrophilic. It is also important to note that CO₂ activation can be achieved in some cases by separate LBs, such as phosphines.⁸⁰

However, sometimes true FLP behavior may not be immediately obvious, as the LB role can be played by the substrate itself, as in cases mentioned above of hydrogenation of imines,¹⁶ amine-substituted benzenes,¹⁸ and *N*-heterocycles.¹⁹ Or, in fact even the solvent may be sufficiently nucleophilic.⁸¹

Finally, in some cases simultaneous presence of both LA and LB is not necessary, as reactions can be performed by adding these 2 reagents stepwise. Catechol borane **75** reacts with the mixture of ^tBu₃P and B(C₆F₅)₃ to form salt **77**

(Scheme 9)⁸². However, from the mechanistic point of view, this reaction includes interaction with one compound in reaction mixture to form intermediate **76**, and the resulting increase of hydridic character of B-H bond leads to possibility of subsequent hydride abstraction by another reagent, $B(C_6F_5)_3$ **5**. Organic synthesis counts many examples of step-by-step reactions with more than one reagent present in the mixture, thus the only factor that makes this example refer to FLP chemistry is that potentially the two reagents in the mixture *could* form a Lewis acid adduct if not for the steric hindrance.



Scheme 9 B-H activation by FLP⁸²

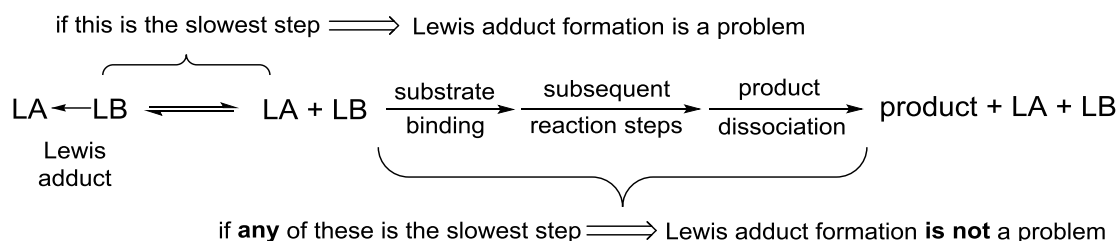
Examples discussed suggest that FLP systems sometimes perform similarly to individual LAs or LBs, thus, it is important to check the reactivity of substrates with the separate LAs and LBs, before making final conclusions on FLP behavior. Nevertheless, many of the aforementioned studies unambiguously show that FLP reactivity cannot be observed without both the LA and LB being present.

1.2.2. “Frustration” and reactivity of Lewis pairs

One of the major and key features of FLP chemistry is the steric inability of the LA and LB to form a Lewis adduct.³⁵ However, while reducing the reactivity of the LA and LB towards each other, steric hindrance also limits substrate scope, since sterically more demanding molecules are less likely to be activated.

The main question when classifying Lewis pairs as either “frustrated” or “not frustrated” is where to draw the line that separates these terms. Lewis adduct formation is an equilibrium process,⁸³ and thus there is both the adduct and separate LA and LB species present in solution. Catalytic activity of such systems will be kinetically determined, depending upon whether adduct dissociation, or LA–LB binding with substrate, or product dissociation or any other reaction step is faster (Scheme 10). If the exchange between LA–LB adduct and the mixture of separate LA and LB is faster than the slowest step in the reaction, then even if the catalyst mainly exists in the adduct form, it can still be active. Thus, adduct formation between LA

and LB should not necessarily lead to a drop in catalytic performance of the FLP system.



Scheme 10 Identifying when Lewis adduct formation has a negative impact on FLP activity

These considerations are supported by multiple literature examples. It was found⁸⁴ that a mixture of 2,6-lutidine and $\text{B}(\text{C}_6\text{F}_5)_3$ can activate hydrogen and show typical FLP reactivity despite observing an equilibrium between the free LA and LB and the Lewis adduct by NMR. Indeed, the two reaction pathways are not mutually exclusive.⁸⁴ Nevertheless, in this particular case, the activation of H_2 was slower than with other bases, presumably due to the fact that some of both the LA and LB exist in an inactive state due to competitive Lewis adduct,⁸⁵ often referred to as a classical Lewis adduct (CLA). However, the same $\text{B}(\text{C}_6\text{F}_5)_3$ -2,6-lutidine system also activates CO_2 faster than $\text{B}(\text{C}_6\text{F}_5)_3$ -2,2,6,6-tetramethylpiperidine,⁶⁴ despite computational studies suggesting that the latter combination of LA and LB should be a more reactive FLP system.⁸⁶

Considering thermodynamics, it can be assumed that non-bonded LA and LB systems should *in general* bind to substrates better than CLAs, because the energy needed for adduct dissociation reduces reactivity.⁸⁷ Nevertheless, CLAs are known to perform FLP chemistry through the equilibrium with free LA and LB in solution.

1.2.3. Reactivity of classic Lewis adducts (CLAs)

Other examples of H_2 activation by mixtures of $\text{B}(p\text{-C}_6\text{F}_4\text{H})_3$ with different phosphines⁸⁸ lead to two important conclusions. Firstly, the stronger and more hindered bases tend to yield FLPs that bind hydrogen irreversibly and form phosphonium borate salts, and it is weaker basicity that becomes a requirement for liberation of hydrogen from the salts formed. A similar effect was observed for *ansa*-aminoboranes⁸⁹ and was shown to be the result of reduced stability of ammonium hydridoborate formed, when a weaker Lewis basic component was used. Secondly, in

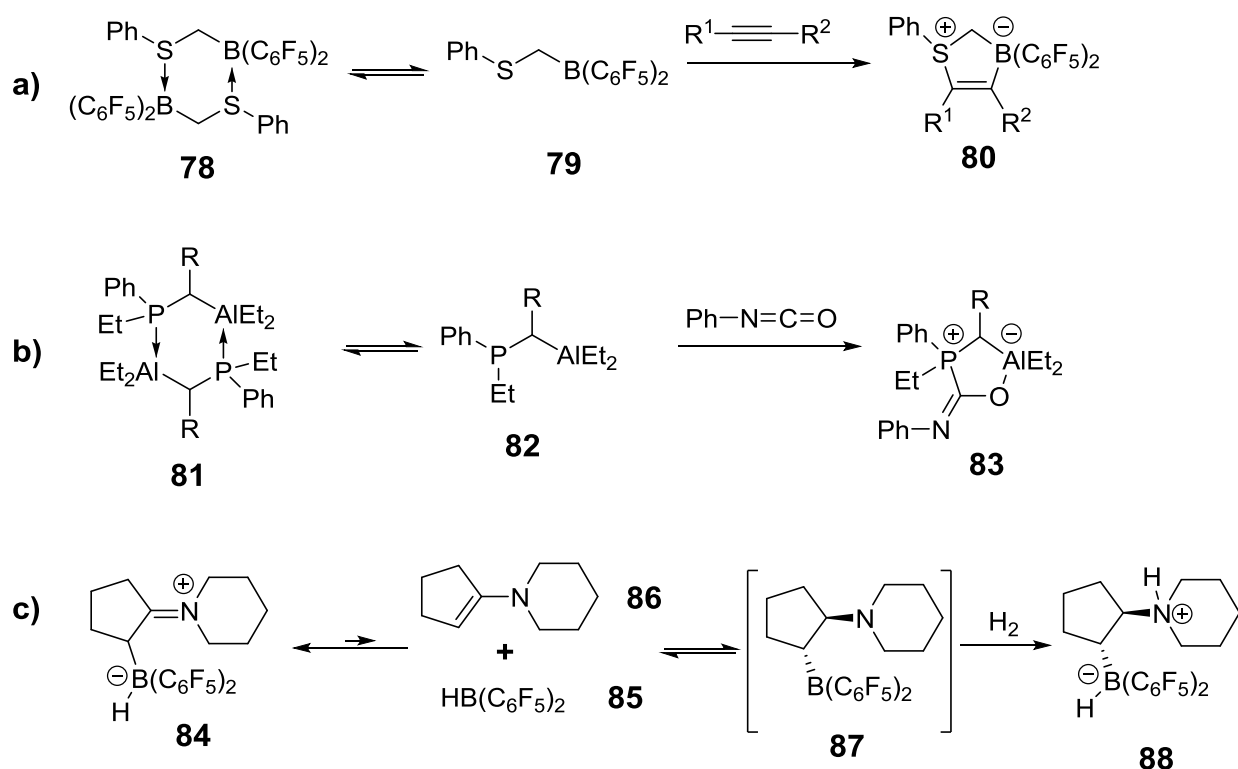
many cases, CLAs have only been shown to be inactive towards H₂ binding; the H-H bond is particularly strong and thus, there is still the possibility for those adducts to activate lower energy bonds.

Alkynes react with both CLAs⁹⁰ and cyclic double Lewis adducts, such as **78** (Scheme 11a).⁹¹ Complex **78** shows that breaking the two donor-acceptor bonds is possible and is driven by interaction with the substrate resulting in complex **80**. Similar activity is observed for Al-P dimer **81** which reacts with CO₂⁹² and other small molecules (Scheme 11b).⁹³ CO₂ can also be activated by CLAs,⁹⁴ and indeed, as early as 1978⁹⁵ it was reported that to achieve efficient catalysis, dimer formation of the bifunctional species is actually *preferred*.

Both the structures of dimers **78** and **81** were identified by X-ray crystallography, and this leads to another important conclusion that is often overlooked, i.e. the existence of interactions between LA and LB centers in solid-state molecular structures of crystalline compounds does not necessarily mean that such species predominate in solution, or equally that this is indicative of the absence of an equilibrium with the free LA and LB. In fact, in some cases, this equilibrium cannot be observed, even by NMR spectroscopy. For example, a mixture of B(C₆F₅)₃ and PPh₃ activated alkynes,⁵⁰ however, NMR spectra of the mixture suggested the presence of adduct only.

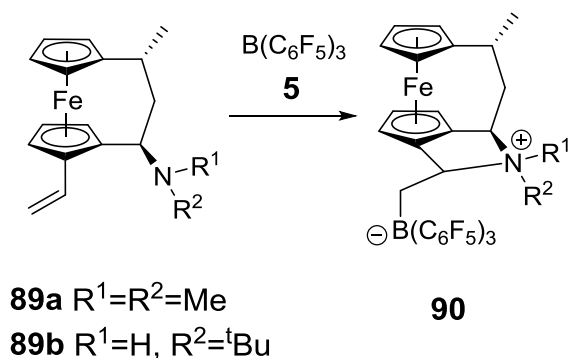
A further demonstration of the importance of a facile LA–LB equilibrium comes from observations of typical FLP reactivity of a precursor of a LA–LB system.⁸³ The Piers borane **85** reacts with enamine **86** to give the iminium salt **84** (Scheme 11c), which was isolated and characterized by NMR and X-ray spectroscopy.⁹⁶ However, exposure of **84** to dihydrogen causes a precipitation of **88** within 5 minutes. This suggests that complex **84** exists in equilibrium with a mixture of free LA **85** and LB **86**, which is also in equilibrium with a small amount of “invisible” hydroboration product **87**. The bifunctional aminoborane **87** is a typical FLP, capable of binding H₂ to yield **88**.

Following the same pattern, the weak adduct between Et₃P and B(C₆F₅)₃ causes ring-opening of THF,⁹⁷ and the adduct of dimethylbenzylamine with B(C₆F₅)₃ reacts with H₂, CO₂, olefins, alkynes and diynes, again due to an equilibrium which makes free LA and LB available for reaction.⁹⁸



Scheme 11 FLP reactivity of LA–LB double adducts **78**⁹¹, **81**⁹³ (a, b) and FLP-precursor compound **84**⁹⁶ (c) through equilibrium with free LA **85** and LB **86**.

An example of FLP reactivity with not very hindered *N,N*-dimethyl LB **89a** was shown by Erker *et al.*⁹⁹ with the 1,2-addition of amine-borane Lewis pairs to olefins (Scheme 12). This approach was extended even to the secondary amine **89b**, which is very likely to reversibly interact with $B(C_6F_5)_3$ **5**, forming a Lewis adduct in equilibrium, but is still able to act as FLP at the [3]Ferrocenophane network (Scheme 12).¹⁰⁰



Scheme 12 FLP addition at the [3]Ferrocenophane network⁹⁹⁻¹⁰⁰

CLAs can also catalyze polymerization reactions.¹⁰¹ Remarkably, the turnover frequency (TOF) for polymerization of γ -methyl- α -methylene- γ -butyrolactone was shown to increase as the catalysts used were changed from FLPs to CLA Ph_3P-

$B(C_6F_5)_3$.¹⁰² Systems in which steric hindrance was too great were inactive in this type of polymerization reactions.

1.2.4. Benefits of reducing Lewis acidity and basicity

It can now be seen that adduct formation does not necessarily lead to inactive FLP systems, and in many cases, conversely increases the performance of Lewis pairs. However, if the equilibrium with the free species is slow or completely shifted to the adduct, the Lewis pair system can indeed become inactive.¹⁰²⁻¹⁰³ In these cases, reducing the likelihood of adduct formation can indeed be achieved through increasing steric hindrance of both LA and LB partners. Unfortunately, this approach can lead to loss of activity, as availability of both the LA and LB drops. This also means that the reactions scope which FLPs can catalyze becomes limited by steric hindrance. Another approach to avoid adduct formation can be the reduction of Lewis acidity and basicity of the FLP components, reducing the strength of LA–LB complexation. This can result in achieving multiple other important goals.

Firstly, even though higher Lewis acidity and basicity can help accelerate substrate activation, it is the rate-determining step that should be considered for tuning LA and LB strength for a particular reaction. In general, high Lewis acidity and basicity slow down product dissociation from the catalyst.¹⁰⁴ The adduct formed between Lewis acid and substrate, as in the case of CO_2 reduction⁶³ or in imine hydrogenations,^{8, 11} can be sufficiently strong that its dissociation can become the rate-determining step. Using a weaker LA facilitates these reactions. Similarly, some FLPs can bind, for example, to benzaldehyde, forming a stable, and thus supposedly, inactive zwitterionic adduct.¹⁰⁵

In the case of FLP-mediated hydrogenations, the rate-limiting step is not always the H_2 activation,⁴³ but can also be the hydrogen transfer.¹² In cases where the rate determining step is the hydride transfer from borohydride, the use of a weaker LA can again improve the performance of the catalyst.¹⁰⁶ Following a similar pattern, $PhB(C_6F_5)_2$ was found to be more effective than $B(C_6F_5)_3$ in transferring the OR group to tin in allylstannylation reactions.¹⁰⁷

Secondly, use of $B(C_6F_5)_3$, and some of its derivatives, may lead to undesirable *ortho*- or *para*-internal catalyst activation,¹⁰⁸ leading to protonolysis of the facile B– C_6F_5 bond^{33, 109} and migration of the pentafluorophenyl group as in known examples of 1,1- and 1,3-carbaborations of terminal alkynes.⁷³

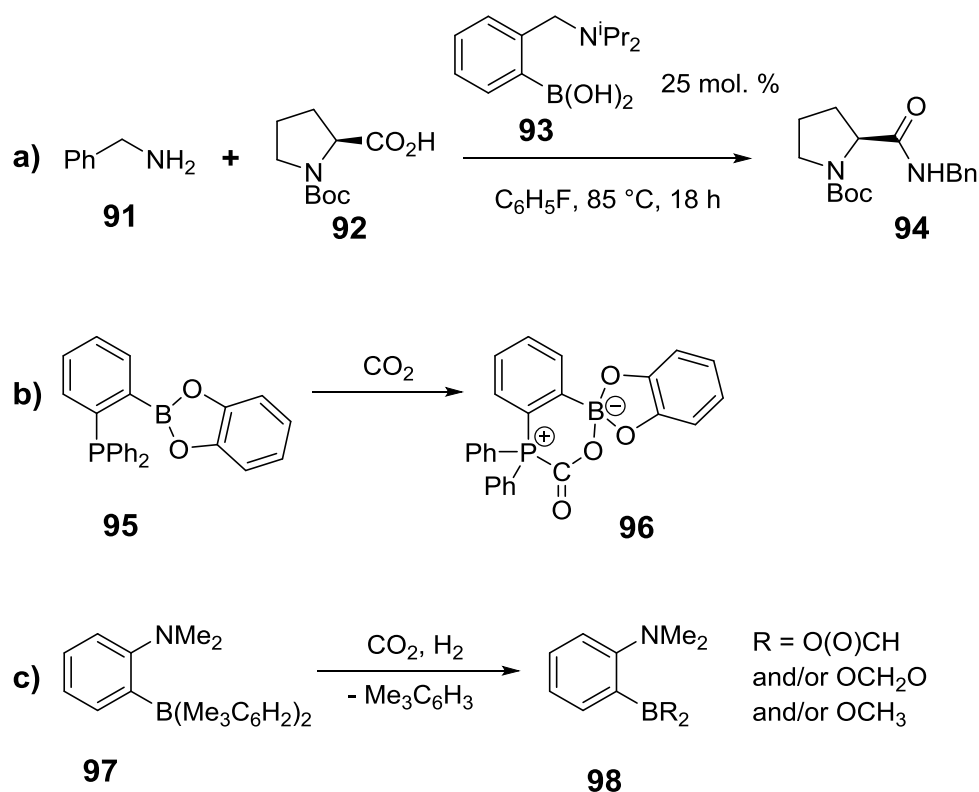
Thirdly, the functional group³⁰ and impurity¹¹⁰ tolerance of catalysts in FLP chemistry can in some cases be an issue. While there are strategies, such as the use of scavengers, that help to increase impurity tolerance,¹¹⁰ reducing the reactivity of LA and LB can also help to improve the performance of FLP catalysts. Careful tuning of the Lewis acidity of the LA and steric requirements of both the LA and LB can even lead to FLP systems that are tolerant to water present in “bench” quality solvents.⁸¹

It is inspiring to see that these principles are becoming more generally recognized and applied. Introduction of two isopropyl groups onto nitrogen in weakly Lewis acidic and basic aminophenylboronic compound **91** (Scheme 13a) is already enough to shift the equilibrium of adduct formation to uncoordinated species,¹¹¹ allowing catalysis of amide formation (Scheme 13a), and similar reactivity is observed even for *N,N*-dimethyl derivative.¹¹² Attempts have been made to reduce the basicity of the LB component of FLPs by the introduction of pentafluorophenyl substituents into the phosphines, which has provided compounds capable of good FLP reactivity.¹¹³ Dihydrogen cleavage was achieved with an “inverse” FLP between a strong LB and a weak LA.¹¹⁴ Dropping the Lewis acidity to the level of an aryl boronate, as in catalyst **95**, still allowed activation and subsequent hydroboration of CO₂ to take place (Scheme 5b);¹¹⁵ a result which again underlines the possibility of using weaker LAs and LBs. Catalyst **97** participated in H₂ activation and provided a route to CO₂ reduction (Scheme 5c),¹¹⁶ and even though it underwent protodeboronation to **98** in the process, the potential of using a non-fluorinated, weakly acidic triarylborane (LA) and unhindered dimethylarylamine (LB) for achieving FLP reactivity has been realized and is a promising development.

1.2.5. Other approaches to avoid Lewis adduct formation

Apart from reducing Lewis acidity and basicity, other methods of preventing Lewis adduct formation between LA and LB are known.

Possibly the most straightforward approach is simply to prevent contact between free LA and LB, by for example, performing reactions in a stepwise manner. Pre-activation of substrate with the LA, followed by subsequent addition of the LB was used for polymerizing a divinyl monomer.¹¹⁷ The existence of a borane-olefin Van der Waals complex in the FLP-mediated reactions with alkenes¹¹⁸ and knowledge of the stepwise character of N₂O capture by phosphine-borane FLPs,¹¹⁹ also suggests that some of these reactions might be attempted stepwise. However, this approach can only be applied for non-interlinked FLPs.



Scheme 13 Weakly Lewis-acidic, weakly hindered compounds performing “bifunctional” and/or “FLP-type” reactivity

Connecting the LA and LB centers with a carefully designed linkage can lead to a reduction in intramolecular adduct formation,¹²⁰ however, the possibility for intermolecular coordination should always be considered.

The energy mismatch of LA and LB orbitals was presumed to enhance reactivity with H₂.¹²¹ Applying “electronic” rather than steric frustration was investigated for metal-ligand multiple-bond complexes, and reactivity similar to that of FLP systems was observed.¹²²

Altering temperature is another tool for manipulating FLP reactivity. “Thermally induced frustration”¹²³ can be observed, when the heating of adduct allows its dissociation and hence, FLP system can become active.¹²⁴ The opposite situation was also reported,¹²⁵ i.e. that adduct formation was shown to be irreversible at r.t., but that FLP reactivity could be observed at -78 °C. An example of a photo-induced dissociation of a LA–LB adduct is also known.¹²⁶

Increasing the H₂ pressure has also been used to initiate its activation by using the unhindered combination of Me₂NH and BH₃.¹²⁷ This combination of LA and LB forms an adduct which is almost inactive to hydrogen at ambient pressures.

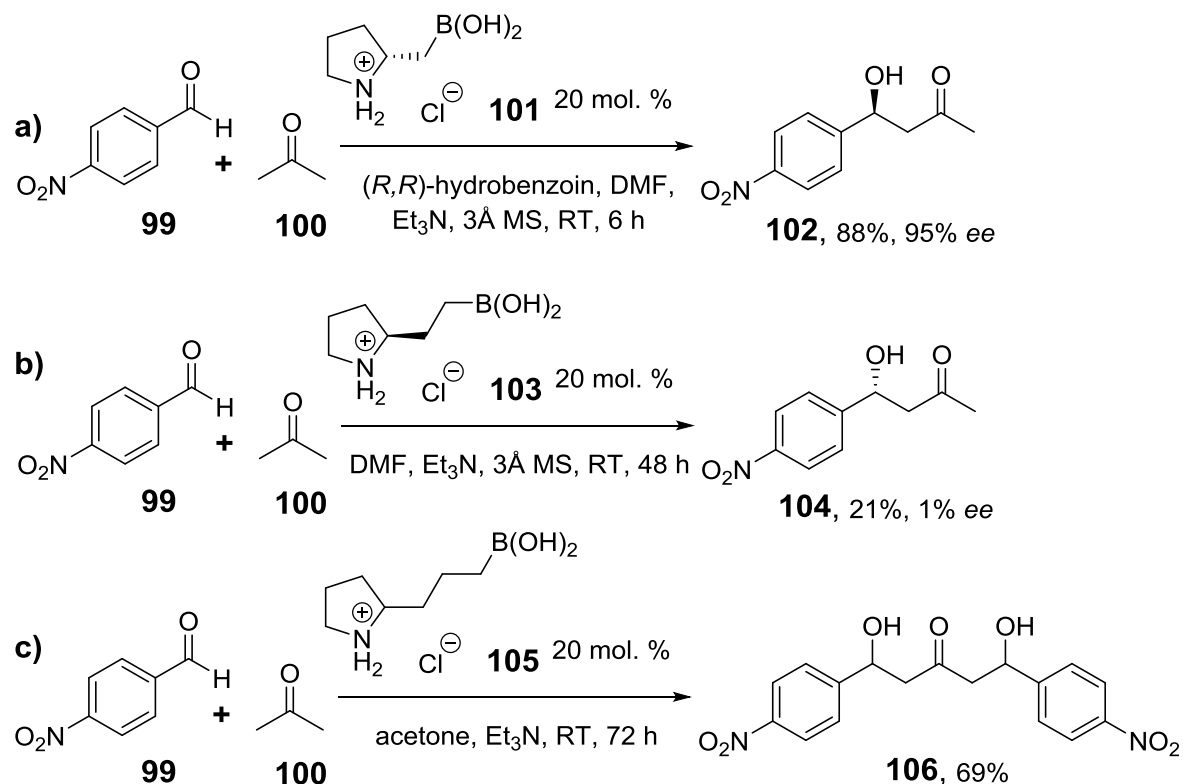
Solvent can play a role in stabilizing FLP adducts, by preventing adduct formation.¹²⁸ In a different example, the introduction of a polyether macrocycle to a reaction medium did not prevent adduct formation, but resulted in stabilizing the product of H₂ activation and thus facilitated this process.¹²⁹

1.2.6. Importance of link between LA and LB centres

It is important to note that, according to definition,¹³⁰ bifunctional catalysis is catalysis by *bifunctional* species, meaning all of the FLP consisting of separate LA and LB should rather be viewed as acting in *concerted* processes.

Catalysts with linked reaction sites lose less entropy when reacting with substrates than do unbound systems,⁸⁶ which improves the reactivity of the connected FLP¹¹⁵ and allows utilization of weaker LA and LB pairs.

Tuning the tether type and length between the two reactive centers is known to have a major effect on bifunctional catalysis. Pyrroline-2-alkylboronic acids **101**, **103** and **105** showed dramatically different reactivity as the length of alkyl chain between LA and LB centers was varied.¹³¹ Homoboroproline **101** was identified as efficient catalyst for enamine-mediated aldol formation with high enantiomeric selectivity (Scheme 14a).



Scheme 14 Impact of tether length between LA and LB centers on reactivity

Increasing the carbon chain length by one methylene group in **103** led to a drop in reactivity and total loss of asymmetric induction (Scheme 14b), while increasing it further by one more CH₂ in **105** completely switched off catalysis of single aldol formation, at the same time opening access to double aldol product (Scheme 14c).

The same applies to FLP systems and for example, it was shown that similar *geminal* and *vicinal* P-B pairs show different reactivity towards cinnamaldehyde.¹³² Changing tether length between 2, 3 and 4 methylene groups had a major effect on FLP reactivity of phosphinoboranes.¹³³ Preorganization of the LA and LB in *geminal* methylene-bridged phosphinoboranes allowed reactions with H₂ and CO₂⁸⁷ even though two phenyl substituents on boron rendered LA center much less acidic than in well-studied pentafluorophenyl substituted boranes.

1.3. Conclusion

The discovery of FLP is an important breakthrough in understanding chemical reactivity and extending catalytic possibilities. At the same time most research groups that joined into investigations of FLP chemistry since 2006 focused only on small molecule activations, as the whole concept of Frustrated Lewis Pairs formulated initially implies significant steric hindrance of both LA and LB components. However, the performance of FLPs is not necessarily diminished by decreasing steric demand or LA and LB strength. In fact, reactivity can be tuned and certainly increased by that approach. Indeed, because Lewis adduct formation is always an equilibrium process, it can be proposed that subtlety of FLP design, i.e. introducing milder Lewis acidity and basicity, reducing hindrance and careful adjustment of tether length between reactive centers, should lead to improved selectivity, reactivity and a significantly increased scope of FLP applications.

Thus this work is, on one hand, devoted to extending the potential of FLP chemistry by using its remarkable principles for design of new bifunctional B-N catalysts for novel applications. On the other hand, investigation of borinic and boronic acids catalytic performance in direct amide formation allowed studying multiple different Lewis adducts formed in reaction mixtures, which helped to understand the mechanism of this remarkable transformation.

2. Results and discussion

2.1. Aims of the project

The original goal of this work was to design and synthesize catalysts that would operate at the boundary between FLP principles and “traditional” bifunctional catalysis. Part I describes synthetic attempts towards these new catalysts. In the process of this work a better understanding of boron chemistry and reactivity aspects of borinic compounds was achieved. Homoboroproline catalyst **176** was successfully applied in nitro-Michael transformation.

In the process of this work multiple diaryl borinic acids of general structure Ar_2BOH were obtained, and it was found, that they have never been probed as catalysts in direct amide formation reaction, while boronic acids $\text{RB}(\text{OH})_2$ are known to efficiently catalyse this process.¹³⁴ However, the mechanism of action of boronic acids in direct amide formation is not yet well understood, while this is crucial for designing better catalysts for this promising, efficient, atom-economic and environmentally benign reaction.¹³⁵

Thus, part II describes investigation of both borinic and boronic acids behaviour in mixtures with substrates for direct amide formation – amines and carboxylic acids – and sheds light on the complex processes and equilibria that occur in these systems with and without presence of molecular sieves.

Finally, non-catalysed, thermal direct amide formation was kinetically investigated in flow and microwave reactors in an attempt to better understand the background processes in direct amide formation and results are reported in the beginning of Part II.

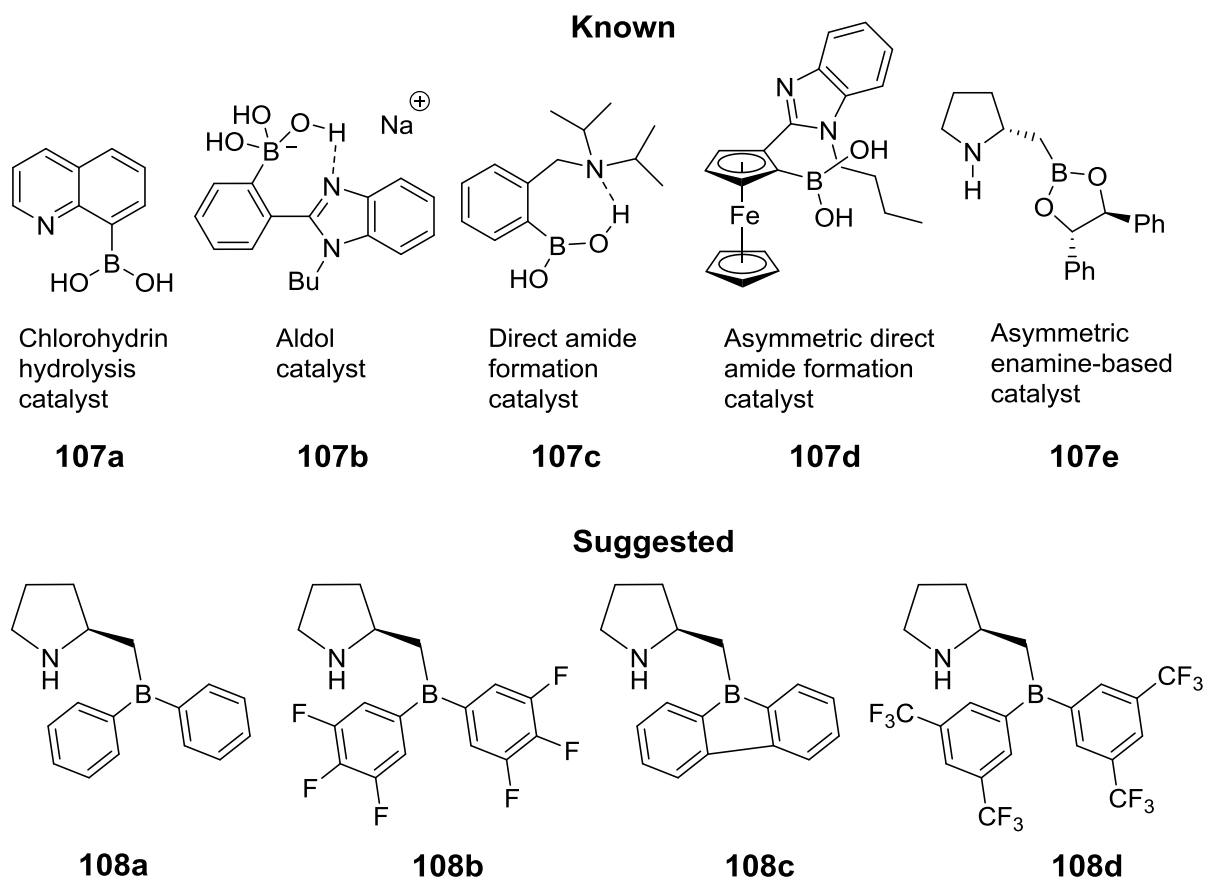
2.2. Part I. New bifunctional B-N catalysts

2.2.1. Design and retrosynthetic analysis of new catalysts

Proline-based boronic acids **107** (Figure 3) were developed as successful catalysts in our group before.¹³⁶ In order to improve applications of such catalysts, investigate further B-N bifunctional systems and to bring our research to the boundary of FLP chemistry, we designed a series of new catalysts **108** (Figure 3). The Lewis acidity of the boron centres in **108b-d** is supposed to be significantly increased compared to boronic acids **107**, but is lower than in general FLP inspired C_6F_5 substituted catalysts. At the same time introducing carbon substituents at boron

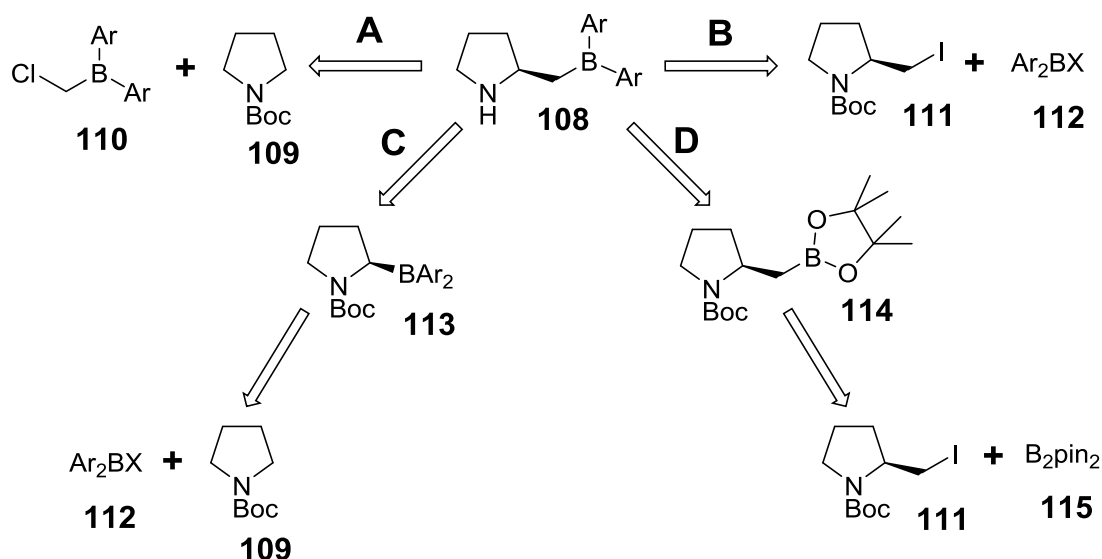
instead of OH groups was expected to reduce the problems of possible reesterifications observed in aldol reactions before. Reduced steric hindrance at LB centre, as compared to FLP bases, should allow catalysis of other organic substrates rather than those generally reported in FLP-related publications. The general retrosynthetic analysis for **108** is shown in Scheme 15.

Figure 3 Known¹³⁶ and suggested new bifunctional B-N catalysts



In order to create the β -boron proline centre, 4 approaches (**A-D**) initially were proposed (Scheme 15). In path **A**, the asymmetric α -lithiation of *N*-Boc pyrrolidine **109** was to be followed by subsequent reaction with diaryl α -chloromethyl borane **110**.

In path **B** the carbon chain with chiral centre is already assembled with iodide **111**, which could be accessed through proline. It was then to be reacted with borinic species **112**, where X could be a halogen or alkoxy group. Another approach **C**, involved asymmetric α -lithiation of **109**, which could be followed by borylation with borinic species **112** to yield α -borylated **113**. A rearrangement reaction with ClCH_2I would yield **108**, as previously reported in our research group on an analogous substrate.¹³⁷ Finally, the **D** approach involved alternative borylation of iodide **111** with B_2pin_2 , with subsequent need for functionalization of boronate **114**.

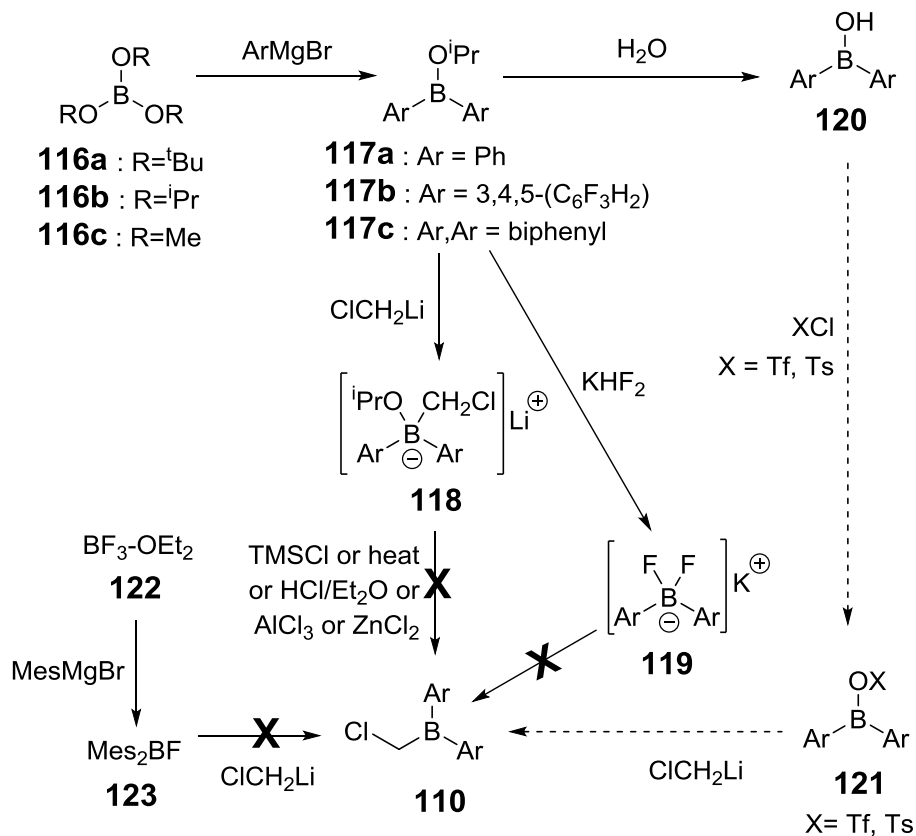


Scheme 15 Retrosynthetic approaches to boranes **108**

2.2.2. Path A. Diaryl α -chloromethyl borane **110** approach

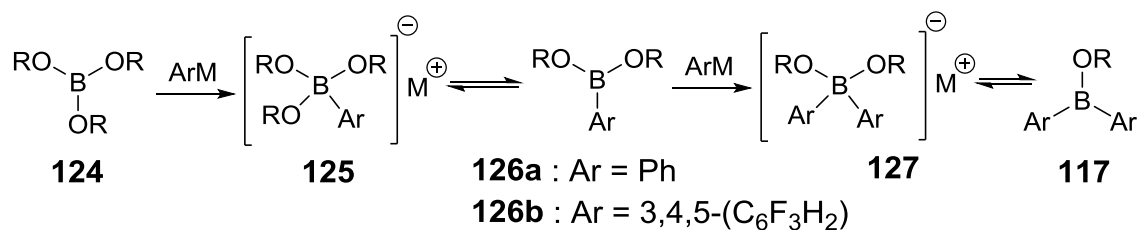
As seen in Scheme 15, diaryl α -chloromethyl borane **110** is a key intermediate in path A. Different synthetic approaches to obtain this compound are summarised in Scheme 16.

2.2.2.1. Borinate synthesis



Scheme 16 Synthetic approaches to borane **110**.

Borinates **117** were suggested as intermediates in the synthesis of **110**, and their synthesis was conducted *via* reactions of organometallic compounds with trialkoxyboranes **116** (Scheme 16). The suggested mechanism of this process¹³⁸ is shown in Scheme 17. First, the aryl nucleophile adds to the boron centre and an “ate”-complex **125** is formed. It then collapses to boronate **126** and is again attacked by an aryl nucleophile to form new “ate”-complex **127**. Finally, the latter collapses to form borinate **117**.

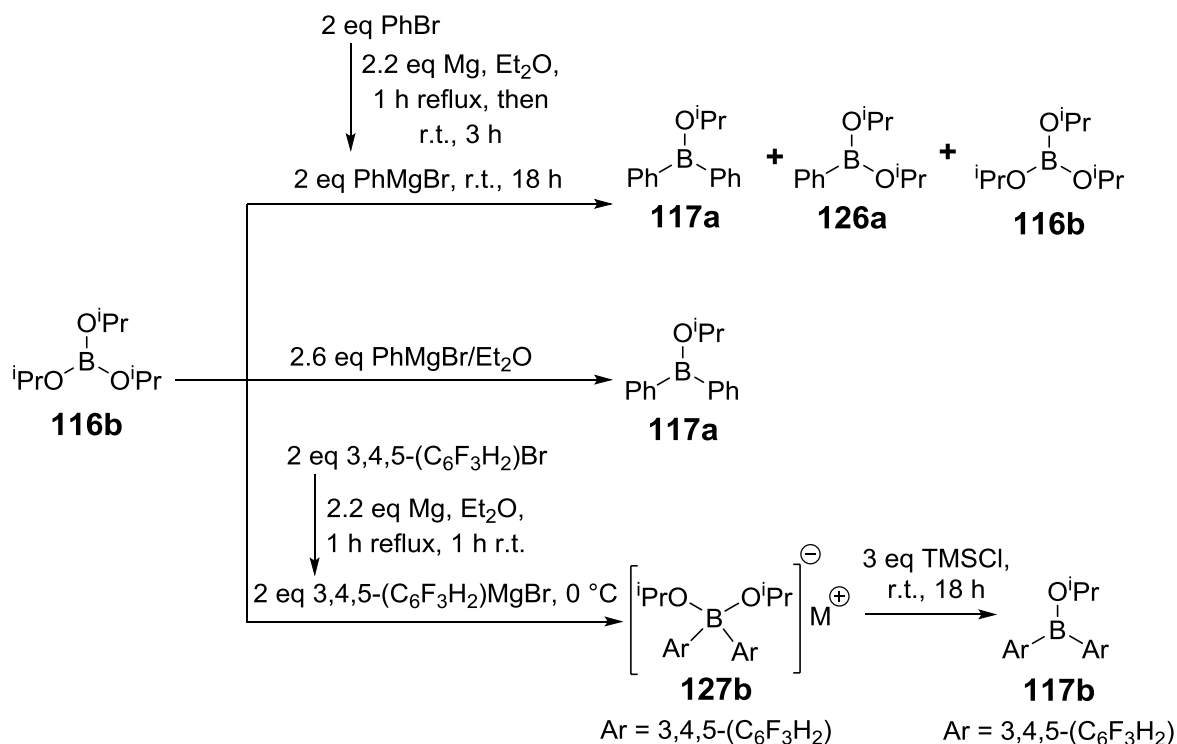


Scheme 17 Suggested¹³⁸ mechanism of borinate **117** formation through “ate”-complexes **125** and **127**, which also explains formation of boronate byproducts **126**

First, tri-*(tert)*-butylborate **116a** was used, but only minor formation of a boronate of type **126** (most likely due to steric hindrance) with conversion of less than 5% was noticed, thus triisopropylborate **116b** was used for further reactions.

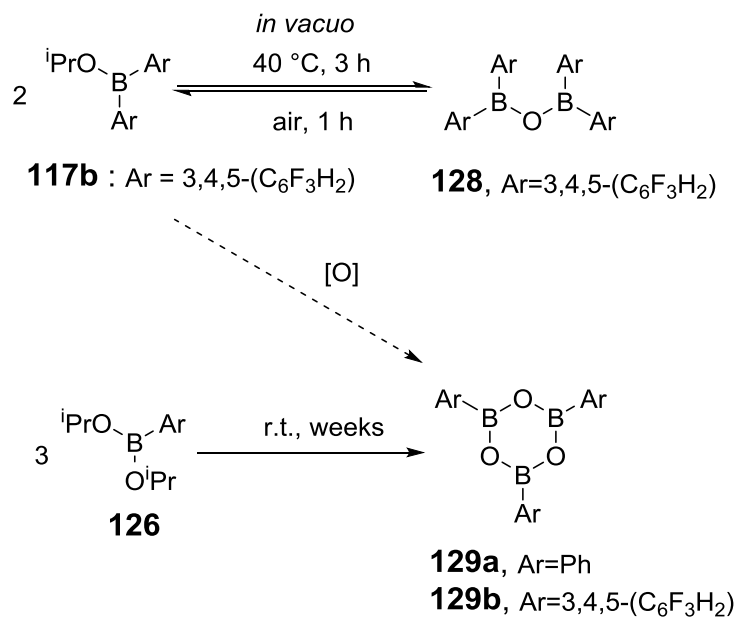
It was reported before¹³⁸ that reacting 2 equivalents of PhMgBr with **116b** was enough to achieve 100% conversion to Ph₂BOⁱPr **117a**. Initial attempts to repeat this process using commercial solution of PhMgBr in THF were unsuccessful. When the concentration of Grignard reagent was determined by titration,¹³⁹ and the amount of reagent adjusted accordingly, conversion was still far from complete as seen by ¹¹B NMR. Finally, preparing 2 equivalents of Grignard reagent from Mg and PhBr in Et₂O with subsequent addition of 1 equivalent of borate **116b** (Scheme 18) resulted, as indicated by ¹¹B NMR, in a mixture of borinate **117a** (δ 44.9, 75%), boronate **126a** (δ 28.3, 18%) and starting borate **116b** (δ 17.5, 7%). This mixture was distilled and the borinate **117a** (containing less than 5% of boronic byproduct) was obtained in 35% overall yield.

It was then found that using 30% excess of commercial PhMgBr in Et₂O led to exclusive formation of Ph₂BOⁱPr **117a** (Scheme 18), however, no borane Ph₃B formation was noticed even when 3 equivalents of PhMgBr were used. Distillation was still required to purify the product **117a** from non-boron containing compounds.



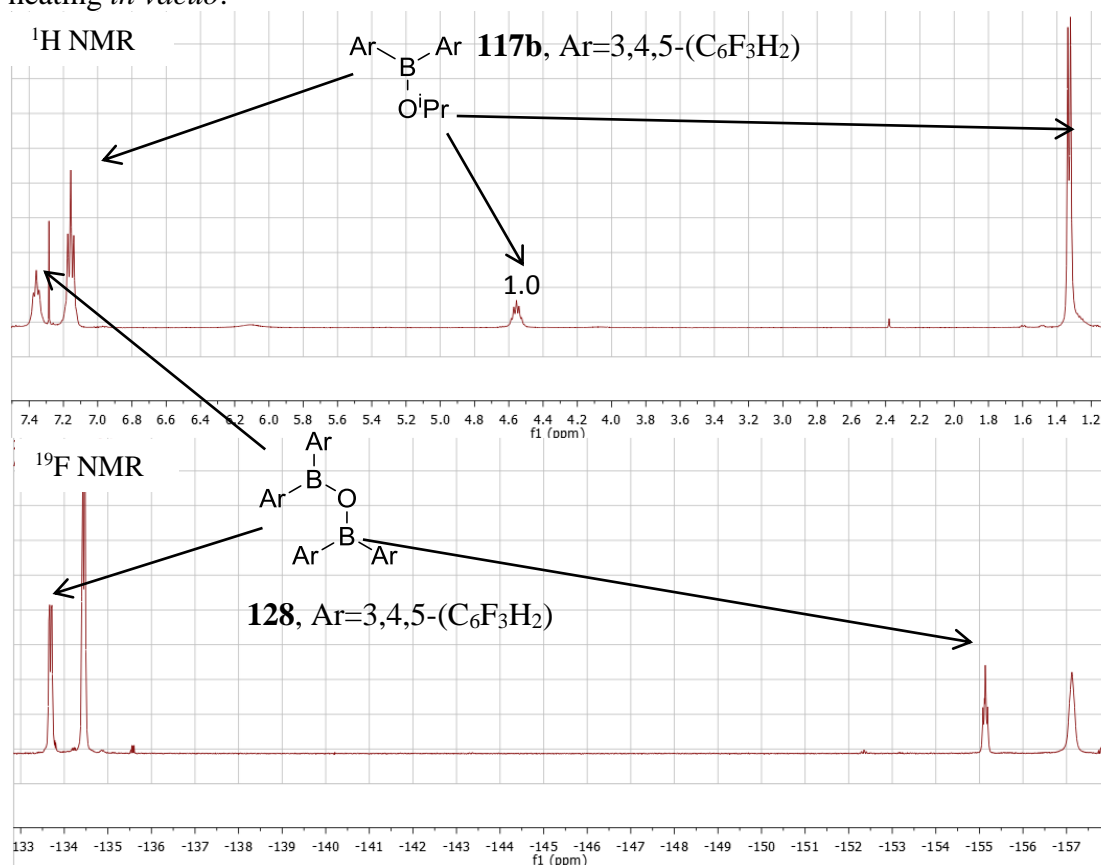
Scheme 18 Synthesis of borinates **117a-b**

In the case of the bis(3,4,5-trifluorophenyl)isopropoxyborane **117b** synthesis, it was enough to use 2 equivalents of 3,4,5-trifluorophenylmagnesium bromide, generated from Mg and aryl halide, to achieve total conversion of borate **116b**, and boronate **126b** was not observed (Scheme 18). However, the “ate”-complex **127b** (Scheme 18), which was formed in this reaction (indicated by ¹¹B NMR, δ 6.2), did not collapse over time, and the reaction mixture needed to be quenched with TMSCl (3 equivalents), which yielded crude borinate **117b**. It was subsequently distilled by Kugelrohr, but it was also found that using HCl and water for the workup of the reaction mixture, followed by addition of isopropanol and removing it *in vacuo* also led to nearly pure borinate **117b** in 82% yield isolated as a brown oil. Evaporation of volatiles needed to be fast and conducted at r.t., as leaving **117b** at 40 °C at 10 mm Hg for 3 hours resulted in partial formation of B-O-B compound **128** (Scheme 19). This was seen in ¹H NMR spectrum by appearance of a new aromatic C-H signal and in the ¹⁹F NMR spectrum by appearance of 2 new groups of signals (Figure 4), although **128** was not isolated. Leaving it in air for 1 hour led to rehydration to **117b**.



Scheme 19 Formation of dehydrated products **128-129**

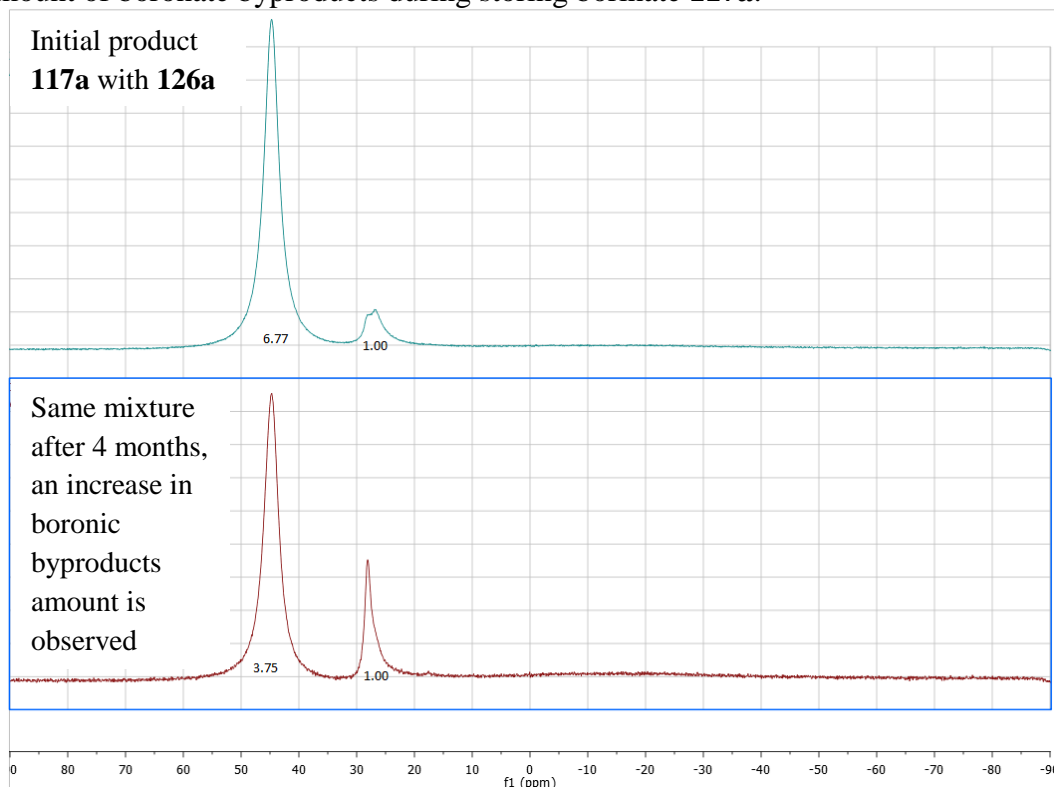
Figure 4 ^1H and ^{19}F NMR (400 and 376 MHz, CDCl_3) spectroscopic data, showing the formation of B-O-B species **128** from borinate **117b** during prolonged heating *in vacuo*:



Over prolonged time during storage at r.t. in a closed flask the boronate byproduct **126a** gradually formed a cotton-like net of curved crystals, presumably of cyclic boroxine **129a**, (Scheme 19) while the main product **117a** remained oily. This was seen in ^{11}B NMR spectra by reduction of boronate peak integral in liquid phase.

The mixture of borinate and crystals was dissolved in ⁱPrOH, and the solvent was then removed *in vacuo*. The ¹¹B NMR spectrum of obtained mixture showed, that over 4 months the total amount of boronate byproducts in the mixture has significantly increased (Figure 5). This can be explained by insertion of O₂ into B-C bond (Scheme 22), which is believed to happen with “ate”-complexes [Ar₂BROR']M **118** as well, and is described below.

Figure 5: ¹¹B NMR (128 MHz, CDCl₃) data, demonstrating the increase of amount of boronate byproducts during storing boronate **117a**:

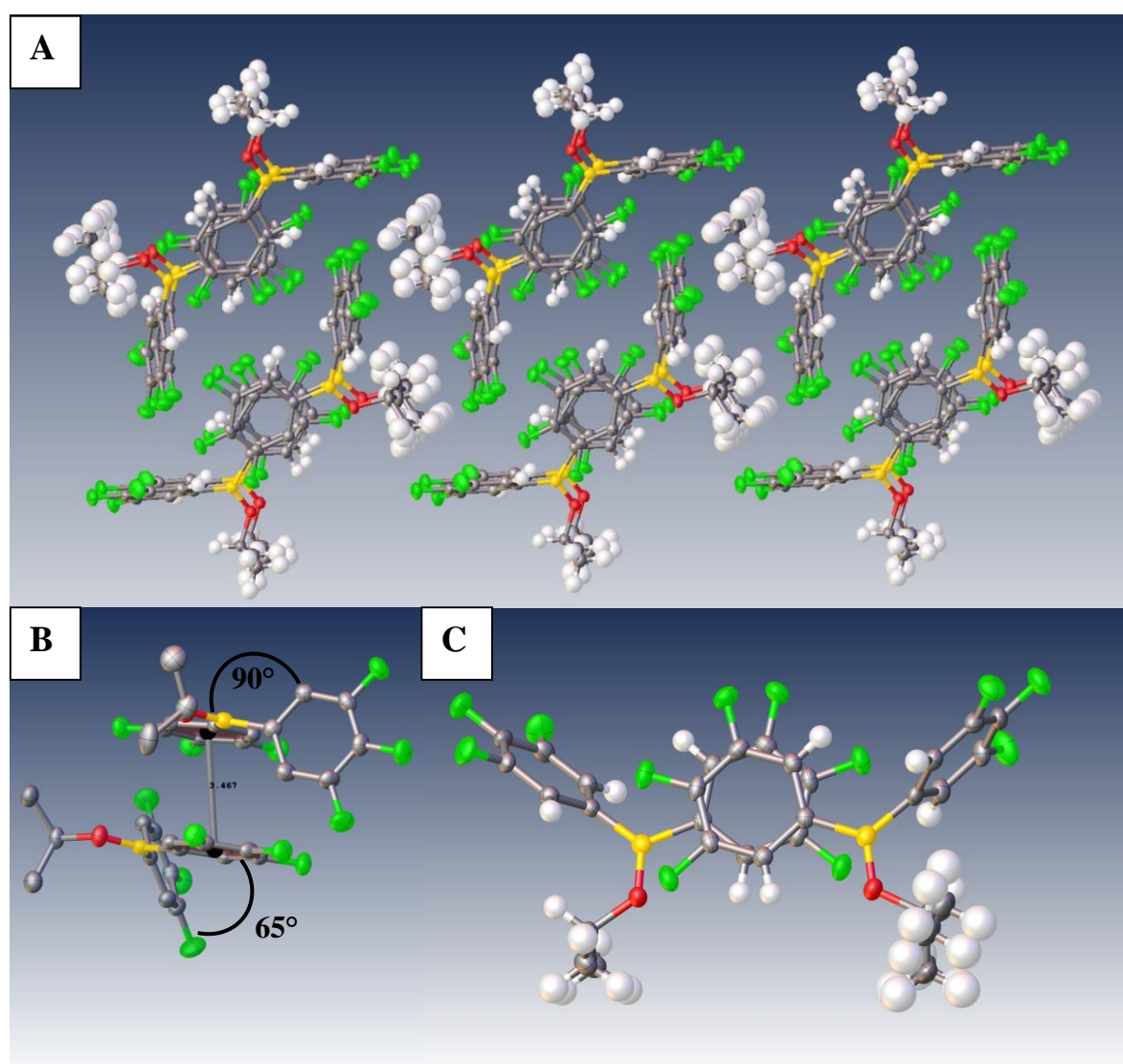


As well as in the case of **117a**, during prolonged storage of **117b** at r.t. a small amount of crystalline cyclic boroxine **129b** (Scheme 19, structure determined by X-Ray, see Supporting Information) was formed. Filtration left **117b** even cleaner; however, crystallisation took months and thus could not be used as the purification process of boronate product. The stability of boronate **117b** and its susceptibility to oxidation by air oxygen, as noticed for **117a**, remains yet unclear.

Although compound **117a** remained in an oily form over a prolonged period of time, the more polar boronate **117b** crystallised after a month of storage. The X-ray analysis of this compound showed that due to steric interactions only one phenyl substituent in the structure was in conjugation with boron, which is common for diaryl-substituted boron compounds. The aromatic rings of adjacent molecules were nearly coplanar (2.571°) and thus formed a long π -stacking structure with distance

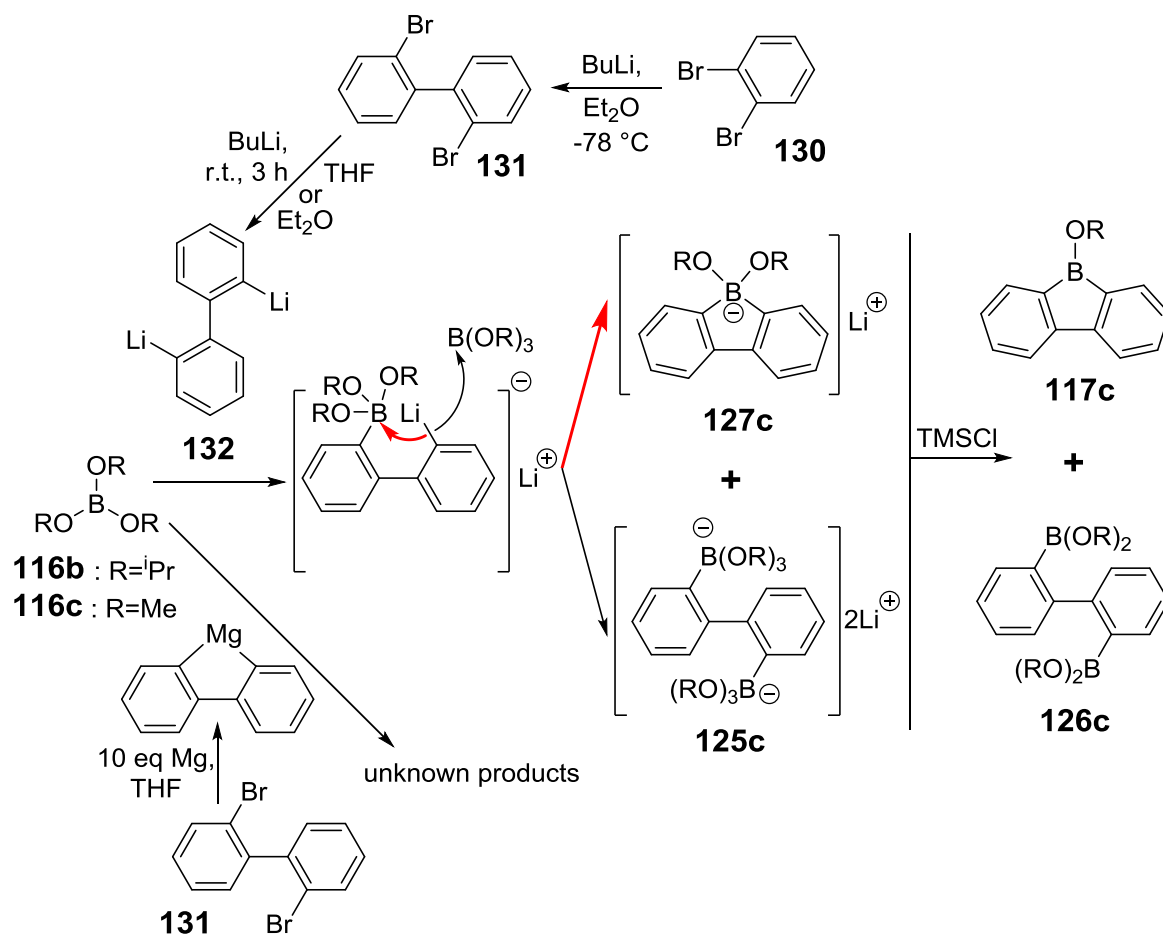
between centres of aromatic rings of 3.467 Å and minimal shift of 0.867 Å (Figure 6, A). The elementary cell contained 2 independent molecules, and the angles between aromatic rings in them were remarkably different. One was nearly perpendicular (89.4°) and another was 64.6° (Figure 6, B). At the same time the angles between non-coplanar rings and the axis of stacking were nearly the same with values of 73.53° and 105.38° (180.00°-105.38° = 74.62°), and when the molecule was aligned along this axis, this symmetry became obvious (Figure 6, C). Thus, it was the π - π stacking interactions that played the major role in molecule organisation.

Figure 6 Crystal structure of borinate **117b** A: generalised view; B: hydrogen atoms omitted for clarity, 90° angle between aromatic planes (top) and 65° angle between same planes (bottom); C: alignment *via* π - π stacking axis reveals symmetry



The initial approach to biphenyl borinate **117c** (Scheme 20) involved treatment of 2,2'-dibromobiphenyl **131**, obtained from 1,2-dibromobenzene **130**¹⁴⁰ (Scheme 20), with 10 equivalents of Mg, which yielded a brownish solution.

However, subsequent addition of $\text{B}(\text{O}^i\text{Pr})_3$ **116b** led to unknown products. When BuLi was used to generate organometallic species, a sediment of presumably **132** formed after stirring reaction mixture at r.t. for 3h in THF (no sediment in Et_2O was observed). Further addition of triisopropylborate **116b** resulted in immediate sediment dissolution and formation of a mixture of stable “ate”-complexes of presumably structures **125c** and **127c**. Quenching this mixture with TMSCl (2 equiv) led to 2:1 mixture of borinate **117c** and starting borate, with only a small amount of boronic species present. Quenching analogous mixture generated in Et_2O led to a 3:2 mixture of borinate and boronate, presumably of structure **126c** (Table 3, entries 1-2).



Scheme 20: Attempted synthesis of borinate **117c**

Attempts to use $\text{B}(\text{OMe})_3$ **116c** (Table 3, entry 3) resulted in major formation of the boronate. This showed, that $\text{B}(\text{OMe})_3$ was too reactive, and after the first attack of the carbanion, the second carbanion centre probably attacked faster a different molecule of $\text{B}(\text{OMe})_3$ (Scheme 20), yielding **125c**, rather than undergoing intramolecular cyclisation to **127c**.

Lowering the temperature of this reaction was thought to make the intramolecular cyclisation more favourable. $\text{B}(\text{OMe})_3$ was added to organometallic

132 at -78 °C in Et₂O. As expected, this resulted in increased formation of borinate (Table 3, entry 4, compared to entry 3), but purification of product was still an issue.

Table 3. Attempted syntheses of **117c**

Entry	B(OR) ₃	Solvent	T of borate addition	Borinate ^a 117c	Boronates ^a (126c)	Mixture of B(OR) ₃ species ^a
1	R= ⁱ Pr	THF	r.t.	60	10	30
2	R= ⁱ Pr	Et ₂ O	r.t.	60	40	-
3	R=Me	Et ₂ O	r.t.	17	63	20
4	R=Me	Et ₂ O	-78 °C	40	40	20
5 ^b	R= ⁱ Pr	Et ₂ O	r.t.	73	-	27

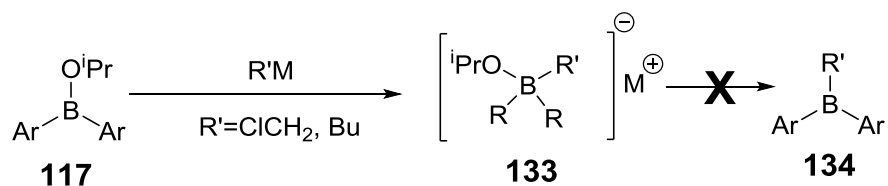
^aDetermined by ¹¹B NMR spectroscopy, ^bMgBr₂ solution added prior to borate

Finally, it was suggested that the nature of the cation could influence the process of complex collapse. Thus, **132** was reacted with MgBr₂ in Et₂O, and then borate **116b** was added to the mixture. This attempt gave the best result (Table 3, entry 5). However, borinate **117c** was not isolated in this study.

2.2.2.2. Borinate approach. Further steps

The next step of synthesis was to convert obtained borinates **117a-b** to borane **110** (Scheme 16). Addition of BuLi to a mixture of borinate **117b** and chloriodomethane at -78 °C led to formation of tetracoordinated boron species, as seen in the ¹¹B NMR spectrum, where the peak at 44 ppm disappeared, and a new peak in the range of 0-5 ppm was formed. This correlated with the previously reported¹³⁸ general mechanism of borane formation (Scheme 21); however, treating the complex with TMSCl did not lead to any detectable amount of borane. Instead, ¹¹B NMR spectroscopy suggested that the obtained product was mainly the starting borinate (or other borinic RR'BOR'' compounds) and some boronate species were also formed. Other attempts were made: borinate **117b** was added to preliminary prepared LiCH₂Cl; use of 2 equivalents of ^tBuLi was tried both with a borinate – ClCH₂I mixture and for the initial generation of LiCH₂Cl with subsequent addition of borinate; simple experiments of reacting borinate with BuLi were conducted as well. In all of cases “ate”-complexes were formed, but TMSCl treatment led either to borinates or to mixtures of borinates with boronates. The same reactions were also carried out with borinate **117a**, the complexes initially formed were quenched without

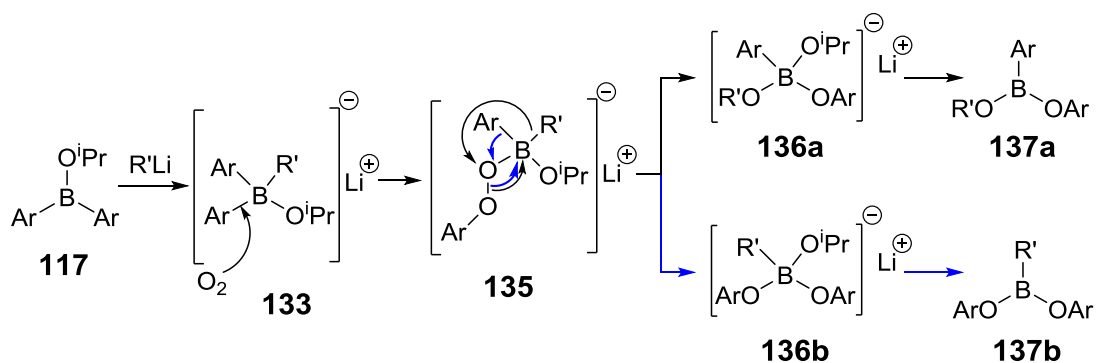
TMSCl addition over time to yield similar mixtures. In some cases, boronates were major species, forming nearly 70% of reaction mixture.



Scheme 21 Supposed mechanism of borane formation from borinates **117a-b**, however in our examples complex does not collapse to form boranes **134**

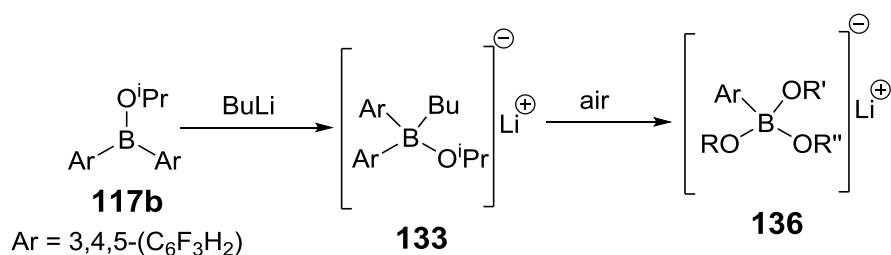
Initially, it was suggested that the isopropoxy substituent was not a good enough leaving group, which could influence this reaction, thus the borinate **117b** was dissolved in MeOH, the solvent was removed (this process was repeated 3 times) and the methoxy analogue of **117b** was formed. However, reacting the latter with LiCH₂Cl and subsequent quenching by TMSCl also did not lead to any borane being formed.

The unexpected formation of boronates in this reaction was investigated further. It was suggested, that complexes **133** may be very sensitive to O₂, and the mechanism of its insertion into B-Ar bond with subsequent generation of boronates **137** was proposed (Scheme 22).



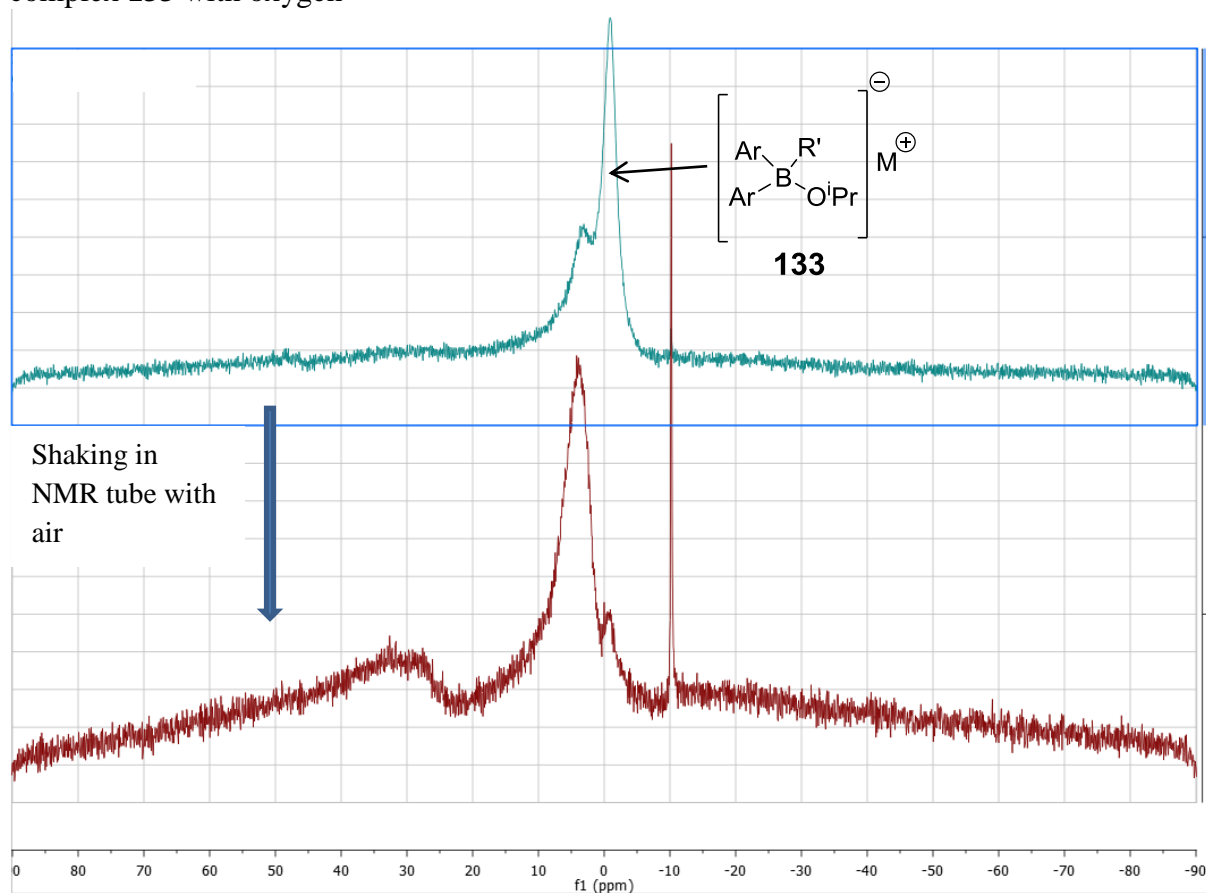
Scheme 22 Suggested mechanism of boronate formation instead of generation of borane Ar₂BR'

The sensitivity of complex **133** towards oxygen was checked experimentally. The species [3,4,5-(C₆F₃H₂)₂B(OⁱPr)Bu]Li was generated by addition of BuLi to borinate **117b**, (Scheme 23) and after running the ¹¹B NMR spectroscopic experiment, air was introduced and NMR tube inverted 3 times, which led to a shift of major product signal in ¹¹B NMR spectrum (Figure 7), which can be explained by generation of new type of complex **135** or **136** with signal in a higher field, compared to initial complex **133**.



Scheme 23 Conversion of initially generated complex **133** to a complex **136** with lower-field ^{11}B NMR shift

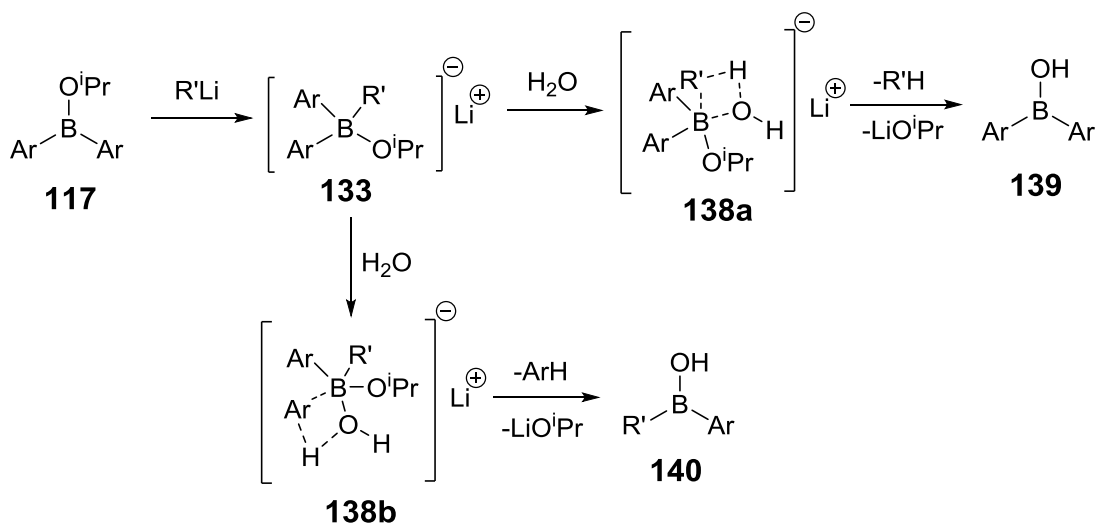
Figure 7 ^{11}B NMR (128 MHz, CDCl_3) spectra of the reaction of “ate”-complex **133** with oxygen



The formation of boronates and borinates can be explained by protodeboronation of complex **133** with water present in the solvent (Scheme 24).

Nevertheless, even most careful conduction of complex generation in dry degassed solvents with subsequent TMSCl quenching did not lead to boranes. In some experiments formation of almost exclusively borinates was observed. Other means of promoting complex collapse were also tried: addition of $\text{HCl}/\text{Et}_2\text{O}$ (prepared from AcCl and MeOH in Et_2O), ZnCl_2 or AlCl_3 all gave similar results. Finally, it was decided to try to promote complex collapse by heat. Surprisingly, either heating at reflux in THF or even in toluene for 3 hours did not lead to any change in ^{11}B NMR

spectroscopic data. Thus, the remarkable thermal stability of these complexes was observed.



Scheme 24 Suggested mechanism of protodeboronation of $[\text{R}_2\text{BR}'\text{O}^i\text{Pr}]\text{Li}$ complex

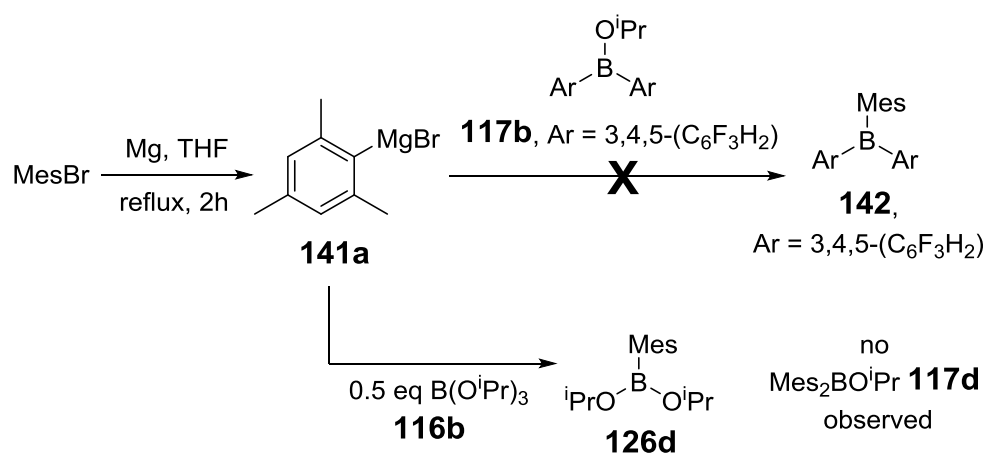
It was then assumed that the nature of the cation could influence the process of complex collapse, thus an exchange reaction between LiCH_2Cl and MgBr_2 was tried. However, insolubility of MgBr_2 in Et_2O at low temperatures and supposed instability of ClCH_2Li species at 0°C or r.t. led to complications. Adding $\text{MgBr}_2/\text{Et}_2\text{O}$ solution to a mixture of BuLi and ClCH_2I at -78°C led to formation of crystalline MgBr_2 , and no borane products were observed after borinate addition.

A reaction of borinate **117b** with PhMgBr was also conducted. An immediate formation of sediment upon addition of Grignard reagent in Et_2O at r.t. was noticed. However, the complex formed did not collapse with addition of 1 equivalent of TMSCl . DMSO solution of the mixture provided a small amount of crystals, but X-Ray showed that it was a Mg^{2+} complex with 2 DMSO and 2 water molecules with 1/4 Br, 7/4 Cl as counterions (see Supporting Information).

A literature search on introducing a third alkyl or aryl substituent to the borinates revealed that this is possible in three main situations: 1) the mesityl substituent can be introduced to 9-boraanthracene-based borinates.¹⁴¹ Introduction of phenyl substituent in similar systems is possible,¹⁴² but product slowly decomposes in solution, and alkyl derivatives could not be obtained due to supposed oxidation. 2) Introduction of aryl group is possible with dimesityl borinates¹⁴³ or other significantly hindered borinates.¹⁴⁴ 3) Borane synthesis from borinates proceeds successfully if there is an additional source of intramolecular stabilisation, such as an O^{145} or N^{146} atom, thus yielding borane “ate”-complexes. These examples underline that extra care

should be taken to avoid possible oxidation, and additional stabilisation or hindrance can help counter this process.

Thus, borinate **117b** was reacted with MesMgBr (Scheme 25) in order to check whether borane formation would be possible in this case. However, the reaction mixture contained only multiple borinic products. This suggested that this system still lacked steric hindrance, most likely due to absence of ortho-substituents on aryl rings in borinate **117b**. In an attempt to generate dimesityl borinate **117d**, MesMgBr was also reacted with 0.5 equivalents of triisopropylborate **116b**, (Scheme 25), however, this reaction, as seen by ^{11}B NMR spectroscopy, resulted only in boronic product formation, supposedly of structure **126d**.

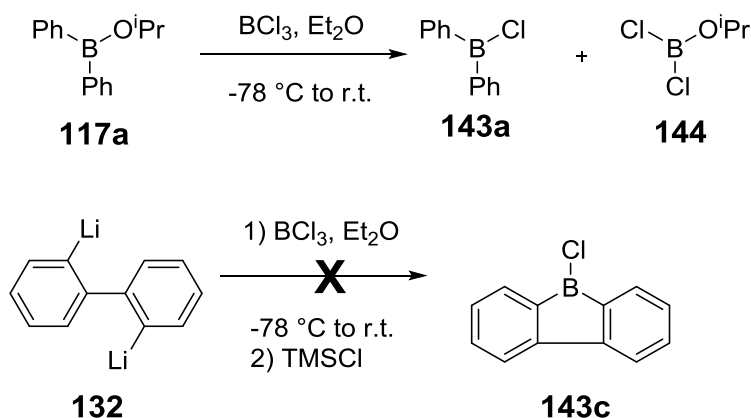


Scheme 25 Attempted reaction of MesMgBr with borinate **117b** and attempted synthesis of borinate **117d**

2.2.2.3. Boron halides approach

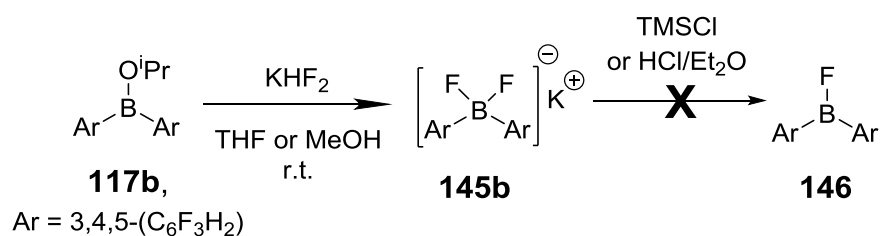
As the borinate approach to boranes had provided many difficulties, attempts were made to synthesize R_2BCl **143** as a different intermediate in $\text{R}_2\text{BR}^{\ominus}$ **110** borane synthesis. It was found that according to the literature,¹⁴⁷ the most generic way of accessing this compound was *via* Me_2SnCl_2 , which is highly toxic. Also known¹⁴⁸ is the comproportionation reaction between borinate **117a** and BCl_3 , which was probed (Scheme 26). According to ^{11}B NMR (δ 63 ppm), the desired R_2BCl **143a** was formed in approximately 60% yield, but its purification proved to be complicated and was not achieved.

As mentioned before, biphenyl borinate **117c** was not isolated, and as it was already shown, borinates **117** could not be converted to boranes **110**. Thus an attempt was made to generate chloride **143c** (Scheme 26). However, direct reaction of dilithium reagent **132** with BCl_3 at -78 °C afforded a complex mixture, which did not produce any R_2BCl products after quenching it with TMSCl (1.5 equiv).



Scheme 26 Approaches to chlorides **143**

The idea of using borinic halides was investigated further, and an approach to R_2BF **146** was probed (Scheme 27).



Scheme 27 Synthesis of $[\text{R}_2\text{BF}_2]\text{K}$ **145b** and an attempt to generate Ar_2BF

Borinate **117b** was reacted with an aqueous solution of 1 equivalent of KHF_2 in MeOH or THF. Unexpectedly, sedimentation of $[\text{R}_2\text{BF}_2]\text{K}$ complex, which was believed to be formed in this reaction, was not observed even when a very small amount of solvent was used. The expected B-F coupling was not seen in either ^{11}B or ^{19}F NMR spectra of the product registered in D_2O . Instead, the boron signal of the product was a broad singlet at δ 6.9 ppm. As the B-F coupling is a known sign of the B-F bond,^{149a} these results initially suggested that D_2O was not a suitable solvent for the product **145b** as hydrolysis of B-F bonds had probably occurred^{149b}. However, the NMR spectra of the product in DMSO-d_6 showed no change. It was then assumed, that using water as solvent for KHF_2 should be avoided, thus, addition of reagent as a solution in MeOH, or as solid was tried. However, the ^{11}B NMR (DMSO-d_6) spectra obtained showed a major broad singlet only, and the signal of the two B-F fluorines in the ^{19}F NMR spectrum was a broad singlet as well (Figure 8). To investigate the nature of product further, the NMR spectra of the product in THF-d_8 were obtained. The fluorine broad signal changed to two uneven broad singlets, and the ^{11}B NMR signal showed a hint of expected triplet character (Figure 8). The lack of coupling can be explained by exchange of fluorine atoms in the rather polar solvents used for

NMR. The structure of $[3,4,5-(\text{C}_6\text{F}_3\text{H}_2)_2\text{BF}_2]\text{K}$ **145b** was unambiguously identified by crystallography (Figure 9). The boron atom was tetrahedral, and potassium was coordinated to 8 fluorine atoms, 4 of which were aromatic fluorines.

Figure 8 ^{11}B and ^{19}F NMR spectra of $[(\text{C}_6\text{F}_3\text{H}_2)_2\text{BF}_2]\text{K}$ **145b**:

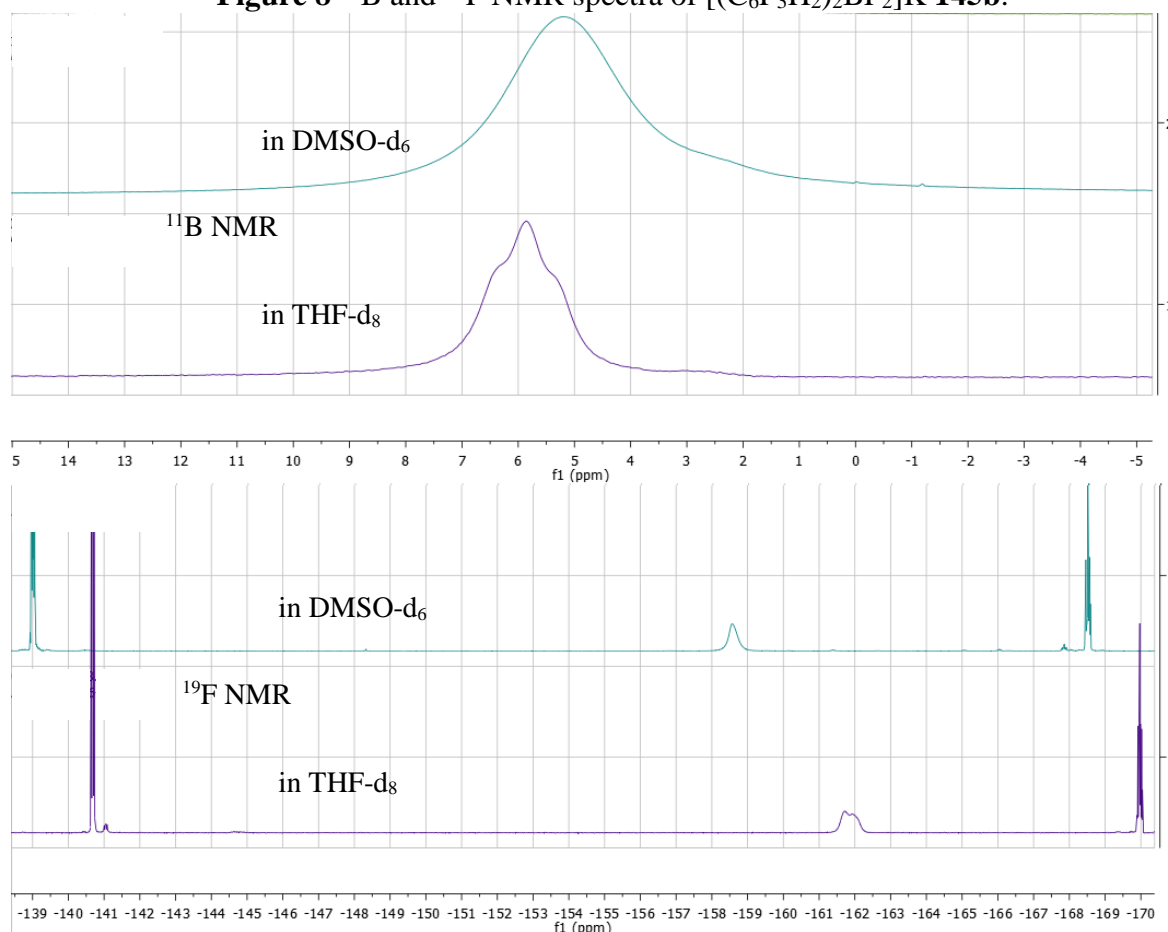
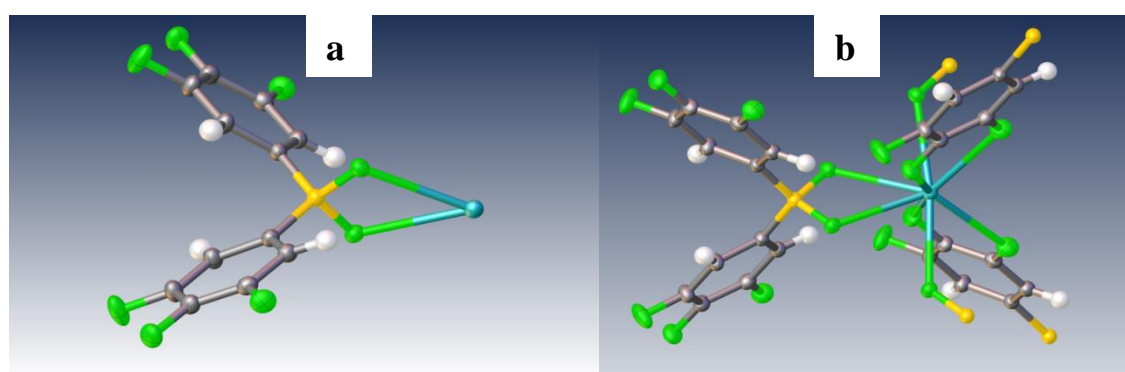


Figure 9 Crystal structure of **145b** (a) and potassium coordination polyhedron (b)



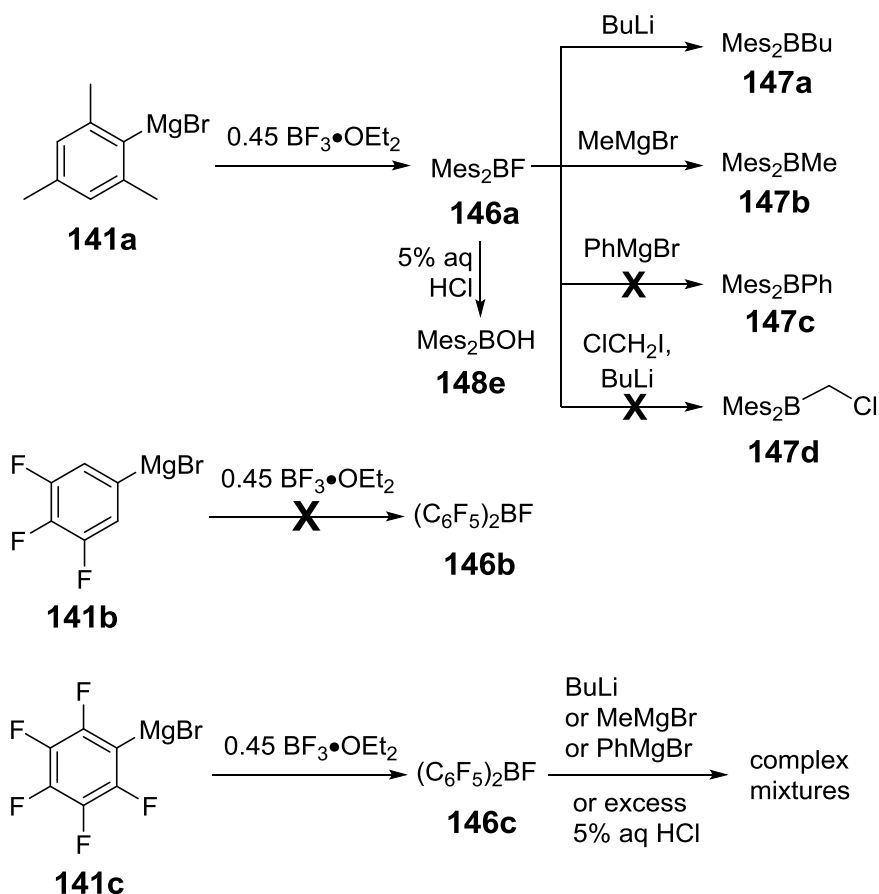
The complex obtained was expected to collapse to $(\text{C}_6\text{F}_3\text{H}_2)_2\text{BF}$ upon addition of TMSCl , but addition of 10 equivalents of TMSCl to the THF-d_8 solution of **145b** in the NMR tube showed that the complex was slowly converted to a complex of a different structure, but the boron atom remained in a tetrahedral configuration and collapse did not occur. However, reacting **145b** with 2 equivalents of TMSCl in

MeCN led to immediate sediment formation and total collapse of the complex to 6:1 borinate : boronate mixture. Similarly, using 2 equivalents of HCl/Et₂O led to immediate total collapse of **145b**, according to ¹¹B NMR spectroscopy, and mixtures of borinates (~60-80%) and boronates (~20-40%) were again obtained, as seen by appearance of signal at ~28 ppm in ¹¹B NMR spectrum and disappearance of broad B-F signal in ¹⁹F NMR spectrum. These results showed again the extreme sensitivity of boron complexes to water and/or oxygen. The reaction pathway with TMSCl is not yet fully understood, as the complex **145b** itself is stable in presence of water, which was used in the reaction solvent system. It is worth mentioning, that ¹¹B NMR spectroscopy signals of R₂BF and R₂BOR' compounds experience rather close shifts with differences rarely exceeding 3 ppm, thus this tool cannot be used to state the absence of R₂BF species. However, the ¹⁹F NMR spectra in all of the above cases showed multiple products and the B-F coupling could not be identified in the mixtures. Finally, Ph₂BOiPr **117a** was also reacted with KHF₂ to yield similar complex **145a**, as seen by ¹¹B and ¹⁹F NMR data, but the product was less pure and was not isolated.

A different approach was also tried with generating borinic fluorides Ar₂BF **146a-c** from BF₃-OEt₂ complex (Scheme 28).

Excess MesMgBr reacted cleanly with BF₃•OEt₂ complex in THF to yield Mes₂BF.¹⁵⁰ However, it should be noted that the temperature of BF₃-OEt₂ addition was of significant importance. Thus, if the reaction was not cooled to 0 °C, a side process of Lewis acid catalysed ring-opening of the solvent THF occurred, and it was difficult to isolate products later. ¹H, ¹¹B and ¹⁹F NMR spectroscopic data of Mes₂BF were identical to that reported in the literature, thus **146a** was used without isolation or further purification.

Both reactions with BuLi/hexanes and MeMgBr/Et₂O yielded boranes of supposed structures Mes₂BBu **147a** and Mes₂BMe **147b**, respectively, in ~30% yield (determined by ¹¹B NMR). In these cases, stable “ate”-complexes were not formed, so collapse with TMSCl was not necessary. However, separation of the product boranes **147** was complicated. Observing these products was an important proof that boranes can indeed be obtained by these reactions, however, we had no synthetic interest in boranes **147a-c** on their own, thus they were not isolated. A solution of Mes₂BF in THF did not react with 1 equivalent of PhMgBr/Et₂O at r.t.



Scheme 28 Synthesis of borinic fluorides **146a-c** and attempts to convert them to boranes **147**

In order to increase the yield of boranes and reduce the amount of boronates formed due to oxidation in these reactions, the Mes_2BF solution in THF was evacuated, redissolved in degassed hexane and reacted with $\text{MeLi}/\text{Et}_2\text{O}$, $\text{BuLi}/\text{hexanes}$ at r.t. and with $\text{ClCH}_2\text{I} + \text{BuLi}/\text{hexanes}$ at -78°C . Reaction with MeLi gave borane **147b** in ~25% yield, and the absence of yield increase can probably be explained by O_2 presence in commercial metalorganic reagent solution. However, reaction with $\text{BuLi}/\text{hexanes}$ led to generation of borane in a higher ~50% yield, though some oxidation to boronates was still observed. Unfortunately, addition of BuLi to a solution of ClCH_2I and Mes_2BF at -78°C did not yield borane **147d**.

Mes_2BF **146a** was also successfully hydrolysed with 5% aq HCl to yield borinic acid **148e**. This borinic acid was stable to air over months and was used in part II of the project.

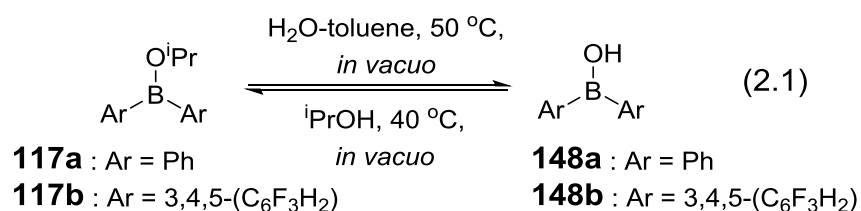
The same Ar_2BF approach was used for $3,4,5\text{-C}_6\text{F}_3\text{H}_2\text{MgBr}$ **141b** and $\text{C}_6\text{F}_5\text{MgBr}$ **141c** in reaction with $\text{BF}_3 \cdot \text{OEt}_2$ (Scheme 28). Interestingly, $(\text{C}_6\text{F}_3\text{H}_2)_2\text{BF}$ **146b** was not generated under these conditions, which supposedly highlights the

importance of *ortho*-substituent on the phenyl ring for boron hindrance and stability of the derivatives. $(\text{C}_6\text{F}_5)_2\text{BF}$ was generated, as seen by ^{11}B NMR spectroscopy, and was reacted with BuLi, MeMgBr and PhMgBr in THF. The reactions were carried out at r.t. and gave rise to several products, including results of oxidation, different complexes and borinic derivatives. However, formation of boranes was noticed only in 1-2% yield. Attempts to collapse complexes with TMSCl did not lead to improved amounts of boranes, and some of the complexes remained stable even in the presence of excess TMSCl. This data underlines that electron-withdrawing substituents at boron make its complexes more stable. Even hydrolysis of $(\text{C}_6\text{F}_5)_2\text{BF}$ with excess aq. HCl yielded a mixture of products.

2.2.2.4. Other approaches

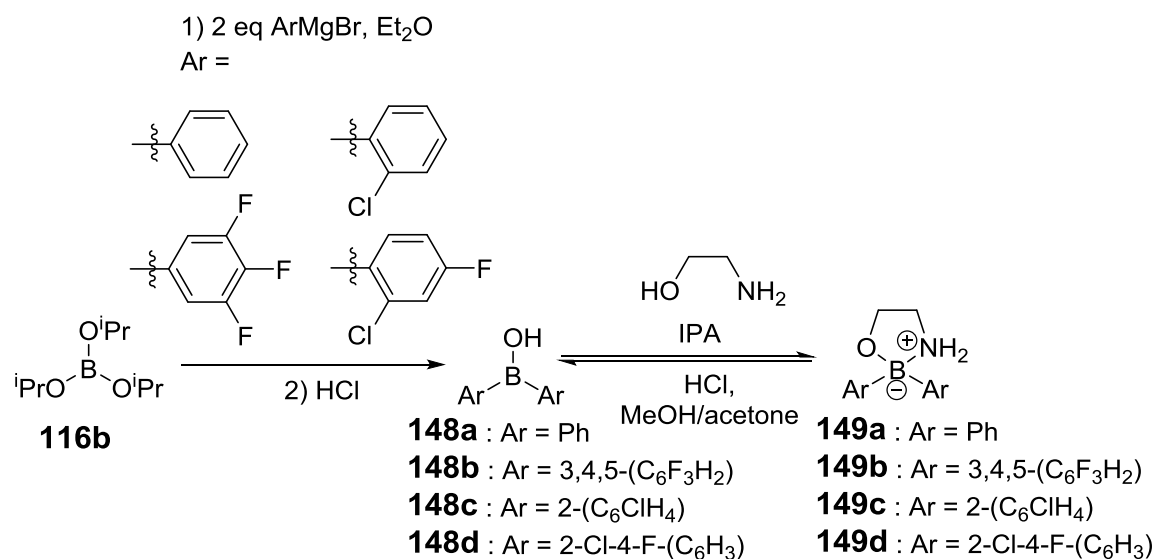
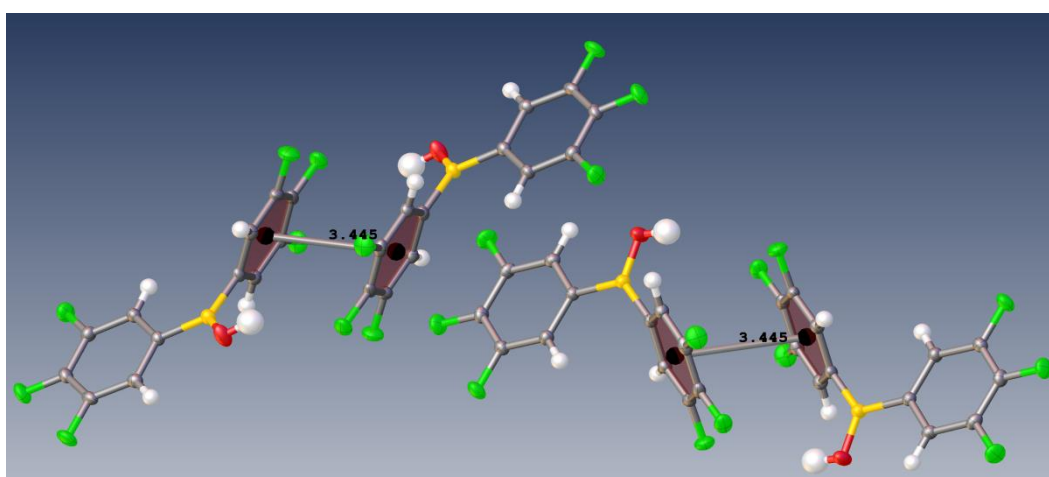
Because the borinic halides approach to boranes also revealed significant complications, other paths were investigated. It was decided to convert the isopropoxyl substituent in the borinate compounds into better leaving groups, as it should have had a significant impact on the collapse of $[\text{Ar}_2\text{BROR}']\text{M}$ **133** complexes.

To access OTs derivative **149b**, it was decided to first convert borinate **117b** into the corresponding borinic acid **148b** (eqn. 2.1). This was achieved by dissolving the borinate in toluene, adding water and removing all volatiles *in vacuo* at 50 °C over 1h. It should be mentioned, that the reverse transformation can be easily achieved by repeating a cycle of dissolving acid **148b** in $i\text{PrOH}$ and removing solvent *in vacuo* at 40 °C several times. This approach was used to purify borinates **117a-b**. It was found that after hydrolysis only borinic acids **148a-b** were soluble in hot petroleum ether, whereas all boronic $\text{ArB}(\text{OR})_2$ **126** derivatives could be filtered off. After hot filtration, pure borinic acid **148b** crystallised in solution and was characterised by X-ray (Figure 10). The π - π interactions were only observed between adjacent molecules, but did not form long stacking chains (Figure 10). The aromatic rings within one molecule formed 59.6° angle.



Both the borinates and borinic acids prepared were not stable (with exception of dimesityl borinic acid **148e**) at r.t. over months of storage, and the best solution was to keep these compounds in bench-stable ethanolamine complex form. After HCl workup of Grignard reactions and pet ether recrystallization, ethanolamine in IPA was added to reaction mixtures and product complexes **149a-d** were crystallised (Scheme 29), at this stage two new aromatic groups, the 2-chlorophenyl and 2-chloro-4-fluorophenyl, were also used. **149b-d** were analysed by X-ray. Borinic acids **148c-d** were only used in direct amide formation research, see below. HCl hydrolysis of products **148** in methanol/acetone yielded pure borinic acids **148a-d** on demand.

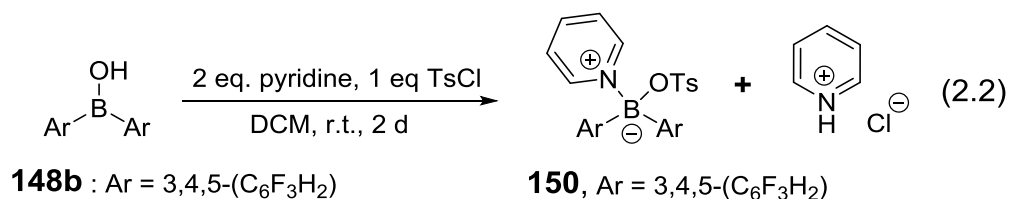
Figure 10 Crystal structure of borinic acid **148b**.



Scheme 29 Synthesis of ethanolamine complexes **149** and their reverse hydrolysis to borinic acids **148**

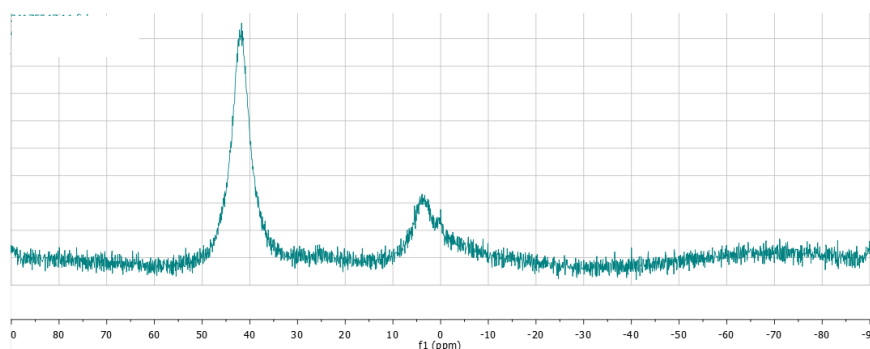
Borinic acid **148b** was reacted with pyridine and tosyl chloride (eqn. 2.2.), the results suggested that pyridine immediately coordinated to boron to form a complex,

and TsCl reacted with the OH group in the presence of 1 more equivalent of pyridine over 2 days to yield **150**. The product of this reaction was not isolated, as removing pyridine from such complex would have been another complication in this path.



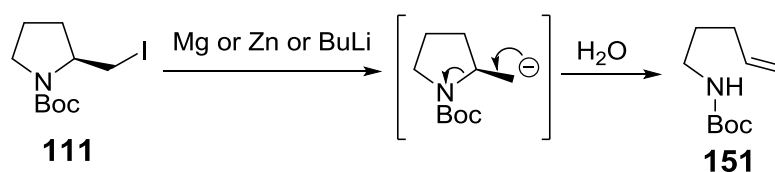
In an attempt to prevent Lewis adduct formation, 1 equivalent of a more hindered base, 2,6-lutidine was used in reaction between borinic acid **148b** and MsCl. This resulted in an equilibrium formation between the “ate”-complex species and free borinic species (Figure 11), indicating FLP formation. It is unclear whether the MsCl reacted under these conditions with the OH group.

Figure 11 ^{11}B NMR spectrum of borinic acid **148b**, 2,6-lutidine and MsCl mixture, showing equilibrium between free borinic species and “ate”-complex



2.2.3. Paths B-C and hydroboration attempt

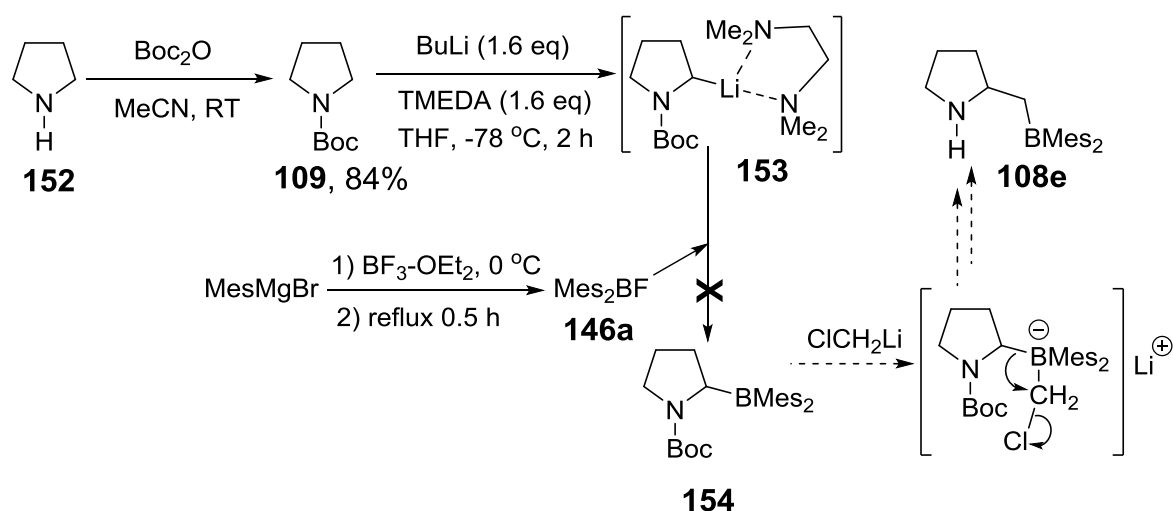
Path B (Scheme 15) was not attempted, as it was known from previous research in our group, that iodide **111** cannot be used for this transformation, as any attempt to generate negative charge on α -carbon results in alkene **151** formation (Scheme 30).



Scheme 30 Elimination reaction, occurring with iodide **111**

Path C was used in an attempt to generate **108e**, a compound with similar B-N arrangement as initial targets **108a-d** (Scheme 31). Synthesis of *N*-Boc pyrrolidine **109** was achieved simply by reacting pyrrolidine **152** with di-*tert*-butyl dicarbonate.^{151a} Subsequent water washing and evaporation of the volatiles yielded

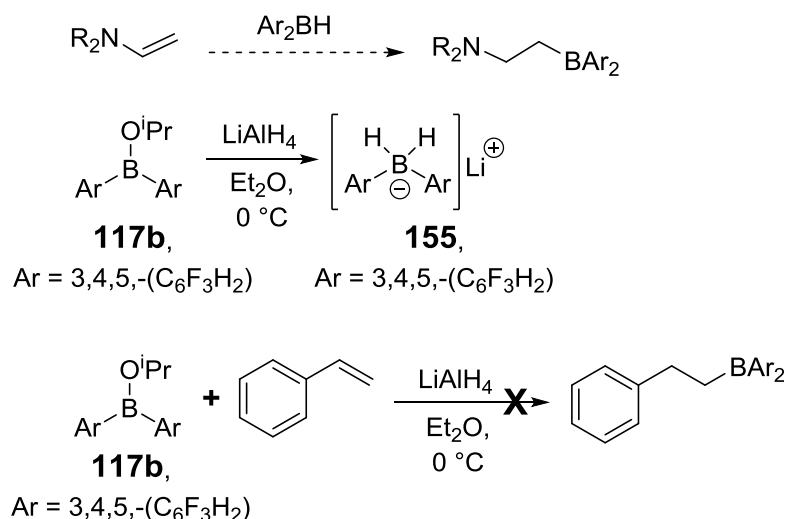
pure **109** in 84% yield. It was known that Mes₂BF **146a** reacts with BuLi to give the corresponding borane. Thus, it was suggested that alpha-lithiation of *N*-Boc pyrrolidine **11** (reaction, investigated by Beak^{151b} and O'Brien^{151c}) with subsequent addition of Mes₂BF should lead to bifunctional system **154**, which can then rearrange with addition of ClCH₂Li to give a structure of type **108**. However, the only species isolated from this reaction was the dimesitylborinic acid. It is supposed that the reagent **146a** is too hindered to react with TMEDA complex **153**. Apart from these issues, it was unclear whether subsequent rearrangement to **108e** would be successful, and whether it would be possible to maintain chirality if **154** was synthesised in an enantioselective reaction with sparteine. Thus path C was not pursued further.



Scheme 31 Path C: attempt to generate bifunctional B-N compound **154** with possible subsequent rearrangement with ClCH₂Li to **108e**

Finally, one more approach was attempted; the reaction between Ar₂BH and an alkene could also yield boranes, and if done with enamines, the desired 1,4-B-N arrangement would be achieved. [Ar₂BH₂]⁻Li⁺ **155** was synthesised through reacting borinate **117b** with 1 equivalent of LiAlH₄ (Scheme 32).

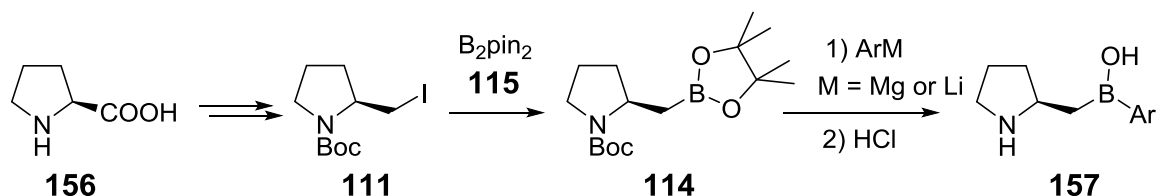
The hydride complex **155** was obtained, as evidenced by the appearance of a triplet in ¹¹B NMR spectrum at -14 ppm, but purification of this complex was not achieved, and using crude product for Ar₂BH generation was unsuccessful. It is also known that such Ar₂BH reagents can be generated *in situ* for hydroboration of alkenes,¹⁵² however, addition of LiAlH₄ to the mixture of borinate **117b** and styrene did not yield any borane (Scheme 32).



Scheme 32 Hydroboration approach

2.2.4. Path D. Borylation with B₂pin₂

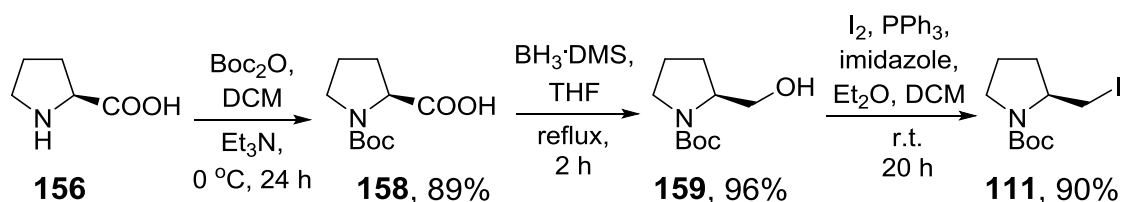
The last path proposed to the bifunctional catalysts **108** (Scheme 15) was to first obtain the intermediate **114**, by borylating iodide **111** with B₂pin₂ **115**, and then introduce the aryl groups to boron. However, with knowledge of borinate behaviour with organometallic compounds, and of the inability to form boranes discussed above, it was unlikely that **114** could be directly converted to **108**. Nevertheless, at this step we developed an interest to form bifunctional borinic compounds **157**, and tried to access them through functionalisation of **114** (Scheme 33).



Scheme 33 Suggested path to alternative borinic bifunctional catalysts **157**

2.2.4.1. Homoboroproline **114** synthesis

Synthesis of iodide **111** (Scheme 34) was based on the previously reported process.¹⁵³ Proline **156** is used as a cheap chiral starting material. Its Boc-protection was simplified and improved: instead of citric acid, 5% HCl was used for workup, and no further washing was needed. Separation, evaporation and recrystallization yielded the product **158** in 89% yield, an increase from 70%. The following reduction to prolinol **159** proceeded smoothly, and it was found that after the workup recrystallization of product was not actually required, evaporation delivered pure white solid **159** in 96% yield, an increase from 80%.

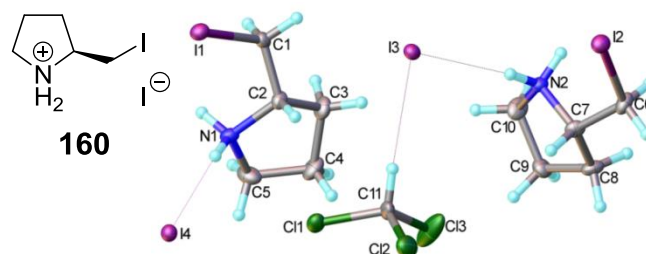


Scheme 34 Synthetic route to iodide **111**

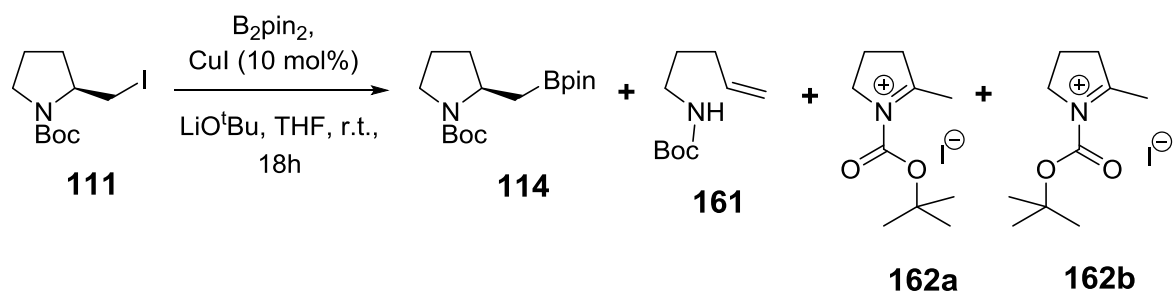
The subsequent iodination was a more sensitive process. The initial attempts to reproduce this reaction only yielded iodide **111** in 40-45% yield. The heterogeneous nature of the reaction and the sticky solid intermediates suggested that stirring problems could hinder the process. Indeed, an improved yield (61%) was achieved by using a mechanical, rather than a magnetic stirrer. Two more alterations allowed further improvements to the yield. First, following the same idea of increasing surface area between reactants, iodine pellets were ground prior to use. Second, application of alternative workup with loading whole crude reaction mixture onto silica and subsequent column chromatography yielded 90% of iodide **111**. The product contained a minor amount of Ph_3P , as seen by ^1H NMR, thus an attempt was made to reduce the loading of both I_2 and Ph_3P to 1 equivalent, however, this led to a reduction in the isolated yield to 45%. Instead of reducing loading of reactants, the Ph_3P impurity in the product was removed with MeI treatment, followed by filtration. It was also shown, that presence of Ph_3P impurity did not have any impact on the yield of subsequent borylation.

During one of iodinations, a small amount of crystals (< 5%) were formed in crude product. They were analysed by X-ray (Figure 12) and the structure suggested that HI could be generated in small amount in this reaction, leading to N -Boc bond cleavage and ammonium salt **160** formation.

Figure 12 X-ray structure of byproduct **160**, isolated from iodination reaction from **159** to **111**



The borylation reaction of **111** to **114** was the most complicated step of this synthesis (Scheme 35, Tables 4-5).



Scheme 35 Synthesis of homoboroproline intermediate **114**

Entry	Borylating reagent	Base	Catalyst	Ligand	Yield of product (¹¹ B NMR)	Yield of product (isolated)
1	B ₂ pin ₂	^t BuOLi, 2 eq	CuI	-	65	34
2	B ₂ pin ₂	^t BuOLi (sublimed), 2 eq	CuI	-	75	20
3	B ₂ pin ₂	^t BuOLi/THF sol-n, 2 eq	CuI	-	80	39
4	B ₂ pin ₂	^t BuOK, 2 eq	CuI	-	0	-
5	B ₂ pin ₂	^t BuOK, 1 eq	CuCl	xanthphos	15	-
6	B ₂ pin ₂	K ₃ PO ₄	Pd ₂ (dba) ₃	^t Bu ₂ MeP•BF ₄	75	-
7	B ₂ Neop ₂	^t BuOLi, 2 eq	CuI	-	25	-
8	B ₂ (OH) ₄	^t BuOLi, 2 eq	CuI	-	0	-
9	B ₂ pin ₂	^t BuOLi, 1 eq	CuI	-	35	-
10	B ₂ pin ₂	^t BuOLi, 1 eq, slow addition	CuI	-	-	43
11	B ₂ pin ₂	^t BuOLi, 2 eq, slow addition	CuI	-	-	42

Table 4 Summary of reaction conditions optimisation for borylation of **111** to **114**

Performing this process under the original reaction conditions with 2 equivalents of ^tBuOLi, 1 equivalent of B₂pin₂, 10 mol.% of CuI in THF yielded only 34% of the homoboroproline **114** after column chromatography (Table 4, Entry 1), and it was not possible to scale the reaction above 0.5 g. The use of freshly sublimed ^tBuOLi increased the yield (Table 4, Entry 2), as determined by ¹¹B NMR, but after column chromatography the product was isolated in only 20% yield.

These initial findings suggested, that apart from actual reaction conditions, the workup could have a significant impact on the yield of the reaction. It was found that if NaOH workup was used instead of HCl, all boron-containing impurities could be removed, however, purification of the product from other byproducts was still needed

and does not lead to improved yield (Table 5, entry 4). Using flash chromatography instead of aqueous workup led to similar result (Table 5, entry 6). Overall, it can be concluded that decomposition of starting material or side reactions occur during reaction step and not during workup and isolation.

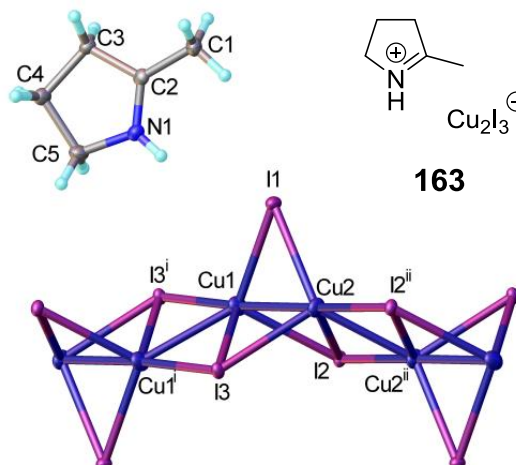
The best result was achieved when using commercial ^tBuOLi solution in THF (Table 4, entry 3). Further attempts to improve this reaction included usage of 1 M solution of ^tBuOK in THF instead of ^tBuOLi (Table 4, Entry 4), which led to an unidentified product and no **114** was generated. Over time a very small amount (<3%) of crystals was formed in crude mixture, and X-ray allowed to identify the structure of this compound (Figure 13). Using only 1 equivalent of ^tBuOK with xanthphos¹⁵⁴ yielded only 15% product as seen in ¹¹B NMR (Table 4, entry 5). A different set of conditions¹⁵⁵ (Table 4, Entry 6), gave promising result, but isolation was not attempted. Use of B₂Neop₂ instead of B₂pin₂ (Table 4, Entry 7) yielded a small amount of homoboroproline, but the main isolated product (35%) was the ring-opened **161**. Borylation of iodide **111** was attempted with B₂(OH)₄ (Table 4, entry 8), however this did not yield any product.

Table 5 Optimising workup conditions for borylation of **111** to **114**

Entry	Loading of iodide 111 (mg)	Workup	Mass after workup (mg)	Isolated yield of 114 after column chromatography
1	500	HCl	610	30%
2	500	HCl	816	32%
3	500	HCl	580	28%
4	400	NaOH	236	23%
5	500	HCl, then NaOH	189	–
6	500	Flash column	600	31%

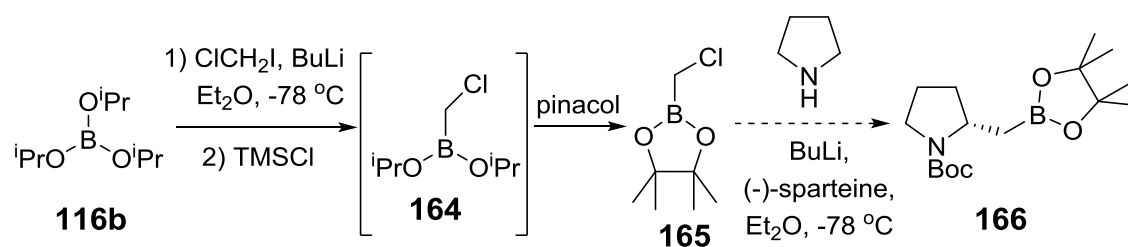
The two byproducts **162a-b** that were isolated in some cases by column chromatography were not fully identified. Simplicity of ¹H NMR spectra of both byproducts suggested an absence of diastereotopic protons as well as an absence of hydrogen bonded to tertiary carbon. ¹¹B NMR showed an absence of boron in both structures. Mass spectra of both isolated byproducts looked very similar, identifying the presence of iodide anion and confirming elemental composition of iminium ion. Finally, the existence of structure **163** suggested that iodide **111** was probably susceptible to elimination. This data led to rationalization of structures of byproducts **162a-b** as shown in Scheme 35.

Figure 13 X-Ray structure of byproduct **163** (Table 4, entry 5)



It was decided to attempt to reduce the amount of base used (Table 5, entry 9) in order to prevent possible deprotonation at the tertiary carbon chiral centre. This, however, yielded a lower amount of product, as seen by ^{11}B NMR. It was then assumed that substrate is exposed to excess of base immediately, whereas B_2pin_2 activation and subsequent borylation occur much slower. Thus, reaction was tried with slow addition *via* a syringe pump of 1 and 2 equivalents of LiO^tBu to the reaction mixture over 6 h (Table 5, entries 10-11). The yield of **114** increased to 42-43%, but surprisingly there was almost no difference between these 2 cases. The amount of isolated byproducts **162a-b** was significantly reduced. The mechanism of this reaction, as well as that of the byproduct formation, remains yet unclear.

It should also be mentioned, that initially it was desired to have access to a different enantiomer of **114**, namely **166**. It was suggested (1,2-shift of the organyl group and substitution of the α -halide pioneered by Matteson¹⁵⁶), this could be achieved using a chiral *ortho*-lithiation of pyrrolidine (Scheme 36). For this purpose compound **165** was synthesized from $\text{B}(\text{O}^i\text{Pr})_3$ and LiCH_2Cl with subsequent addition of TMSCl and pinacol. It is worth mentioning, that **165** was formed even if TMSCl was added only after addition of pinacol to the reaction mixture.

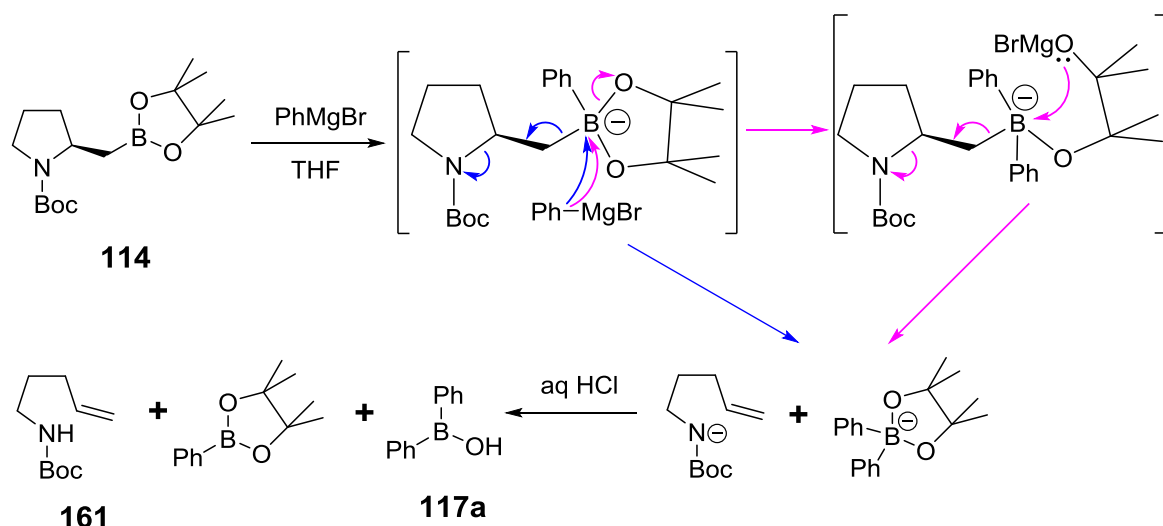


Scheme 36 Synthetic route to enantiomer of **114**, compound **166**

However, the subsequent reaction step to **166** was not attempted due to complications faced with further usage of **114** (see below) as well as low availability and high cost of sparteine, which is used stoichiometrically in this transformation.

2.2.4.2. Attempted derivatisation of homoboroproline **114**

Homoboroproline **114** was reacted with excess (4 equiv.) PhMgBr in an attempt to generate product **157** (Scheme 33). Unfortunately, after HCl workup, the majority of the boron-containing products were boronic, and no starting material remained, which means that boron was disconnected from proline structure (Scheme 37). The only borinic product formed in the reaction was identified as Ph₂BOH. Reaction with 1 equiv. of PhMgBr or BuLi also did not lead to formation of borinic product.

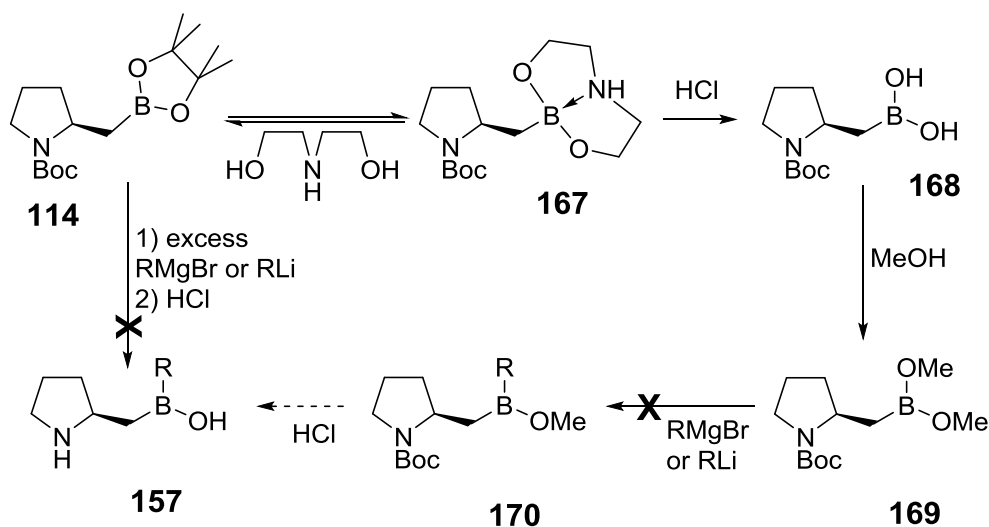


Scheme 37 Supposed mechanism of reaction between homoboroproline **114** and PhMgBr

It was assumed, that the pinacol substituent was probably preventing the “ate”-complex from collapsing to the borinic acid. For this purpose it was decided to re-esterify **114** to an analogous methoxy derivative **169**. This was achieved through diethanolamine derivative **167** (Scheme 38).

Interest in synthesis of **167** was revived as it was hoped that it could provide an alternative pathway to the workup step of homoboroproline **114** synthesis. It is known¹⁵⁷ that addition of diethanolamine to pinacolboronic esters leads to precipitation of the resulting complex of type **167** (Scheme 38). However, introduction of 1 equivalent of diethanolamine/ⁱPrOH to homoboroproline **114** did not lead to crystallisation of **167**. As seen in results of ¹¹B NMR spectroscopy (Figure 14,

A), the equilibrium between **114** and **167** is established, and is not pushed further to **167** due to absence of crystallisation, which was not achieved in Et₂O either.



Scheme 38 Synthetic attempts to generate bifunctional borinic acids **157**

Reaction of homoboroproline **114** with three equivalents of diethanolamine with subsequent evaporation of pinacol led to almost complete conversion to adduct **6** (Figure 14, B), but solubility (and consequently reactivity) became an issue, as the product formed a very thick gel. In order to get complete conversion, at least 3 cycles of dilution/evaporation were required. Another issue was that the product contained excessive diethanolamine. However, an efficient procedure was developed so that this process could be conducted by Kugelrohr distillation.

Initially, **114** was heated in diethanolamine at 120 °C at 1 Torr, but it led to partial distillation of homoboroproline **114** and the yield of complex **167** was very low. Thus, pinacolate **114** was first heated at 60 °C at 1 Torr in excess of diethanolamine (5 equivalents), which acted as solvent, and under these conditions pinacol was distilled off, and the equilibrium was pushed towards the product **167**. After 1 hour, the temperature was raised to 120 °C, when diethanolamine also distilled off. The product gel was dissolved in Et₂O, and slow evaporation in air at r.t. yielded crystalline **167**, which was characterised by X-ray (Figure 15). This ethanolamine workup process could also be used for the workup of the borylation reaction described above, however, the yields were not improved, which again underlined that it is the reaction conditions that should be further optimised.

Figure 14 Results of ^{11}B NMR spectroscopy for reaction of homoboroproline **114** with 1 equivalent of diethanolamine at r.t. (A) and with 3 equivalents of diethanolamine after 3 evaporation/dilution cycles (B).

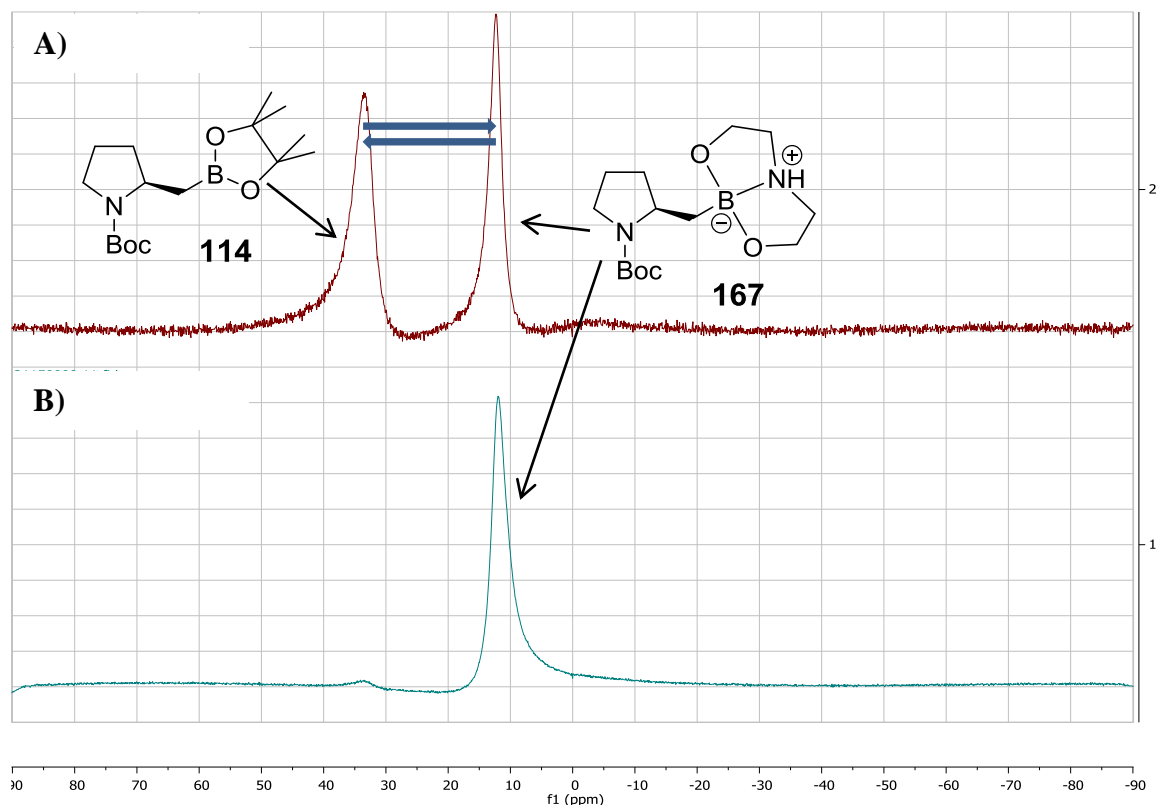
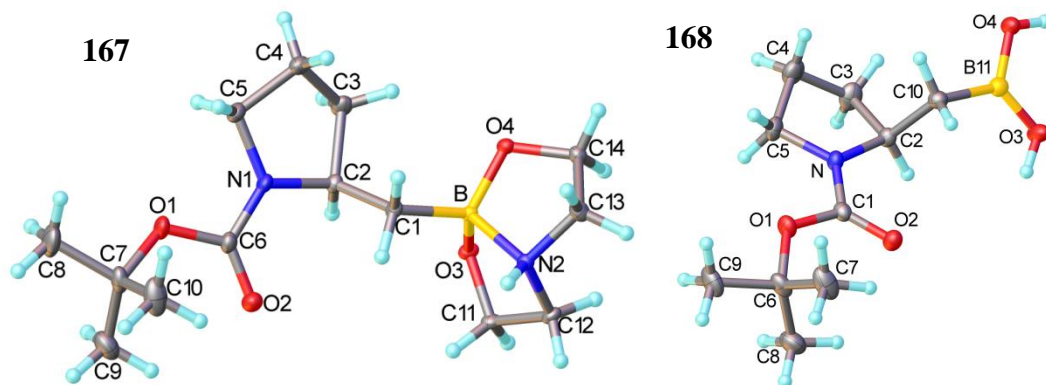
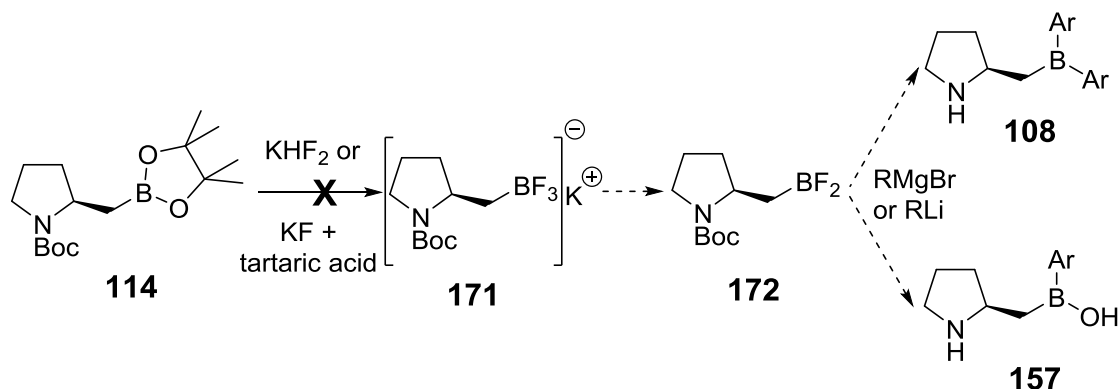


Figure 15 X-Ray structures of diethanolamine adduct **167** and N-protected boronic acid **168**.



Diethanolamine complex **167** was also successfully reacted with 5% aq HCl to yield N-protected boronic acid **168** (Scheme 38), which also crystallised (Figure 15). However, further esterification with MeOH (without product **169** isolation) and subsequent reaction with PhMgBr did not lead to borinic product **157**. This suggested that elimination outlined in Scheme 37 is the main reaction pathway in this case as well.

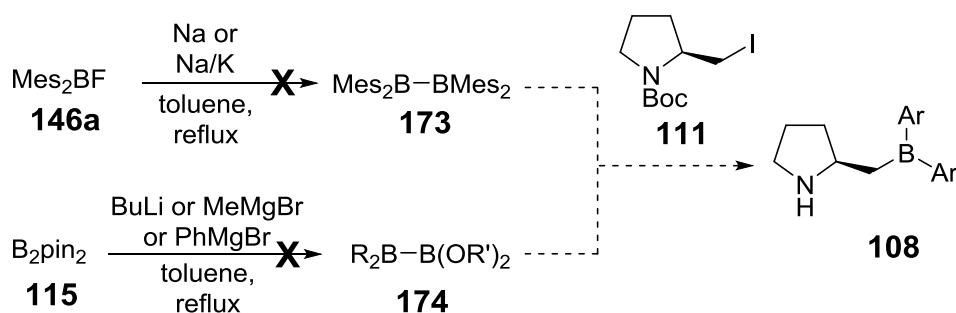
Boron halide compound **172** (Scheme 39) was suggested as an alternative intermediate for synthesis of catalysts **108** and **157**.



Scheme 39 Attempted fluorinations of **114**

Again, it is known that reacting the pinacolboronic esters with KHF_2 ¹⁵⁸ or KF in a mixture with tartaric acid¹⁵⁹ yields the $[\text{RBF}_3]\text{K}$ complexes, that crystallises from solution. In the case of **114** the desired trifluoroborate **171** was only formed in very low yield (< 5%), and surprisingly, under the milder conditions of KF and tartaric acid, only the products of elimination and ring-opening of the proline were observed.

Ring-opening was seen during all attempts to introduce the aryl substituent to boron in homoboroproline derivatives. One last approach to **108** was suggested through generation of Ar_2BBAr_2 **173** species, so that using these instead of B_2pin_2 during the borylation step of **111** could directly produce the compounds of interest (Scheme 40). Another idea was to generate $\text{R}_2\text{BB}(\text{OR}')_2$ **174**, as using such reagents for borylation could reveal, which group would transfer ($\text{R}_2\text{B}-$ or $(\text{R}'\text{O})_2\text{B}-$) and could contribute to general understanding of B-B chemistry.



Scheme 40 The Ar_2BBAr_2 and $\text{R}_2\text{BB}(\text{OR}')_2$ approaches to catalysts **108**.

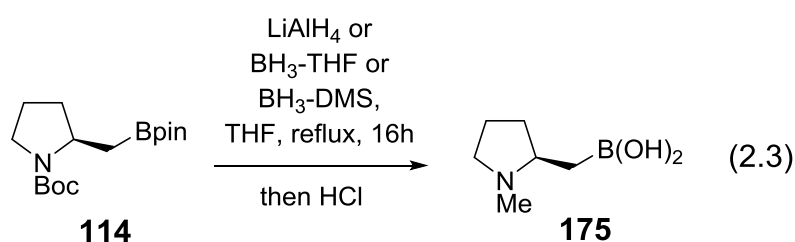
For this purpose, a reaction between boron fluoride **146a** and Na in degassed toluene with reflux was attempted (Scheme 40), as Na was used for similar $(\text{R}_2\text{N})_2\text{BX}$ dimerization.¹⁶⁰ In our case, the B-B product was not obtained, probably due to

significant steric hindrance of mesityl groups. It is known¹⁶¹ that Mes₂BF can generate Mes₂B• radical when reacted with Na/K alloy, so we attempted a similar process hoping for the dimerization of radicals, but this was not successful either.

It was also interesting to check how B₂pin₂ **115** would react with excess BuLi, MeMgBr and PhMgBr, as this potentially could result in products **174**. “Ate”-complexes were formed in all cases, but unfortunately, pinacolate substituents on boron atoms hindered the process of their collapse and the reaction was largely reversible, which again underlines oxygenophilicity of boron.

A reduction of **114** was also tried, in order to generate compound **175** (eqn. 2.3). Bifunctional boronic acid **175** is a different type of bifunctional catalyst of interest, as it does not have the N-H bond of **108** or **157**, thus it will not form enamines, imines or hydrogen bonds with ketones or aldehydes, but the lone pair on nitrogen could still be active and could participate in catalysis in a more “FLP”-like way.

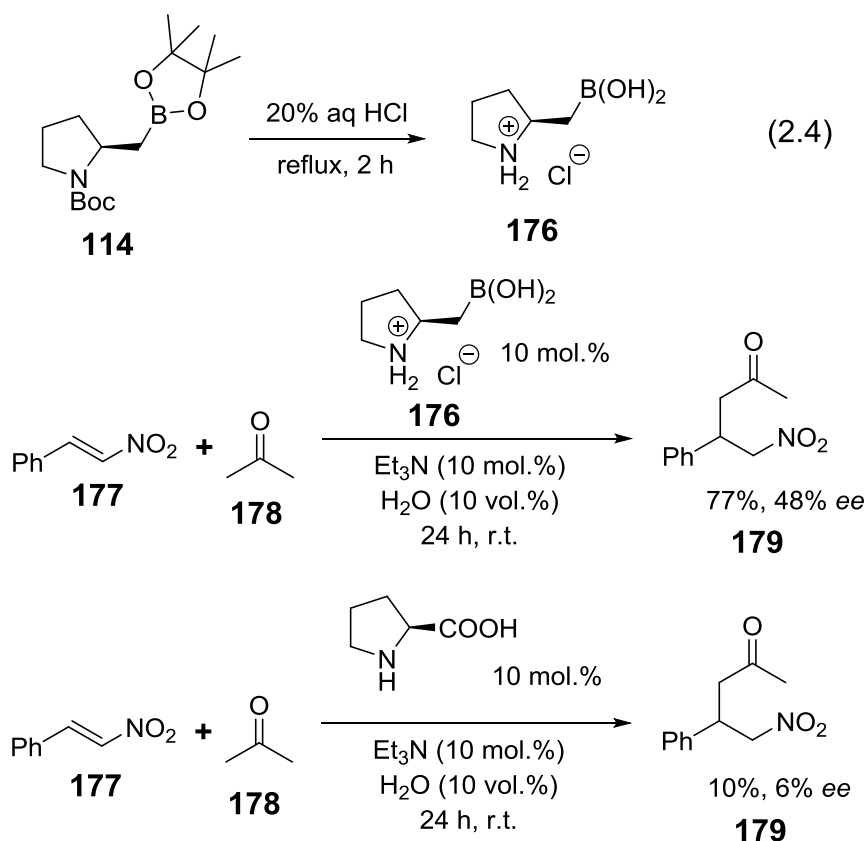
An initial attempt with excess of LiAlH₄ yielded after workup only 19% of organic material, which was not pure. However, the accurate mass data, obtained on this mixture suggested that the major component was product **175**. It was assumed that the majority of product was lost during workup, but subsequent reduction with BH₃-THF yielded no product. Finally, full consumption of starting material was seen by ReactIR (see Part II for introduction to the instrument) when 5 equivalents of BH₃-DMS were used. However, the crude product contained large amounts of boric acid and was impossible to separate.



2.2.4.3. Attempted catalysis with homoboroproline derivative **176**

Acid hydrolysis of the homoboroproline led to deprotection of the *N*-Boc group and loss of pinacol (eqn. 2.4), resulting in compound **176** which has previously been shown to be catalytically active in the aldol reaction. This product was attempted as the catalyst in nitro-Michael addition (Scheme 41) and yielded 77% product with 48% *ee* after 24 h. The identical reaction with *L*-proline as catalyst only gave 10% of product with 6% *ee* after 24 h, thus homoboroproline **176** was almost 8 times more

active than proline and provided fairly good chiral control too. The synthesis of racemic standard for the product of nitro-Michael addition was initially attempted with pyrrolidine as catalyst, however under these conditions a byproduct was generated, which was difficult to separate. Instead, the reaction was attempted with racemic proline, and after 7 days of stirring at r.t. product (48%) was isolated by column chromatography.



Scheme 41 Application of homoboroproline catalyst **176** in nitro-Michael reaction

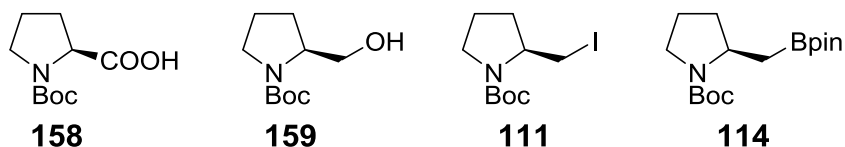
2.2.5. NMR analysis of proline derivatives

Understanding the peculiarities of ¹H and ¹³C NMR spectra of some of the compounds obtained is important for future insights into their mechanism of action and of catalysts derived from these structures. Indeed, the complications arising from the presence of rotamers, diastereotopic protons, exchange processes and hydrogen bonding can create difficulties in signal assignment, but when resolved, shed light on the chemistry of these compounds and equilibria in these systems.

2.2.5.1. Analysis of diastereotopic protons and rotamers

The existence of diastereotopic protons was first identified in 1957, when symmetry was used to explain the inequivalence of geminal protons in various compounds, in addition to previous arguments based solely on bond rotation¹⁶². Diastereotopic protons are now defined by IUPAC¹⁶³ as being: “Constitutionally equivalent atoms or groups of a molecule which are not symmetry related. Replacement of one of two diastereotopic atoms or groups results in the formation of one of a pair of diastereomers.” In many cases, the resulting spectrum has two separate signals for the magnetically inequivalent diastereotopic protons, with coupling to each other giving equal doublet splittings; in some, the geminal coupling is such that these signals merge into just one. Because of the presence of a chiral centre in synthesized *S*-proline-based compounds (Figure 16), all of the CH₂ protons are diastereotopic, and this was observed in some of ¹H NMR spectra (see below).

Figure 16 Compounds, that were analysed by NMR methods more particularly



The partial π -character of the amide bond in the Boc protecting group, combined with the freedom restriction of the proline ring, means that compounds **158**, **159**, **111** and **114** experience slowed internal rotation around B-N bond. Taking into account the timescale of NMR experiments, this means that separate rotamers of compounds in question can often be observed in NMR spectra. Unlike the proton diastereotopicity, this effect can be seen in the ¹³C NMR spectra, for example in case of iodide **111** (Figure 17). The pattern of rotamers appearance in the NMR spectra is generally not consistent, or easily predictable, and the ratio of rotamers is not necessarily 1:1, although in this case, it is very close.

Various 2D NMR techniques can be used to identify pairs of diastereotopic protons and to distinguish them from pairs of rotamers. COSY allows seeing that two protons are diastereotopic even if their appearance in ¹H NMR is significantly different from one another (Figure 18). For example, in case of *N*-Boc prolinol **159** signals of H-2 diastereotopic protons lie to both sides of the H-3 signals, and are coupled to each other, to H-3 and H-1 protons as well. This allowed unambiguous assignment of the signals in ¹H NMR spectrum of **159**, and, similarly, for **114**.

Figure 17 Fragment of ^{13}C NMR spectrum of iodide **111**, showing duplicated signals, indicative of rotamers

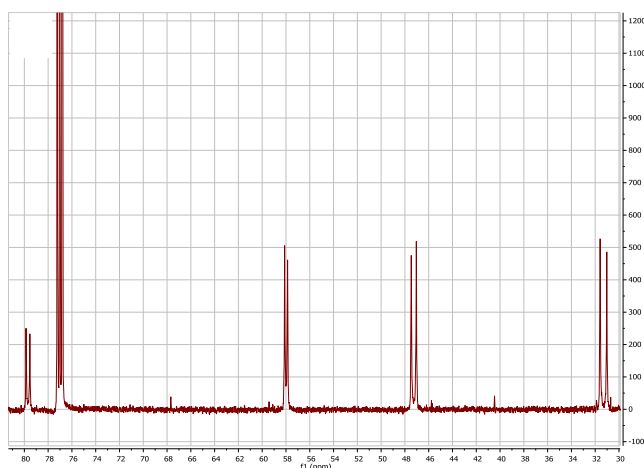
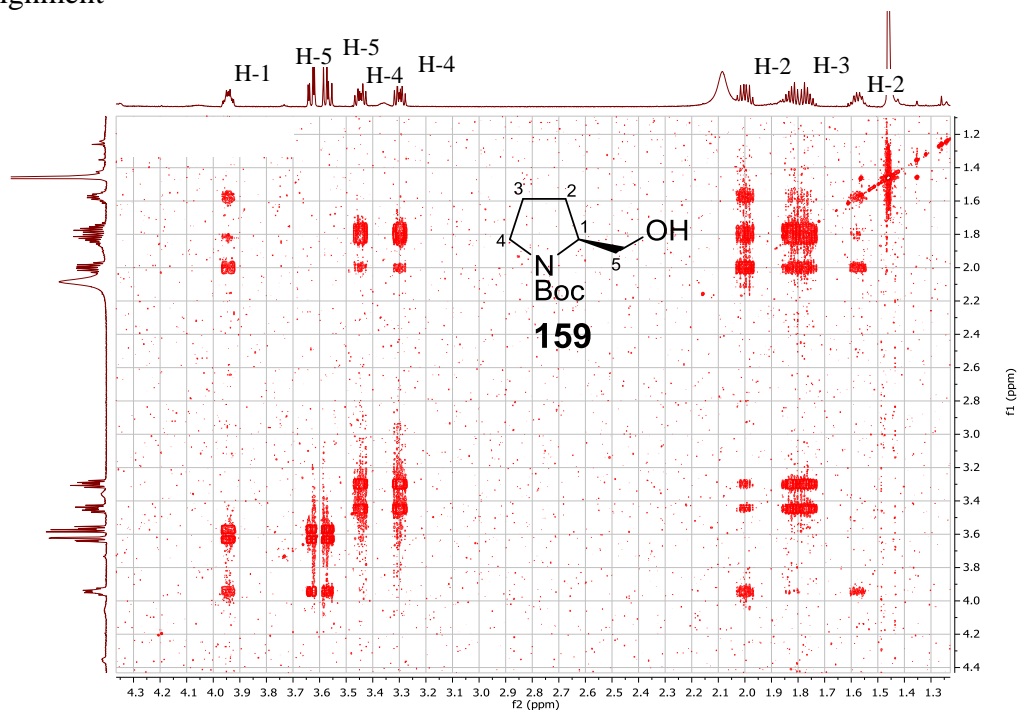


Figure 18 ^1H COSY NMR spectrum of the prolinol **159**, allowing full signal assignment

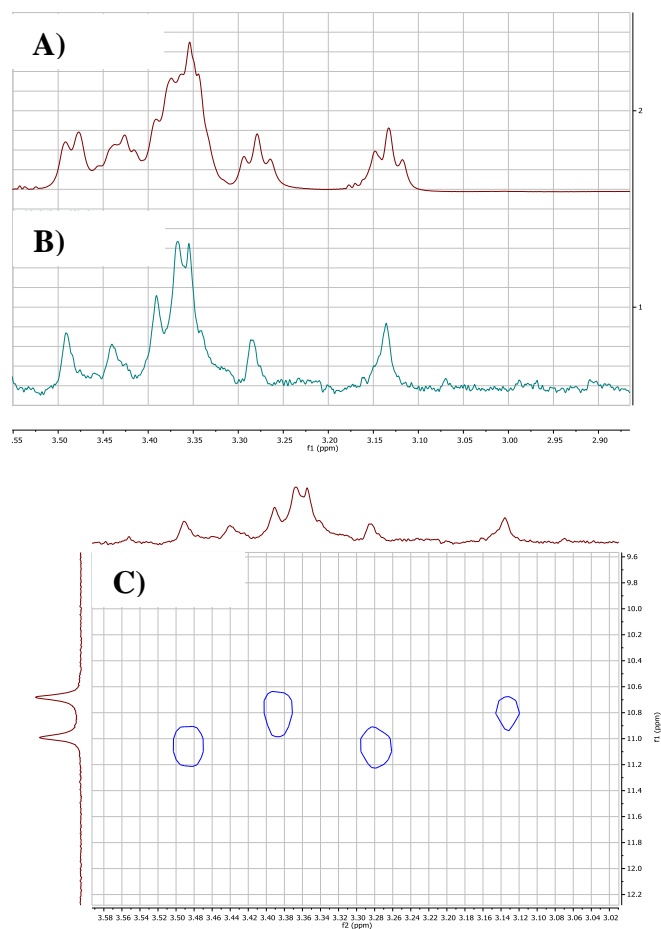


However, if rotamers make the spectrum more complicated, it becomes impossible to complete the assignment by means of COSY only. The best technique in these cases is HSQC, which shows correlation of protons of one rotamer to one carbon signal, and protons of other carbon couple to the other carbon. This allowed assignment of protons in the ^1H NMR spectra of **158**.

Identifying signals from different conformers is sometimes difficult in the presence of exchange because signals from different conformers often overlap. Here pure shift techniques can be used to remove the problem, provided that signals are not

too broad, using pure shift techniques to collapse multiplets into singlets, as in Figures 19 and 21. These techniques allow the removal, in our case, of H-H coupling, thus collapsing proton signals to singlets. Such attempts have been made since mid-1970s;¹⁶⁴ however, have not gained popularity until recently. They can be united under the overarching term of “pure shift”¹⁶⁵ method. In this study, the PSYCHE¹⁶⁶ (Pure Shift Yielded by Chirp Excitation) technique was used.

Figure 19 ^1H (A), ^1H PSYCHE (B) and ^1H PSYCHE – HSQC (C) fragments of iodide **111** NMR spectra

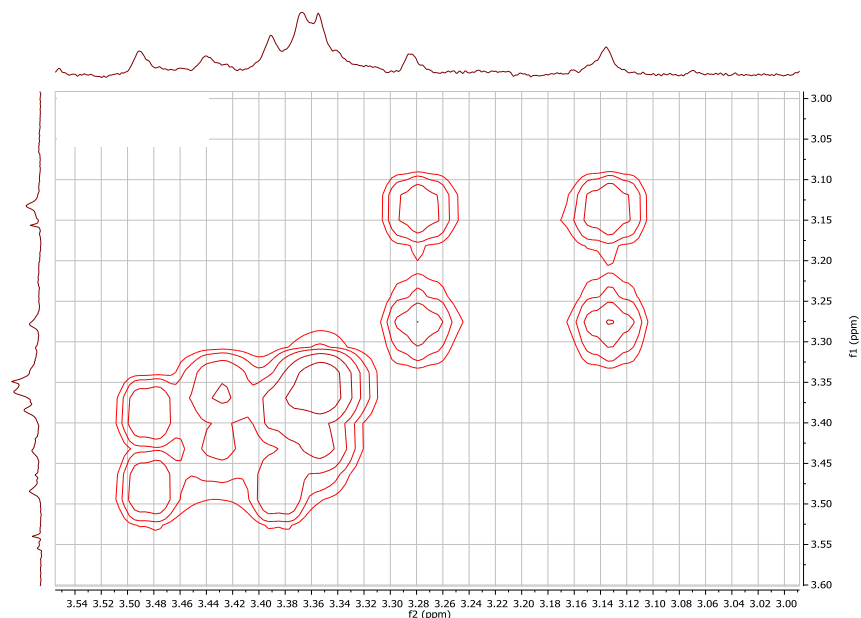


It can be seen (Figure 19, A), that a region in ^1H NMR spectrum of iodide **111** is quite complex. Performing the PSYCHE experiment on the same sample (Figure 19, B) revealed 4 separate proton signals, and PSYCHE-coupled HSQC (Figure 19, C) allowed unambiguous assignment of diastereotopic H-5 protons of two rotamers, 2 protons correlate to one carbon signal, and two other protons correlate to the carbon signal of the other rotamer.

Finally, another tool that helps with identifying rotamers is EXSY. What makes this experiment useful in our case is that it allows to correlate the exchanging

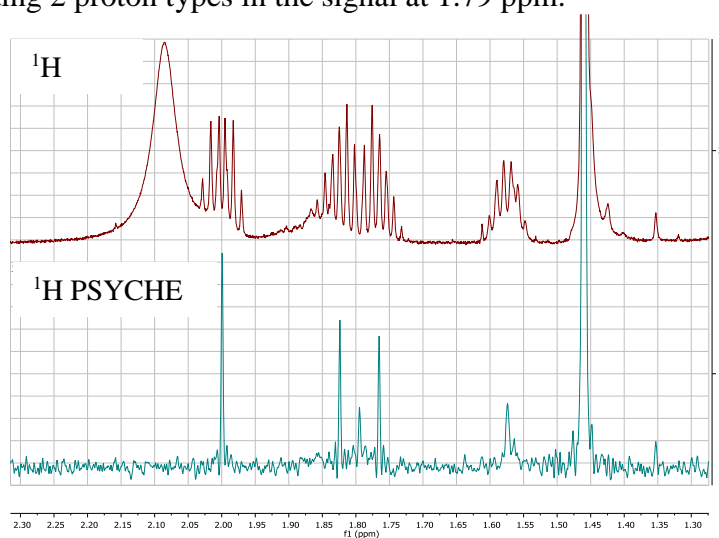
protons, for example in the same case of iodide 111 (Figure 20), and in this case PSYCHE makes picture clearer as well.

Figure 20 EXSY ^1H PSYCHE – ^1H PSYCHE spectrum of iodide 111 indicating correlations between exchanging H-5 protons



Another example of PSYCHE usage (Figure 21) can allow to clearly identify diastereotopic protons H-3 in prolinol **159**, showing that the multiplet at 1.79 ppm actually contains two separate signals. Note, that a smaller signal at 1.79 ppm in PSYCHE spectrum is an artefact, known in the PSYCHE method.

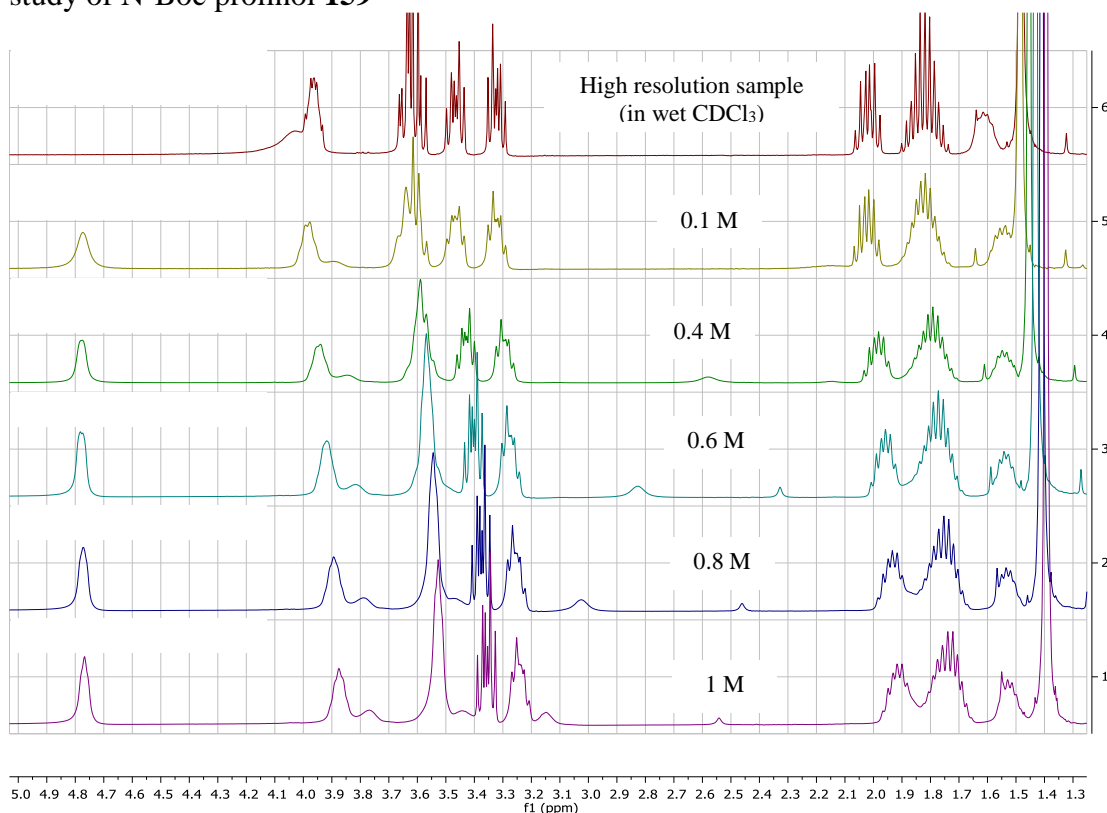
Figure 21 ^1H and ^1H PSYCHE NMR spectra fragments of the prolinol **159**, indicating 2 proton types in the signal at 1.79 ppm.



2.2.5.2. ^1H NMR resolution in prolinol **159** spectra

An interesting ^1H NMR effect was accidentally found when obtaining ^1H NMR spectra of *N*-Boc prolinol **159**. In some cases, the resolution of spectrum was greatly increased, so that all main coupling constants could be identified, including those for diastereotopic protons interactions (Figure 22, top). Originally, this effect was thought to be concentration dependent, however, a concentration study between 0.1 M and 1 M solutions did not reveal any change of resolution (Figure 22). Some signals, however, shift significantly as concentration changes.

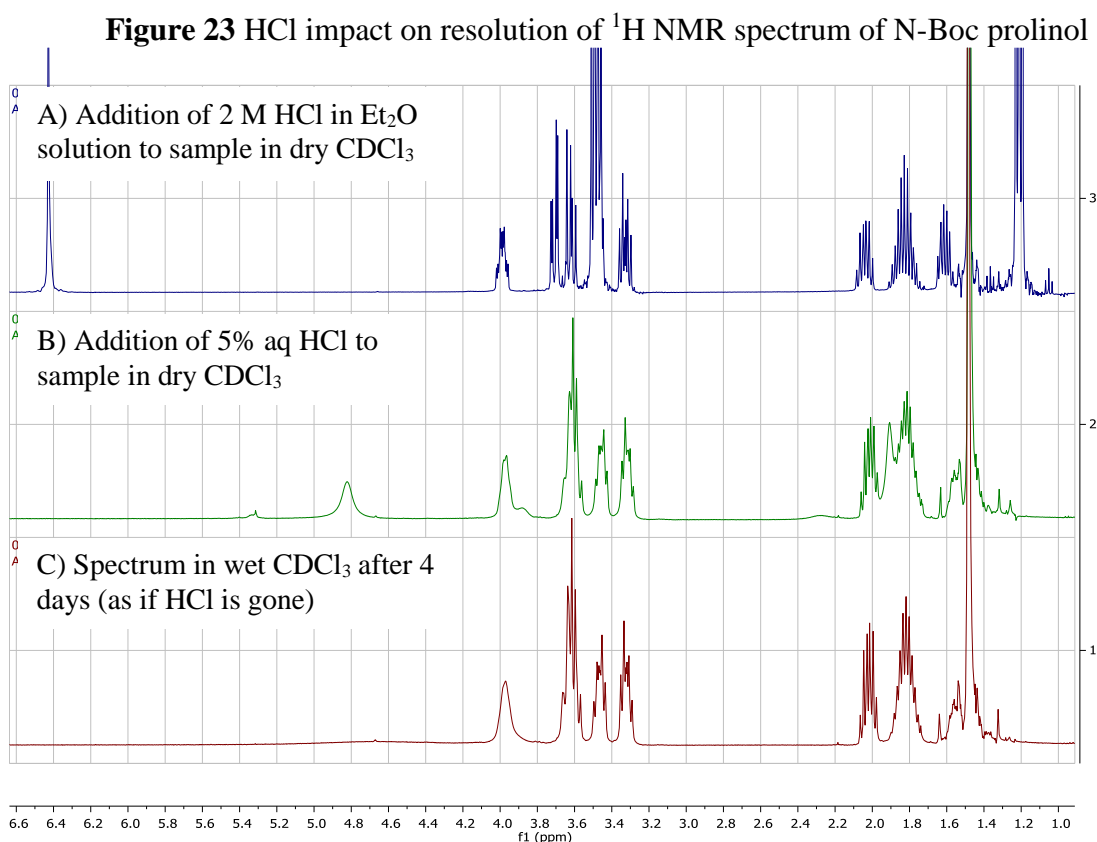
Figure 22 Accidentally obtained increased resolution and concentration NMR study of *N*-Boc prolinol **159**



It was then found, that resolution appears when wet CDCl_3 is used for sample preparation, whereas in dry deuterated chloroform signals remain broad. However, when shaking the dry CDCl_3 sample with a drop of water, no better resolution is obtained. Consequently, it was suggested that resolution might be changing due to presence of HCl in wet CDCl_3 , as far as chloroform is known to undergo slow light induced decomposition to HCl and dichlorocarbene.¹⁶⁷ However, when chloroform is dried (for example, with molecular sieves), HCl can, supposedly, escape solution, as there is almost no more water to trap it, and the pH of solution will rise. This effect was confirmed by introducing molecular sieves to wet CDCl_3 and observing the drop

of resolution in ^1H spectrum, as well as storing wet CDCl_3 over sodium carbonate overnight, which also resulted in the loss of resolution.

The resolution increased most when a drop of 2 M HCl in Et_2O was added to the sample (Figure 23, A). Surprisingly, shaking solution of **159** in dry CDCl_3 with a drop of 5% aq HCl did not yield improved resolution (Figure 23, B), which can be explained by very low solubility of water and HCl in chloroform, meaning most of acid remains in aqueous layer. Another unusual finding was that over 4 days a sample, prepared with wet CDCl_3 , completely lost resolution, just as if chloroform became dry and HCl was removed (Figure 23, C).

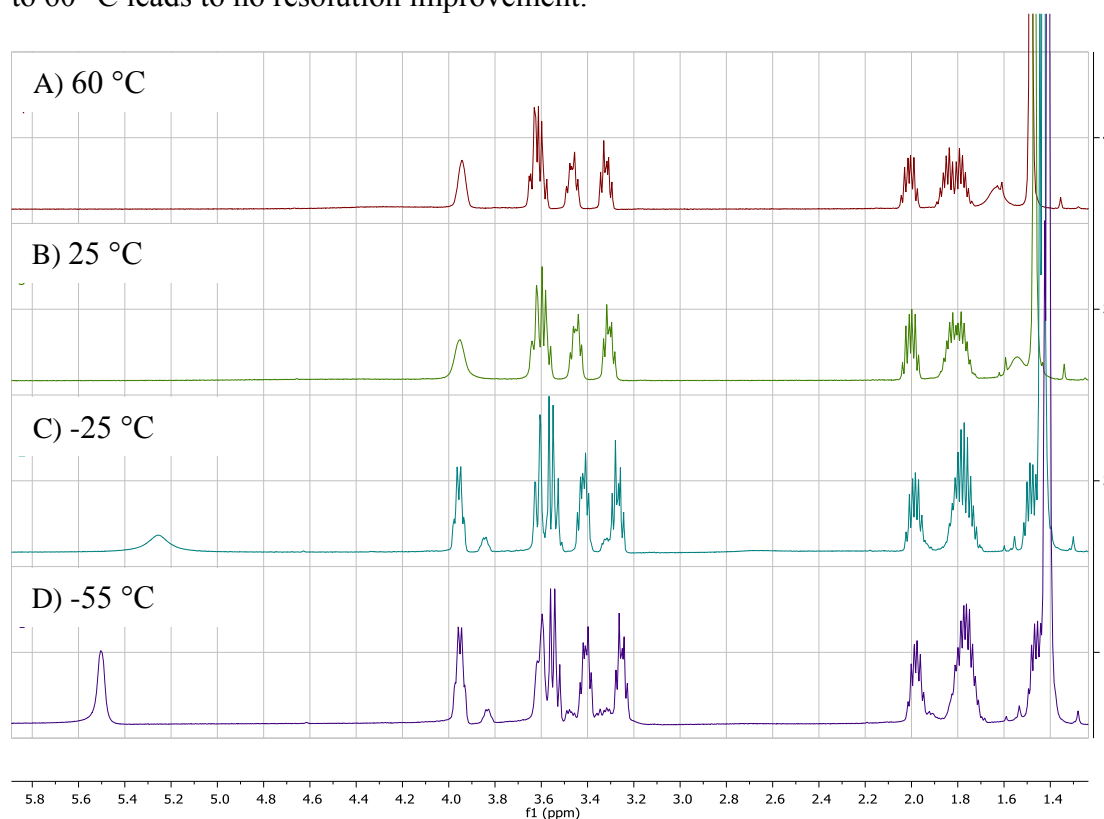


It was important to identify the influence of HCl on resolution of ^1H NMR spectrum. First, the molecule in question is an amide, thus one can expect an energy barrier of rotation around N-C bond. It means that the spectrum observed at r.t. could either indicate fast rotation around N-C bond and the average of 2 rotamers observed, or completely the opposite, i.e. fully locked rotation and only 1 rotamer. It was suggested, that the O-H proton could be hydrogen bonding intramolecularly to the carbonyl oxygen of Boc group (Figure 24, A), forming a 7-membered ring and thus locking rotation around amide bond. This would explain the HCl effect, as once added to the solution it would interrupt hydrogen bonding and C-N bond rotation would

improve, leading to increased resolution in ^1H NMR spectrum. The X-ray structure of **159** was recorded and showed, that such $\text{O-H}\cdots\text{O}=\text{C}$ coordination existed in solid state, but was intermolecular, rather than intramolecular (see Appendix 1).

In order to further verify this, a VT study was conducted (Figure 24). VT ^1H NMR confirmed free rotation around N-C bond at r.t., because at higher temperatures spectrum did not change and at lower temperatures a second set of signals, presumably of the second rotamer, was seen in a $\sim 1:9$ ratio. This underlined that the nature of low resolution could be different, for example, intermolecular hydrogen bonds could lead to agglomeration of molecules into a macromolecule, which would rotate slower and this would result in decreased ^1H NMR resolution, while addition of HCl would break these intermolecular coordinations and improve resolution.

Figure 24 VT ^1H NMR study of prolinol 159, A) 60 °C, B) 25 °C, C) -25 °C, D) -55 °C. Note rotamers can be seen at -25 °C, and even better at -55 °C, but heating to 60 °C leads to no resolution improvement.

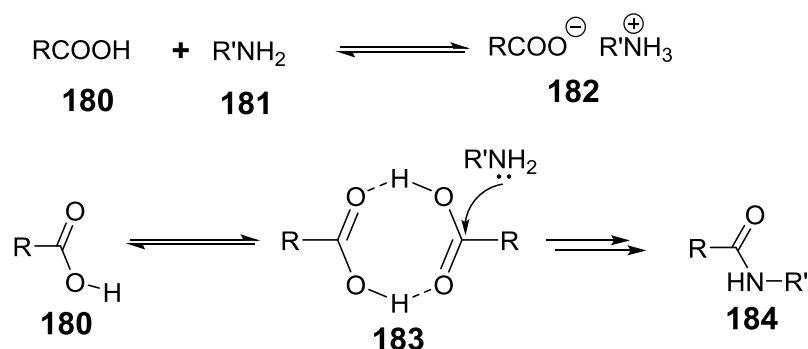


2.3. Part II. Direct amide formation

As noted above, borinic acids Ar_2BOH **148** were synthesized in the course of this work. It was noted, that by then they have not been tried as catalysts in direct amide formation reactions (but they were used in chloroacylations and chlorosulfonylations^{168a}, couplings of glycosyl methanesulfonates^{168b} and in synthesis of β -glycosylceramides^{168c}), even though analogous boronic acids $\text{ArB}(\text{OH})_2$ were known to catalyse this process. Thus, it was decided to apply borinic acids in reactions between carboxylic acids and amines in refluxing toluene, however, the initial results were difficult to interpret, and it was decided to study the background, non-catalytic direct amide formation in order to better understand these systems and processes. It was also noticed, that the mechanism of this non-catalytic direct interaction between carboxylic acid and amine, leading to an amide, is not fully known, and we hoped to gain insights into it.

2.3.1. Non-catalysed, background thermal direct amide formation

Formally, non-catalysed direct amide formation only involves 2 reactants, a carboxylic acid **180** and an amine **181**. However, other processes are also involved, e.g. ammonium salt **182** formation equilibrium (Scheme 41). This makes analysis of these mixtures more complicated and is probably the reason why the mechanism of direct non-catalysed amide formation is not fully understood,¹³⁴ and even the order of this transformation had not been identified. One of the reasonable hypotheses behind the mechanism of non-catalysed direct amide formation suggests that the carboxylic acid undergoes self-activation towards amine nucleophilic attack by forming a dimer **183** (Scheme 41).



Scheme 41 Possible processes in direct amide formation reaction systems and one of the possible mechanisms

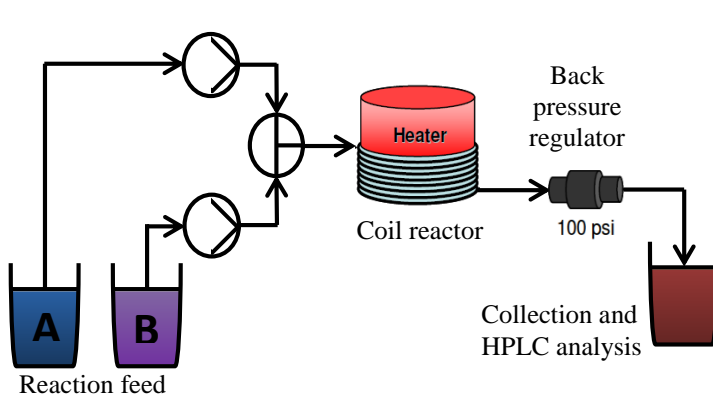
The batch process, which involves Dean-Stark water removal, was not suitable for this investigation, as it is extremely engineering-dependant, and in order to get reproducible results the same equipment should be used. Batch reactions also take long time, thus it was decided to apply flow reactor technology for this project.

2.3.1.1. Amide formation: Flow reactor

A few studies focussed on investigating amide formation in flow reactors under homogeneous conditions, however, that research is focussed on magnesium-¹⁶⁹ or aluminium-mediated¹⁷⁰ amidations of esters. Direct amide formation, i.e. reaction between carboxylic acid and amine, was also applied in flow, but these processes were heterogeneous with application of enzyme-¹⁷¹ or silica-based¹⁷² catalysis.

For the purposes of non-catalysed study a homogeneous 2-feed setup with a simple T-type mixer was used (Figure 25).

Figure 25 Flow scheme, configuration and instrument used for amide formation



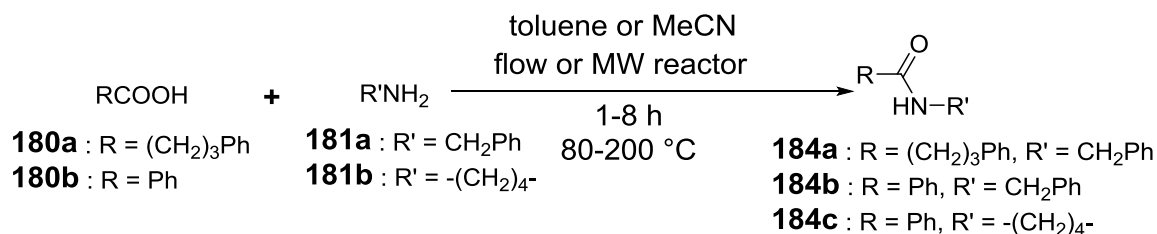
formation

System Configuration	
Reactor type	Coil
Material	PTFE High Temp
Volume	52.0 ml
Coil Temp	100 – 150 °C
System Dead Volume	0.50 ml
Min and Max Pressure	5 bar, 12 bar
Coil Residence Time	1 – 4 h
Flow Rate of reagents	0.11 – 0.43 ml/min
Reagents Ratio	1:1, 1:2, 2:1
Substrates	Benzylamine + 4-phenylbutyric acid
Substrates	Benzylamine + benzoic acid
Substrates	Pyrrolidine + benzoic acid
Solvents	Toluene



The main investigated pair of reagents was 4-phenylbutyric acid **180a** and benzylamine **181a** in toluene (Scheme 42), as this is a fairly thermally active combination, which also does not form insoluble ammonium salt at r.t., which could

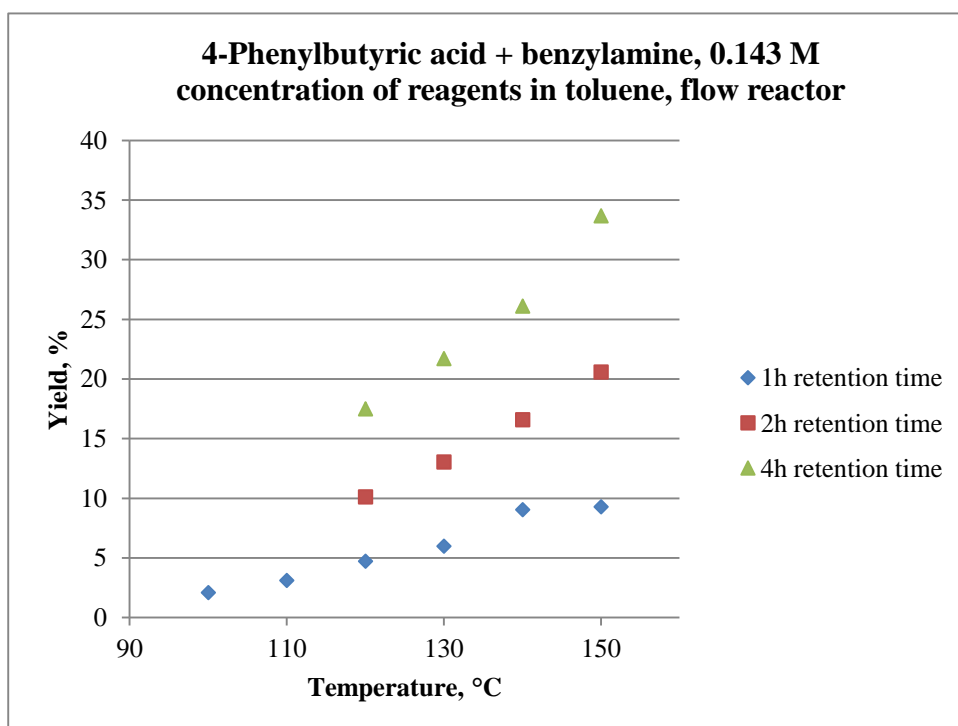
block the flow reactor. The yield of amide was determined with reverse phase HPLC (see Supporting Information for calibration graphs) First, temperature dependencies at different retention times were acquired (Figure 26). It is worth mentioning, that due to the use of back-pressure regulator it was possible to conduct reactions at temperatures above the boiling point of the solvent, which allowed to decrease retention times while generating a significant yield of the amide.



Scheme 42 Attempted direct amide formation in flow and microwave reactors

Attempts were then made to obtain dependencies of amide yield on reagent concentration, but at this point lack of reproducibility of the results made the results hard to interpret. However, two conclusions were made on the basis of observed data; that the yield increased linearly with concentration of both reagents and that the yield increased if acid concentration was kept the same, but amine concentration dropped. These conclusions were further investigated when amide formation was conducted in a microwave reactor.

Figure 26 Temperature and retention time impact on flow conversion for 4-phenylbutyric acid + benzylamine, 0.143 M concentration of reagents in toluene, flow reactor

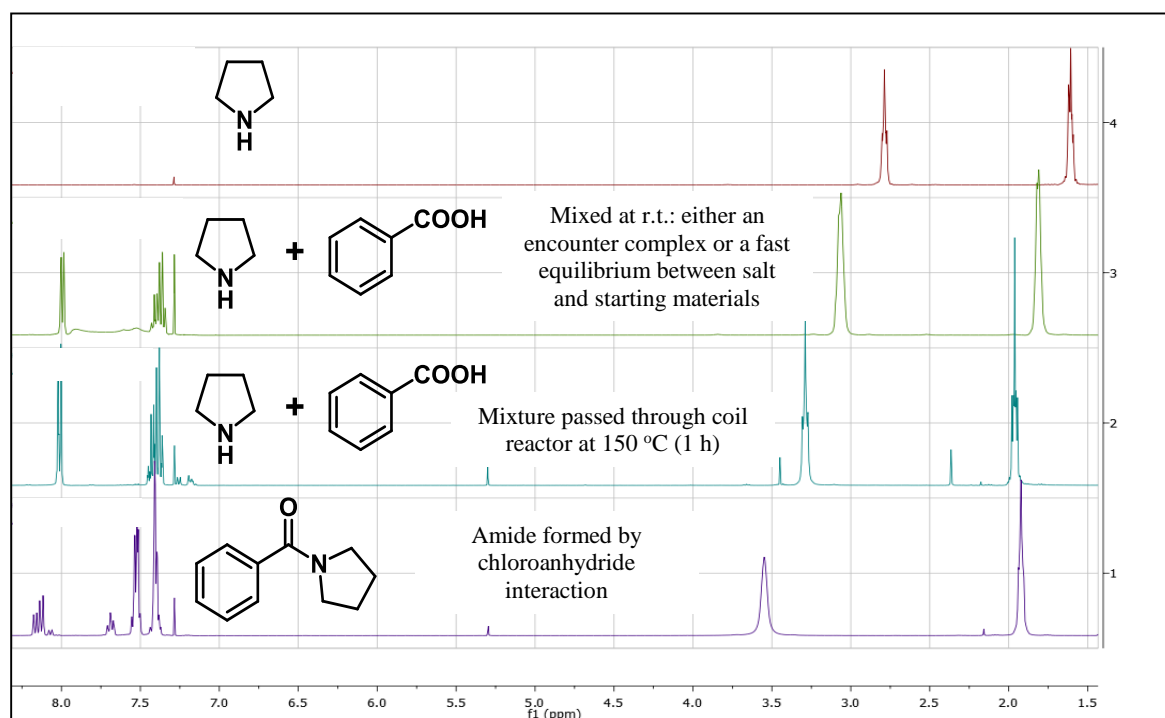


phenylbutyric acid – benzylamine system

It was found that ammonium salt formed in the system benzoic acid-benzylamine and therefore blocked the entrance to the flow reactor. This problem could be partially solved by preheating reagents before mixing, however, salt then blocked the exit of reactor, as conversion was far from full, thus this system was not investigated further.

No amide formation was observed for the system pyrrolidine – benzoic acid. When mixing these reagents at r.t. no ammonium salt formation was seen. However, after passing this mixture through the flow reactor at 150 °C for 4 h, crystals of ammonium salt were formed in the resulting solution, as confirmed by X-ray (see Supporting Information), and the ^1H NMR signals of crude mixture were shifted compared to r.t. mixture (Figure 27). This observation suggested that salt formation was facilitated by heating in the reactor, whereas at r.t. most likely an encounter complex, or a fast equilibrium between ammonium salt and mixture of free acid and amine, was formed.

Figure 27 Pyrrolidine interaction with benzoic acid at r.t. and after passing through flow reactor



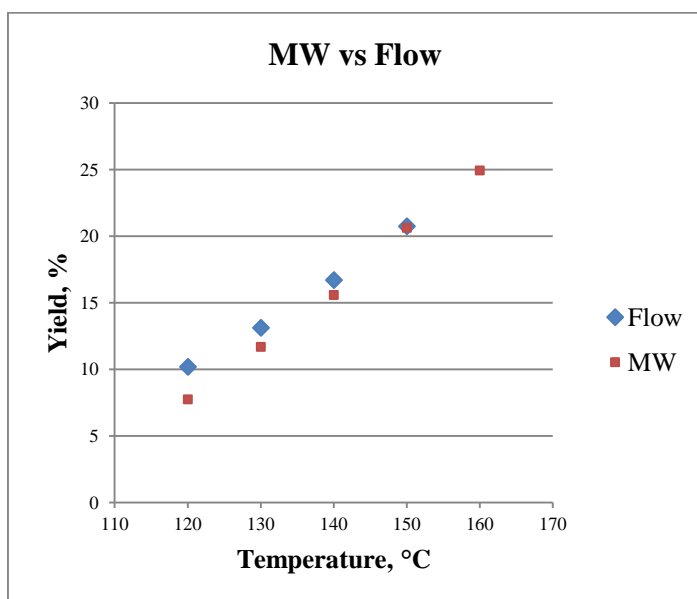
For this comparison amide **184c** was synthesized by interaction of pyrrolidine with benzoyl chloride and Et_3N . The TLC after the reaction showed two spots, and it was possible to identify one of them as the product by using a new TLC-MS method. The instrument (see Experimental) collected bits of silica with compound on it from spots on TLC, and MS analysis showed that one of them was target amide. Such

techniques can significantly simplify column chromatography and product identification.

2.3.1.2. Amide formation: Microwave reactor

Because reproducibility in the flow system was not sufficient, PTFE tubing limited the possible reaction temperature to 150 °C, retention times were limited to 4 h because of pumps speed and reactor volume, and certain amine-acid combinations generated ammonium salt that blocked the flow reactor, further investigations of direct thermal amide formation were conducted in the microwave reactor. The results in the same conditions correlated well with the results in flow (Figure 28). The same reaction conditions (PhCH₂NH₂ **181a** 0.143 M, Ph(CH₂)₃COOH **180a** 0.143 M, toluene, 2 h reaction time, no stirring), were used in most subsequent experiments and will be referred to as “standard” onwards.

Figure 28 Comparing yields of amide formation in flow and microwave reactors (PhCH₂NH₂ 0.143 M, Ph(CH₂)₃COOH 0.143M, toluene, 2 h reaction time)



Reproducibility in the MW reactor was better, and the temperature could be raised to 200 °C, which allowed a more detailed investigation of retention time and temperature influence on yield of *N*-benzyl-4-phenylbutyramide **184a** (Figure 29).

A few experiments, identifying the impact of stirring and of the presence of molecular sieves, were conducted (Figure 30). It was found, that stirring while in the microwave reactor, despite the mixture appearing to be homogeneous, improved the yield. The impact of molecular sieves (with stirring) was unclear. At elevated temperature, water absorbance on molecular sieves is a fast equilibrium process,

meaning water removal from reaction mixture is not efficient, and it was possible that molecular sieves were merely hindering stirring.

Figure 29 Influence of reaction time and temperature on yield of amide

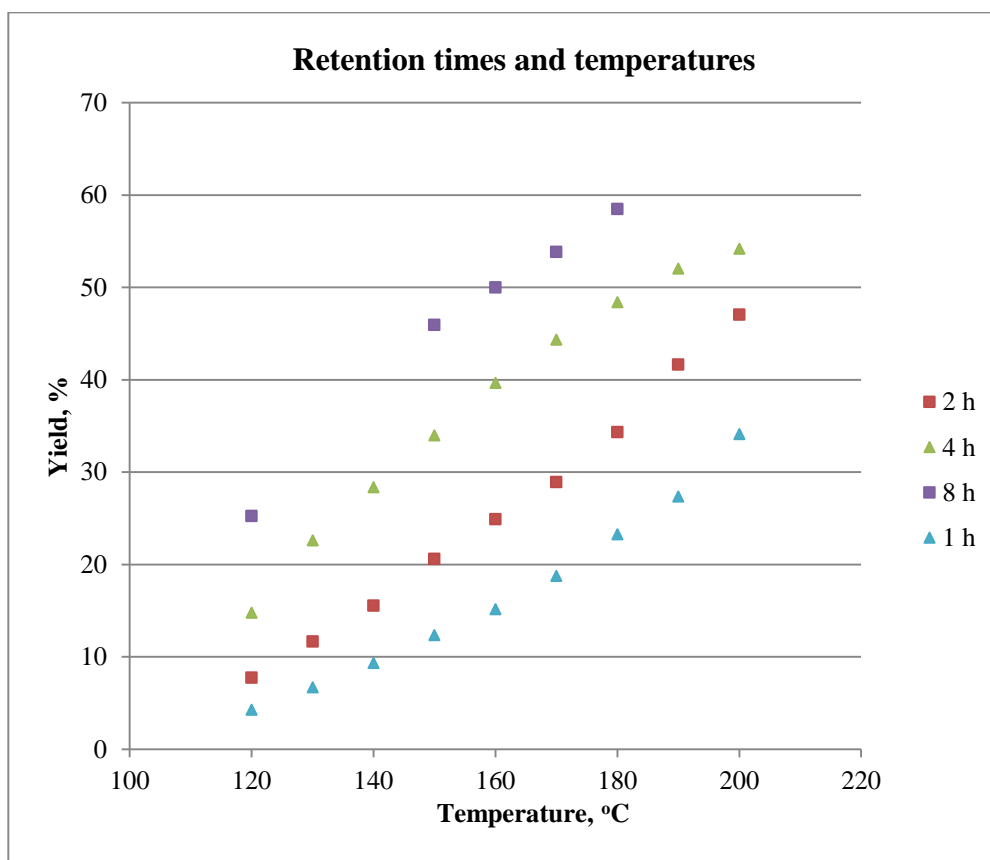
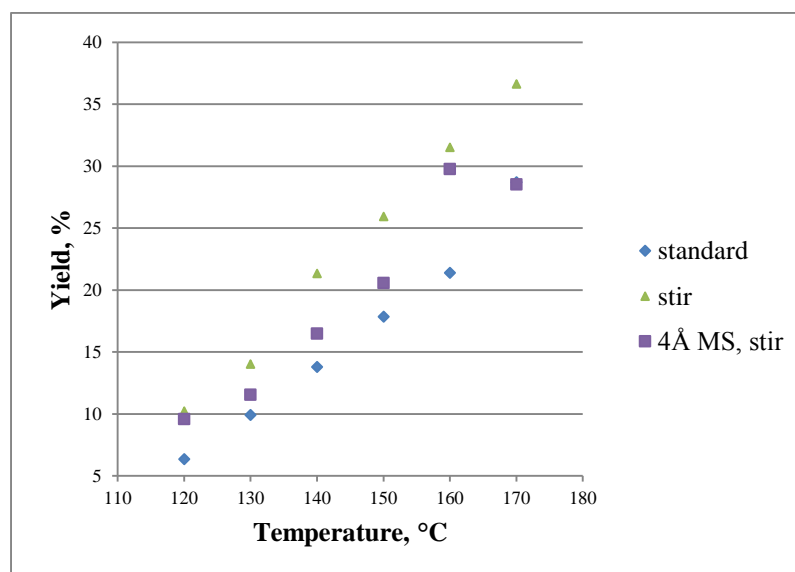


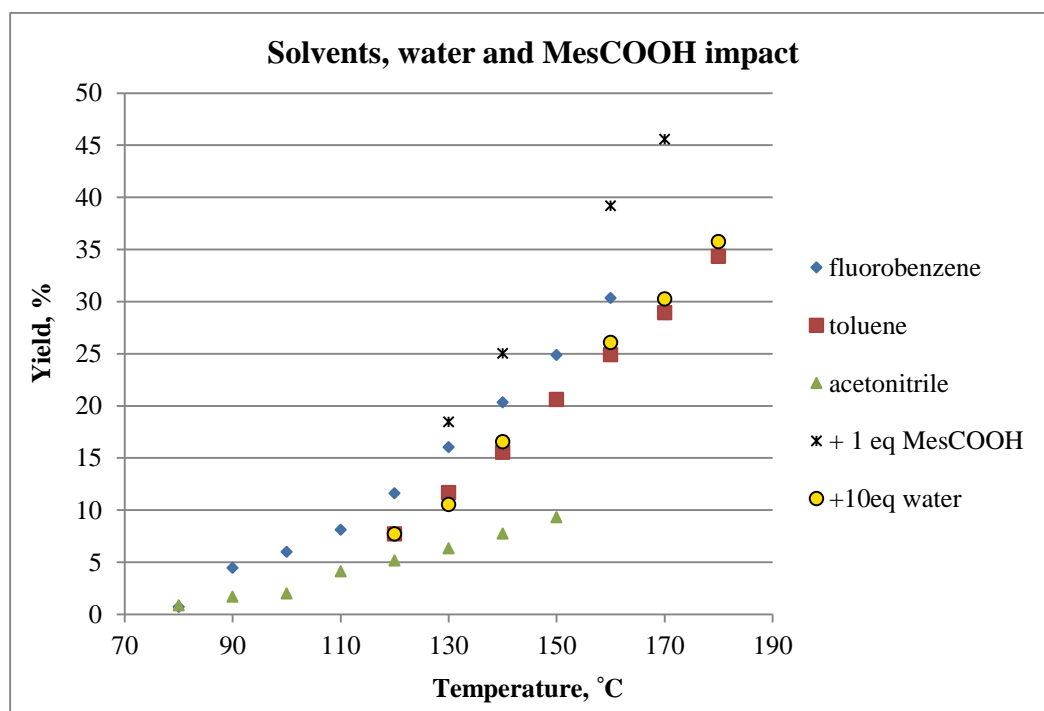
Figure 30 Stirring and 4Å MS impact on amide yield as compared to standard conditions



A solvent study revealed that fluorobenzene was a better solvent than toluene for this reaction, while reactions in MeCN were inferior (Figure 31). The impact of

the presence of water was also analysed. Surprisingly, when 1 equivalent of water was introduced to reaction mixture, no change in amide yield as compared with standard conditions was noticed. In order to verify this, a reaction was conducted with 10 equivalents of water present, and exactly the same amide yield was observed (Figure 31, yellow points). This finding was an important confirmation for the idea that amide formation is not a reversible process and that amide hydrolysis with water cannot take the same mechanistic path as thermal amide formation.

Figure 31 Solvent effect, water and MesCOOH impact on direct amide formation yields (standard conditions)



In order to find evidence or disprove the hypothesis of carboxylic acid dimer **183** (Scheme 41) being a key intermediate in the amide formation mechanism, an equivalent of mesityl carboxylic acid was added to the reaction mixture (Figure 31, black stars). Mesityl carboxylic acid is significantly hindered and does not form amide under these conditions, which was verified by ^1H NMR, but it is still capable of forming carboxylic acid dimer, both with itself and with active substrate, i.e. 4-phenylbutyric acid. The yield of 4-phenylbutyrylbenzamide was substantially increased in this case, which is in agreement with the hypothesis. An attempt to quantify this increase is possible. With 2 rough approximations that $\text{Ph}(\text{CH}_2)_3\text{COOH}$ (A) and MesCOOH (B) have equal rate constants for carboxylic acid dimer formation for AA, AB and BB, and that carboxylic acid dimer formation is a 1st order reaction,

then taking into account equal concentrations of (A) and (B), the conclusion can be made that dimers should be in a statistical mixture AA:AB:BB 1:2:1.

$$[AA]=k[A], [BB]=k[B], [AA]+[BB]+[AB]=k[A+B]$$

$$[A]=[B]$$

$$[AB]=2[AA]=2[BB]$$

$$\text{Thus, } [AA]+[AB] = 0.75([AA]+[AB]+[BB])$$

$$\text{System 1: } [A] = x, [AA]_1=kx$$

$$\text{System 2: } [A]=[B]= x,$$

$$[AA]_2+[AB]_2=0.75([AA]+[AB]+[BB])=0.75k([A+B])=0.75(2kx)=1.5x$$

The dimers, active towards amine attack, are only AA and AB, their total concentration is $\frac{3}{4}$ of total dimer concentration. This leads to a theoretical 1.5 times increase in the AA and AB concentration after introducing 1 equivalent of MesCOOH, as compared to AA concentration in the system with Ph(CH₂)₃COOH alone. Now making a final assumption that amide formation is 1st order with respect to the carboxylic acid dimer, the increase in amide yield in system 2 compared to system 1 should be 1.5 as well. The average experimental increase in amide yield observed after addition of 1 equivalent of MesCOOH, as compared to standard conditions, was 1.58. This further 0.08 improvement can be explained by the ammonium salt equilibrium being pushed to carboxylic acids by excess of ammonium salt, thus leading to higher free carboxylic acid concentration in solution.

A series of experiments were made in order to confirm the linear dependence between yield of amide and concentration of both reagents (Figure 32), which was initially observed in the flow reactor. In order to further understand the reaction mechanism and impact of starting materials on kinetics, another study was conducted. First, acid concentration was kept constant, and amine concentration was varied (Figure 33, blue points). Then, a complimenting series of experiments were conducted with amine concentration being constant and acid concentration varying (Figure 33, red points). These data suggested that the increase in yield when reducing amine concentration was due to the significant impact of the excess of carboxylic acid on the yield. However, the increase of yield with raising amine concentration was not rationalized yet. Interestingly, the dependence of yield on excess of carboxylic acid was almost linear. Unfortunately, these observations, despite being interesting, do not directly lead to conclusions on reaction order. However, the increase of yield with

excess of carboxylic acid gave further support to the carboxylic acid dimer mechanism, discussed above.

Figure 32 Dependency of amide yield on concentration of both carboxylic acid and amine

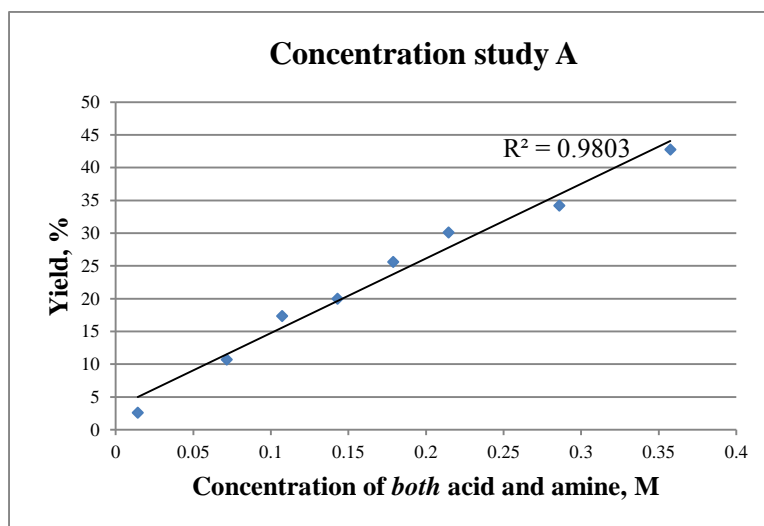
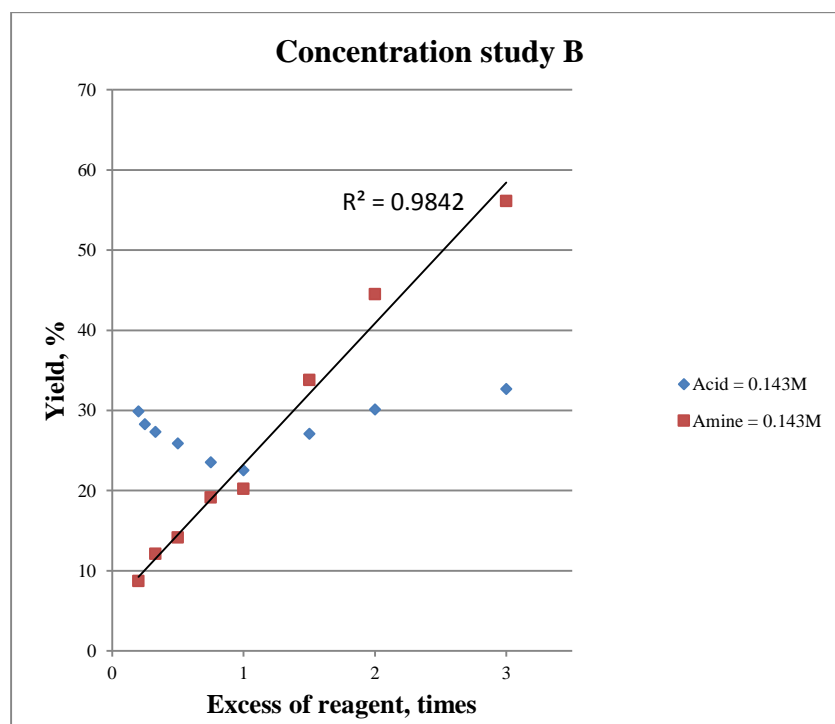


Figure 33 Dependency of amide yield on excess of carboxylic acid (red points) or amine (blue points)



It was noticed, that in most experiments the yield of studied thermal amide formation between 4-phenylbutyric acid and benzylamine did not exceed 60-70%. This was in good correlation with previous studies of this reaction as a batch process.¹⁷³ A single experiment was attempted, when a concentrated (0.358 M) mixture of acid and amine was kept at 150 °C for 8h. This yielded only 73% of amide.

In order to better understand the nature of the yield limitation in this process, a product inhibition study was attempted. Reaction mixtures were loaded with 0.5 equivalent of product amide, and the reaction was run under the standard conditions (Figure 34). Despite the fact that resulting dataset seemed to have a higher error, all the data points showed lower yield obtained in this experiment as compared to standard. This suggested that a degree of product inhibition could indeed be taking place.

Figure 34 Product inhibition study

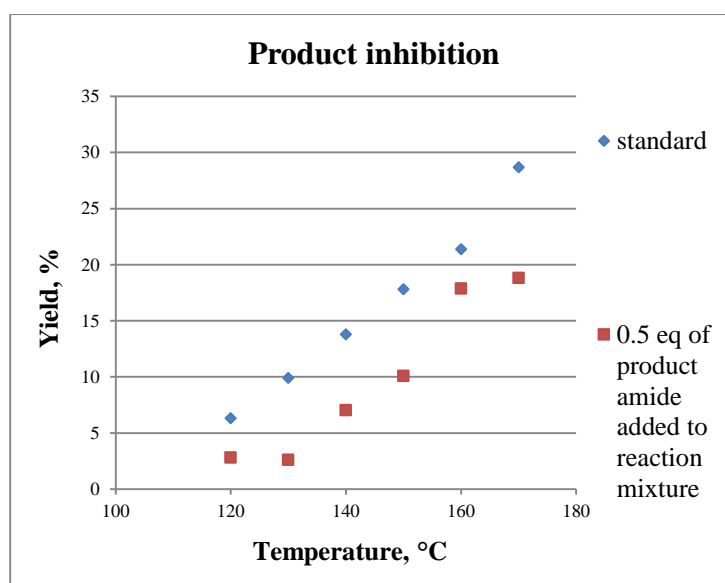
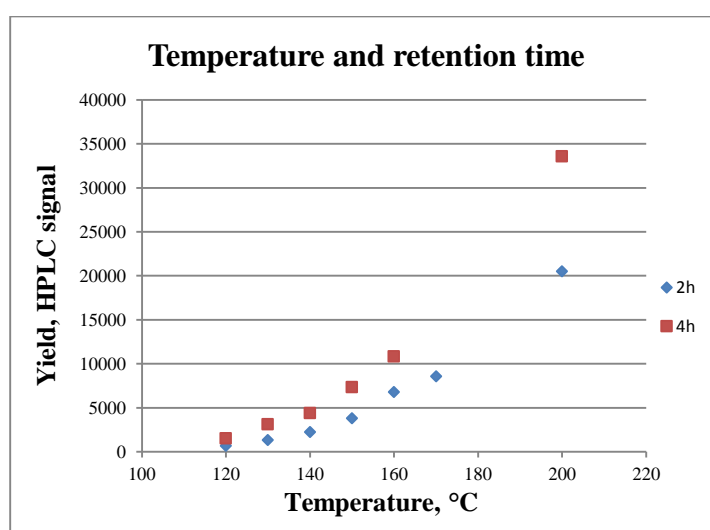


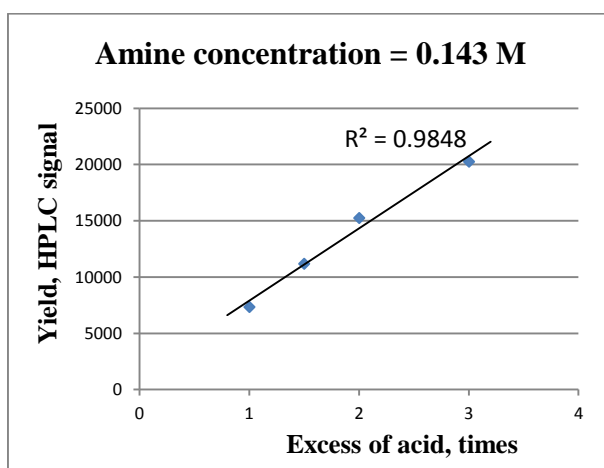
Figure 35 Temperature and retention time impact on amide yield in PhCOOH (0.143 M) – PhCH₂NH₂ (0.143 M) system



It was also decided to check whether the trends observed for this reaction were the same for other acid – amine systems. Benzoic acid – benzylamine reaction could

be analysed in microwave reactor, because ammonium salt formation at r.t. was not problematic, as it quickly dissolved when the mixture was heated. The temperature dependence (Figure 35) was not linear, but the yield linearly depended on adding an excess of benzoic acid (Figure 36), just as in the 4-phenylbutyric acid – benzylamine system (Figure 33, red points).

Figure 36 Dependency of amide yield on excess of carboxylic acid



In order to better understand the mechanism of this transformation, a kinetic study was attempted. MeCN was selected as solvent, as it is polar enough to measure pseudo-pH of reaction mixtures, and the amide yields are low enough for initial rate measurement.

In order to measure only the yields in the linear part of the kinetic profile, conditions and concentrations were adjusted to maintain yields observed under 10% (PhCH₂NH₂, Ph(CH₂)₃COOH, MeCN, 1-4 h reaction time, no stirring). Previous studies showed a quite complex impact of varying amine concentration on amide yields, while dependency on carboxylic acid excess appeared more clear. Thus, a study was carried out when benzylamine concentrations were maintained at the same level of 0.0715 M, 4-phenylbutyric acid concentration was varied between 0.0536 and 0.143 M and yields were measured at different reaction times. The results are shown in Figure 37, and linear approximations allowed plotting initial rates versus acid concentration, as shown in Figure 38.

Unfortunately, the obtained dependency could not be approximated as neither linear nor squared equation (2nd power trendline showed on graph). This can be explained by the existence of other processes happening in the same system, as discussed above. For example, it might be that amide formation is first or second order based upon the carboxylic acid dimer **183**, but its concentration will depend on

concentration of free carboxylic acid, which in its turn depends on ammonium salt concentration. The latter will be influenced by the ratio of carboxylic acid/amine, and the actual concentration of active species can remain obscure, thus not allowing identification of the order of this reaction in attempted study.

Figure 37 Concentration study for amide formation (PhCH_2NH_2 , $\text{Ph}(\text{CH}_2)_3\text{COOH}$, MeCN)

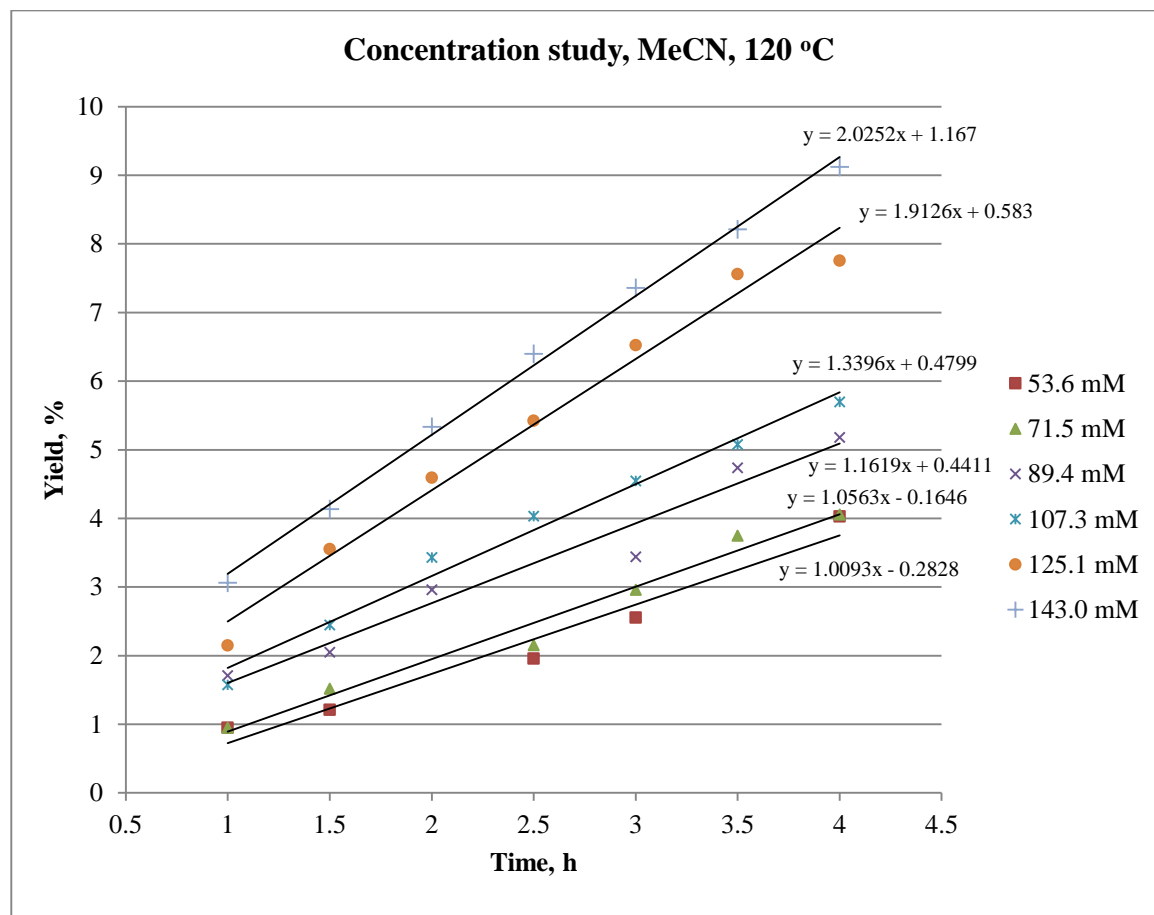
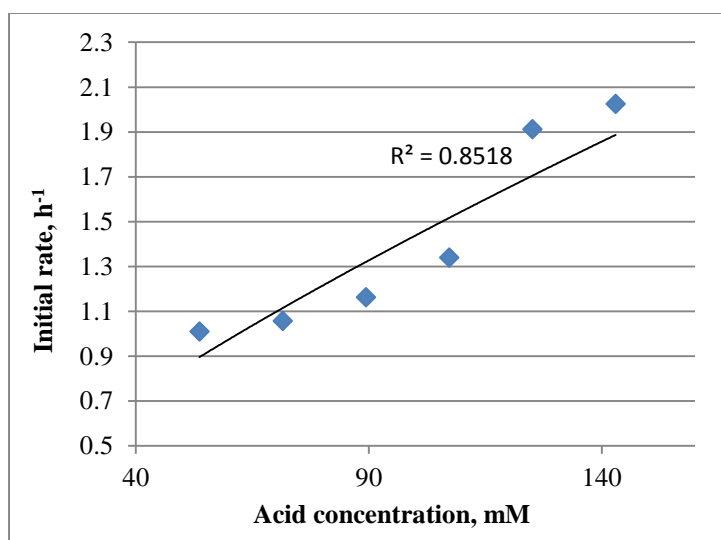


Figure 38 Plotting initial rates vs carboxylic acid concentration

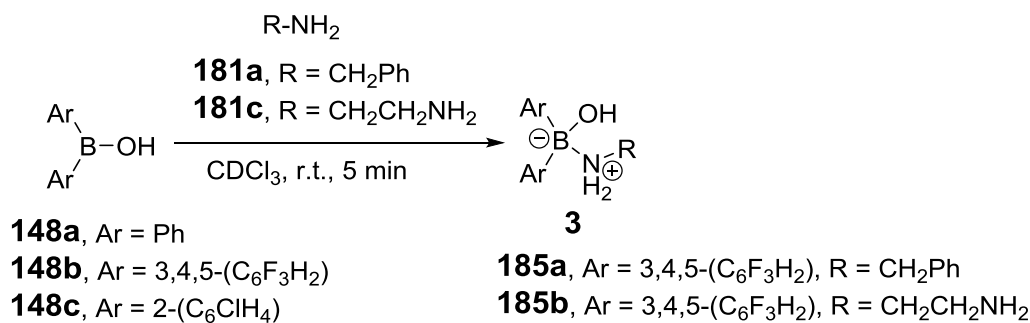


2.3.2. Boron-catalysed direct amide formation

2.3.2.1. Interactions of borinic and boronic acids with amines

Borinic acids **148a-c** were found to interact with benzylamine **181a** and ethylenediamine **181c** at r.t. in DCM or CDCl₃ (Scheme 43). ¹¹B NMR indicated in all cases that a boron “ate”-complex was formed (Figure 39), and when bis-3,4,5-trifluorophenylborinic acid **148b** was used, the products **185a-b** crystallised and were isolated, allowing X-ray structure verification (Figure 40). This suggested that Lewis adducts **185** were formed in all cases. In case of **185a**, the dimeric coordination *via* NH···O hydrogen bonding in solid state was observed (Figure 40).

Borinic acids also interacted with N-Me benzylamine, and ¹¹B NMR indicated formation of an “ate”-complex, but ¹H NMR suggested that multiple species were formed. No products were isolated from these experiments.



Scheme 43 Reactions between borinic acids **148a-c** and amines at r.t.

Figure 39 A general picture observed in ¹¹B NMR in all cases of mixing borinic acids **148a-c** with amines **181a, c**

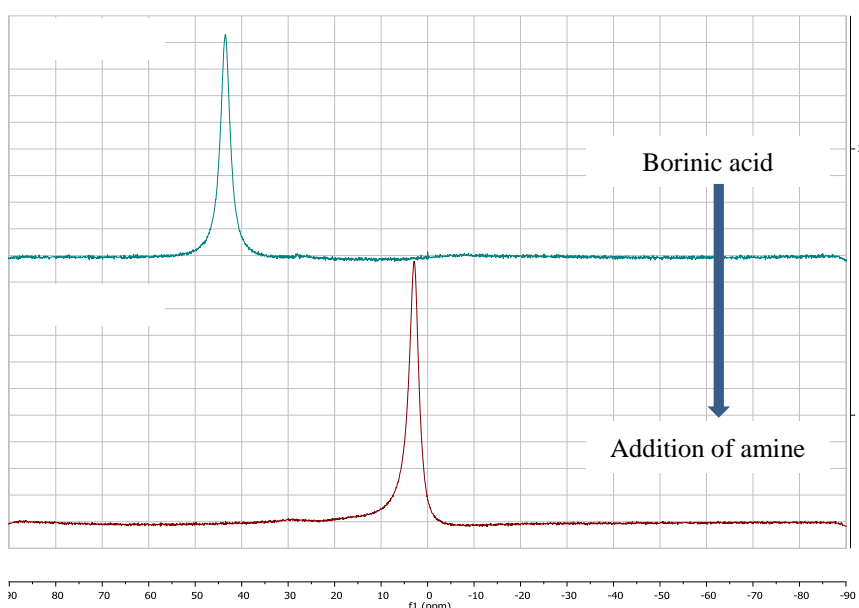
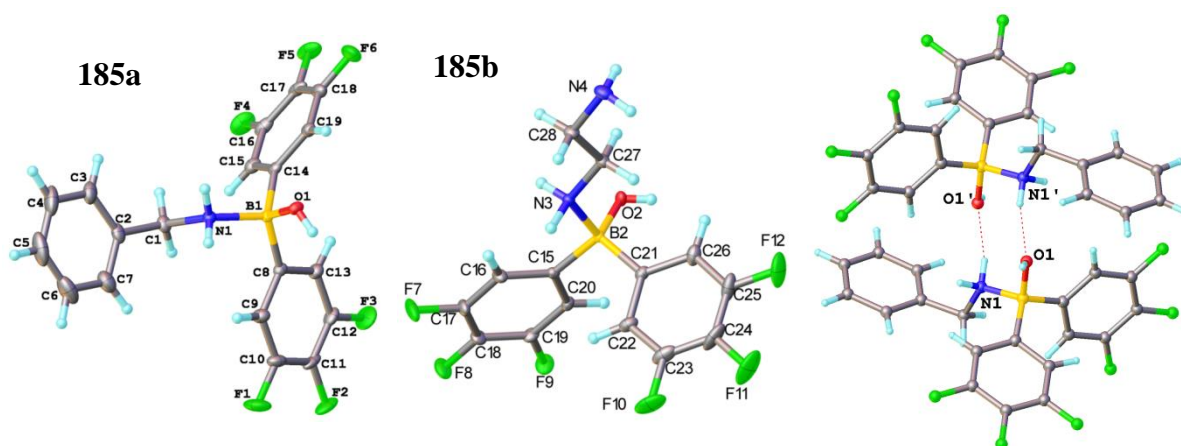
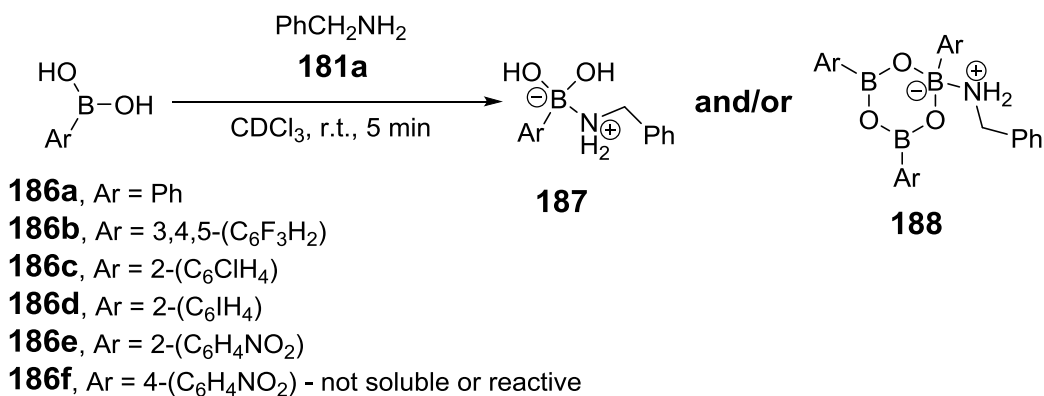


Figure 40 X-Ray structures of Lewis adducts **185a-b** and dimeric coordination *via* hydrogen bonding in **185a**



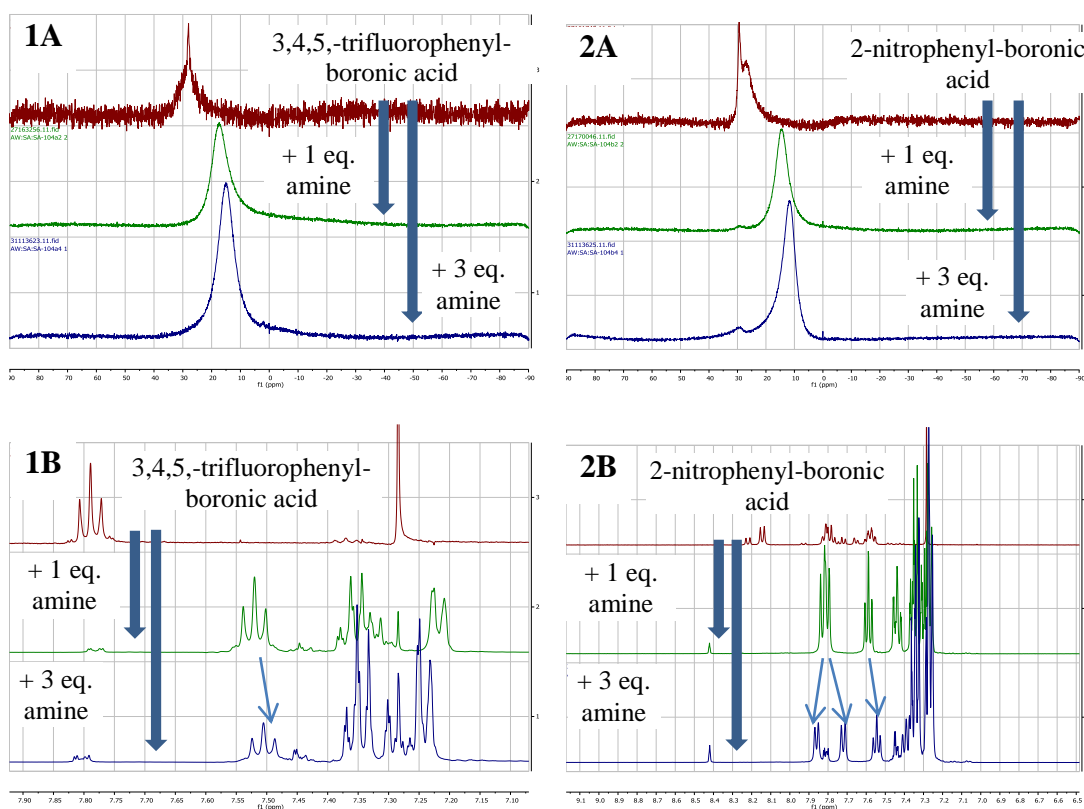
Multiple boronic acids were used in the study of their interaction with amines. Phenyl- **186a**, 3,4,5-trifluorophenyl- **186b**, and 4-nitrophenylboronic **186f** acids were not sufficiently soluble in chloroform. 2-nitrophenyl- **186e** and particularly 2-chlorophenyl- **186c** and 2-iodophenylboronic acids **186d** showed better solubility. It is also worth noting that boronic acids can form different boroxines, i.e. cyclic (RBO)₃ (see below for structures) species, during storage and those are the common impurities, often appearing in ¹¹B NMR at the same 30 ppm region as boronic acids.

Interaction of boronic acids **186** with 1 equivalent of benzylamine **181a** in all cases, apart from 4-nitrophenylboronic acid **186f**, resulted in greatly improved solubility of the boronic acids in chloroform and partial coordination of amine to boronic species was observed by a shift in ¹¹B NMR from 30 ppm to the region of 15-20 ppm in all cases (Figure 41, 1A, 2A). An additional result supporting that this is an equilibrium Lewis adduct coordination, was the interaction between 1 equivalent of 3,4,5-trifluorophenylboronic acid **186b** and 3 equivalents of benzylamine. It showed a further shift of ¹¹B NMR signal to lower field (Figure 41, 1A), and indicated a further shift of ¹H signal of aromatic C-H of boronic acid to lower field as well (Figure 41, 1B), suggesting a shift of equilibrium between free boronic species and Lewis adduct to the latter. When *o*-nitrophenylboronic acid was used, the same tendency in ¹¹B NMR was seen (Figure 41, 2A), however, in the ¹H NMR, the shifts were different and could not be rationalised (Figure 41, 2B). It should be noted, however, that this data also suggests that boroxine formation with one or more coordinated molecules of amine, quickly exchanging between boron centres, is possible. It was impossible to identify whether **187** or **188** was the main species in these reactions.



Scheme 44 Reactions between boronic acids **179a-e** and amines at r.t.

Figure 41 ¹¹B (**1A**, **2A**) and ¹H (**1B**, **2B**) NMRs of reactions between 3,4,5-trifluorophenyl boronic acid (**1A**, **1B**) and 2-nitrophenylboronic acid (**2A**, **2B**) with 1 and 3 equivalents of benzylamine in CDCl₃ at r.t.

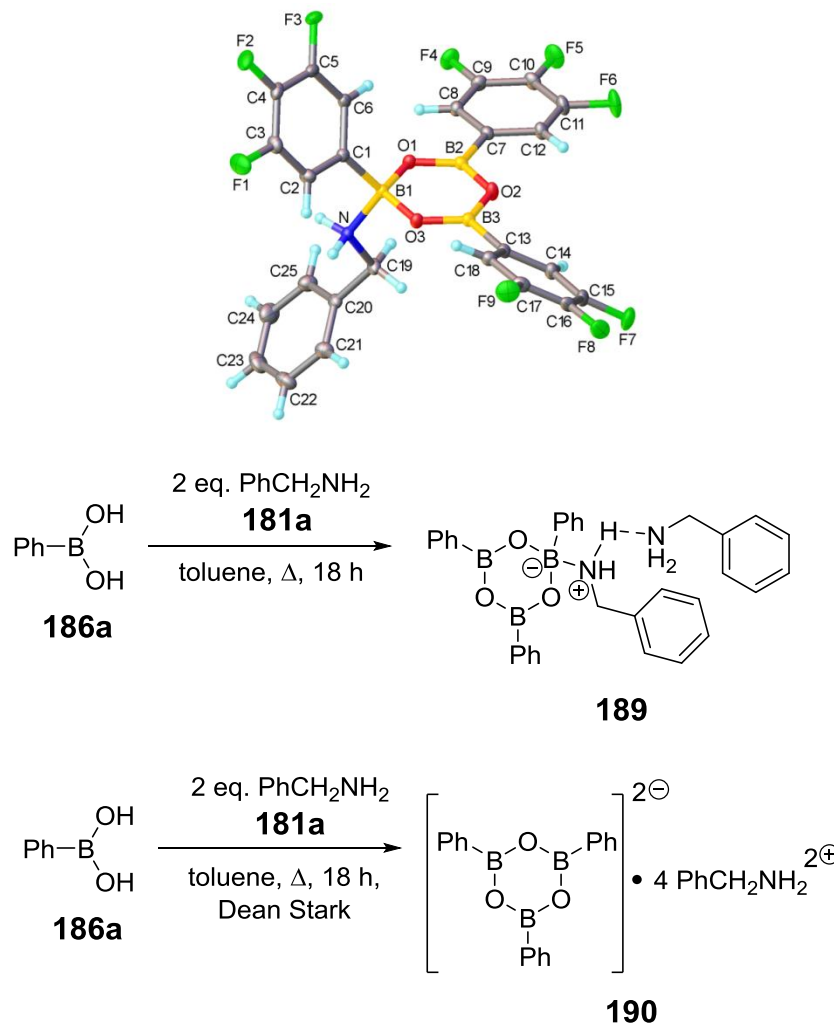


Over 2 days complex **188a** of boroxine with 1 molecule of benzylamine crystallised out from the mixture of 3,4,5-trifluorophenylboronic acid **186b** and benzylamine **181a**, and was characterised by X-Ray (Figure 42). Analogous result was obtained with ethylenediamine **181c**.

Another transformation was attempted: phenylboronic acid **186a** was refluxed with 2 equivalent of benzylamine **181a** in toluene for 18 hours (Scheme 45), and from the obtained oil, crystals of boroxine adduct **189** with 2 molecules of benzylamine

were formed (Figure 43). When the same reaction was conducted with Dean-Stark water removal apparatus, a different complex **190** of boroxine with 4 molecules of benzylamine was formed (Figure 43).

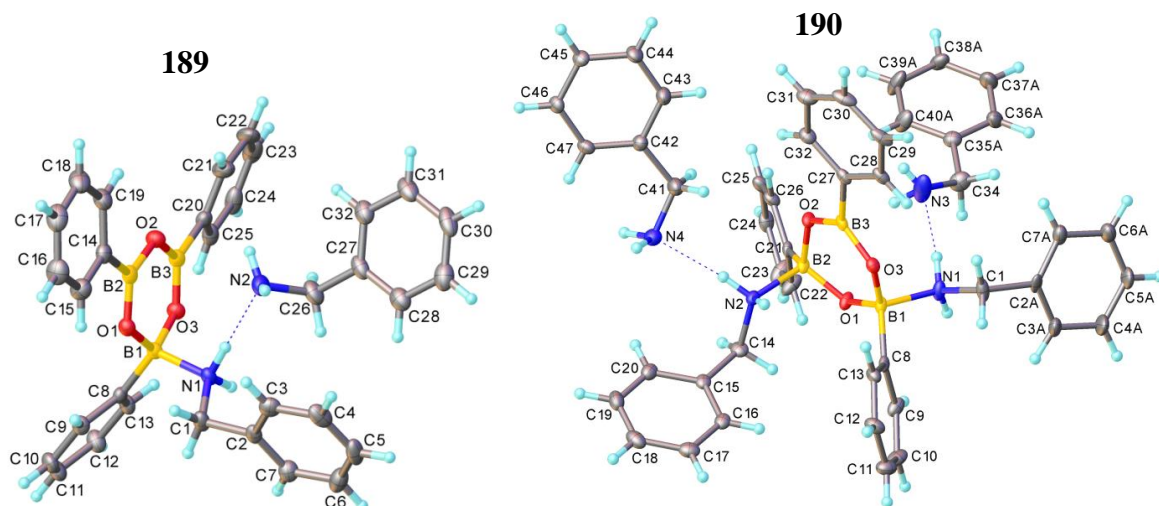
Figure 42 3,4,5,-trifluorophenylboroxine adduct with benzylamine **188a**



Scheme 45 Interactions between boronic acids and benzylamine, yielding boroxine-amine Lewis complexes

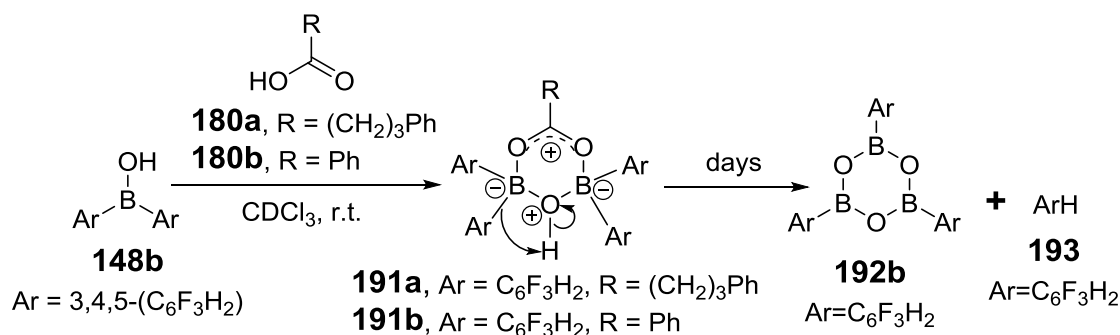
It should be mentioned, that these compounds could only be crystallised in the presence of excess of benzylamine, and removing the latter was not possible, thus the isolated yields could not be reported. The crude yields were 97-98%. Excess of benzylamine also made NMR analysis more difficult, whereas when mixed stoichiometrically with 2 or 4 equivalents of benzylamine, boroxines were not sufficiently soluble in CDCl_3 . Inability to reproduce the crystallisation of complex **189** led to lack of analytical data for this compound.

Figure 43 X-Ray structures of boroxine-amine Lewis adducts **189** and **190**



2.3.2.2. Interactions of borinic and boronic acids with carboxylic acids

Bis-3,4,5-trifluorophenylborinic acid **148b** was reacted with 4-phenylbutyric acid **180a** and benzoic acid **180b** (Scheme 46). In both cases, after 5 minutes of mixing, ^{11}B NMR showed partial formation of “ate”-complex and a small amount of boronic species (Figure 44). However, over the period of 6 days borinic acid completely protodeboronated and only boronic species could be seen, boroxine **185b** crystallised from the reaction mixtures and 1,2,3-trifluorobenzene **186** was formed.



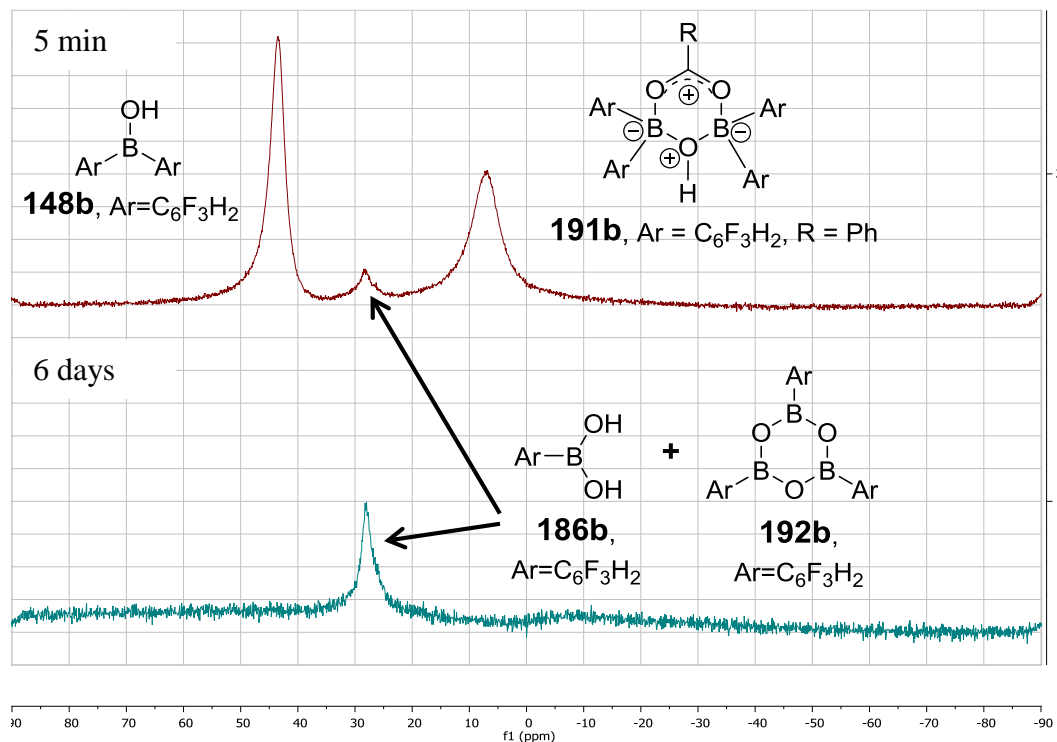
Scheme 46 Interactions between borinic acid **148b** and carboxylic acid **173a**

It is supposed that the reaction proceeds through intermediates **184**. The analogous cyclic boroxine-carboxylate compound was reported before with pentafluorophenyl substituents on the boron atoms.¹⁷⁴ Another result, that generally supported the possibility of **191a** formation, was a peak in the accurate mass spectrum of a different complex **195a** (see below) at 725.1340 (Calcd. 725.1343).

In general, it was difficult to observe interactions between boronic acids **186** and carboxylic acids **180**. No change was observed upon mixing 3,4,5-

trifluorophenyl- or 4-nitrophenylboronic acids with 4-phenylbutyric acid, but this was probably due to low solubility of these boronic acids in chloroform.

Figure 44 ^{11}B NMRs of a mixture of bis-3,4,5-trifluorophenylboronic acid **148b** with benzoic acid after 5 min and 6 days upon mixing.



In the case of 2-nitrophenylboronic acid **186e**, no immediate conclusion could be made on its reactivity towards 4-phenylbutyric acid **180a**. ^{11}B NMR showed a slight change upon mixing the two compounds; however, the main signal position remained the same (Figure 45). ^1H NMR spectrum showed disappearance of boronic OH signal and loss of resolution of boronic acid aromatic protons signals, however, their position remained the same and the shift of aliphatic CH₂ protons signals of carboxylic acid was too small to make any conclusion (Figure 46). Upon heating, the solubility of the boron-containing compound(s) significantly increased, and a set of aromatic signals slightly different from starting boronic acid signals appeared. It is also worth noticing, that broad peak of carboxylic COOH proton remained seen in the ^1H NMR over the course of the reaction. ^{11}B NMR also indicated some protodeboronation occurring over 2 days of heating, with the formation of borate species.

A ReactIR study was conducted for a stoichiometric reaction between phenylboronic acid **148a**, benzylamine **181a** and 4-phenylbutyric acid **180a**. It was noticed that upon mixing carboxylic and boronic acids some interaction occurred, as

seen by appearance of two new species in the region of 1630 cm^{-1} and 1670 cm^{-1} (Figure 47, pink).

Figure 45 ^{11}B NMR results of 2-nitrophenylboronic acid interaction with 4-phenylbutyric acid.

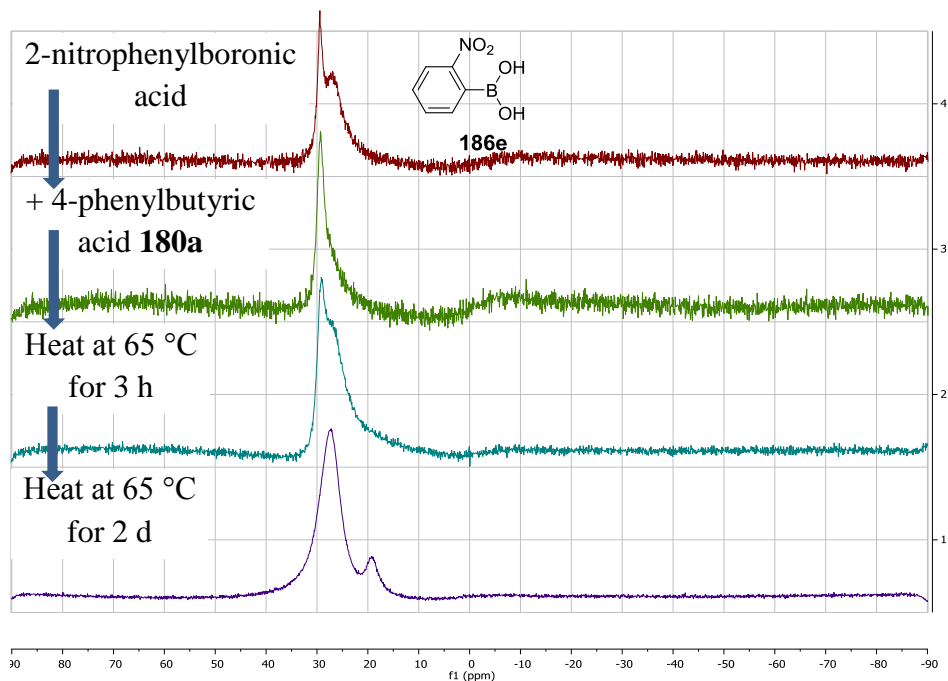
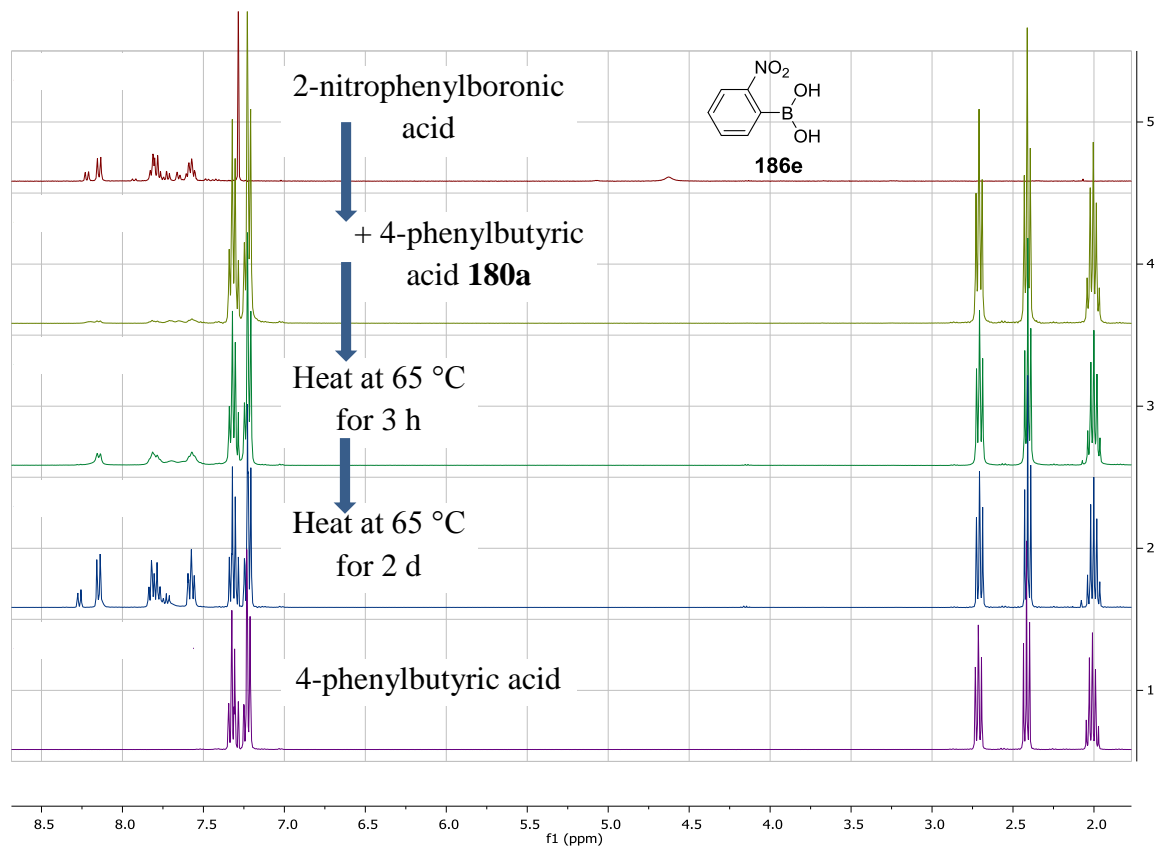


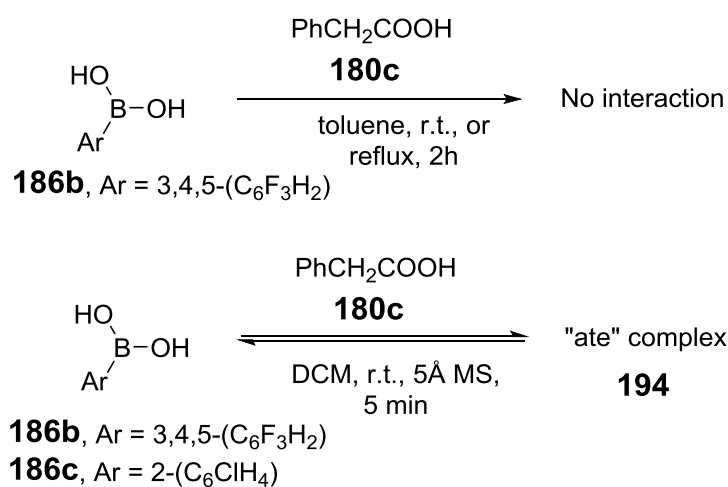
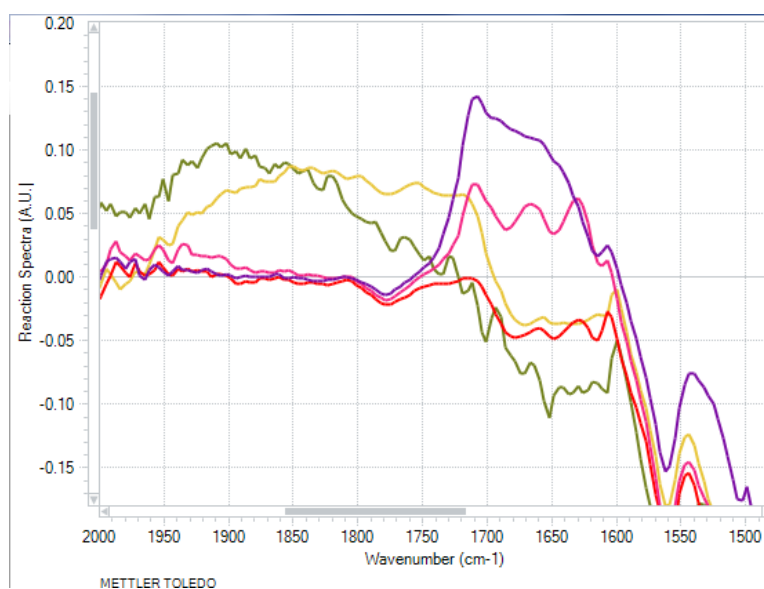
Figure 46 ^1H NMR results of 2-nitrophenylboronic acid interaction with 4-phenylbutyric acid.



Their intensity reduced upon addition of the amine (Figure 47, red), and completely disappeared upon heating, while the amide peak at the 1600 cm⁻¹ appeared (Figure 47, yellow, green). Unfortunately, this unusual result could not be reproduced and subsequent studies suggested a lack of interaction of phenylboronic acid **148a** with carboxylic acid in such systems.

Another ReactIR test between 3,4,5-trifluorophenylboronic acid **186b** and phenylacetic acid **180c** (Scheme 47) showed a total absence of any interactions between these two compounds at r.t., during and after 2 h of reflux. All the NMR data suggested that **186b** and **180c** remained totally unreacted.

Figure 47 ReactIR data on interactions between phenylboronic acid, benzylamine and 4-phenylbutyric acid. Purple: starting carboxylic acid. Pink: addition of benzenboronic acid. Red: addition of amine. Green: 5 min of reflux. Yellow: 2 h of reflux.

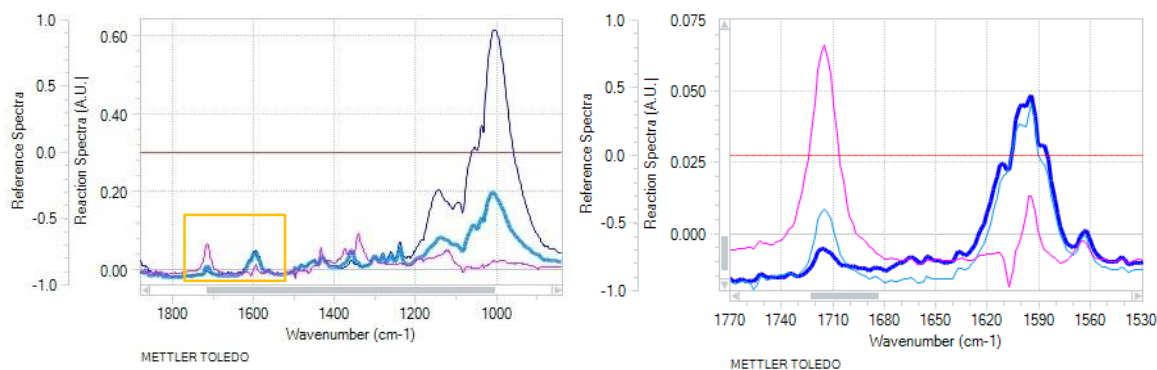


Scheme 47 Boronic acids **186b-c** interactions with carboxylic acid **180c**

On the other hand, both 3,4,5-trifluorophenylboronic acid **186b** and 2-chlorophenylboronic acid **186c** reacted with phenylacetic acid **180c** at r.t. in the presence of 5Å MS. The IR showed a shift of carbonyl peak of carboxylic acid from 1710 cm⁻¹ region to 1590-1600 cm⁻¹ (Figure 48).

In order to better understand the nature of this reaction, a similar process was conducted in an NMR tube. Addition of 5Å MS to a mixture of boronic acid and carboxylic acid, and addition of 5Å MS to the boronic acid, followed by adding carboxylic acid, produced identical NMR spectra. Also, mixing carboxylic acid with boronic acid showed no changes in ¹¹B NMR, and ¹H NMR suggested absence of interactions between components until 5Å MS are introduced.

Figure 48 ReactIR indication of boronic **186c** and carboxylic acids interaction. Pink: a mixture of carboxylic acid and boronic acid. Light blue: addition of 5Å MS. Dark blue: addition of more 5Å MS.



Figures 49a and 50a show the ¹¹B and ¹H NMR spectra for 2-chlorophenylboronic acid **186c**. The signals changed as 5Å MS were introduced (Figures 49b, 50b). A similar picture was observed after refluxing **186c** in toluene for 2 h with Dean-Stark apparatus, a common setup for boroxine synthesis, thus it was assumed that the species observed after 5Å MS addition to boronic acids (similar effect was observed for **186a-b**) were the corresponding boroxines **192**.

If boronic acid and carboxylic acid were premixed, the addition of a tiny bit of 5Å MS led to partial formation of boroxine (Figures 49c, 50c). This, along with the observation that boroxine signals remain in the mixture throughout, suggested that boroxine formation occurs prior to any other interactions, and that boroxine is always in equilibrium in such systems, in some cases even before 5Å MS addition. The addition of further amounts of 5Å MS led first to the appearance of the “ate”-complex signal at 4 ppm (Figures 49d, 50d), and even bigger amounts allowed a further equilibrium shift from boroxine to this complex (Figures 49e, 50e).

Figure 49 ^{11}B NMR spectra showing interactions between 2-chlorophenylboronic acid **186c**, phenylacetic acid **180c** and 5 Å MS. A: 2-chlorophenylboronic acid **186c**; B: addition of 5 Å MS to (A); C: addition of a tiny amount of 5 Å MS to a mixture of boronic and carboxylic acid; D: addition of more 5 Å MS; E: addition of even more 5 Å MS

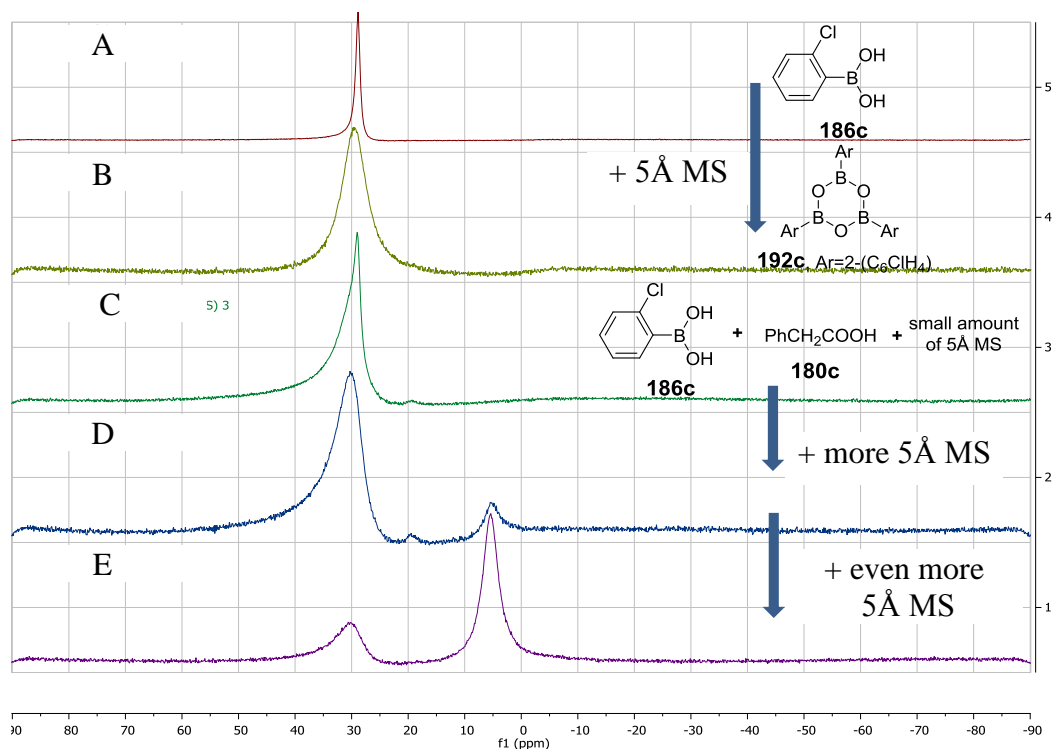
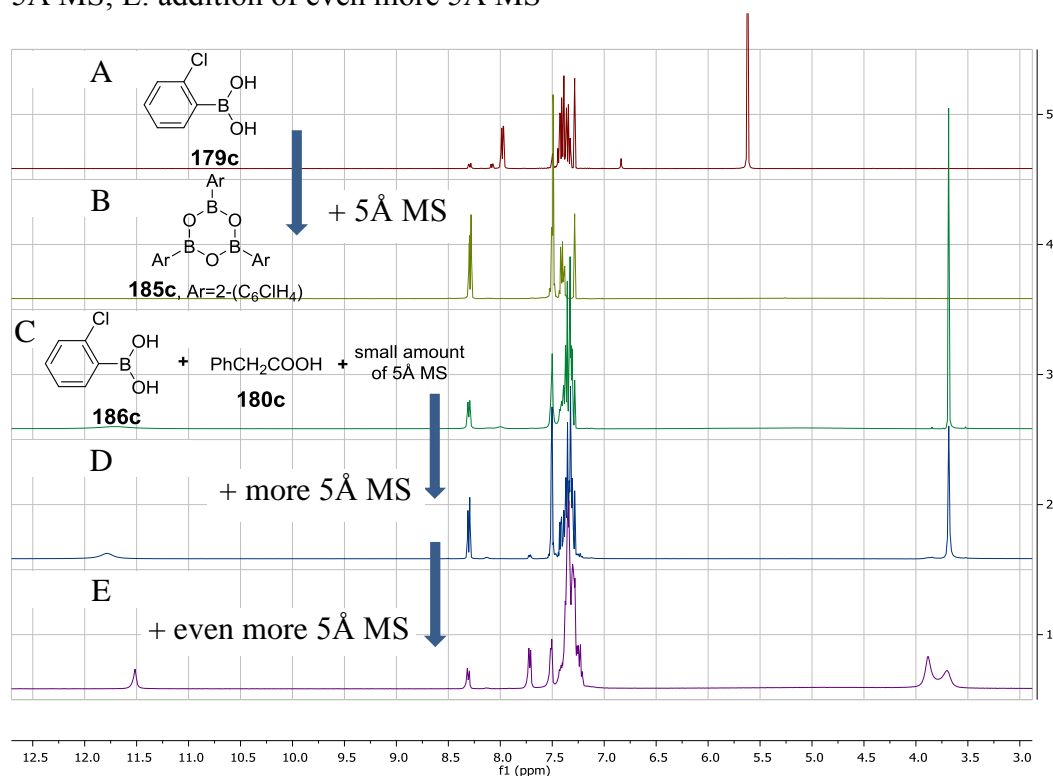


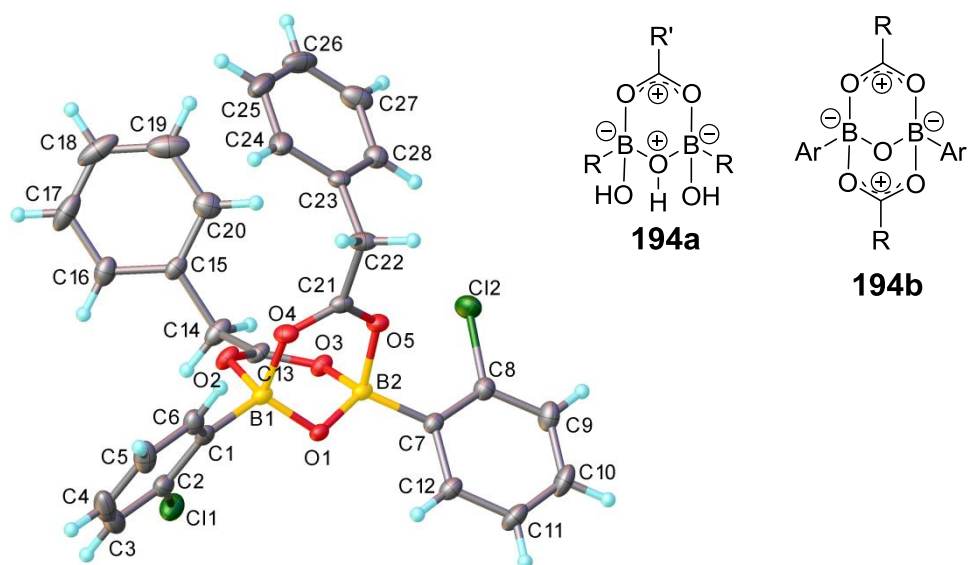
Figure 50 ^1H NMR spectra showing interactions between 2-chlorophenylboronic acid **186c**, phenylacetic acid **180c** and 5 Å MS. A: 2-chlorophenylboronic acid **186c**; B: addition of 5 Å MS to (A); C: addition of a tiny amount of 5 Å MS to a mixture of boronic and carboxylic acid; D: addition of more 5 Å MS; E: addition of even more 5 Å MS



It should be noted, that an excess of the carboxylic acid also shifted the equilibrium in this reaction to the “ate”-complex, however, 5 Å MS had a much more profound impact. Over prolonged periods of time mixtures slowly decomposed, forming boric (B(OR)₃) species, as suggested by ¹¹B NMR.

These observations allowed us to propose 2 possible structures for complex **194** (Figure 51). The system 2-chlorophenylboronic acid **186c** – phenylacetic acid **180c** – 5 Å MS – CHCl₃ was kept under inert atmosphere in a bigger flask containing pentane. The solvent exchange allowed crystallisation, and the isolated monocrystal was analysed with X-ray, the result of which (Figure 51) proved our suggestion of **194b** structure to be correct.

Figure 51 Suggested structures of complex **194** and the X-ray analysis result



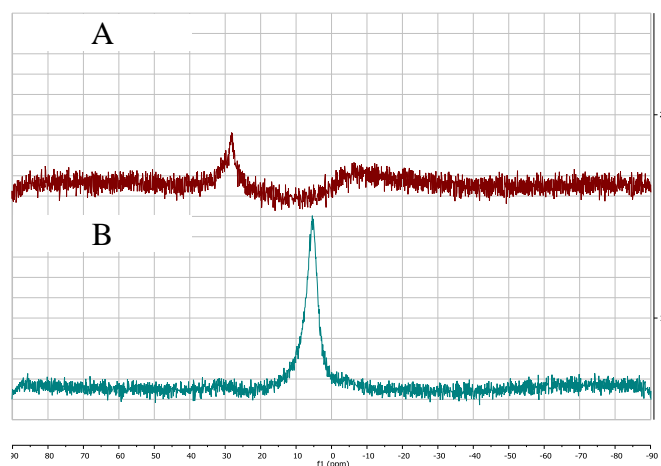
It should also be noted, that in the presence of 4 Å MS < 10% of complex **194b** was formed, suggesting that 5 Å MS pore size is probably ideal for orchestration of such transformation.

Interestingly, phenylacetic acid **180c** was able to significantly increase the solubility of 3,4,5-trifluorophenylboronic acid **186b**, which is barely soluble in chloroform, through formation of similar species **194** (Figure 52). A similar picture was observed between benzoic acid and 2-chlorophenylboronic acid, indicating that other carboxylic acids can also coordinate to boronic acid in this way.

Attempts were made to isolate analogous B-O-B dicarboxylates of type **187b**. Attempts with phenylboronic acid and 3,4,5-trifluorophenylboronic acid only yielded crystalline boroxines, while success was achieved with 2-iodophenylboronic acid (see Appendix 1). These findings underlined the importance of *ortho*-substituent in

arylboronic acids, especially for crystallisation. Without such *ortho*-substituent corresponding boroxines are not destabilised and act as a thermodynamic sink, crystallising out from solution and dragging the equilibria away from the “ate”-complex.

Figure 52 3,4,5-trifluorophenylboronic acid **186b** (A) is transformed to “ate”-complex **194** with phenylacetic acid **180c** (B) and its solubility in CDCl₃ is increased.

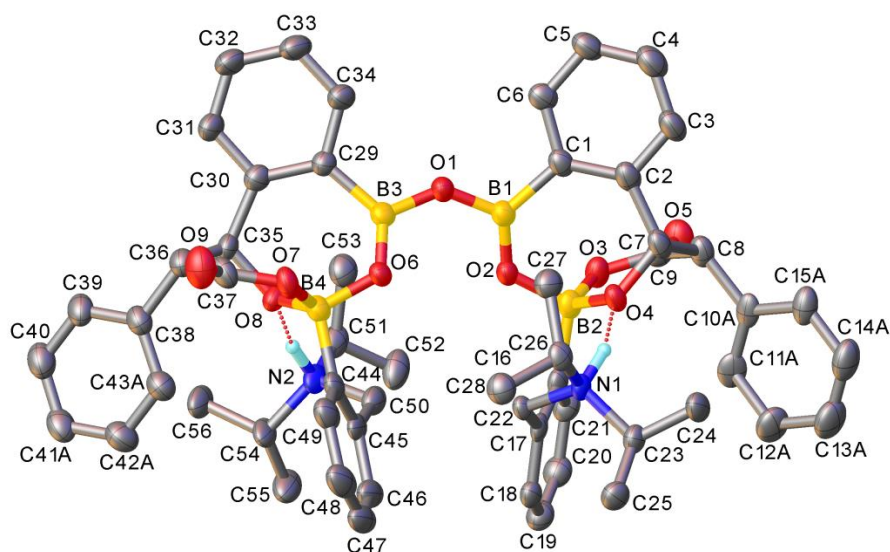


Finally, when *N,N*-diisopropyl-2-(aminomethyl)phenylboronic acid¹⁷⁵ was used under the same conditions, no crystallisation initially occurred, however, after a week a very small amount of crystals was obtained. X-ray analysis identified the unexpected structure (Figure 53). Crystals quickly decomposed and could not be characterised, but ¹H NMR of the mixture showed weak (< 1%) peaks which could be attributed to the CH-CH₂ protons of the newly formed C-C bond. Initially, it was suggested, that this is the result of borylation of the carboxylic acid reductive dimer, however, later we came to conclusion that it is more likely that a benzylic attack had occurred on the boronic acid, leading to elimination of diisopropylamine, which can be protonated, as seen from the X-ray. However, the formation of hydroxyl group on the same carbon remains not understood.

This result underlined once again the complexity of systems, containing boron compounds and the need for their thorough and in-depth investigation. Many species can be formed in such systems on smaller scale, and some of them might potentially play catalytic role too.

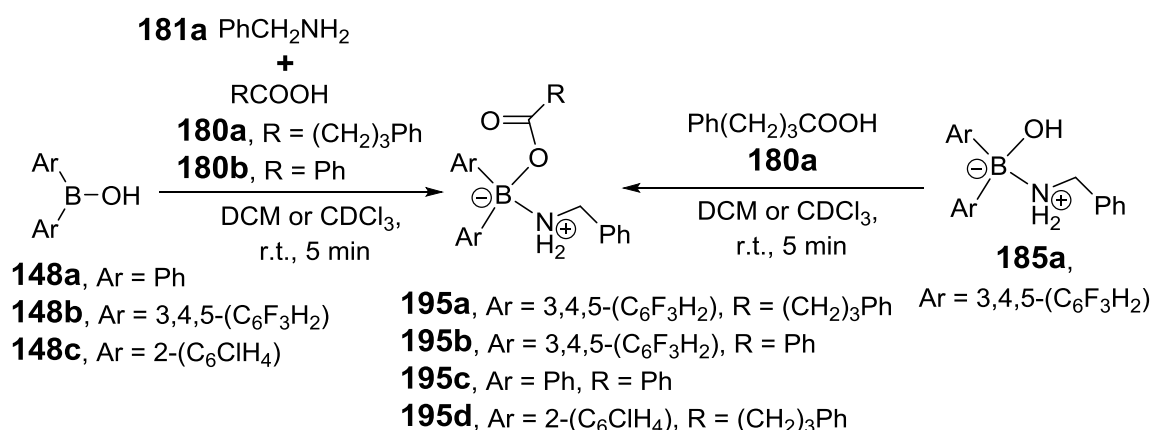
The formation of remarkable complexes **194** opened a new suggestion for the possible mechanism of boronic-acid catalysed direct amide formation (this reaction is always performed in presence of molecular sieves), which is discussed in chapter 2.3.2.5.

Figure 53 X-ray analysis of product that crystallised from the mixture of *N,N*-diisopropyl-2-(aminomethyl)phenylboronic acid, phenylacetic acid and 5 Å MS in CHCl₃/pentane.



2.3.2.3. Interactions of borinic and boronic acids with carboxylic acids and amines

Borinic acids **148a-c** were reacted with 1 equivalent of carboxylic acids **180a-b** and 1 equivalent of benzylamine **181a** (Scheme 48). In under 5 minutes, the “ate”-complexes **195** were formed, and many of them crystallised after slow evaporation, allowing X-ray identification of these products as amino-carboxylate borinic complexes (Figure 54). The NMR data supported this conclusion. It is important to note that reacting preformed amine-boronic acid Lewis adduct **185a** with carboxylic acid gives the same product **195a** (Scheme 48).

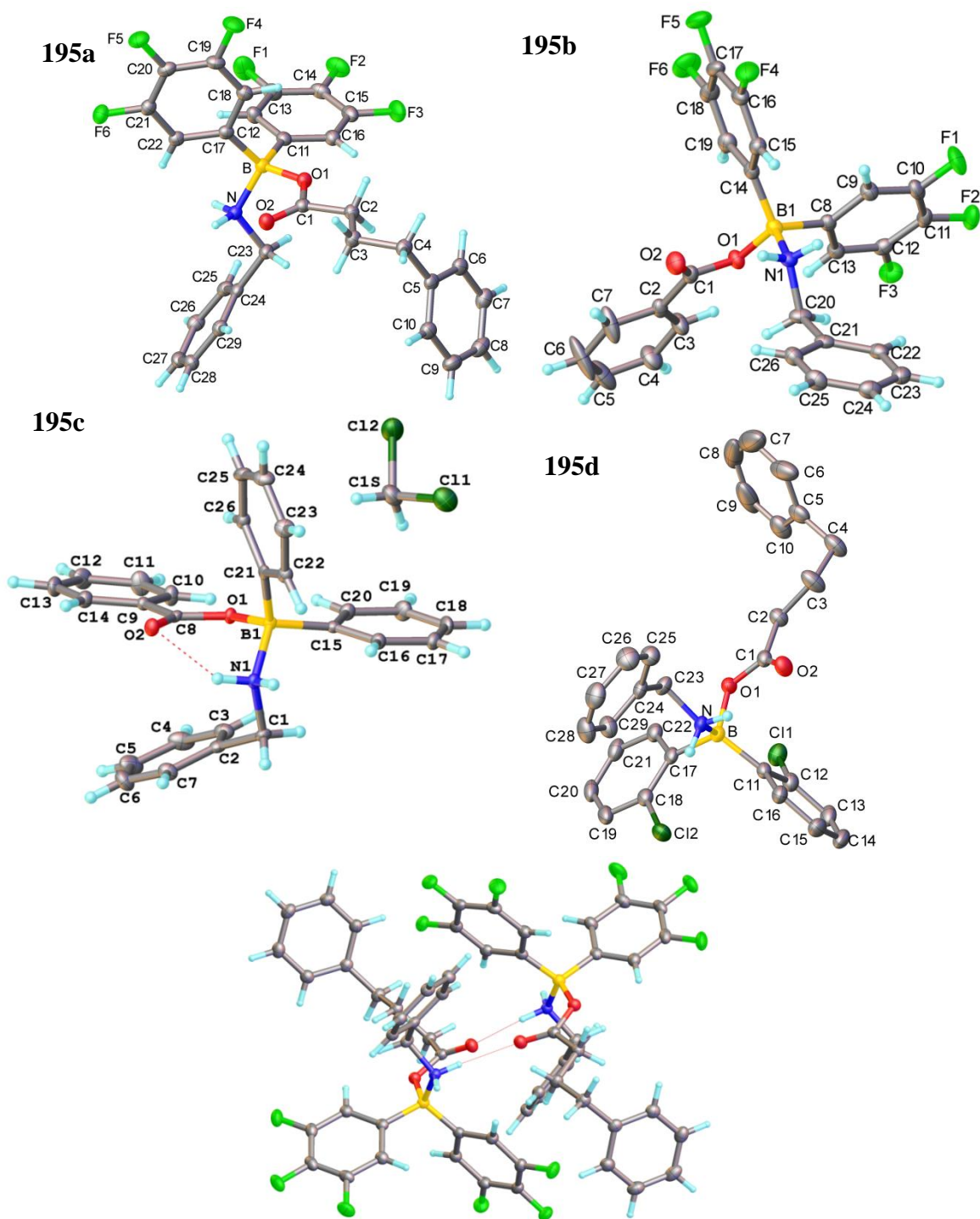


Scheme 48 Formation of amino-carboxylic borinic complexes **195**

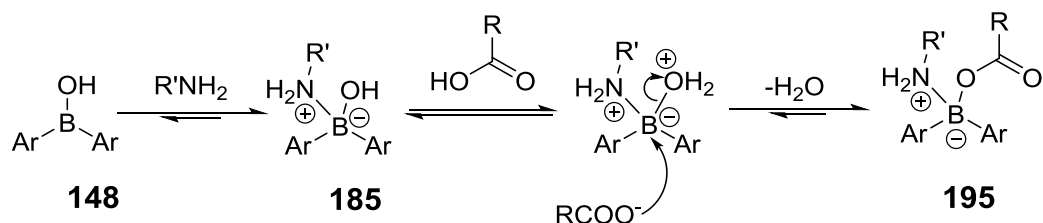
This observation allowed us to suggest a mechanism, where amine attacks borinic acid first, and an S_N2-like attack of carboxylate follows (Scheme 49).

The aminocarboxylate complex **195c** was less stable in solution, most likely due to reduced electrophilicity of boron centre. It existed in equilibrium with, supposedly, carboxylic acid and amine, their ammonium salt and other compounds, which made NMR analysis difficult.

Figure 54: X-ray structures of amino-carboxylate borinic complexes **195** and example of dimeric coordination *via* hydrogen bonding in **195a**



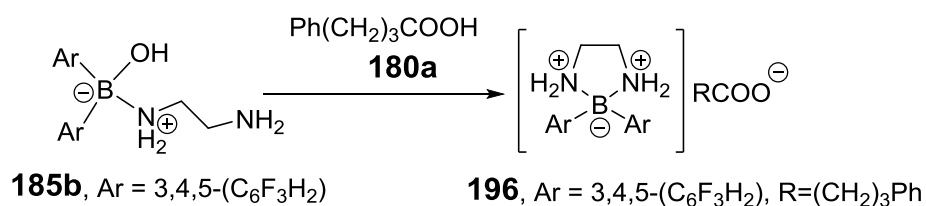
Borinic acid **148b** was also reacted with benzylamine and *para*-toluenesulphonic acid, however, complex was not formed in this case.



Scheme 49 Suggested mechanism of complex **195** formation

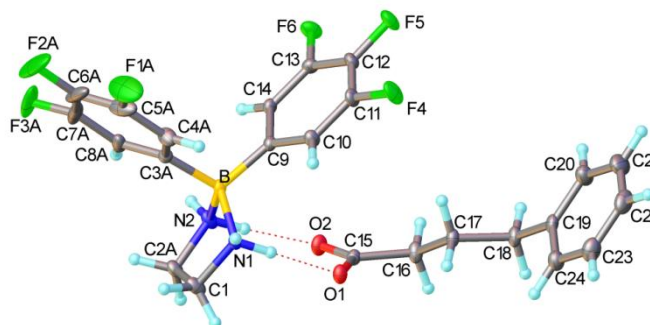
It seems that carboxylate group in these amino-carboxylate complexes **188** is activated and can undergo nucleophilic attack by an amine to yield an amide (see for S_N1 and S_N2 reactions at boron in Lloyd-Jones work¹⁷⁶). However, neither reacting these complexes with additional equivalents of amine, nor heating them showed any amide formation. Complex **195a** and showed surprising stability towards 5% aq HCl. Heating **195a** in chloroform at 60 °C did not lead to any change in the NMR spectra. Heating at 60 °C in toluene produced mixed unidentified boronic species. Attempts to deprotonate the ammonium cation in **195a** with excess of Hünig's base or proton sponge failed; these bases did not react with complex **195a** even when heated to 60 °C in chloroform. The complex reacted with $Bu_4NOH/MeOH$ and with Et_4NBr . In both cases, "ate"-complexes of other structures were formed, but were not identified.

A final attempt to force amide formation from complexes **195** was the introduction of a free intramolecular amine group. For this purpose ethylenediamine **181c** was used. As mentioned before (Scheme 43), it interacted stoichiometrically with bis-3,4,5-trifluorophenyl borinic acid **148b** to yield Lewis adduct **185b**, however, reacting this complex with 4-phenylbutyric acid **180a** yielded an unexpected product **196** (Scheme 50), a double Lewis adduct with carboxylate counter-ion, which was doubly coordinated to N-H hydrogens in crystal form (Figure 55). The same identification problems regarding equilibria with multiple other compounds in solution, as mentioned for **195c**, was observed in the case of product **196**.



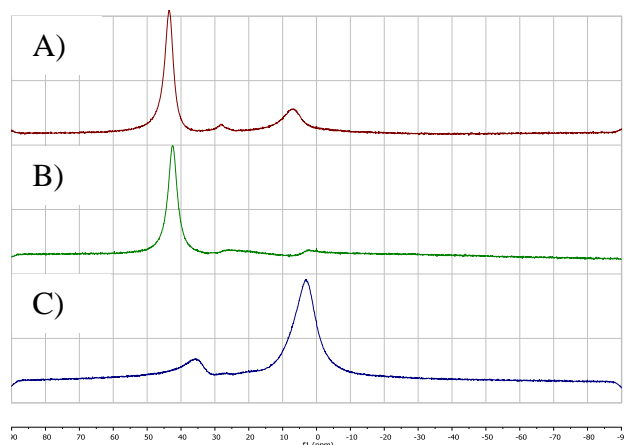
Scheme 50 Formation of double Lewis adduct **196** instead of amino-carboxylic complex **195**

Figure 55 X-Ray structure of unusual complex **196**



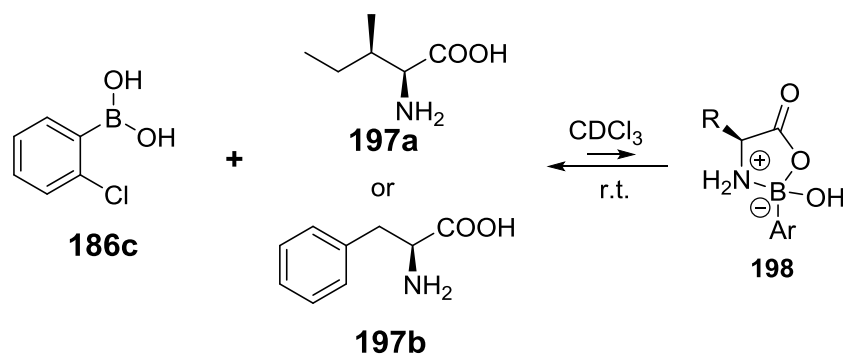
Bis-3,4,5-trifluorophenyl borinic acid **148b** was also reacted with aniline. Because of the significant involvement of the nitrogen lone pair in conjugation with the aromatic ring and its low basicity, the interaction was expected to be weak. Indeed, a barely noticeable amount of complex was generated under these conditions (Figure 56, B), and over time boroxine **192b** crystallised from solution. It has been previously mentioned that the interaction between this borinic acid and 4-phenylbutyric acid **180a** led to partial “ate”-complex formation, however, when all 3 components were mixed together, much more “ate”-complex was formed (Figure 56).

Figure 56 ^{11}B NMR spectra of reactions of $(\text{C}_6\text{F}_3\text{H}_2)_2\text{BOH}$ **148b** with 4-phenylbutyric acid **180a** (A), with aniline (B) and with both 4-phenylbutyric acid and aniline (C).



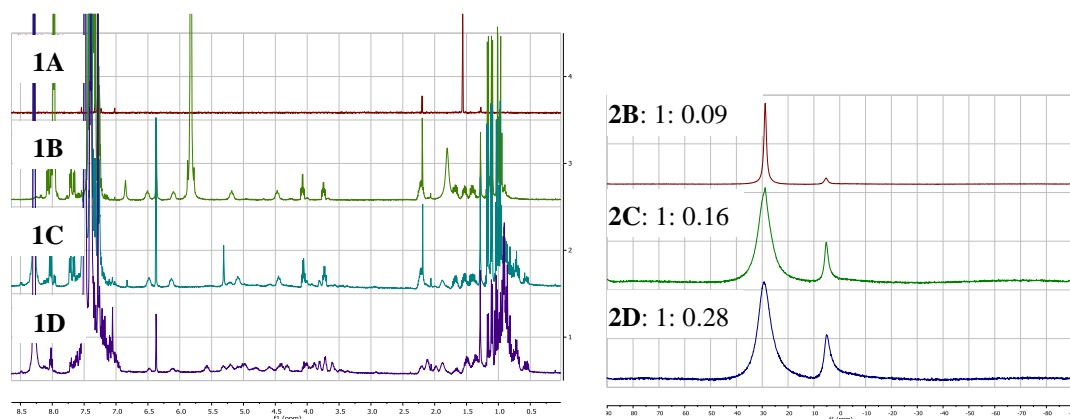
The ^{11}B NMR spectra of reactions of 3,4,5-trifluorophenyl- or 2-nitrophenylboronic acids with benzylamine and 4-phenylbutyric acid in all cases showed a signal around 20 ppm as seen for interaction with amine only. In case of 3,4,5-trifluorophenylboronic acid **186b** the same boroxine-amine adduct **188b**, that was formed when boronic acid was mixed with amine only, crystallised from reaction mixture.

2-chlorophenylboronic acid **186c** was also reacted with aminoacids *L*-isoleucine **197a** and *L*-phenylalanine **197b** in CDCl₃ (Scheme 51). It was reported before¹⁷⁷ that aminocarboxylate cyclic complexes **198** can be formed between aminoacids and boronic acids in DMSO. Our experiment supported this idea. Both aminoacids were virtually insoluble in chloroform (Figure 57, 1A for example with isoleucine), however when 1 equivalent of 2-chlorophenylboronic acid was added, 8% of the “ate”-complex was formed, as seen by ¹¹B NMR (Figure 57, 2B), and in ¹H NMR spectrum signals of aliphatic protons appeared (Figure 57, 1B). The subsequent addition of 5 Å MS pushed this equilibrium further to 14% of “ate”-complex (Figure 57, 1C, 2C), and overnight the ¹H NMR spectrum became more complex (Figure 57, 1D), possibly indicating partial dipeptide formation, while there was already 22% of “ate”-complex(es) in the mixture (Figure 57, 2D). A similar picture was observed for phenylalanine.



Scheme 51 Interaction of 2-chlorophenylboronic acid **186c** with aminoacids **197**

Figure 57 Interaction between isoleucine and 2-chlorophenylboronic acid in CDCl₃. Left: ¹H NMRs, Right: ¹¹B NMRs. **1A**: solid isoleucine in NMR tube with CDCl₃, insoluble. **1B**, **2B**: Addition of 2-chlorophenylboronic acid, aliphatic signals appear. **1C**, **2C**: Addition of 5 Å MS. **1D**, **2D**: Mixture over 16 h.



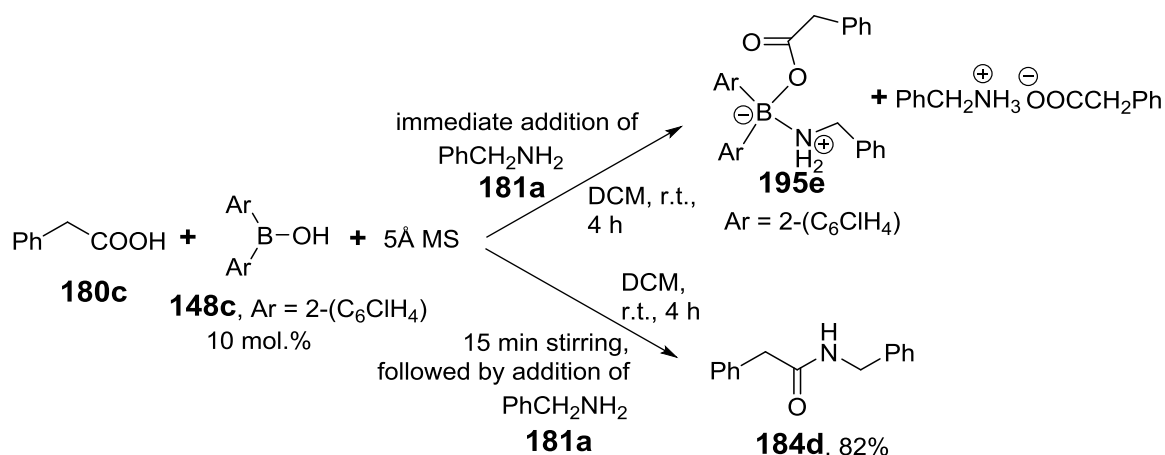
Finally, boric acid B(OH)₃ and its anhydride B₂O₃ were both not soluble in CDCl₃ even after adding benzylamine. Nevertheless, addition of phenylacetic acid to

these mixtures resulted in some “ate”-complex observed in ^{11}B NMR, and its amount increased after the addition of 5Å MS.

2.3.2.4. Borinic and boronic acids in direct amide formation

Borinic acids were not found to have any impact on the direct amide formation reactions. The experiments at elevated temperature gave data that was hard to interpret, but no proof of activity was obtained. The r.t. amidation reaction in the presence of 5Å MS was studied more thoroughly.

In the process of this work, a paper was published,¹⁷⁸ noting that borinic acids are efficient catalysts for amidation reactions and peptide formation. When reproducing published results (Scheme 52), we found the following: if the carboxylic acid **180c** was stirred with catalyst (bis-2-chlorophenylborinic acid **148c**) and 5Å MS in DCM for 15 min, and after this benzylamine **181a** was added (as the published experimental suggests), the reaction proceeded with 82% yield. However, if all the components were mixed simultaneously and no prestir period was applied, there was no conversion to amide at all.

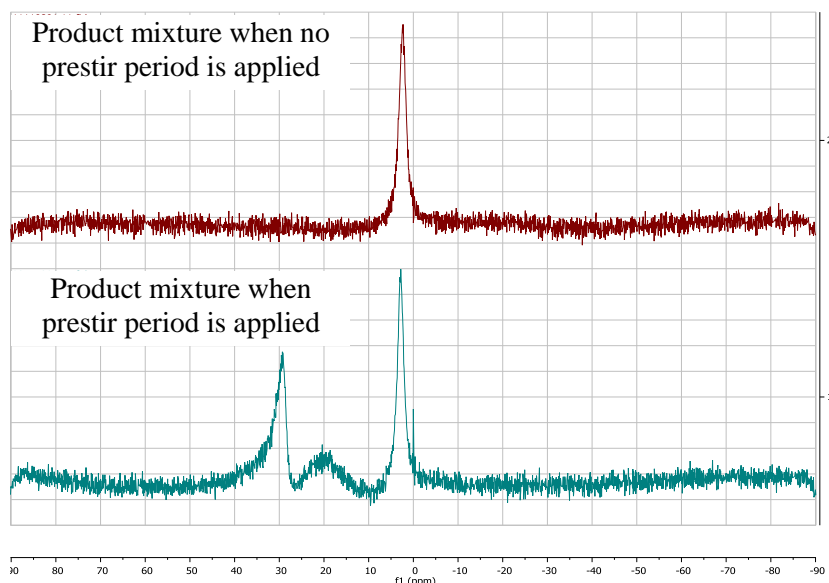


Scheme 52: Applying bis-2-chlorophenylborinic acid **148c** as catalyst in direct amide formation

^{11}B NMR (and ^1H NMR) of the product mixture, obtained by simultaneous mixing of reagents, suggested that borinic acid remained in amino-carboxylate borinic complex **195e** form (Figure 58). The same reaction performed with 4-phenylbutyric acid **180a** showed the same set of signals as for **195d**, verifying aminocarboxylate complex formation in this reaction. The ^{11}B NMR of the product mixture obtained when the carboxylic acid and borinic acid were prestirred, showed the presence of mainly 2 species: boronic acid and unknown “ate”-complex. No signal for the borinic acid was observed. This result suggested, that during the prestir period, borinic acid

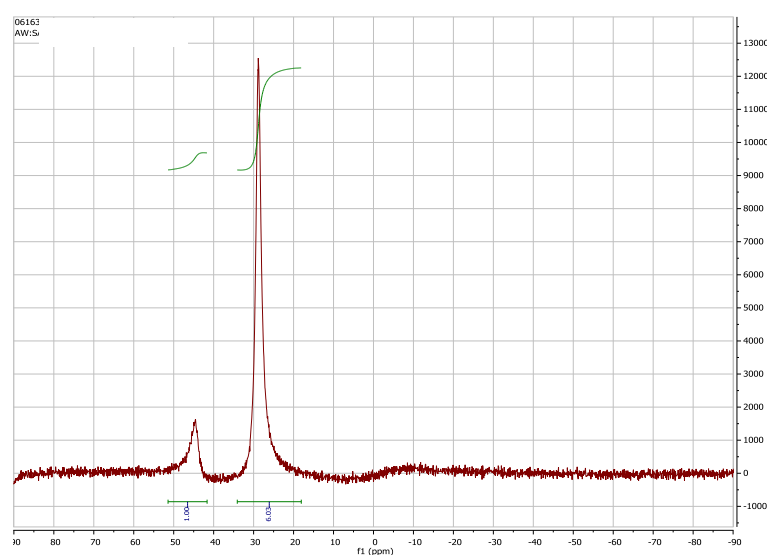
protodeboronated to the boronic acid, and the latter acted as catalyst in amide formation.

Figure 58: ^{11}B NMRs of mixtures of benzylamine, phenylacetic acid, 10 mol.% bis-2-chlorophenylboronic acid and 5Å MS in DCM after 4 h (see Scheme 9); with or without 15 min prestirring of carboxylic acid, boronic acid and MS.



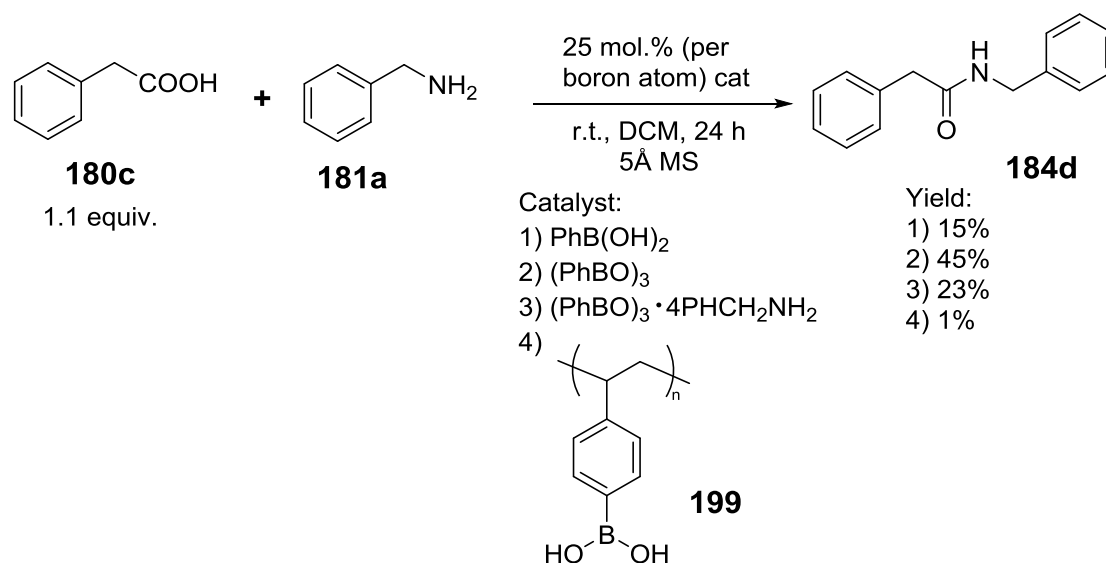
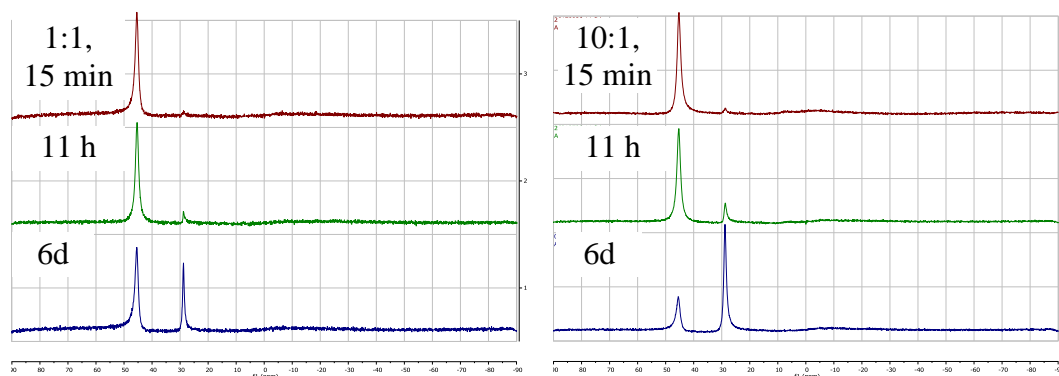
This was further verified by filtering and evaporating the mixture of 10% 2-chlorophenylboronic acid, phenylacetic acid and 5Å MS after 15 min stirring, and recording the NMR spectra. In this case a 1:6 ratio of borinic to boronic species was observed (Figure 59).

Figure 59 ^{11}B NMR of a 1:1 mixture of phenylacetic acid **180c** and bis-2-chlorophenylboronic acid **148c** in presence of 5Å MS in DCM after 15 min at r.t.



It should also be noted, that protodeboronation of borinic acid to boronic acid occurred very slowly if no 5 Å MS were added. The excess carboxylic acid slightly facilitated this process (Figure 60). Finally, when 4 Å MS were used, no amidation was seen at all, which suggested that 5 Å MS were obligatory for fast protodeboronation to give boronic acid.

Figure 60 Slow protodeboronation of borinic acid in CDCl₃ without 5 Å MS is faster when excess of carboxylic acid is used. 1:1 and 10:1 ratios of 4-phenylbutyric acid : bis-2-chlorophenylborinic acid **148c**



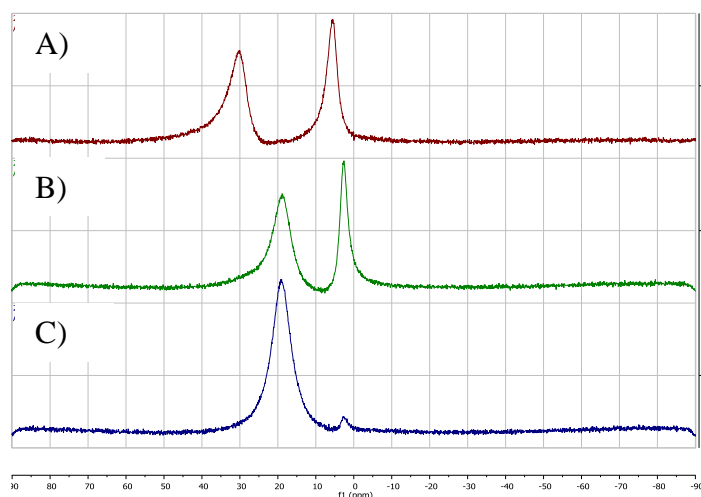
Scheme 53 Direct amide formation with various phenylboronic compounds.

Direct amide formation between benzylamine **181a** and 2-phenylacetic acid **180c** was attempted at r.t. in DCM in the presence of activated 5 Å MS with 4 different catalysts at 25 mol.% per boron atom loadings (Scheme 53): phenylboronic acid **186a**, phenylboroxine **192a**, phenylboroxine complex with 4 molecules of benzylamine **190** (loading of benzylamine reduced to match concentration with other reactions) and the polymeric catalyst **199** on the basis of 4-vinylphenylboronic acid, synthesised in our group by Tom Barber. The amount of amide product was

determined by ^1H NMR, but the results were not easy to interpret. Boroxine showed best activity, which is most likely due to a smaller overall amount of water in the system. The polymeric catalyst was shown to perform well in toluene under reflux with Dean-Stark conditions (results not yet published), but it did not catalyse direct amide formation at r.t.

In order to better understand what processes are going on in the system of boronic acid, carboxylic acid and amine, another NMR study was conducted. After mixing 2-chlorophenylboronic acid **186c**, phenylacetic acid **180a** and 5 Å MS, equilibrium with the dicarboxylate B-O-B complex **195b**, was established (Figure 61). Then, amine was added to the mixture. The boroxine peak in ^{11}B spectrum was shifted to 20 ppm, a signal similar to ^{11}B NMR signal of adducts **188-190** obtained when mixing boronic acids with amines only. The dicarboxylate signal was quickly (< 8 min) shifted to slightly higher field, and a new “ate”-complex at 3 ppm was formed. Overnight, amide was formed and all boron “ate”-complexes eventually collapsed.

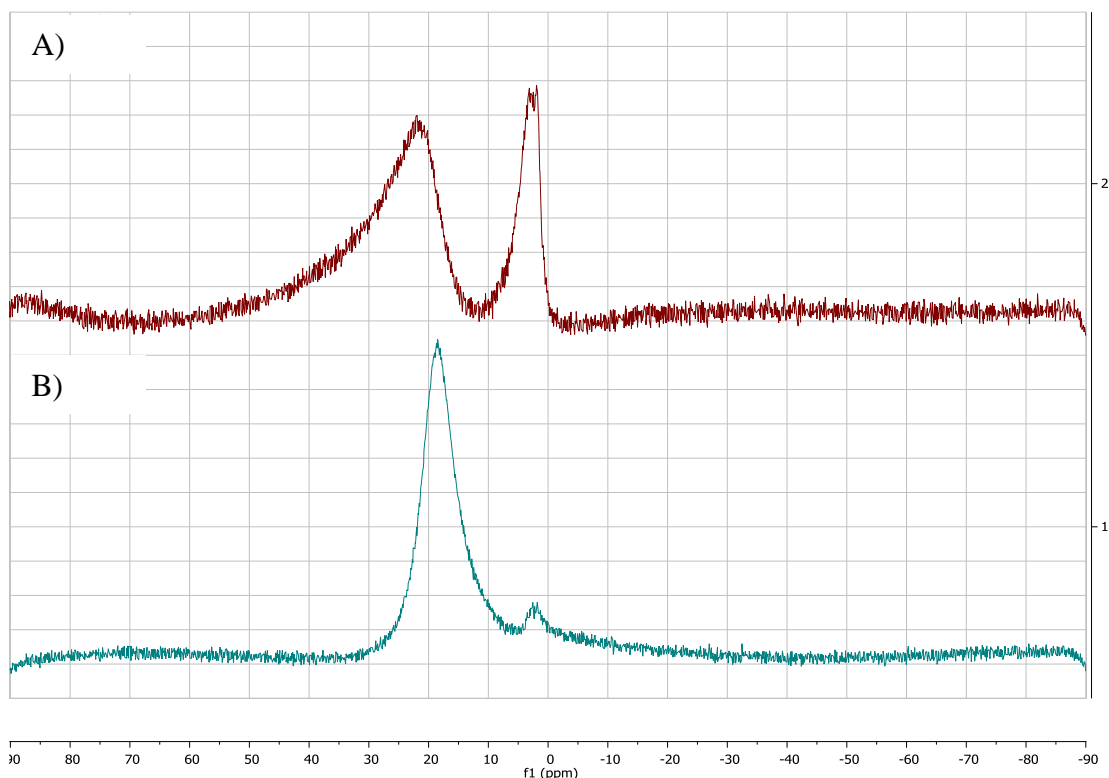
Figure 61 A) Mixture of 1:1 2-chlorophenylboronic acid **186c** with phenylacetic acid **180c** and 5 Å MS; B) addition of 1.5 equiv of benzylamine **181a**, 8 min; C) 18 h, ^1H NMR shows complete conversion to amide and remaining excess amine left.



It was also surprising that the order of mixing of the 3 components had a significant impact on the reaction profile in the ^{11}B NMR. Premixing the boronic acid with carboxylic acid and 5 Å MS yielded, after subsequent amine addition, an approximately 1:1 ratio of the “ate”-complex to the “boroxine-amine” species with signal at 20 ppm in ^{11}B NMR spectrum, as seen in Figure 61, B and 62. However, premixing the boronic acid with amine and 5 Å MS with subsequent addition of the carboxylic acid yielded a mixture with a much smaller amount of “ate”-complex

(<10% of the mixture). This can be explained by “trapping” of boronic acid in the form of boroxine with amine. Nevertheless, on a 1:1:1 scale no change in amide yield after 18 h was noticed.

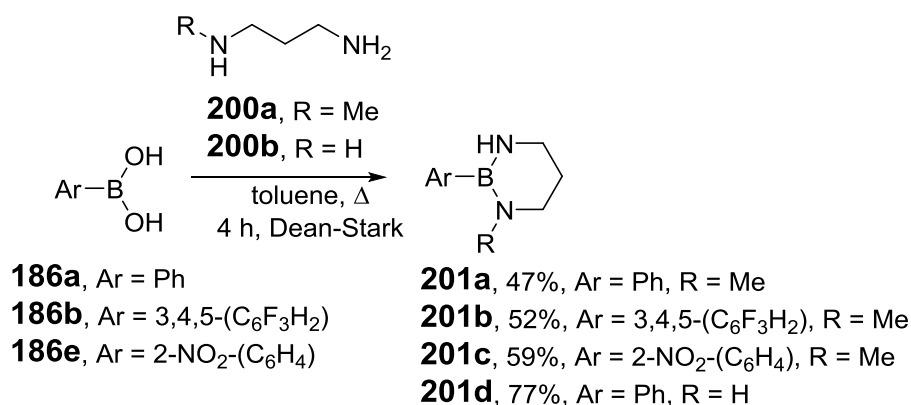
Figure 62 ^{11}B NMRs: A) premixing boronic acid and carboxylic acid with 5Å MS and subsequent addition of amine; B) premixing boronic acid and amine with 5Å MS and subsequent addition of carboxylic acid



2.3.2.5. Boronic diamides

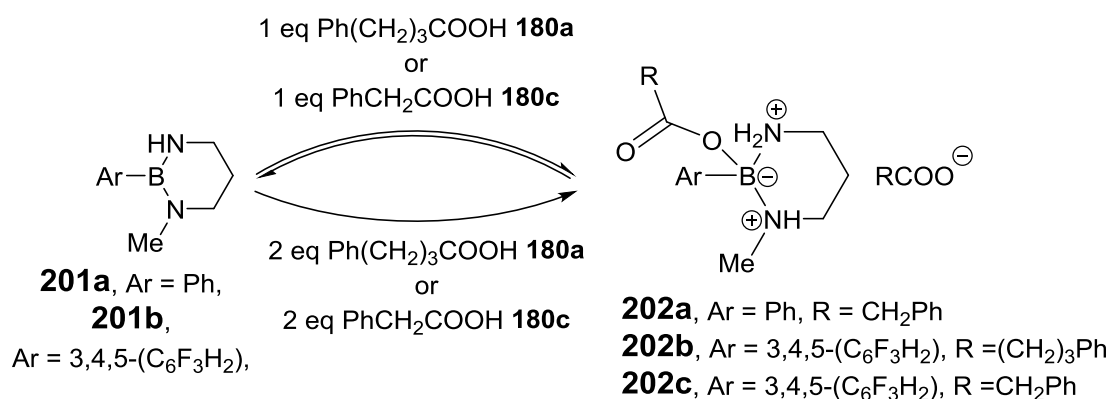
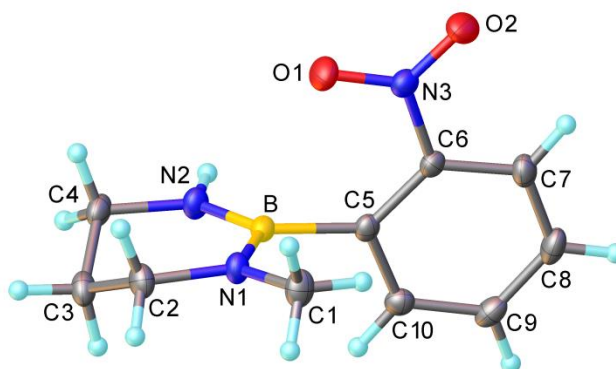
Even though attempts to react benzylamine with boronic acids only yielded boroxine, an example was found,¹⁷⁹ that boronic acids can react with *N*-methyl-1,3-diaminopropane **200a** in refluxing toluene with Dean-Stark removal of water to yield the boronic diamide. This reaction was attempted with phenyl- **186a**, 3,4,5-trifluorophenyl- **186b** and 2-nitrophenylboronic acids **186e** (Scheme 54), and boronic diamides **201** were formed and purified by distillation in all cases. The non-methylated 1,3-diaminopropane was also reacted with phenylboronic acid (Scheme 54). However, diamides **201b** and **201d** were not obtained in pure form, as it seems that they distilled together with ~20% of the diamine, and that this impurity could not be removed. Diamide **201c** crystallised over time, allowing X-ray structure confirmation (Figure 63). Unfortunately, the instability of this product to air and/or water was underestimated, and it was lost during recrystallization attempts. It was

impossible to reproduce its synthesis, because the reaction seemed to be sensitive towards impurities, and commercially purchased 2-nitrophenylboronic acid is frequently of low purity. This led to lack of analytical data on product **201c**.



Scheme 54 boronic diamides **201** formation

Figure 63 X-ray structure of boronic diamide **201c**



Scheme 55 Interaction of boronic diamides **201a-b** with carboxylic acids at r.t.

Diamides **201a** and **201b** reacted with 1 equivalent of 4-phenylbutyric acid **180a** at r.t. in CDCl_3 in 5 min to give an equilibrium with the new “ate”-complex **202** (Scheme 55, Figure 64), and the equilibrium remained stable over 3 days. Addition of 5 Å MS had absolutely no impact on this equilibrium. However, addition of a second equivalent of 4-phenylbutyric acid allowed the reaction to proceed to completion.

Repeating the experiment with phenylacetic acid **180c** allowed crystallisation of product **202c**, and X-ray crystallography allowed identification of its structure (Figure 65). It is chemically similar to the diadduct **196** that was isolated with borinic acid, which underlines that B-N Lewis adduct bonds can be favoured in different systems. This complex was not found to collapse to amide at r.t.

Figure 64 ^{11}B NMR, indicating interaction between boronic diamide **201b** and 1 and 2 equivalents of 4-phenylbutyric acid in CDCl_3 at r.t.

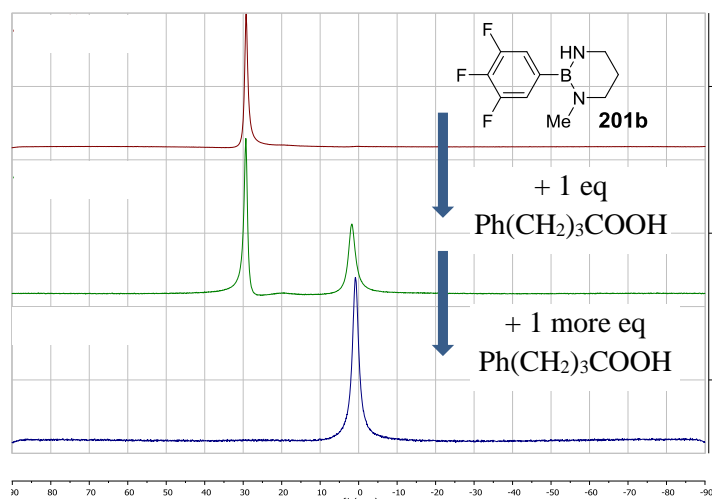
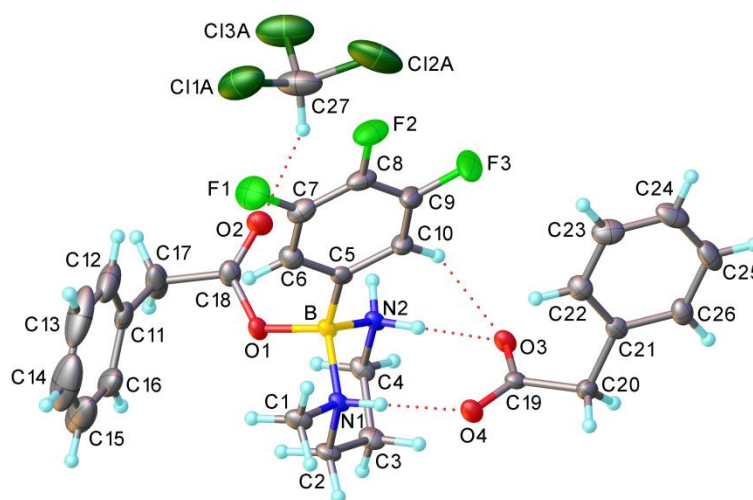


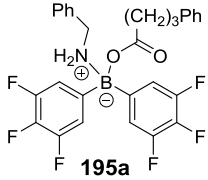
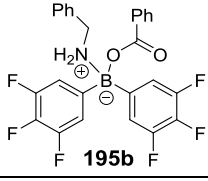
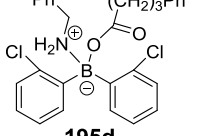
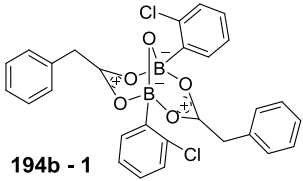
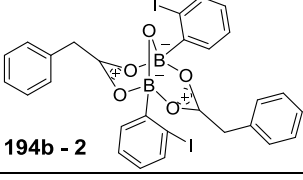
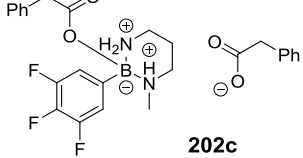
Figure 65 X-ray structure of complex **202c**



The selected analytical data on various forms of boron carboxylate compounds, obtained during this project, is summarised in Table 6. It should be noted, that B-O-B dicarboxylates **194** show similar C-O and “C=O” stretches, and C-O is much shorter than usual, while “C=O” is longer – actually, they can no longer be unambiguously distinguished. Compounds **194** also have the longest B-O bonds from the selection, likely due to significant steric hindrance in bicyclic system. In case of adduct **202c**, the C=O and C-O stretches of the not-covalently-bonded carboxylate are

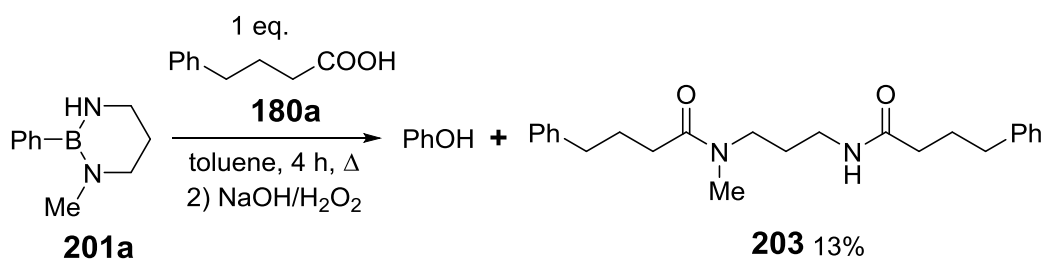
also very similar (1.250; 1.263 Å), due to double hydrogen bonds and more even charge distribution, as compared to the bonded carboxylate (1.205; 1.329 Å)

Table 6 Data on carbonyl C=O IR stretches, ^{13}C NMR of carbonyl carbon, C=O, C-O and B-O bond lengths and ^{11}B NMRs of selected compounds, isolated in this project.

Structure	^{11}B NMR	^{13}C NMR (C=O)	IR (C=O)	B-O, Å	C=O or "C=O", Å	C-O, Å
 195a	1.4	178.83	1677	1.49	1.214	1.323
 195b	1.9	170.89	1665	1.491	1.219	1.324
 195d	2.5	177.99	1678	1.499	1.216	1.319
 194b - 1	5.3	184.52	1705	1.548; 1.571	1.27	1.276
 194b - 2	5.5	184.65	1698	1.550; 1.584	1.256	1.276
 202c	0.8	178.92; 173.00	1702; 1611?	1.476	1.205; 1.250	1.329; 1.263
PhCH ₂ COOH	-	177.23 ¹⁸⁰	1715			

Refluxing diamide **201a** with 1 equivalent of 4-phenylbutyric acid **180a** in toluene (Scheme 56) gave an oily mixture of multiple boron-containing compounds. Treating it with NaOH/H₂O₂ resulted in breaking the B-C bond and phenol was isolated, but another product that was obtained was diamide **203**, as seen by ^1H NMR, IR and mass spectrometry. It is possible that monoamide, if it was formed, was lost during column chromatography. It should be noted, that a reaction in identical conditions was attempted between *N*-Me-1,3-diaminopropane **200a** and 4-

phenylbutyric acid **180a** in order to check the direct reactivity of amine and acid, but in this case no amide was formed. This reaction underlined that B-N interactions can play a remarkable role in direct amide formation, catalysed by boron species.



Scheme 56 Reaction of boronic diamide **191a** with 4-phenylbutyric acid **173a**

Finally, it should be mentioned that dimesityl boronic acid **148e**, that was not reactive with either carboxylic acids or amines at r.t. formed borinic amide **204** when refluxed in toluene (eqn. 2.5). This product was also formed, isolated and crystallised when Mes₂BOH was attempted as the catalyst in direct amide formation reaction (no improvement in amide yield as compared to background thermal reaction was noticed) (Figure 66).

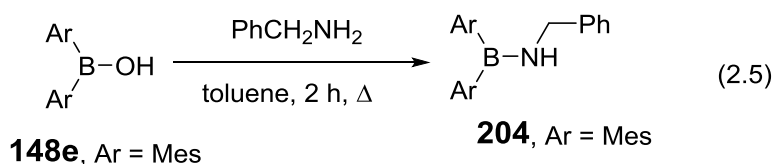
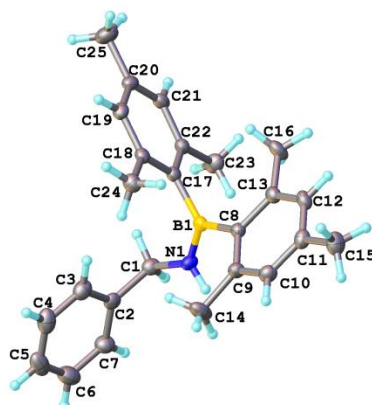


Figure 66 X-Ray structure of borinic amide **204**



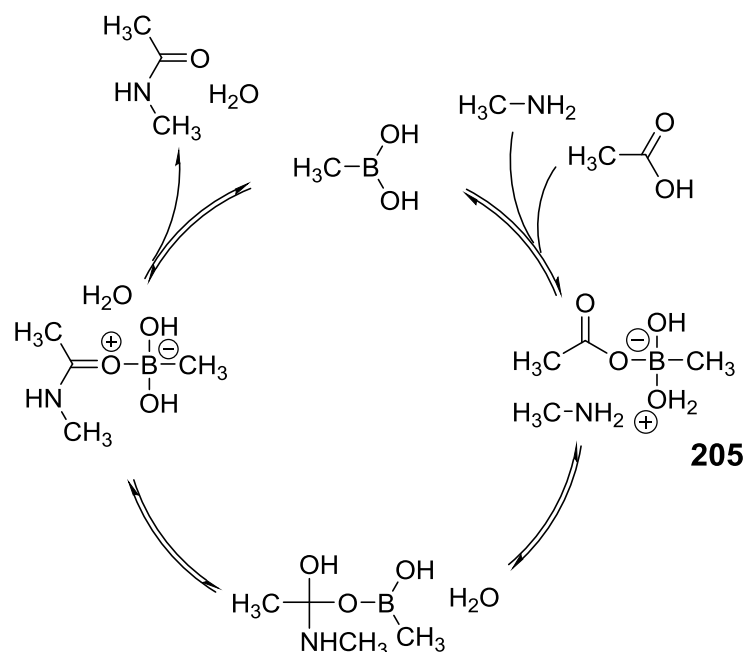
2.3.2.6. Mechanistic conclusions on boronic acid catalysed direct amide formation

The results, discussed above, suggested three key insights into the mechanism of action of boronic acids in amide formation.

First, following the isolation of multiple boron derivatives as Lewis adducts with amines, it is obvious that B-N interactions plays a significant role. Different B-N

coordinated compounds are definitely formed in equilibrium in the reaction mixtures, but it remains an open question whether they play the role of an active catalyst. However, this concept has not been looked at before, as the widely accepted mechanism¹⁸¹ for this reaction includes boronic acid interaction with the carboxylic acid, and the obtained boronic carboxylate **205** is considered to be activated enough for subsequent nucleophilic amine attack (Figure 67). However, if this pathway was possible, borinic acids, having even stronger Lewis acidity, could also catalyse amide formation. However, we have shown, that this is not the case. Consequently, the mechanism of boronic acids action in direct amide formation is different and still needs more attention.

Figure 67 Currently accepted mechanism for boronic acids role in direct amide formation

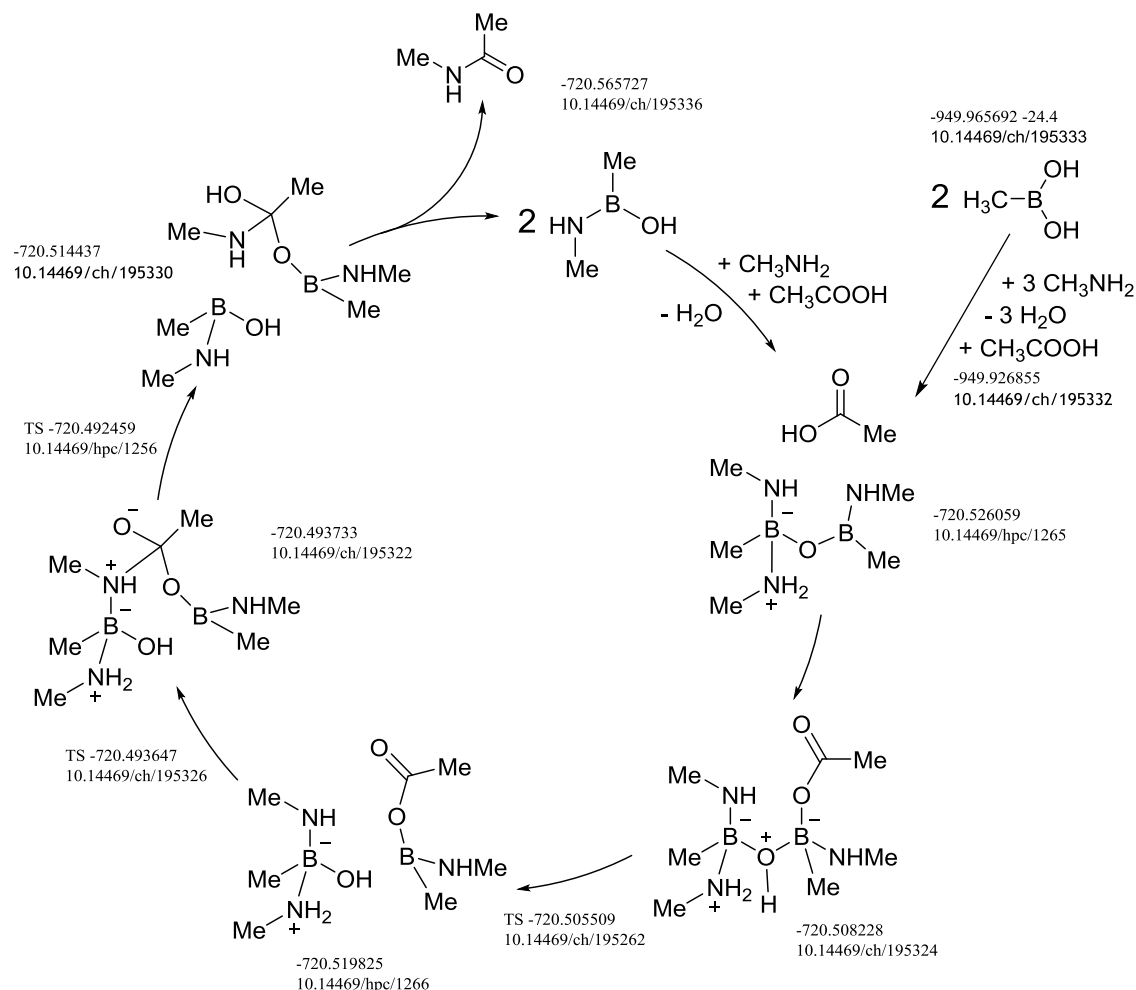


Second, the likelihood of boroxines formation and achieved isolation of dicarboxylate B-O-B complex **194** suggest that intermediates, containing multiple boron atoms can be formed in these systems. These two principles were united and a catalytic cycle was designed (Figure 68). Thanks to efforts of Prof. Henry Rzepa, the energies for this catalytic cycle were calculated by DFT.

Third, it is also possible, that double carboxylate activation, achieved in **194b**, could be enough for subsequent nucleophilic amine attack, thus **194b** could be the active catalytic species in this reaction. On one hand, the ¹³C NMR of this compound shows the carbonyl peak at 184 ppm (Figure 69), which indicates that the carbonyl centre is more electrophilic than that of carboxylic acid. On the other hand, the signal of carbonyl C=O bond at ~1700 cm⁻¹ in IR (as compared to 1715 cm⁻¹ stretch for

phenylacetic acid) suggested that nucleophilic attack is less likely to occur. Finally, formally positive charges are located on carboxylate carbon atoms in **194b**.

Figure 68 Suggested new catalytic cycle, utilising principles of B-O-B species formation and B-N coordinations possibility



At this stage, another catalytic cycle, involving dicarboxylate of **194b** type was calculated by Henry Rzepa at ICL (Figure 70). It turned out to be more energetically favoured than other approaches. Also, it was shown, that a bridging oxygen atom can move between two borons, making the system asymmetric, and rendering one boron atom more electrophilic, which could, in turn, activate one of the two carboxylates towards nucleophilic attack by amine.

In order to verify this idea of reactivity further, an additional experiment was conducted. Complex **194b** was formed, as always, in equilibrium with planar boronic species, and this equilibrium was pushed to the “ate”-complex as far as it was possible with excess of 5 Å MS. This created a mixture, containing 85% of B-O-B dicarboxylate complex **194b** (Figure 71, A).

Figure 69 ^{13}C NMRs of a mixture of phenylacetic acid **180c** and bis-2-chlorophenylboronic acid **186c** in presence of 5 Å MS, which contains dicarboxylate B-O-B complex **194b** (top), and the NMR of same mixture after adding amine (+18 h) – signal at 184 ppm is gone

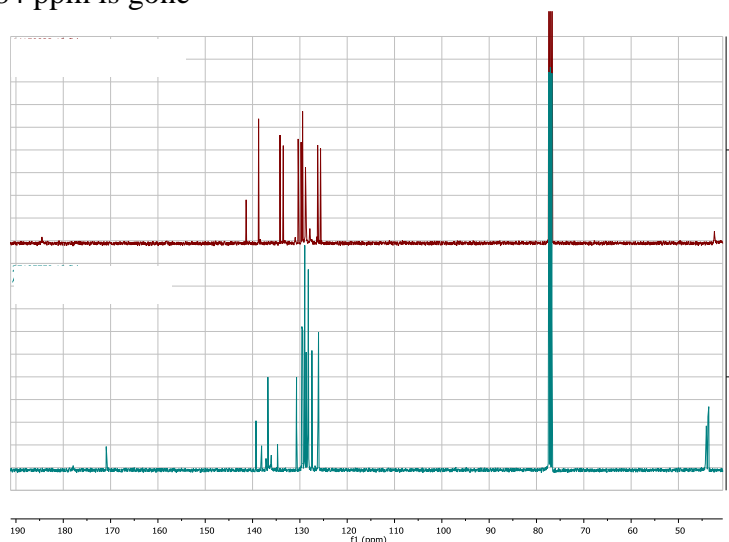
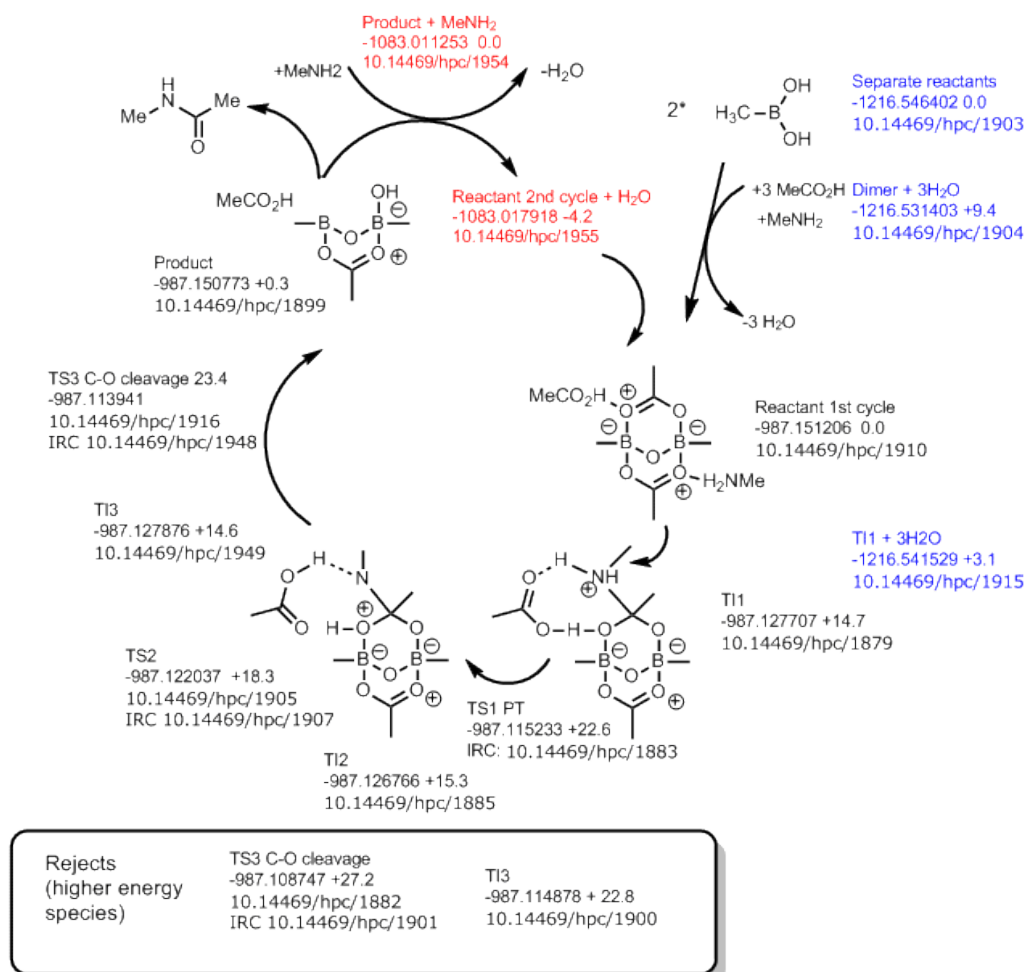


Figure 70 A catalytic cycle for amide formation, involving the isolated B-O-B dicarboxylate **194b** type of species

Cycle collection DOI: [10.14469/hpc/1854](https://doi.org/10.14469/hpc/1854) Project DOI: [10.14469/hpc/1620](https://doi.org/10.14469/hpc/1620)



A calculated amount of amine, 1:1 to complex **194b** (i.e. $0.5 \text{ equiv.} \times 0.85 = 0.43 \text{ equiv.}$ of amine to initially loaded carboxylic and boronic acids) was added (Figure 71, B). Surprisingly, even after 2.5 h, only $< 1\%$ of amide was generated, and ^{11}B NMR showed that part of the B-O-B dicarboxylate complex signal remained (δ 5 ppm), while part was transformed to 2 different “ate”-complexes with ^{11}B NMR signal in a higher field (δ 3 ppm, 1 ppm). Astonishingly, ^1H NMR showed a pattern that was familiar from boronic acids research: 2 signals, at 3.46 and 6.20 ppm look identical to those of *borinic* aminocarboxylate **195c** for CH_2 and NH_2 groups (Figure 73). This observation, together with the knowledge that aminoacids can form aminocarboxylate complexes with boronic acids, suggested, that in substoichiometric amine conditions, aminocarboxylate complexes can be formed in direct amide formation systems as well (Scheme 57). After adding 43% more amine (2^{nd} equivalent per B-O-B dicarboxylate complex), already after 20 minutes a significant amount of amide was seen (Figure 71, C), and over 48 h it increased to $\sim 30\%$ yield (Figure 71, D), which was much lower than the amine loading (85%), but the aminocarboxylate signals could still be seen.

Figure 71 ^{11}B NMRs of A) mixture of 2-chlorophenylboronic acid **186c** and phenylacetic acid **180c** resulting in equilibrium between B-O-B dicarboxylate **194b** (δ 5 ppm) and boronic species (δ 30 ppm); B) addition of 1 equivalent (per “ate”-complex **194b**) of benzylamine, after 2.5 h; C) Addition of 2^{nd} equivalent of benzylamine, 20 min; D) Same mixture over 48 h.

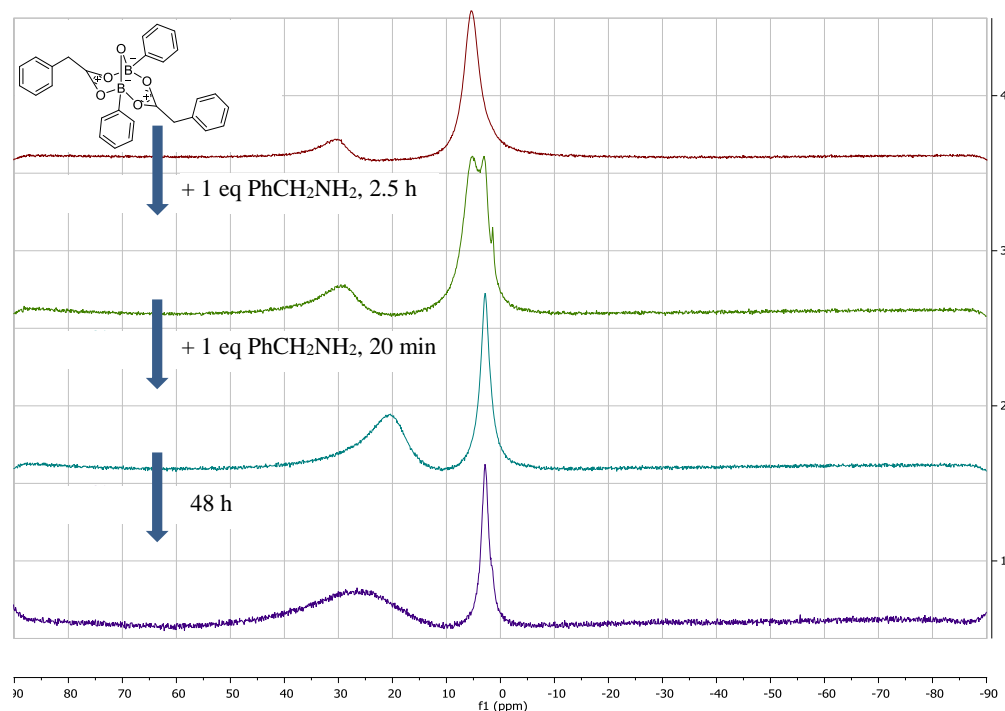


Figure 72 ^1H NMRs of A) mixture of 2-chlorophenylboronic acid **186c** and phenylacetic acid **180c** resulting in equilibrium between B-O-B dicarboxylate **194b** (δ 5 ppm) and boronic species (δ 30 ppm); B) addition of 1 equivalent (per “ate”-complex **194b**) of benzylamine, after 2.5 h; C) Addition of 2nd equivalent of benzylamine, 20 min; D) Same mixture over 48 h.

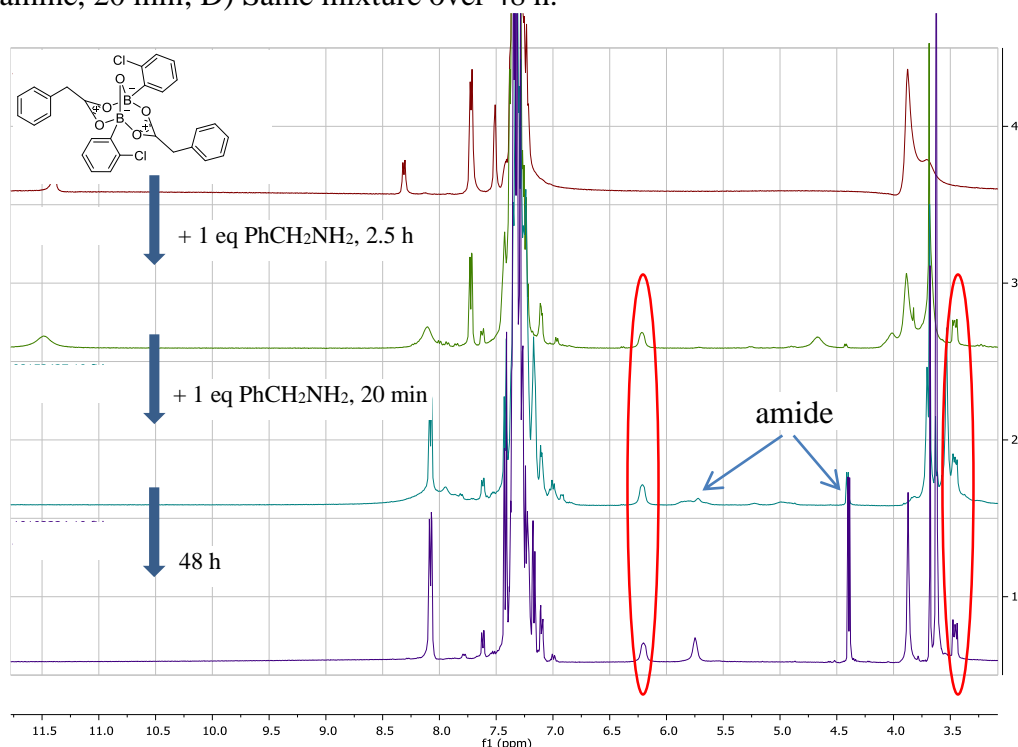
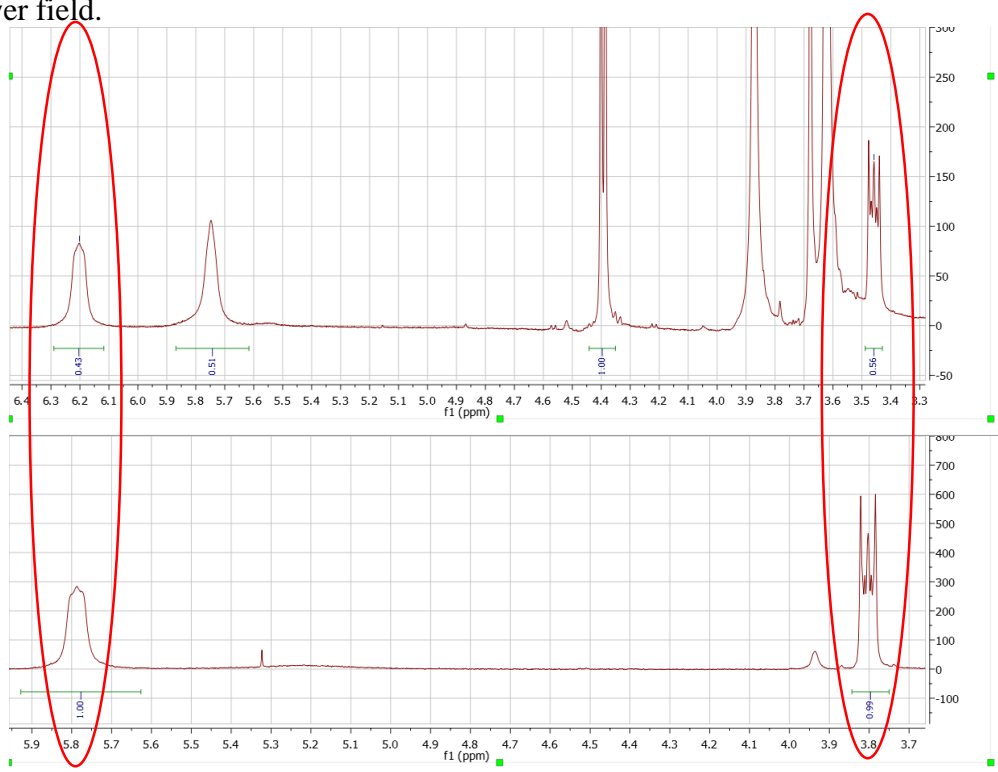
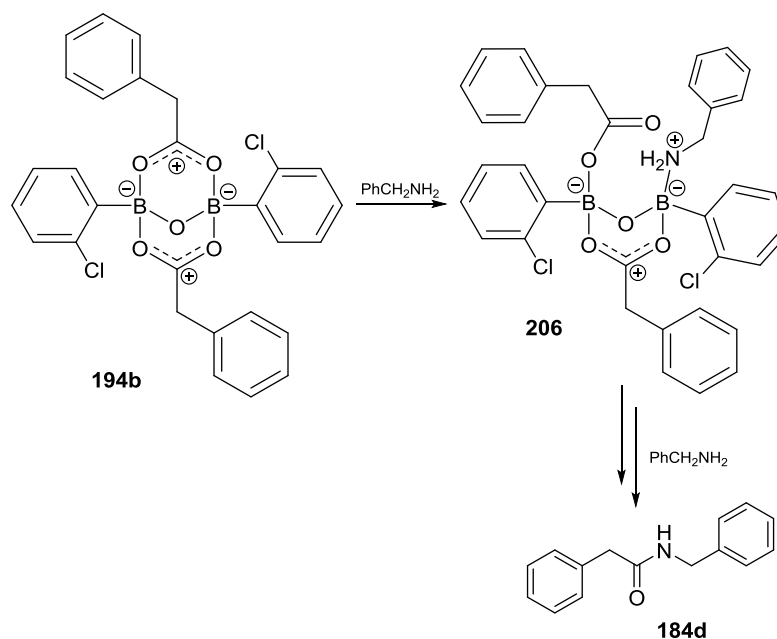


Figure 73 Comparing ^1H NMR of the reaction mixture after 48 h (top, fragment of Figure 70, D) with ^1H NMR of borinic aminocarboxylate **195c** (bot, note that all borinic aminocarboxylates **195a-d** look very similar in terms of 2 signals in question). Note identical multiplicity of 2 signals, but chemical shifts are different, just as they should: in borinic (more Lewis acidic) case the amino CH_2 signal is in the lower field.





Scheme 57 Suggested transformation of B-O-B dicarboxylate “ate”-complex **194b** upon addition of amine

These findings do not necessarily state that the boronic B-O-B aminocarboxylate “ate”-complex **206** is the active catalytic species (even though this is possible) or an intermediate in this process, but, according to accumulated data this species is definitely formed in equilibria in these systems, which again underlines the importance of B-N interactions and the likelihood of bifunctional role of B-O-B systems.

2.4. Conclusions and future work

The results of literature research unambiguously show that decreasing steric hindrance and electronic strength of LA and LB components, along with careful design of tether length will help broaden the scope of frustrated Lewis pairs applications.

Despite new designed catalysts **108** and **157** were not accessed, diverse synthetic attempts provided multiple important insights into borinate chemistry. Susceptibility to oxidation and protodeboronation, inability to form boranes and inability to access these compounds from proline derivatives broaden our understanding of boron chemistry and will help to develop more efficient pathways to bifunctional B-N systems.

Homoboroproline catalyst **176** was successfully applied in nitro-Michael reaction, allowing good conversion and significant *ee*% of the product. Substrate scope, conditions and kinetic investigations should follow.

Studies of non-catalysed direct amide formation underlined the complexity of carboxylic acid – amine systems even before the catalyst was introduced. The carboxylic acid dimer could indeed be the active species undergoing amine attack in this transformation, as multiple observations supported this hypothesis.

Boron chemistry was again shown to be a complex area, where multiple boron centres can orchestrate complicated catalytic processes. Similarity was found on three of boron oxidation level: boric acid, boronic acids and borinic acid all interacted with amines and carboxylic acids with formation of aminocarboxylates and other “ate” complexes. Understanding of these processes achieved through NMR investigations and isolation of multiple intermediates is of big importance for the design of more efficient catalysts for the promising applications in direct amide formation. Mastering this reaction, the only byproduct of which is water, is particularly important in the light of waste production and atom inefficiency of most currently used methods for amide synthesis.

Isolation of the remarkable **194** complexes under these conditions can also be viewed along with the findings, reported earlier by Ishihara¹⁸² on acyloxyboron species: it is indeed likely that they have observed the similar di-coordinated species in their work.

The future work in this area should include further studies on compound **206** and analysis of whether it is the catalytic species or the thermodynamic sink in amide formation. As far as it was shown with one example, that more than 50% of amine per boron atom is needed to achieve catalyst turnover and conversion into amide, this should be further verified in other boronic acid – carboxylic acid – amine – molecular sieves systems.

The difference of 4Å and 5Å MS action in this reaction can also be further looked at. This can also include the more in-depth comparison of boronic acids and corresponding boroxines reactivity in direct amide formation.

In the area of non-catalysed direct amide formation, studies can be designed in order to determine kinetics of ammonium salt formation and, possibly, of carboxylic acid dimer formation, and with this data understanding of the kinetics of actual amide formation might be achieved.

3. Experimental

3.1. General Information

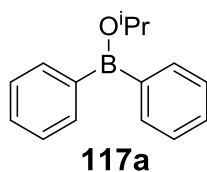
All starting materials and solvents were obtained commercially from standard chemical suppliers and were used as received unless otherwise stated. Anhydrous Et₂O was purchased from Fisher Scientific. Other dry solvents were prepared using the Innovative Technology Inc. solvent purification system, or dried by known methods. This included standing over 4 Å molecular sieves for 24 h in case of toluene, THF and CDCl₃ or distillation from sodium and benzophenone under Ar in case of THF. ClCH₂I was distilled from CaH₂. Alkyl lithium reagents were titrated prior to use¹³⁶. Air- and moisture-sensitive reactions were performed using general Schlenk techniques and all glassware for use was oven dried for at least 6 hours at 140 °C and cooled in the flow of argon. Reactions were carried out at r.t. unless otherwise stated. “Evaporation” refers to removal of volatiles *in vacuo*. Magnetic stirrer bar was used for stirring reactions. Sensitive reagents were stored under Ar and were introduced with a syringe through rubber septa. Evaporations were carried out at 10-20 mm Hg using a Büchi rotary evaporator and water bath followed by evaporation to dryness *in vacuo* (<2 mmHg). “Overnight” means 16-18 h. Column chromatography was performed using 60 Å silica gel purchased from Aldrich. TLC was performed on Merck aluminium-backed pre-coated plates and were analysed by UV at 254 and 365 nm. Crystals suitable for X-ray analysis were obtained by vapour diffusion with EtOAc/pentane unless otherwise stated.

NMR spectra were recorded using Bruker Avance-400 MHz spectrometer at frequencies of 400, 101, 128 and 376 MHz for ¹H, ¹³C, ¹¹B and ¹⁹F, respectively. NMR data was collected in dry CDCl₃ unless otherwise stated and is reported as follows: chemical shift (δ, ppm), multiplicity, spin-spin coupling constants (J, Hz), integration and assignment, where possible. H_{na} and H_{nb} denote diastereotopic protons; H_n and H_{n'} (or equivalently, C_n and C_{n'}), denote rotamers. Aromatic carbons next to boron atom are not reported in ¹³C NMR. Mass spectra were obtained using ASAP (LCT Premier XE), ESI (TQD mass spectrometer with Acquity UPLC photodiode array detector) or EI (Shimadzu QP-2010-Ultra) techniques; accurate mass values were measured on QtoF Premier mass spectrometer. IR spectra were obtained using FT1600 series or PerkinElmer UATR Two spectrometers. HPLC reverse phase analysis was carried out on an Agilent 110 series instrument, fitted with a Perkin

Elmer series 200 degasser with Gemini 5 μ C18 110 Å column (150 \times 4.60 mm) fitted with guard cartridge (4 \times 3.0 mm). Elemental analysis was performed using an Exeter Analytical E-440 Elemental Analyser. Melting points were determined using an Electrothermal apparatus and were uncorrected. Flowsyn reactor with 52 mL FEP flow coil was used for investigation of amide formation in flow and Biotage MW reactor with R4 or R8 arm was used for microwave studies. The *in situ* IR spectroscopy monitoring was carried out with ReactIR 4000 instrument equipped with MCT detector; ConcIRT window = 1900 – 900 cm^{-1} . Advance setting: Laser WN = 7901 – 415 cm^{-1} ; Apodization = Happ General. Probe: Prob A DiComp (Diamond) connected *via* K6 Conduit (16mm prob); Sampling 4000-6500 at 8 cm^{-1} resolution; Scan option: auto select, gain 2 \times .

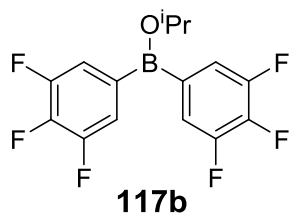
3.2. Synthetic procedures

Synthesis of isopropoxydiphenylborane **117a**¹³⁸:



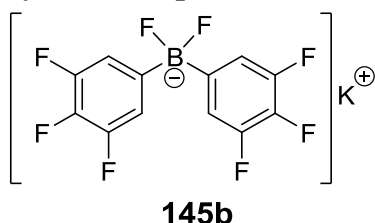
Mg turnings (1.69 g, 70.2 mmol) were stirred under Ar for 30 mins, followed by the addition of anhydrous Et_2O (100 mL) and a crystal of I_2 . Part of PhBr (0.5 g, 3.2 mmol) was added and the mixture was left to stir until the start of reaction, indicated by disappearance of the iodine colour. The remaining PhBr (10.02 g, 63.8 mmol) was then added dropwise. After the addition was complete, the mixture was heated at reflux for 1 h, then left at r.t. for 2 h. It was cooled to 0 $^\circ\text{C}$, $\text{B}(\text{O}^i\text{Pr})_3$ (6.0 g, 31.9 mmol) was added and the mixture was left overnight. Mixture was evaporated and Kugelrohr distillation was carried out to collect 4.90 g of a mixture of desired borinate and boronate **126a**. The latter was then distilled off at 112-116 $^\circ\text{C}$ 3 Torr, leaving undistilled product **117a** (2.50 g, 35% yield, 87% purity). ^1H NMR δ 7.73 – 7.71 (m, 4H, $\text{C}_{\text{Ar}}\text{-H}$), 7.55 – 7.47 (m, 6H, $\text{C}_{\text{Ar}}\text{-H}$), 4.72 (sept, $J = 6.1$ Hz, 1H, CH), 1.40 (d, $J = 6.1$ Hz, 6H, CH_3). ^{11}B NMR δ 45.

Synthesis of isopropoxy(di-3,4,5-trifluorophenyl)borane **117b**:



Mg turnings (1.762 g, 73.4 mmol) were stirred under Ar for 30 mins, followed by the addition of anhydrous Et₂O (110 mL) and a crystal of I₂. Part of 3,4,5-trifluorobromobenzene (0.5 g, 2.4 mmol) was added and the mixture was left to stir until the start of reaction, indicated by disappearance of the iodine colour. The remaining aryl bromide reagent (13.64 g, 64.6 mmol) was then added dropwise. After the addition was complete, the mixture was heated at 40 °C for 1 h, then left at r.t. for 1 h. It was cooled to 0 °C, B(OⁱPr)₃ (6.0 g, 31.9 mmol) was added, and the mixture was left to warm to r.t. overnight. TMSCl (10.00 g, 95.7 mmol) was added. In 24 h inorganic sediment was filtered off, water was added to the filtrate, organic layer was separated, evaporated and the residue was dissolved in ⁱPrOH, which was then removed *in vacuo*. The ⁱPrOH workup was carried out 2 more times, and the product was dissolved in toluene, which was also evaporated together with any remaining water at 40 °C. **117b** with less than 5% of **126b** was obtained as brown oil (8.64 g, 82%), which crystallised over 1 month of storage at r.t. Mp 48 – 51 °C. ¹H NMR δ 7.19 – 7.12 (m, 4H, C_{Ar}-H), 4.55 (sept, *J* = 6.1 Hz, 1H, CH), 1.33 (d, *J* = 6.1 Hz, 6H, CH₃). ¹¹B NMR δ 42. ¹⁹F NMR δ -134.36 – -134.56 (br m, 4F, CH-CF), -156.93 – -157.32 (br s, 2F, CH-CF-CF). ¹³C NMR δ 151.21 (ddd, *J* = 252.6, 9.8, 2.8 Hz, CH-CF), 141.28 (dt, *J* = 256.3, 17.1 Hz, CH-CF-CF), 116.60 – 118.43 (m, CH-CF), 71.06, 24.60. IR ν_{max} (neat)/cm⁻¹ 1526, 1418, 1346, 1037, 869, 714, 668.

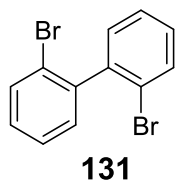
Synthesis of potassium difluorobis(3,4,5-trifluorophenyl)borate **145b**:



KHF₂ (0.071 g 0.91 mmol) was added to a solution of borinate **117b** (0.3g, 0.91 mmol) in 1 mL of MeOH. After stirring the mixture overnight it was evaporated, leaving product **145b** as white solid (0.312 g, 98%). Mp 241 - 242 °C. ¹H NMR (DMSO-d₆) δ 7.01 – 6.93 (m, 2H, C_{Ar}-H). ¹¹B NMR (DMSO-d₆) δ 5. ¹⁹F NMR (DMSO-d₆) δ -139.01 (dd, ¹J_{CF} = 20.65, ²J_{CF} = 8.87 Hz, 4F, CH-CF), -158.30 –

159.36 (br s, 2F, BF), -168.40 – -168.58 (m, 2F, CH-CF-CF). ^{13}C NMR (DMSO- d_6) δ 150.00 (ddd, $J = 248.5, 9.2, 1.8$ Hz, CH-CF), 136.81 (dt, $J = 242.6, 16.0$ Hz, CH-CF-CF), 114.20 – 113.93 (m, CH-CF). IR ν_{max} cm^{-1} 1405, 1321, 992, 852, 711, 691.

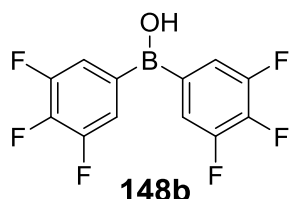
Synthesis of 2,2'-dibromobiphenyl **131**¹⁸³:



To a stirred solution of 1,2-dibromobenzene (4.9 g, 20.76 mmol) in THF (40 mL) under Ar at -78 °C BuLi (2.05 M in hexanes, 10.38 mmol) was added dropwise. The reaction mixture was allowed to warm to r.t. overnight, water was added, mixture was extracted with Et₂O three times, organic layer separated, dried and evaporated. Subsequent recrystallization from EtOH yielded 1.77 g (55%) of white solid **131**.

Mp $76 - 77$ °C (lit. $79-80$ °C¹⁷⁸). ^1H NMR δ 7.74 – 7.70 (m, 2H, C_{Ar}-H), 7.45 – 7.39 (m, 2H, C_{Ar}-H), 7.33 – 7.26 (m, 4H, C_{Ar}-H).

Bis-(3,4,5-trifluorophenyl)borinic acid **148b**:



Procedure A) Borinate **117b** (0.5 g, 1.5 mmol) was dissolved in toluene (10 mL) and water (5 mL) was added, the mixture was then evaporated *in vacuo* at 45 °C. This procedure was repeated twice to yield a brownish sediment, which was then dissolved in toluene and evaporated *in vacuo* again to remove the trace amounts of water. Hexane was added to the crude product and the mixture was heated to the boiling point. It was then evaporated to half the volume and left at r.t. overnight, which yielded white solid borinic acid **148b** (0.341 g, 78%). Mp $68.5 - 69$ °C. ^1H NMR δ 7.40 – 7.32 (m, 4H, C_{Ar}-H), 6.11 (br s, 1H, OH). ^{13}C NMR δ 151.35 (ddd, $J = 253.4, 9.6, 2.9$ Hz, CH-CF), 142.15 (dt, $J = 257.4, 15.3$ Hz, CH-CF-CF), 118.40 – 118.05 (m, CH-CF). ^{11}B NMR δ 44. ^{19}F NMR δ -133.58 – -133.71 (m, 4F, CH-CF), -155.00 – -155.17 (m, 2F, CH-CF-CF). IR ν_{max} (neat)/ cm^{-1} 3611, 1610, 1528, 1419, 1349, 1191, 1036, 972, 864, 713, 622. Anal. Calcd for C₁₂H₅BOF₆: C, 49.71; H, 1.74. Found: C, 49.88; H, 1.75.

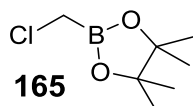
Procedure B) Mg turnings (1.137 g, 47.4 mmol) were stirred under Ar for 30 mins, followed by the addition of anhydrous THF (60 mL) and a crystal of I₂. Part of 3,4,5-trifluorobromobenzene (0.5 g, 2.4 mmol) was added and the mixture was left to stir until the start of reaction, indicated by disappearance of the iodine colour. The rest of this reagent (9.5 g, 45.0 mmol) was added dropwise. After the addition was complete, the mixture was heated at 40 °C for 1 h, then left at r.t. for 1 h. It was cooled to 0 °C, B(OⁱPr)₃ (4.23 g, 22.5 mmol) was added, and the mixture was left to warm to r.t. overnight. 5% HCl was added and the mixture was extracted with Et₂O 3 times, organic layer was dried and evaporated. The crude was redissolved in hot hexane, filtered and evaporated to yield 6.12 g (94%) of lightly-brown solid **148b**.

All analytical data was identical to that of product obtained in procedure A).

Procedure C) See “borinic acids synthesis” *via* hydrolysis of ethanolamine complexes below.

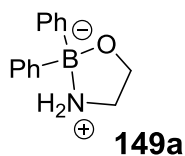
Synthesis of 2-(chloromethyl)-4,4,5,5-tetramethyl-1,3,2-dioxaborolane

165:



To a mixture of B(OⁱPr)₃ (5.0 g, 26.6 mmol) and ClCH₂I (4.69 g, 26.6 mmol) BuLi solution (2.04M in hexanes, 26.6 mmol) was added dropwise under Ar at -78 °C. The mixture was left to warm to r.t. overnight, then pinacol (3.19 g, 26.6 mmol) and TMSCl (3.24 mL, 26.6 mmol) were added. Solution was evaporated to provide a mixture of oil and sediment, Et₂O was added, mixture filtrated through celite, concentrated again and Kugelrohr distillation yielded 4.19 g (89% yield, 90% purity) of slightly yellow oil **165** ¹H NMR δ 2.98 (s, 2H, CH₂), 1.31 (s, 12H, CH₃). ¹¹B NMR δ 31. IR ν_{max} (neat)/cm⁻¹ 2978, 2361, 1472, 1372, 1325, 1141, 967, 846, 674.

Bis-phenylborinic acid – ethanolamine complex **149a**¹⁸⁴:

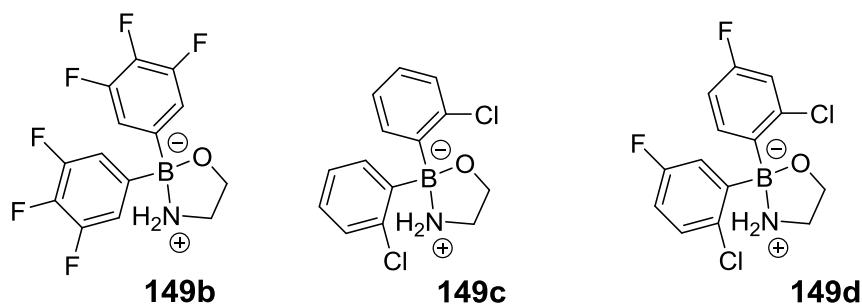


To dry THF (20 mL) triisopropylborate (0.5 g, 2.66 mmol) was added at 0 °C, followed by PhMgBr (3 M sol-n in Et₂O, 5.32 mmol). The reaction mixture was warmed to r.t., after 16 h 5% aq HCl (8 mL) was added, the mixture was stirred for 10 min and extracted with ether. After reducing the volume to ca. 5 mL *in vacuo*,

diethanolamine (1 M solution in ⁱPrOH, 2.66 mmol) was added. After 30 min the mixture was evaporated and recrystallization from EtOH yielded compound **149a** (0.363 g, 56%).

¹H NMR δ 7.50 – 7.46 (m, 4H, C_{Ar}-H), 7.34 – 7.29 (m, 4H, C_{Ar}-H), 7.27 – 7.21 (m, 2H, C_{Ar}-H), 4.22 – 4.03 (br s, 2H, NH₂), 4.03 (t, *J* = 6.3 Hz, 2H, CH₂), 3.07 – 3.00 (m, 2H, CH₂). ¹¹B NMR δ 6.

Synthesis of other borinic acid – ethanolamine complexes:



Mg turnings (2.1 equiv.) were stirred under Ar for 30 mins, followed by the addition of anhydrous THF (1 mL per 1 mmol of halide) and a crystal of I₂. Part of aryl halide (0.1 equiv.) was added and the mixture was heated to ca. 40 °C until the start of reaction, indicated by disappearance of the iodine colour. Then a mixture of remaining aryl halide (1.9 equiv.) and trimethylborate (1 equiv.) was added dropwise, and the reaction mixture was left to stir at r.t. overnight. Then 5% aq HCl was added, mixture was washed with Et₂O twice, organic fractions united, dried and evaporated. Residue was then redissolved in IPA and ethanolamine (1 equiv.) was added. Subsequent addition of Et₂O or hexane led to crystallisation of product as white solid.

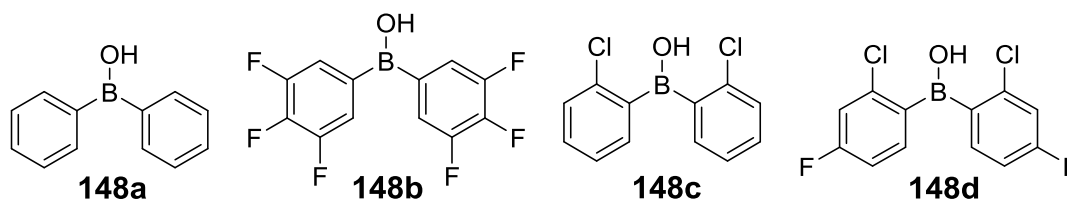
Bis-(3,4,5-trifluorophenyl)borinic acid ethanolamine complex **149b**: 59%. Mp 210 – 212 °C. ¹H NMR δ 7.09 – 6.97 (m, 4H, C_{Ar}-H), 4.15 – 4.04 (m, 2H, CH₂), 3.31 – 3.16 (br s, 2H, CH₂). ¹¹B NMR δ 5. ¹³C NMR (DMSO-d₆) δ 155.18 (ddd, *J* = 248.9, 9.3, 2.3 Hz, CH-CF-CF), 142.37 (dt, *J* = 246.4, 15.5 Hz, CF-CF-CF), 119.58 – 119.23 (m, CH-CF), 67.91, 46.69. ¹⁹F NMR δ -135.51 – -135.66 (m, 4F, *m*-C_{Ar}-F), -163.26 – -163.45 (m, 2F, *p*-C_{Ar}-F). IR ν_{max} (neat)/cm⁻¹ 3347, 3086, 2872, 1607, 1520, 1405, 1318, 1206, 1131, 1071, 1031, 992, 862, 783, 726, 670. Anal. Calcd for C₁₄H₁₀BF₆NO: C, 50.49; H, 3.03; N, 4.21. Found: C, 49.92; H, 3.06; N, 4.26.

Bis-(2-chlorophenyl)borinic acid ethanolamine complex **149c**: 41%. Mp 213 – 215 °C. ¹H NMR δ 7.38 – 7.33 (m, 2H, C_{Ar}-H), 7.32 – 7.29 (m, 2H, C_{Ar}-H), 7.23 – 7.15 (m, 4H, C_{Ar}-H), 5.40 – 5.05 (br s, 2H, NH₂), 4.09 (t, *J* = 6.5 Hz, 2H O-CH₂), 3.24 (pent, *J* = 6.5 Hz, 2H, N-CH₂). ¹¹B NMR δ 6. ¹³C δ NMR 137.90, 136.01, 129.18,

128.61, 126.34, 63.27, 41.59. IR ν_{\max} (neat)/ cm^{-1} 3305, 2862, 1580, 1418, 1279, 1250, 1198, 1148, 1076, 1024, 919, 767, 745, 724. Anal. Calcd for $\text{C}_{14}\text{H}_{14}\text{BCl}_2\text{NO}$: C, 57.10; H, 4.96; N, 4.61. Found: C, 57.20; H, 4.80; N, 4.76.

Bis-(2-chloro-4-fluorophenyl)borinic acid ethanolamine complex **149d**: 11%. Mp 188 – 190 °C. ^1H NMR δ 7.32 – 7.25 (m, 2H, $\text{C}_{\text{Ar}}\text{-H}$), 7.10 – 7.05 (m, 2H, $\text{C}_{\text{Ar}}\text{-H}$), 6.95 – 6.88 (m, 2H, $\text{C}_{\text{Ar}}\text{-H}$), 5.38 – 4.90 (br s, 2H, NH_2), 4.09 (t, $J = 6.5$ Hz, 2H O-CH_2), 3.27 (pent, $J = 6.5$ Hz, 2H, N-CH_2). ^{11}B NMR δ 6. ^{13}C δ NMR 162.22 (d, $J = 248.4$ Hz, $\underline{\text{C}}\text{F}$), 137.82 (d, $J = 9.6$ Hz), 136.95 (d, $J = 7.8$ Hz), 116.48 (d, $J = 23.5$ Hz), , 113.62 (d, $J = 18.9$ Hz), 63.23, 41.67. ^{19}F NMR δ -113.97 – -114.08 (m). ^{11}B NMR δ 6. IR ν_{\max} (neat)/ cm^{-1} 3065, 1678, 1588, 1473, 1373, 1251, 1197, 1069, 1033, 932, 888, 849, 823, 798, 746, 701.

Synthesis of borinic acids¹⁷⁵



A 100 mg of ethanolamine complex **149** was dissolved in 2 ml of 1:1 mixture of acetone and MeOH, 3 mL 5% aq HCl was added and the mixture was stirred for 5 min, then extracted with 10 mL Et₂O twice, the organic layers were combined, dried and evaporated to yield borinic acids **148** as colourless oils.

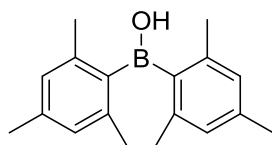
Bis-(phenyl)borinic acid **148a**: 89%. ^1H NMR δ 7.90 – 7.82 (m, 4H, $\text{C}_{\text{Ar}}\text{-H}$), 7.54 – 7.43 (m, 6H, $\text{C}_{\text{Ar}}\text{-H}$), 6.03 – 5.80 (br s, 1H, OH). ^{11}B NMR δ 46.

Bis-(3,4,5-trifluorophenyl)borinic acid **148b**: 82%. All analytical data was identical to that reported above.

Bis-(2-chlorophenyl)borinic acid **148c**: 83%. ^1H NMR δ 7.50 – 7.45 (m, 2H, $\text{C}_{\text{Ar}}\text{-H}$), 7.45 – 7.40 (m, 4H, $\text{C}_{\text{Ar}}\text{-H}$), 7.34 – 7.29 (m, 2H, $\text{C}_{\text{Ar}}\text{-H}$). ^{11}B NMR δ 45.

Bis-(2-chloro-4-fluorophenyl)borinic acid **148d**: 93% (90% purity). ^1H NMR δ 7.51 – 7.43 (m, 2H, $\text{C}_{\text{Ar}}\text{-H}$), 7.20 – 7.12 (m, 2H, $\text{C}_{\text{Ar}}\text{-H}$), 7.07 – 6.99 (m, 2H, $\text{C}_{\text{Ar}}\text{-H}$), 3.90 – 3.78 (br s, 1H, OH). ^{11}B NMR δ 45.

Bis-(mesityl)borinic acid **148e**:

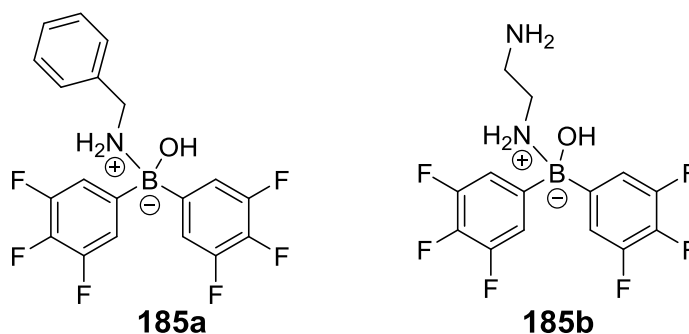


148e

Mg turnings (1.20 g, 50 mmol) were stirred under Ar for 30 mins, followed by the addition of anhydrous THF (100 mL) and a crystal of I₂. Part of mesityl bromide (0.50 g, 2.5 mmol) was added and the mixture was heated to ca. 50 °C until the start of reaction, indicated by disappearance of the iodine colour. Heating was turned off and the remaining mesityl bromide (9.45 g, 47.5 mmol) was added dropwise. The mixture was brought to reflux, after 2.5 h it was cooled to 0 °C and BF₃-OEt₂, (3.37 g, 23.8 mmol) was added, the mixture was brought to reflux again and after 1.5 h was cooled down, 5% HCl was added, mixture was extracted with Et₂O (3 x 50 mL), dried, evaporated and recrystallization from hot hexane yielded 3.43 g (54%) of white solid **148e**.

Mp 136 – 139 °C (lit. 140 °C¹⁵⁰). ¹H NMR δ 6.84 (s, 4H, C_{Ar}-H), 5.92 (s, 1H, OH), 2.30 (s, 6H, *p*-C_{Ar}-CH₃), 2.29 (s, 12H, *o*-C_{Ar}-CH₃). ¹¹B NMR δ 50. ¹³C NMR δ 141.11, 138.94, 128.37, 22.44 (*o*-C_{Ar}-CH₃), 21.19 (*p*-C_{Ar}-CH₃). IR ν_{max} (neat)/cm⁻¹ 3272, 2919, 1739, 1609, 1424, 1256, 1161, 1070, 1030, 843, 730, 666, 575. Anal. Calcd for C₁₈H₂₃BO: C, 81.22; H, 8.71. Found: C, 81.14; H, 8.54.

Synthesis of bis-(3,4,5-trifluorophenyl)borinic acid – amine complexes

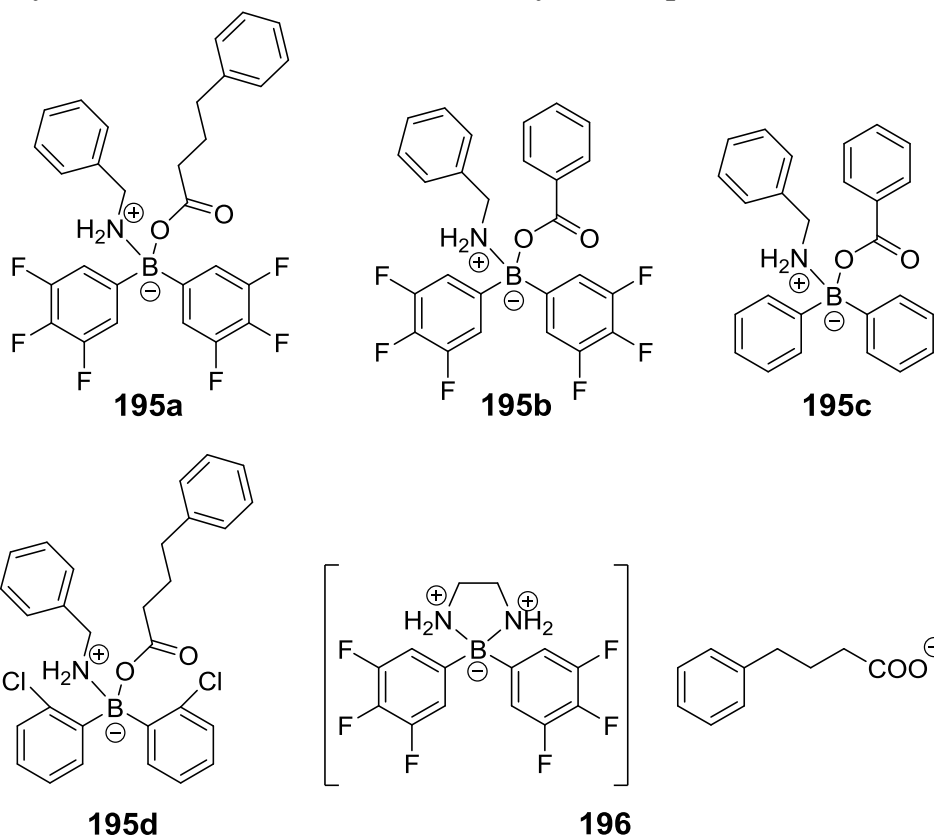


To DCM (10 mL) was added bis-(3,4,5-trifluorophenyl)borinic acid **1** (0.1 g, 0.34 mmol), followed by amine (0.34 mmol, 1 equiv.). The reaction mixture was stirred at r.t. for 5 min and was evaporated to dryness. The crude product was used without further purification. Crystals suitable for X-Ray analysis were obtained by slow recrystallization from DCM.

Bis-3,4,5-trifluorophenylborinic acid benzylamine complex **185a**: Mp 118 – 122 °C. ^1H NMR 7.38 – 7.43 (m, $\text{C}_{\text{Ar}}\text{-H}$, 3H), 7.16 – 7.21 (m, $\text{C}_{\text{Ar}}\text{-H}$, 2H), 6.93-7.00 (m, 4H, $(\text{C}_6\text{F}_3\text{H}_2)_2$), 3.77 (s, 2H, CH_2), 2.63 – 3.89 (br s, 2H, NH_2). ^{13}C NMR δ 151.20 (dm, $J=251.8$ Hz, CH-CF-CF), 137.51 – 140.03 (m, CF-CF-CF), 135.58, 129.65, 129.22, 128.05, 114.51 – 114.87 (m, CH-CF), 45.87. ^{11}B NMR δ 3. ^{19}F NMR δ -135.11 – -135.43 (br s, 4F, CH-CF-CF), -162.82 – -163.44 (br s, 2F, CF-CF-CF). IR ν_{max} (neat)/ cm^{-1} 3679, 2957, 1610, 1522, 1403, 1319, 1024, 734, 700. Anal. Calcd for $\text{C}_{19}\text{H}_{14}\text{BNOF}_6$: C, 57.46; H, 3.55; N, 3.53. Found: C, 57.52; H, 3.54; N, 3.54.

Bis-3,4,5-trifluorophenylborinic acid ethylenediamine complex **185b**: Mp 88 – 93 °C. ^1H NMR 7.04 – 6.95 (m, 4H, $\text{C}_{\text{Ar}}\text{-H}$), 2.80 (s, 4H, CH_2), 2.23 – 1.59 (br s, 4H, NH_2). ^{13}C NMR 150.03 (dd, $J = 247.4, 8.8$ Hz, CH-CF-CF), 136.92 (dm, $J = 244.3$ Hz, CH-CF-CF), 115.10 – 114.70 (m, CH-CF), 44.10. ^{11}B NMR δ 1. ^{19}F NMR δ -135.83 – -136.05 (m, 4F, CF-CH), -164.01 – -164.27 (m, 2F, CF-CF-CF). IR ν_{max} (neat)/ cm^{-1} 2962, 1607, 1520, 1405, 1316, 1104, 1023, 983, 909, 852, 759, 736, 688.

Synthesis of borinic acid aminocarboxylate complexes 195-196:



Borinic acid (1 equiv.) was dissolved in DCM at r.t. (10 mL). Amine was added (1 equiv.), followed by carboxylic acid (1 equiv), and after 5 min stirring the

mixture was evaporated to dryness. The crude products were used without further purification.

Bis(3,4,5-trifluorophenyl)-borinic acid benzylamine-4'-phenylbutanoate **195a**: Mp 162–163 °C. ^1H NMR δ 7.37 – 7.42 (m, 3H, $\text{C}_{\text{Ar}}\text{-H}$), 7.29 – 7.35 (m, 2H, $\text{C}_{\text{Ar}}\text{-H}$), 7.19 – 7.25 (m, 3H, $\text{C}_{\text{Ar}}\text{-H}$), 7.13 – 7.18 (m, 2H, $\text{C}_{\text{Ar}}\text{-H}$), 6.91–6.98 (m, 4H, CH-CF), 5.65 – 5.75 (br s, NH_2), 3.60–3.64 (m, 2H, $\text{NH}_2\text{-CH}_2$), 2.69 (t, $J=7.5$ Hz, 2H, CO-CH_2), 2.48 (t, $J = 7.5$ Hz, 2H, $\text{CO-CH}_2\text{-CH}_2\text{-CH}_2$), 2.03 (pent, $J = 7.5$ Hz, 2H, $\text{CO-CH}_2\text{-CH}_2$). ^{13}C NMR δ 178.83, 151.15 (ddd, $J = 250.9, 12.5, 2.5$ Hz, CH-CF-CF), 141.23, 138.77 (dt, $J = 250.9, 12.5$ Hz, CF-CF-CF), 134.11, 129.64, 129.51, 128.47, 128.45, 128.40, 126.07, 114.42 – 114.61 (m, CH-CF), 45.80, 35.96, 35.26, 26.72. ^{11}B NMR δ 1. ^{19}F NMR δ -135.41 – -135.53 (m, 4F, CH-CF-CF), -162.99 – -163.13 (m, 2F, CF-CF-CF). IR ν_{max} (neat)/ cm^{-1} 3262, 1677, 1524, 1409, 1322, 1273, 1030, 754, 700, 681. ESI-LRMS (negative ion) m/z 542.16 [M-H], 453.12 [M-PhCH_2], 289.12 [$\text{M-PhCH}_2\text{NH}_2\text{-Ph(CH}_2)_3\text{CO}$], 163.09 [$\text{Ph(CH}_2)_3\text{COO}$]. HRMS: Calcd for $\text{C}_{29}\text{H}_{23}^{10}\text{BNO}_2\text{F}_6$ 541.1762, found 541.1757. Anal. Calcd for $\text{C}_{29}\text{H}_{24}\text{BNO}_2\text{F}_6$: C, 64.11; H, 4.45; N, 2.58. Found: C, 63.80; H, 4.47; N, 2.48.

Bis(3,4,5-trifluorophenyl)-borinic acid benzylaminobenzoat **195b**: Mp 197 – 200 °C. ^1H NMR 8.21 – 8.24 (m, 2H, $\text{C}_{\text{Ar}}\text{-H}$), 7.63 – 7.69 (m, 1H), 7.53 – 7.59 (m, 3H, $\text{C}_{\text{Ar}}\text{-H}$), 7.40 – 7.43 (m, 2H, $\text{C}_{\text{Ar}}\text{-H}$), 7.22 – 7.26 (m, 2H, $\text{C}_{\text{Ar}}\text{-H}$), 7.01 – 7.08 (m, 4H, CF-CH), 5.70 (br s, 2H, NH_2), 3.72 – 3.77 (m, 2H, CH_2). ^{13}C NMR δ 170.89, 160.00, 149.97, 134.18, 133.33, 131.76, 129.94, 129.71, 129.57, 128.58, 128.49, 122.92, 114.36 – 114.61 (m, CH-CF), 45.92. ^{11}B NMR δ 2. ^{19}F NMR δ -135.09 – -135.20 (m, 4F, CH-CF-CF), -162.71 – -162.86 (m, 2F, CF-CF-CF). IR ν_{max} (neat)/ cm^{-1} 3291, 3201, 1665, 1575, 1521, 1410, 1318, 1266, 1135, 1011, 758, 700, 647. ESI-LRMS (negative ion) m/z 500.10 [M-H], 424.09 [M-Ph], 380.11 [M-PhCO_2]. HRMS: Calcd for $\text{C}_{26}\text{H}_{17}^{10}\text{BNO}_2\text{F}_6$ 499.1293, found 499.1296, calcd for $\text{C}_{20}\text{H}_{13}^{10}\text{BNO}_2\text{F}_6$ 423.0998, found 423.0980, calcd for $\text{C}_{19}\text{H}_{13}^{10}\text{BNF}_6$ 379.1100, found 379.1082. Anal. Calcd for $\text{C}_{26}\text{H}_{18}\text{BNO}_2\text{F}_6$: C, 62.30; H, 3.62; N, 2.79. Found: C, 61.61; H, 3.61; N, 2.76.

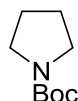
Bis-(phenyl)borinic acid benzylaminobenzoate **195c**: Mp 107 – 108 °C. ^1H NMR (50% purity; assignment on the basis of comparison with benzylamine and benzoic acid ^1H NMR data) δ 8.34 – 8.27 (m, 2H, $\text{C}_{\text{Ar}}\text{-H}$), 8.11 – 8.00 (m, 8H, $\text{C}_{\text{Ar}}\text{-H}$), 7.48 – 7.40 (m, 10H, $\text{C}_{\text{Ar}}\text{-H}$), 5.92 – 5.68 (br m, 2H, NH_2), 3.86 – 3.76 (m, 2H, CH_2). ^{13}C NMR: peaks of the product could not be identified (see Supporting Information).

^{11}B NMR δ 4. IR ν_{max} (neat)/ cm^{-1} 3239, 3033, 1693, 1638, 1574, 1514, 1387, 1349, 1312, 1260, 1154, 963, 891, 844, 756, 697, 656.

Bis-(2-chlorophenyl)borinic acid benzylamine-4-phenylbutanoat **195d**: Mp 136 – 137 °C. ^1H NMR δ 7.64 – 7.58 (m, 2H, $\text{C}_{\text{Ar}}\text{-H}$), 7.45 – 7.38 (m, 4H, $\text{C}_{\text{Ar}}\text{-H}$), 7.34 – 7.28 (m, 4H, $\text{C}_{\text{Ar}}\text{-H}$), 7.25 – 7.13 (m, 10H, $\text{C}_{\text{Ar}}\text{-H}$), 6.68 – 6.47 (br m, 2H, NH_2), 3.66 – 3.59 (m, 2H, N-CH_2), 2.65 (t, $J = 7.4$ Hz, 2H, OC-CH_2), 2.47 (t, $J = 7.4$ Hz, 2H, $-\text{CH}_2$), 2.04 (pent, $J = 7.4$ Hz, 2H, $\text{OC-CH}_2\text{-CH}_2\text{-CH}_2$), ^{13}C NMR δ 177.99, 141.72, 137.06, 135.35, 134.98, 129.43, 129.25, 128.93, 128.51, 128.40, 128.34, 128.22, 125.93, 125.88, 45.83, 36.14, 35.29, 26.83. ^{11}B NMR δ 2. IR ν_{max} (neat)/ cm^{-1} 3281, 3198, 1678, 1591, 1388, 1370, 1338, 1279, 1244, 1188, 1006, 922, 851, 745, 700, 629.

Bis-(3,4,5-trifluorophenyl)borinic acid ethylenediamine 4-phenylbutanoate dicomplex **196**: Mp 136 – 143 °C. ^1H NMR: peaks of product could not be identified (see Supporting Information). ^{11}B NMR δ 2. ^{19}F NMR δ -135.86 – -136.02 (m, 4F, CH-CF), -163.68 – -163.91 (m, 2F, CH-CF-CF). IR ν_{max} (neat)/ cm^{-1} 2925, 1610, 1526, 1507, 1400, 1330, 1222, 1122, 1041, 844, 740, 699, 507. Anal. Calcd for $\text{C}_{24}\text{H}_{23}\text{BF}_6\text{N}_2\text{O}_2$: C, 58.09; H, 4.67; N, 5.65. Found: C, 58.45; H, 4.76; N, 5.70.

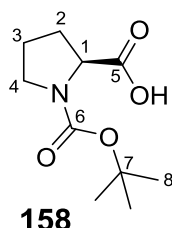
***Tert*-butyl pyrrolidine-1-carboxylate **109**¹⁵¹**



Pyrrolidine (10.0 g, 139 mmol) was dissolved in MeCN (250 mL) and Boc_2O (30.3 g, 139 mmol, 1 equiv.) was added. The mixture was stirred for 1 h, evaporated, redissolved in hexane, washed with water, separated, dried and evaporated to yield 20.1 g (84%) of **109** as yellowish oil.

^1H NMR δ 3.38 – 3.19 (m, 4H, $\text{CH}_2\text{-N}$), 1.89 – 1.74 (m, 4H, $\text{CH}_2\text{-CH}_2\text{-N}$), 1.44 (s, 9H, CH_3).

***N*-(*tert*-butoxycarbonyl)-(*S*)-proline **158**:**

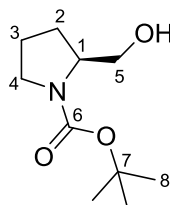


158

To an ice-cold suspension of S-proline (9.0 g, 78.3 mmol) in DCM (180 mL) Et₃N (14.2 mL, 102.4 mmol) was added, followed by Boc₂O (23.9 g, 109.62 mmol) in DCM (20 mL). After stirring at r.t. for 2h, 5% HCl (150 mL) was added. Mixture was extracted into Et₂O, organic layer washed with brine (60 mL), water (60 mL) and dried to give the crude product. It was recrystallized from hot EtOAc by adding hexane and leaving the mixture in the freezer overnight to yield 15.05 g (89%) of solid white product.

Mp 130 – 133 °C (lit. 123 – 126 °C¹⁵³). ¹H NMR (with rotamers present, but hard to define, so given as multiplets with a range of chemical shifts) δ 4.20-4.38 (m, 1H, H₁), 3.30-3.60 (m, 2H, H₄), 2.21-2.31 (m, 1H, H_{2b}), 2.00-2.14 (m, 1H, H_{2a}), 1.91-1.99 (m, 1H, H_{3b}), 1.82-1.91 (m, 1H, H_{3a}), 1.37-1.50 (m, 9H, H₈). ¹³C NMR (with two rotamers present) δ 178.87 (C_{5'}), 175.46 (C₅), 156.20 (C_{6'}), 153.86 (C₆), 81.24 (C_{7'}), 80.31 (C₇), 59.06 (C_{1'}), 58.90 (C₁), 46.93 (C_{4'}), 46.31 (C₄), 30.81 (C_{2'}), 28.69 (C₂), 28.37 (C_{8'}), 28.25 (C₈), 24.29 (C_{3'}), 23.63 (C₃). IR ν_{max} (neat)/cm⁻¹ 2978, 2896, 1734, 1635, 1424, 1208, 1160, 1128, 898, 852, 775. ESI-LRMS (positive ion) *m/z* 238.05 [M+Na]. HRMS: Calcd for C₁₀H₁₇NO₄Na 238.1055, found 238.1069. Anal. Calcd for C₁₀H₁₇NO₄: C, 55.8; H, 7.96; N, 6.51. Found: C, 56.04; H, 8.07 N, 6.25.

(S)-N-(tert-Butoxycarbonyl)-2-(hydroxymethyl)pyrrolidine 159:



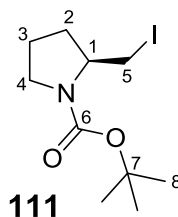
159

To a solution of N-(tert-butoxycarbonyl)-(S)-proline (14.50 g, 67.4 mmol) in dry THF (125 mL) under Ar, BH₃•DMS (5.64 g, 74.2 mmol) was added dropwise and the reaction mixture was refluxed for 2 h. After cooling to r.t., ice was added, the aqueous layer was extracted with Et₂O, washed with 5% aq NaOH (2 x 30 mL), then with water, separated, dried and evaporated to yield 12.97g (96%) of colourless oil, which crystallised overnight.

Mp 56 – 59 °C (lit. 55 – 60 °C). ¹H NMR (no rotamers) δ 3.96-3.91 (m, 1H, H₁), 3.63 (dd, J=11.1, 3.3, 1H, H_{5b}), 3.57 (dd, J=11.1, 7.6, 1H, H_{5a}), 3.45 (dt, J=10.8, 7.0 Hz, 1H, H_{4b}), 3.30 (dt, J=10.8, 6.8 Hz, 1H, H_{4a}), 2.03-1.96 (m, 1H, H_{2b}), 1.86-1.73

(m, 2H, H₃), 1.62-1.53 (m, 1H, H_{2a}), 1.46 (s, 9H, H₈). ¹³C NMR (no rotamers) δ 109.99 (C₆), 80.24 (C₇), 67.35 (C₅), 59.95 (C₁), 47.43 (C₄), 28.73 (C₂), 28.44 (C₈), 23.92 (C₃). IR ν_{max} (neat)/cm⁻¹ 3431, 2981, 2873, 1652, 1399, 1161, 1129, 1055, 909, 776, 565. ESI-LRMS (positive ion) *m/z* 224.46 [M+Na]. HRMS: Calcd for C₁₀H₁₉NO₃Na 224.1263, found 224.1277. Anal. Calcd for C₁₀H₁₉NO₃: C, 59.61; H, 9.49; N, 6.96. Found: C, 59.68; H, 9.52 N, 6.96.

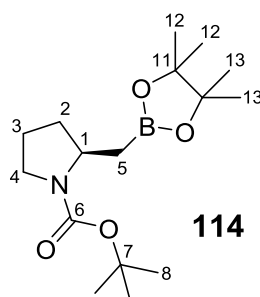
(S)-N-(tert-Butoxycarbonyl)-2-(iodomethyl)pyrrolidine 111:



To a suspension of imidazole (1.76 g, 25.96 mmol) and PPh₃ (5.21 g, 19.88 mmol) in Et₂O (150 mL) at 0 °C under Ar, iodine, (ground pellets, 4.99 g, 19.63 mmol) was added in portions over 30 min during intense stirring with mechanical stirrer. Solution of (2*S*)-*N*-(tert-butoxycarbonyl)-2-(hydroxymethyl)pyrrolidine (2.65 g, 13.17 mmol) in DCM (20 mL) was added, and the mixture stirred overnight at r.t. The reaction mixture was then dissolved in DCM, mixed with silica and column chromatography (EtOAc:hex 1:1) yielded 3.72 g (91%) of product as white solid.

Mp 38 – 41 °C (lit. 38 – 40 °C). ¹H NMR (with rotamers 1:1) δ 3.92-3.79 (m, 1H, H₁), 3.52-3.47 (m, 0.5H, H_{5b}), 3.47-3.41 (m, 0.5H, H_{4b}), 3.41-3.32 (m, 2H, H_{4a}, 4a', 4b, 5b), 3.29 (t, J=8.9, 0.5H, H_{5a}), 3.14 (t, J=9.1, 0.5H, H_{5a}), 2.10-1.98 (m, 1H, H_{2b}), 1.95-1.83 (m, 2H, H_{3b,2a}), 1.83-1.76 (m, 1H, H_{3a}), 1.48-1.42 (m, 9H, H₈). ¹³C NMR (with two rotamers present) δ 154.38 (C₆'), 154.04 (C₆), 79.86 (C₇'), 79.54 (C₇), 58.12 (C₁'), 57.87 (C₁), 47.47(C₄'), 47.04 (C₄), 31.58 (C₂'), 31.03 (C₂), 28.46 (C₈), 23.47 (C₃'), 22.80 (C₃), 10.99 (C₅'), 10.68 (C₅). IR ν_{max} (neat)/cm⁻¹ 2973, 2869, 1675, 1389, 1364, 1165, 1113, 766, 544. Anal. Calcd for C₁₀H₁₈NO₂: C, 38.45; H, 5.76; N, 4.44. Found: C, 38.60; H, 5.83 N, 4.50.

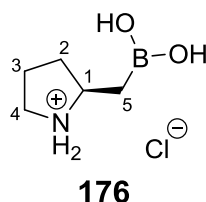
(R)-2-(Pinacolato)borylmethyl-*N*-*tert*-butoxycarbonyl-pyrrolidine 114



To (*S*)-*N*-Boc-2-(iodomethyl)pyrrolidine (0.5 g, 1.608 mmol) under Ar dry THF (8 mL) was added, followed by B₂pin₂ (0.408 g, 1.608 mmol), LiO^tBu (1.46 mL of 2.2 M solution in THF, 3.216 mmol) and CuI (0.031 g, 0.161 mmol). Reaction mixture turned black and was stirred at r.t. for 16 h, before adding 5 mL of 5% HCl, and stirring for another 5 minutes. The mixture was extracted with Et₂O, dried, and evaporated to give the crude oil, which was then purified by column chromatography (EtOAc:hex 1:1) to yield 0.162 g (32%) of product as colourless oil.

¹H NMR (signals for main rotamer) δ 3.96-3.89 (m, 1H, H₁), 3.37-3.26 (m, 2H, H₄), 2.05-1.97 (m, 1H, H_{2b}), 1.89-1.78 (m, 1H, H_{3b}), 1.75-1.68 (m, 1H, H_{3a}), 1.59-1.52 (m, 1H, H_{2a}), 1.45-1.43 (m, 9H, H₈), 1.39 (dd, *J* = 15.7, 3.6 Hz, 1H, H_{5b}), 1.22 (s, 6H, H₁₂) 1.21 (s, 6H, H₁₃), 0.95 (dd, *J* = 15.7, 10.3 Hz, 1H, H_{5a}). ¹³C NMR δ 154.44 (C₆), 82.93 (C₁₁), 78.82 (C₇), 54.21 (C₁), 46.24 (C₄), 33.11 (C₂), 28.54 (C₈), 24.87 (C₁₂/C₁₃), 24.66 (C₁₂/C₁₃), 23.39 (C₃), 18.54 – 17.98 (br s, C₅). IR ν_{max} (neat)/cm⁻¹ 2975, 1690, 1390, 1365, 1318, 1141, 1108, 882, 848, 772. LRMS⁺ *m/z* 311.19 [M]. Calcd for C₁₆H₃₁¹⁰BNO₄ 311.2382, found 311.2402.

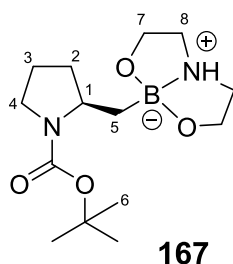
(R)-2-(boronomethyl)pyrrolidin-1-ium chloride 176:



To (*R*)-2-(Pinacolato)borylmethyl-*N*-*tert*-butoxycarbonyl-pyrrolidine (0.1 g, 0.322 mmol) 20% HCl (1.7 mL) was added, and refluxed for 2 h. The mixture was cooled to rt, washed with Et₂O (3 x 20 mL) and evaporated fully, to isolate a pale brown oil (48 mg, 90.2%)

^1H NMR (D_2O) δ 3.62-3.53 (m, 1H, H_1), 3.21-3.10 (m, 2H, H_4), 2.13-2.06 (m, 1H, H_{2b}), 1.97-1.89 (m, 1H, H_{3b}), 1.88-1.80 (m, 1H, H_{3a}), 1.53-1.43 (m, 1H, H_{2a}), 1.22 (dd, $J = 15.8, 6.5$ Hz, 1H, H_{5b}), 1.09 (dd, $J = 15.8, 9.6$ Hz, 1H, H_{5a}). ^{13}C NMR δ 58.15 (C_1), 44.68 (C_4), 31.43 (C_2), 23.04 (C_3), 18.72 – 17.04 (br s, C_5).

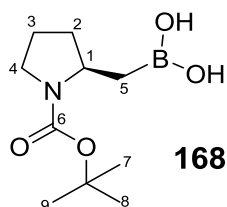
(*R*)-2-(boronomethyl)-*N*-*tert*-butoxycarbonyl-pyrrolidine diethanolamine complex 167:



To (*R*)-2-(Pinacolato)borylmethyl-*N*-*tert*-butoxycarbonyl-pyrrolidine (0.244 g, 0.78 mmol) diethanolamine (0.412 g, 3.90 mmol, 5 equiv.) was added, the mixture was heated in the bulb-to-bulb distillation apparatus at 60 °C (1 Torr) for 1 h. The temperature was then increased to 120 °C, and after 1 h the undistilled residue was cooled to r.t., dissolved in Et_2O and slow evaporation in air yielded 0.133 g (74%) of product as colourless crystals.

Mp 194 – 205 °C. ^1H NMR δ 7.92 – 7.52 (br s, 1H, NH), 4.11 – 3.62 (m, 5H), 3.40 – 3.15 (m, 4H), 2.88 – 2.72 (m, 2H), 2.03 – 1.85 (m, 2H), 1.84 – 1.74 (m, 1H), 1.71 – 1.63 (m, 1H), 1.46 (s, 9H, CH_3), 0.82 (dd, $J = 15.4, 5.1$ Hz, 1H, C_{5a}), 0.65 (dd, $J = 15.4, 3.8$ Hz, 1H, C_{5b}). ^{11}B NMR δ 12. IR ν_{max} (neat)/ cm^{-1} 3087, 2876, 1679, 1395, 1240, 1174, 1063, 1043, 988, 939, 879, 840, 791, 750, 676, 543.

(*R*)-2-(boronomethyl)-*N*-*tert*-butoxycarbonyl-pyrrolidine 168



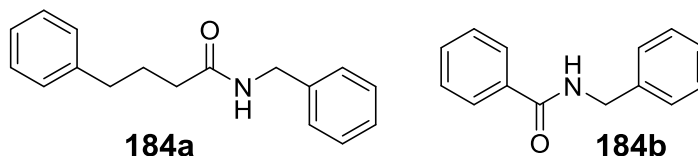
(*R*)-2-(boronomethyl)-*N*-*tert*-butoxycarbonyl-pyrrolidine diethanolamine complex **167** (110 mg 0.37 mmol) was dissolved in Et_2O (5 mL) and 5% aq HCl (5 mL) was added. The mixture was vigorously stirred for 10 minutes, then organic layer

was separated, dried and evaporated to yield 66 mg (85%) of product **168** as white solid.

Mp 106 – 112 °C. ^1H NMR (signals for main rotamer) δ 4.18 – 4.05 (m, 1H, H_1), 3.37 – 3.28 (m, 2H, H_4), 2.00 – 1.89 (m, 2H), 1.88 – 1.80 (m, 1H), 1.65 – 1.55 (m, 1H), 1.45 (br s, 9H, CH_3), 1.32 – 1.23 (m, 1H), 1.03 – 0.92 (m, 1H). ^{13}C NMR δ 80.51, 54.00, 46.26, 34.54, 28.59, 28.47, 23.17. IR ν_{max} (neat)/ cm^{-1} 3291, 2972, 1653, 1408, 1365, 1341, 1218, 1149, 1121, 958, 854, 821, 774, 543. Anal. Calcd for $\text{C}_{10}\text{H}_{20}\text{BNO}_4$: C, 52.43; H, 8.8; N, 6.11. Found: C, 51.96; H, 8.56 N, 5.74.

Direct amide formation

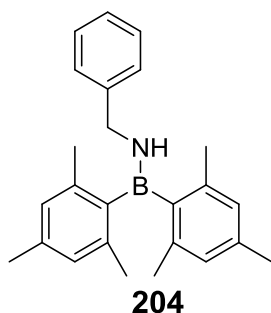
To a round bottom flask was added toluene (20 mL), followed by benzylamine (to achieve 0.143 M) and carboxylic acid (to achieve 0.143 M). The solution was heated at reflux for 24 h with Dean-Stark apparatus, and the yield of amide was determined by HPLC. Similar processes were conducted using the flow reactor and microwave reactor (see Results and Discussion).



N-benzyl-4-phenylbutyramide 184a ^1H NMR δ 7.39 – 7.33 (m, 2H, $\text{C}_{\text{Ar}}\text{-H}$), 7.33 – 7.27 (m, 5H, $\text{C}_{\text{Ar}}\text{-H}$), 7.24 – 7.16 (m, 3H, $\text{C}_{\text{Ar}}\text{-H}$), 5.82 – 5.54 (br s, 1H, NH) 4.46 (d, $J = 5.6$ Hz, 2H, $\text{CH}_2\text{-N}$), 2.69 (t, $J = 7.6$ Hz, 2H, $\text{CH}_2\text{-C(O)}$), 2.24 (t, $J = 7.6$ Hz, 2H, $\text{CH}_2\text{-C}_{\text{Ar}}$), 2.03 (pent, $J = 7.4$ Hz, 2H, $\text{CH}_2\text{-CH}_2\text{-N}$).

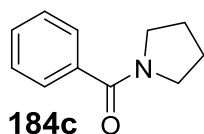
N-benzylbenzamide 184b ^1H NMR δ 7.84 – 7.79 (m, 2H, $\text{C}_{\text{Ar}}\text{-H}$), 7.55 – 7.50 (m, 1H, $\text{C}_{\text{Ar}}\text{-H}$), 7.48 – 7.43 (m, 2H, $\text{C}_{\text{Ar}}\text{-H}$), 7.41 – 7.36 (m, 4H, $\text{C}_{\text{Ar}}\text{-H}$), 7.36 – 7.30 (m, 1H, $\text{C}_{\text{Ar}}\text{-H}$), 6.67 – 6.26 (br s, 1H, NH), 4.68 (d, $J = 5.7$ Hz, 2H, CH_2).

When hydroxydimesitylborane **148e** was applied as a catalyst (10 mol. %) in identical process, column chromatography (EtOAc:hex 1:1) allowed isolation of 4% of boranamine **204**.



N-benzyl-1,1-dimesitylboranamine 204 Mp 92 – 95 °C. ^1H NMR δ 7.31 – 7.37 (m, 2H, $\text{C}_{\text{Ar}}\text{-H}$), 7.22 – 7.28 (m, 3H, $\text{C}_{\text{Ar}}\text{-H}$), 6.85 (s, 2H, $\text{CH}_3\text{-C-CH}$), 6.80 (s, 2H, $\text{CH}_3\text{-C-CH}$), 4.75 (t, $J = 7.0$ Hz, 2H, NH_2), 4.24 (d, $J = 7.0$ Hz, 2H, CH_2), 2.32 (s, 9H), 2.27 (s, 3H), 2.26 (s, 6H). ^{13}C NMR δ 141.14, 140.38, 137.40, 136.98, 128.52, 128.37, 127.66, 127.56, 126.95, 48.58, 22.83, 22.36, 21.11, 20.98. ^{11}B NMR δ 43. IR ν_{max} (neat)/ cm^{-1} 3389, 2916, 1607, 1487, 1453, 1299, 1240, 1030, 852, 753, 695, 624, 484. Anal. Calcd for $\text{C}_{25}\text{H}_{30}\text{BN}$: C, 84.51; H, 8.51; N, 3.94. Found: C, 84.34; H, 8.56; N, 3.84.

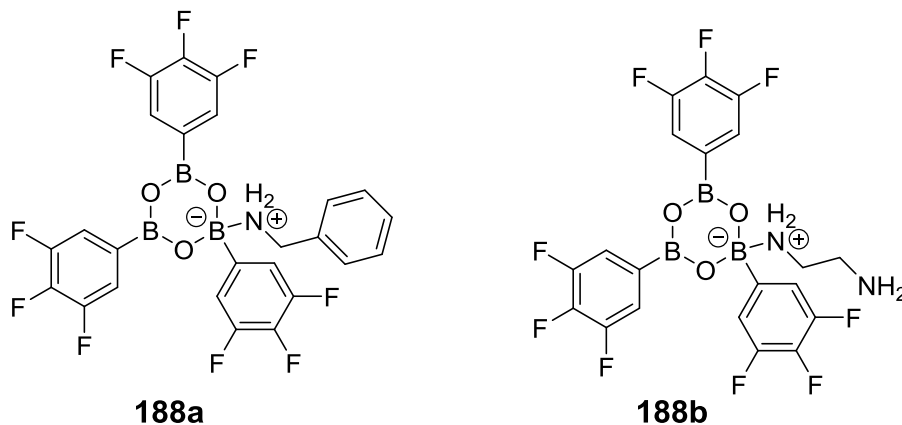
N-Benzoylpyrrolidine 184c¹⁸⁵



Pyrrolidine (1 g, 14.08 mmol) and Et_3N (1.7 g, 16.9 mmol, 1.2 equiv.) were added to DCM (30 mL) at 0 °C, then benzoyl chloride (1.98 g, 14.08 mmol, 1 equiv.) was added dropwise. White sediment was formed and the mixture was allowed to stir at r.t. overnight, then water (20 mL) was added. Separation of organic layer, drying and evaporation yielded crude mixture, which was purified with column chromatography (EtOAc:hex 1:1) to yield amide **184c** (1.3 g, 53%) as pale yellow oil. Identification of product spot on the TLC plate was performed with TLC-MS technique (LRMS⁺ m/z 175.5 [M], performed on Advion expression CMS equipped with Plate Express for reading/analysing planar surfaces; positive ion analysis from atmospheric pressure chemical ionisation).

^1H NMR δ 7.60 – 7.35 (m, 5H, $\text{C}_{\text{Ar}}\text{-H}$), 3.72 – 3.37 (br s, 4H), 2.02 – 1.82 (br s, 4H).

Synthesis of 3,4,5-trifluorophenylboroxine – amine complexes 188a

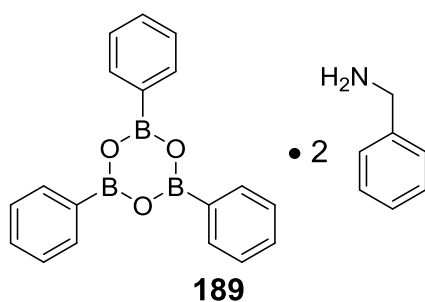


3,4,5-trifluorophenylboronic acid (0.10 mmol) was added to the NMR tube, followed by CDCl_3 (0.7 mL) and amine (0.03 mmol benzylamine or ethylenediamine). The tube was reversed 10 times, full dissolution was not achieved. Over time crystals suitable for X-ray analysis were formed in the tube.

3,4,5-trifluorophenylboroxine – benzylamine complex 188a: Mp 205 – 207 °C. ^1H NMR δ 7.58 – 7.48 (m, 6H, CF-CH), 7.43 – 7.32 (m, 3H, NC...C_{Ar}-H), 7.28 – 7.23 (m, 2H, NC...C_{Ar}-H), 3.93 (s, 2H, CH₂), 3.09 – 2.24 (br s, 2H, NH₂). ^{13}C NMR δ 151.20 (dm, $J = 251.2$ Hz, CH-CF-CF), 141.15 (dm, $J = 254.4$ Hz, CF-CF-CF), 137.23, 129.30, 128.57, 127.74, 116.95 – 116.73 (m, CH-CF), 45.62. ^{11}B NMR δ 19. ^{19}F NMR δ -135.30 – -135.45 (br m, 4F, CH-CF-CF), -158.11 – -158.46 (br m, 2F, CF-CF-CF). IR ν_{max} (neat)/ cm^{-1} 3337, 2981, 1612, 1526, 1430, 1357, 1323, 1268, 1220, 1131, 1030, 1019, 859, 762, 725, 700, 662, 615. Anal. Calcd for $\text{C}_{25}\text{H}_{15}\text{B}_3\text{F}_9\text{NO}_3$: C, 51.70; H, 2.60; N, 2.41. Found: C, 51.56; H, 2.59 N, 2.44.

3,4,5-trifluorophenylboroxine – ethylenediamine complex 188b: Mp 241 – 242 °C. ^1H NMR δ 7.46 – 7.41 (m, 6H, CF-CH), 2.73 (s, 4H, CH₂), 1.78 – 1.15 (br s, 4H, NH₂). ^{13}C NMR (CF-CF-CF carbon not reported) δ 151.06 (dm, $J = 250.3$ Hz, CH-CF), 116.36 – 116.18 (m, CH-CF), 44.24. ^{11}B NMR δ 19. ^{19}F NMR δ -136.00 – -136.18 (m, 6F, CH-CF), -160.21 – -160.51 (br s, 3F, CH-CF-CF). IR ν_{max} (neat)/ cm^{-1} 3349, 2964, 1607, 1583, 1518, 1425, 1408, 1352, 1314, 1273, 1211, 1137, 1018, 901, 874, 782, 720, 659.

Synthesis of phenylboroxine complex with 2 benzylamine molecules 189:

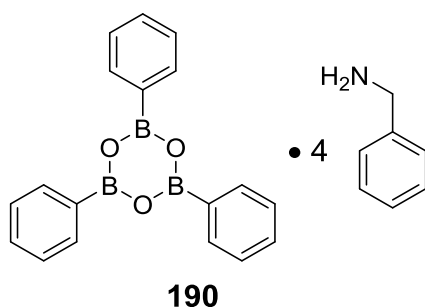


Phenylboronic acid (0.2 g, 1.64 mmol) and benzylamine (0.351 g, 3.28 mmol, 2 equiv.) were added to toluene (10 mL) and mixture was refluxed for 2 h. Obtained solution was evaporated to yield 0.51 g of pale yellow oil, which crystallised overnight.

^1H NMR δ 8.15 – 8.06 (m, 6H, C_{Ar}-H), 7.52 – 7.43 (m, 9H, C_{Ar}-H), 7.40 – 7.30 (m, 6H), 7.25 – 7.17 (m, 4H), 3.90 (s, 4H) ^{13}C NMR δ 138.95, 133.76, 129.79,

129.02, 127.93, 127.68, 127.65, 45.38. ^{11}B NMR δ 20. Anal. Calcd for $\text{C}_{25}\text{H}_{24}\text{B}_3\text{NO}_3$: C, 73.06; H, 6.32; N, 5.33. Found: C, 72.32; H, 6.29; N, 5.19.

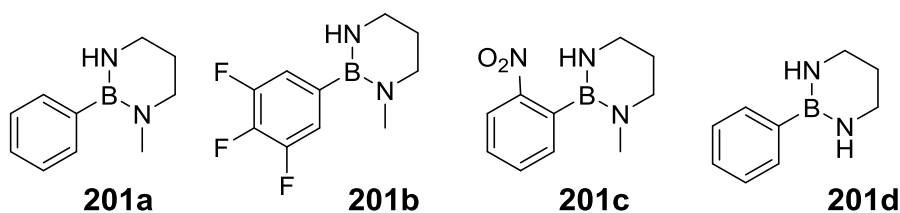
Synthesis of phenylboroxine complex with 4 benzylamine molecules **190**:



Phenylboronic acid (2.0 g, 16.4 mmol) and benzylamine (3.5 g, 32.8 mmol, 2 equiv.) were added to toluene (60 mL) and mixture was refluxed for 2 h with Dean-Stark apparatus. Obtained solution was evaporated to yield 5.2 g of colourless oil, which crystallised overnight.

Mp 56 – 56.5 °C. ^1H NMR (with slight excess of benzylamine present) δ 8.12 – 8.05 (m, 6H, B- $\text{C}_{\text{Ar}}\text{H}$... $\text{C}_{\text{Ar}}\text{H}$) 7.48 – 7.42 (m, 9H, B- $\text{C}_{\text{Ar}}\text{H}$... $\text{C}_{\text{Ar}}\text{H}$) 7.39 – 7.32 (m, 8H, N- $\text{C}_{\text{Ar}}\text{H}$... $\text{C}_{\text{Ar}}\text{H}$), 7.32 – 7.25 (m, 12H, N- $\text{C}_{\text{Ar}}\text{H}$... $\text{C}_{\text{Ar}}\text{H}$), 3.89 (s, 8H, CH_2), 2.27 – 2.01 (br s, 8H, NH_2). ^{13}C NMR δ 141.56, 133.72, 129.73, 128.74, 127.63, 127.31, 127.25, 46.04. ^{11}B NMR δ 20. IR ν_{max} (neat)/ cm^{-1} 3368, 3310, 3267, 3025, 1607, 1495, 1440, 1359, 1304, 1257, 1210, 1192, 1125, 1016, 911, 843, 729, 701, 672, 614.

Synthesis of boronic diamides¹⁷⁵



Known and new boronic diamides **201a-d** were synthesized according to the procedure, reported in the literature.¹⁷⁵

1-methyl-2-phenyl-1,3,2-diazaborinane, 201a: 47%. ^1H NMR δ 7.51 – 7.43 (m, 2H, $\text{C}_{\text{Ar}}\text{H}$), 7.39 – 7.30 (m, 3H, $\text{C}_{\text{Ar}}\text{H}$), 3.18 – 3.10 (m, 2H, $\text{CH}_2\text{-NH}$), 3.06 (t, $J = 5.9$ Hz, 2H, $\text{CH}_2\text{-NMe}$), 2.93 – 2.82 (m, 1H, NH), 2.74 (s, 3H, CH_3), 1.98 (pent, $J = 5.8$ Hz, 2H, $\text{CH}_2\text{-CH}_2\text{-N}$). ^{11}B NMR δ 29.

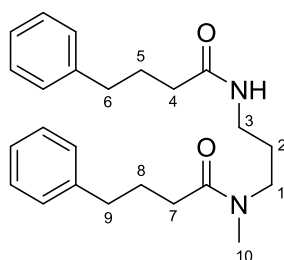
1-methyl-2-(3,4,5-trifluorophenyl)-1,3,2-diazaborinane, 201b: 59%. ^1H NMR δ 7.04 – 6.96 (m, 2H, $\text{C}_{\text{Ar}}\text{H}$), 3.12 – 3.04 (m, 2H, $\text{CH}_2\text{-NH}$), 3.00 (t, $J = 5.9$ Hz, 2H, $\text{CH}_2\text{-NMe}$), 2.84 – 2.74 (m, 1H, NH), 2.65 (s, 3H, CH_3), 1.93 (pent, $J = 5.8$ Hz,

2H, $\text{CH}_2\text{-CH}_2\text{-N}$). ^{13}C NMR δ 150.85 (dm, $J = 250.8$ Hz, CH-CF-CF), 139.22 (dt, $J = 250.2, 15.3$ Hz, CH-CF-CF), 115.96 – 115.63 (m, CH-CF-CF), 48.57, 30.28, 38.56, 27.14. ^{11}B NMR δ 28. ^{19}F NMR δ -136.59 – -136.73 (m, 2F, CH-CF), -162.72 – -162.88 (m, 1F, CH-CF-CF). IR ν_{max} (neat)/ cm^{-1} 3470, 2855, 1607, 1510, 1485, 1457, 1405, 1361, 1321, 1271, 1232, 1151, 1086, 1033, 859, 730, 675, 650.

1-methyl-2-(2-nitrophenyl)-1,3,2-diazaborinane, 201c: 52%. ^1H NMR δ 8.16 – 8.11 (m, 1H, $\text{C}_{\text{Ar-H}}$), 7.63 – 7.57 (m, 1H, $\text{C}_{\text{Ar-H}}$), 7.51 – 7.41 (m, 2H, $\text{C}_{\text{Ar-H}}$), 3.25 – 3.08 (br s, 2H, CH_2), 3.08 – 2.91 (br s, 2H, CH_2), 2.72 – 2.59 (br s, 1H, NH), 2.41 (s, 3H, CH_3), 2.02 (pent, $J = 5.8$ Hz, 2H, $\text{CH}_2\text{-CH}_2\text{-N}$). ^{11}B NMR δ 29.

2-phenyl-1,3,2-diazaborinane, 201d: 77%. ^1H NMR δ 7.51 – 7.45 (m, 2H, $\text{C}_{\text{Ar-H}}$), 7.36 – 7.32 (m, 3H, $\text{C}_{\text{Ar-H}}$), 3.33 – 3.09 (br m, 6H, $\text{CH}_2\text{-NH}$ and NH), 1.96 – 1.87 (m, 2H, $\text{CH}_2\text{-CH}_2\text{-N}$). ^{11}B NMR δ 28.

***N*-methyl-4-phenyl-*N*-(3-(4-phenylbutanamido)propyl)butanamide 203**

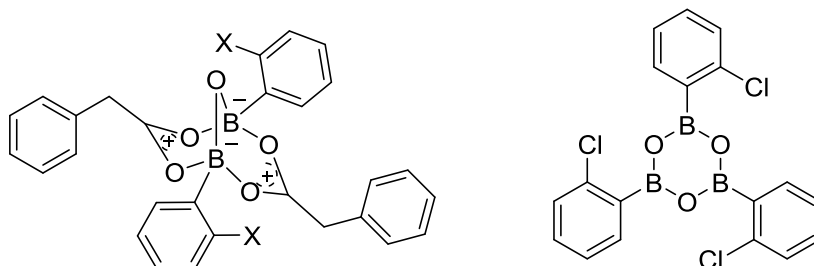


1-methyl-2-phenyl-1,3,2-diazaborinane **201a** (0.1 g, 0.57 mmol) was added to toluene (15 mL) in a round bottom flask, followed by 4-phenylbutyric acid (0.094 g, 0.57 mmol, 1 equiv.). The mixture was refluxed for 4 h, then cooled, NaOH (0.115 g, 20% aq sol-n, 0.57 mmol, 1 equiv.) and H_2O_2 (0.056 g, 35% aq. sol-n, 0.57 mmol, 1 equiv.) were added, the mixture was stirred vigorously for 10 minutes, then water (10 mL) was added, organic layer was separated, dried and evaporated. Column chromatography (EtOAc:hex, 1:4) allowed isolation of 47 mg (35%) of phenol, and subsequent wash with DCM:MeOH 5:1 yielded 14 mg (13%) of diamide **203**.

^1H NMR (signals for main rotamer) δ 7.34 – 7.25 (m, 4H, $\text{C}_{\text{Ar-H}}$), 7.25 – 7.16 (m, 6H, $\text{C}_{\text{Ar-H}}$), 6.94 – 6.77 (m, 1H, NH), 3.46 (t, $J = 6.1$ Hz, 2H, H_1), 3.20 – 3.13 (m, 2H, H_3), 2.93 (s, 3H, H_{10}), 2.74 – 2.62 (m, 4H, H_6, H_9), 2.4 – 2.32 (m, 2H, H_7), 2.30 – 2.22 (t, 2H, H_4), 2.05 – 1.93 (m, 4H, H_5, H_8), 1.67 (pent, $J = 6.1$ Hz, 2H, H_2). ^{13}C NMR δ 173.83, 172.96, 141.73, 141.48, 128.50, 128.45, 128.42, 128.32, 126.01, 125.83, 44.31, 36.29, 35.36, 35.31, 35.17, 35.12, 32.66, 27.34, 26.61, 26.57. IR ν_{max}

(neat)/cm⁻¹ 3310, 3027, 2930, 2860, 1723, 1628, 1603, 1543, 1496, 1452, 1403, 1250, 1129, 1077, 1030, 912, 747, 699, 564, 491. LRMS⁺ *m/z* 381.03 [M].

Synthesis of B-O-B dicarboxylate complexes **194**



In the NMR tube boronic acid (0.1 mmol) was dissolved in dry CDCl₃ (0.7 mL), 5 Å MS were added (in case of X = Cl derivative **194b** at this stage ¹H and ¹¹B NMR were obtained, suggesting the presence of (RBO)₃ boroxine **192c**, and the data is reported below, even though compound was not isolated). Then phenylacetic acid (0.1 mmol) was added. The product was observed in NMR, and crystals suitable for X-ray analysis were obtained by vapour diffusion (CDCl₃/pentane), but it was impossible to separate them from molecular sieves, thus the isolated yield is not reported. The maximum obtained NMR yield (¹¹B NMR) was 85% (see Supporting Information).

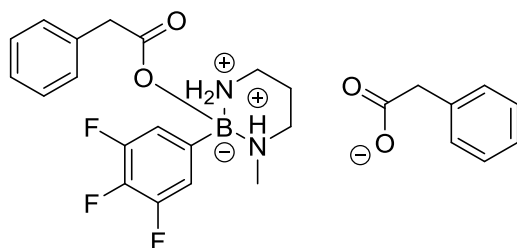
Boroxine **192c**: ¹H NMR δ 8.33 – 8.26 (m, 3H, C_{Ar}-H), 7.54 – 7.46 (m, 6H, C_{Ar}-H), 7.44 – 7.36 (m, 3H, CH₂). ¹¹B NMR δ 29.

X = Cl, **di-2-chlorophenylboronic B-O-B di-2-phenylacetate 194b – 1**: Mp 152 – 160 °C. ¹H NMR (in mixture with boroxine **192c** and phenylacetic acid **180c**) δ 7.75 – 7.68 (m, 2H, C_{Ar}-H), 7.38 – 7.19 (m, 18H, C_{Ar}-H), 3.88 (s, 4H, CH₂). ¹³C NMR δ 184.52, 141.36, 134.20, 133.51, 130.36, 129.75, 129.46, 129.42, 128.82, 126.24, 125.63, 42.40. ¹¹B NMR δ 5. IR *v*_{max} (neat)/cm⁻¹ 3348, 3087, 1607, 1579, 1520, 1405, 1318, 1259, 1206, 1131, 1105, 1071, 1030, 992, 861, 783, 726, 673, 644.

X = I, **di-2-iodophenylboronic B-O-B di-2-phenylacetate 194b – 2**: Mp 108 – 110 °C. ¹H NMR (in mixture with boroxine **192d** and phenylacetic acid **180c**) δ 7.92 – 7.87 (m, 2H, C_{Ar}-H), 7.75 – 7.69 (m, 2H, C_{Ar}-H), 7.39 – 7.26 (m, 12H, C_{Ar}-H), 7.05 – 6.98 (m, 2H, C_{Ar}-H), 3.91 (s, 4H, CH₂). ¹³C NMR δ 184.65, 140.79, 139.88, 139.39, 134.52, 133.41, 130.08, 129.72, 128.89, 127.32, 126.88, 100.86, 42.47. ¹¹B NMR δ 5. IR *v*_{max} (neat)/cm⁻¹ 3283, 1698, 1581, 1460, 1416, 1344, 1241, 1124, 998, 812, 751, 700, 678.

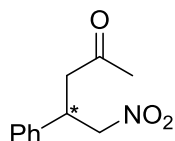
1-methyl-2-(3,4,5-trifluorophenyl)-1,3,2-diazaborinane di-2-phenylacetate

202c:



1-methyl-2-(3,4,5-trifluorophenyl)-1,3,2-diazaborinane **201b** (33 mg, 0.143 mmol, 1 equiv.) and phenylacetic acid (39 mg, 0.286 mmol, 2 equiv.) were dissolved in CHCl_3 (2 mL). After 10 minutes of stirring the mixture was evaporated to yield 70 mg (97%, 80% purity) of colourless oil. A crystal suitable for X-ray analysis was obtained as described in the general experimental information. ^1H NMR δ 11.17 – 10.36 (br s, 2H, NH_2^+), 7.43 – 7.30 (m, 5H, $\text{C}_{\text{Ar}}\text{-H}$), 7.31 – 7.18 (m, 5H, $\text{C}_{\text{Ar}}\text{-H}$), 7.06 – 6.96 (m, 2H, CF-CH), 5.76 – 4.82 (br s, 1H, NH^+), 3.76 (s, 2H), 3.55 (s, 2H), 3.09 – 2.98 (m, 1H), 2.97 – 2.84 (m, 1H), 2.80 – 2.65 (m, 1H), 2.61 – 2.48 (m, 1H), 2.47 – 2.30 (m, 2H), 2.13 (s, 3H, CH_3). ^{13}C NMR δ 178.92, 173.00, 151.08 (dm, $J=250.7$ Hz, CH-CF-CF), 139.66 (dt, $J = 251.9$ Hz, 15.3 Hz, CH-CF-CF), 137.53, 134.32, 129.28, 129.24, 128.90, 128.33, 127.59, 126.12, 115.60 – 115.27 (m, CH-CF), 48.74, 44.87, 43.64, 38.18, 36.11, 21.59. IR ν_{max} (neat)/ cm^{-1} 2706, 1702, 1611, 1533, 1496, 1454, 1440, 1413, 1377, 1306, 1282, 1154, 1136, 1034, 1006, 912, 728, 648.

Catalysed nitro-Michael addition reaction¹⁸⁶



To acetone (4 mL) β -nitrostyrene (0.149 g, 1 mmol) was added, followed by catalyst (*L*-proline or racemic proline or (*R*)-2-(boronomethyl)pyrrolidin-1-ium chloride **176**; 10 mol.%), Et_3N (10 mg, 0.1 mmol, 10 mol.%) and water (0.5 mL). The mixture was stirred at r.t. for 24 h, evaporated and column chromatography (EtOAc:hex 1:3) yielded product **179** as white solid (10% when *L*-proline or racemic proline were used, 77% with homoboroproline **176**). It was analysed by chiral HPLC and product obtained with racemic proline as catalyst was used as racemic standard.

5-nitro-4-phenylpentan-2-one **179**, *ee* 6% (with L-proline), *ee* 48% (with catalyst **176**): ^1H NMR δ 7.39 – 7.21 (m, 5H, $\text{C}_{\text{Ar}}\text{-H}$), 4.72 (dd, $J = 12.3, 6.9$ Hz, 1H, $\text{CH}_2\text{-N}$), 4.62 (dd, $J = 12.4, 7.7$ Hz), 4.03 (pent, $J = 7.2$ Hz, 1H, CH), 2.94 (d, $J = 7.0$ Hz, 2H, $\text{CH}_2\text{-C}_{\text{Ar}}$), 2.14 (s, 3H, CH_3). ^{13}C NMR δ 205.35, 138.81, 129.09, 127.92, 127.38, 79.46, 46.15, 39.06, 30.41. HPLC analysis: Chiralcel–OJ-H column, Hexane:IPA 85:15, flow rate = 1.0 mL/min, wavelength 210 nm, $R_t = 37.8$ min (minor), 59.5 min (major).

4. Appendix 1

Selected X-ray data (for all X-ray data, see Supporting information)

Di-2-iodophenylboronic B-O-B di-2-phenylacetate 194b – 2

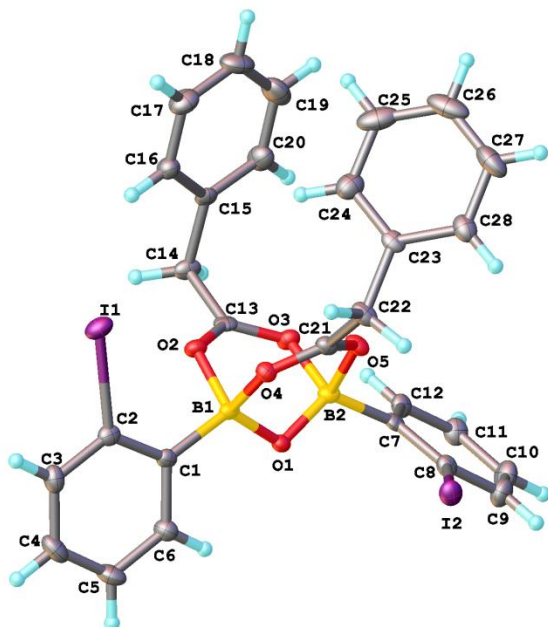


Table 1 Crystal data and structure refinement for 16srv431.

Identification code	16srv431
Empirical formula	C ₂₈ H ₂₂ B ₂ I ₂ O ₅
Formula weight	713.87
Temperature/K	120.0
Crystal system	triclinic
Space group	P-1
a/Å	10.6350(5)
b/Å	11.4814(5)
c/Å	12.2457(6)
α/°	83.1389(18)
β/°	87.0947(19)
γ/°	64.1817(17)
Volume/Å ³	1336.36(11)
Z	2
ρ _{calc} /g/cm ³	1.774
μ/mm ⁻¹	2.390
F(000)	692.0
Crystal size/mm ³	0.22 × 0.15 × 0.05
Radiation	MoKα (λ = 0.71073)
2θ range for data collection/°	4.906 to 59.998
Index ranges	-14 ≤ h ≤ 14, -16 ≤ k ≤ 16, -17 ≤ l ≤ 17
Reflections collected	21913
Independent reflections	7764 [R _{int} = 0.0289, R _{sigma} = 0.0381]

Data/restraints/parameters	7764/0/334
Goodness-of-fit on F ²	1.036
Final R indexes [I>=2σ (I)]	R ₁ = 0.0286, wR ₂ = 0.0538
Final R indexes [all data]	R ₁ = 0.0448, wR ₂ = 0.0580
Largest diff. peak/hole / e Å ⁻³	0.83/-0.60

Table 2 Fractional Atomic Coordinates ($\times 10^4$) and Equivalent Isotropic Displacement Parameters ($\text{Å}^2 \times 10^3$) for 16srv431. U_{eq} is defined as 1/3 of the trace of the orthogonalised U_{ij} tensor.

Atom	x	y	z	U(eq)
II	13829.4(2)	6682.6(2)	3394.7(2)	23.43(5)
I2	7152.3(2)	12796.0(2)	3475.9(2)	21.89(5)
O1	9826.0(16)	10592.3(14)	1867.7(12)	14.3(3)
O2	11206.3(16)	8305.1(14)	1675.5(12)	16.5(3)
O3	9011.4(16)	9243.3(15)	1035.2(13)	17.9(3)
O4	10569.3(16)	9055.9(15)	3494.5(12)	15.1(3)
O5	8385.7(17)	9687.3(15)	2918.3(12)	18.5(3)
C1	12432(2)	9550(2)	2375.2(18)	15.1(4)
C2	13695(2)	8535(2)	2753.9(18)	17.3(5)
C3	14945(3)	8642(2)	2709(2)	22.9(5)
C4	14967(3)	9796(3)	2266(2)	28.1(6)
C5	13742(3)	10835(3)	1890(2)	26.4(6)
C6	12501(3)	10711(2)	1955.1(19)	19.9(5)
C7	7223(2)	11531(2)	1360.6(18)	15.3(4)
C8	6510(2)	12635(2)	1911.8(18)	17.4(5)
C9	5301(3)	13681(2)	1499(2)	25.3(5)
C10	4761(3)	13644(3)	510(2)	27.0(6)
C11	5418(3)	12566(2)	-57.6(19)	22.8(5)
C12	6623(2)	11535(2)	362.1(18)	18.5(5)
C13	10260(2)	8348(2)	1062.8(18)	16.7(5)
C14	10601(3)	7256(2)	376.4(18)	20.4(5)
C15	10251(2)	6225(2)	1027.8(18)	16.0(4)
C16	11231(3)	5272(2)	1750(2)	21.1(5)
C17	10940(3)	4311(2)	2331(2)	29.4(6)
C18	9676(3)	4297(3)	2208(2)	34.6(7)
C19	8680(3)	5254(3)	1511(2)	34.6(7)
C20	8965(3)	6219(3)	922(2)	26.4(6)
C21	9315(2)	9245(2)	3663.6(18)	17.0(5)
C22	8909(3)	8944(2)	4812.8(18)	21.2(5)
C23	8117(2)	8118(2)	4899.2(18)	18.0(5)
C24	8688(3)	6903(2)	4525(2)	28.1(6)
C25	7968(4)	6136(3)	4675(2)	38.8(7)
C26	6699(3)	6580(3)	5202(2)	39.8(8)
C27	6124(3)	7789(3)	5559(2)	36.4(7)
C28	6818(3)	8563(3)	5405(2)	24.3(5)
B1	10974(3)	9481(2)	2321(2)	15.5(5)
B2	8650(3)	10351(2)	1776(2)	16.6(5)

Atom	U_{11}	U_{22}	U_{33}	U_{23}	U_{13}	U_{12}
I1	30.71(10)	15.40(8)	21.23(9)	-0.72(6)	-5.27(7)	-7.01(7)
I2	21.97(9)	26.11(9)	19.29(8)	-8.41(6)	0.90(6)	-10.59(7)
O1	15.9(8)	14.2(7)	14.0(8)	-1.8(6)	2.4(6)	-7.8(6)
O2	21.3(9)	13.6(7)	16.2(8)	-3.1(6)	0.1(6)	-8.8(7)
O3	20.4(9)	15.5(8)	17.9(8)	-3.0(6)	-3.2(6)	-7.4(7)
O4	17.1(8)	18.0(8)	11.3(7)	-0.7(6)	-0.4(6)	-8.7(6)
O5	21.0(8)	24.6(8)	13.9(8)	1.9(7)	-0.8(6)	-14.5(7)
C1	18.9(11)	16(1)	12.3(10)	-4.1(9)	2.2(8)	-8.9(9)
C2	22.6(12)	17.9(11)	11.3(10)	-1.8(9)	1.5(9)	-8.7(9)
C3	16.8(12)	30.3(13)	19.3(12)	-3.6(10)	0.3(9)	-7.9(10)
C4	26.5(14)	42.5(16)	24.0(13)	-3.0(12)	3.9(11)	-23.7(12)
C5	33.6(15)	30.1(14)	24.0(13)	3.8(11)	-1.1(11)	-23.1(12)
C6	22.2(12)	22.2(12)	17.6(11)	-0.3(10)	-1.8(9)	-12(1)
C7	17.4(11)	19.6(11)	12.4(10)	-0.3(9)	3.3(8)	-12.0(9)
C8	18.3(12)	22.2(12)	13.1(11)	-2.6(9)	2.4(9)	-10.2(10)
C9	23.6(13)	24.0(13)	22.9(13)	-7.2(11)	2.4(10)	-4.4(10)
C10	21.5(13)	26.9(13)	23.6(13)	0.2(11)	-3.2(10)	-2.4(10)
C11	24.4(13)	29.1(13)	13.0(11)	-0.9(10)	0.0(9)	-10.1(11)
C12	18.6(12)	22.5(12)	13.5(11)	-2.6(9)	3.7(9)	-8.4(10)
C13	25.2(13)	13.5(10)	13.7(11)	3.1(9)	1.4(9)	-11.7(9)
C14	32.6(14)	18.0(11)	12.8(11)	-3.5(9)	0.2(10)	-12.6(10)
C15	21.8(12)	13.4(10)	14.1(11)	-4.6(9)	1.3(9)	-8.4(9)
C16	21.6(12)	18.8(11)	22.8(12)	-1.6(10)	-0.8(10)	-8.7(10)
C17	37.9(16)	20.5(13)	24.6(14)	3.8(11)	-2.6(12)	-9.0(11)
C18	52.2(19)	31.2(15)	31.0(15)	-1.4(12)	7.6(13)	-29.1(14)
C19	32.4(16)	44.0(17)	39.5(16)	-10.9(14)	2.5(13)	-26.4(14)
C20	24.3(13)	25.9(13)	30.0(14)	-3.4(11)	-6.5(11)	-11.1(11)
C21	20.9(12)	18.3(11)	15.4(11)	-2.9(9)	1.1(9)	-11.7(9)
C22	24.9(13)	31.6(13)	12.1(11)	1.1(10)	0.0(9)	-17.7(11)
C23	21.2(12)	23.9(12)	10(1)	4.7(9)	-2.7(9)	-12(1)
C24	35.0(15)	24.5(13)	22.1(13)	-0.6(11)	1.6(11)	-11.1(11)
C25	68(2)	23.8(14)	27.1(15)	5.2(12)	-14.0(15)	-22.6(14)
C26	53(2)	50.9(19)	31.3(16)	19.0(14)	-17.8(14)	-41.4(17)
C27	28.4(15)	54.5(19)	31.6(15)	12.3(14)	-3.6(12)	-26.7(14)
C28	21.9(13)	30.3(13)	18.6(12)	4.1(10)	-0.8(10)	-11.0(11)
B1	19.8(13)	13.2(11)	14.9(12)	-3.9(10)	3.2(10)	-8.1(10)
B2	21.1(13)	16.5(12)	14.0(12)	-1(1)	0.8(10)	-10.1(10)

Atom	Atom	Length/ \AA	Atom	Atom	Length/ \AA
I1	C2	2.123(2)	C7	B2	1.588(3)
I2	C8	2.121(2)	C8	C9	1.389(3)
O1	B1	1.403(3)	C9	C10	1.380(4)
O1	B2	1.406(3)	C10	C11	1.380(3)
O2	C13	1.266(3)	C11	C12	1.382(3)
O2	B1	1.567(3)	C13	C14	1.496(3)
O3	C13	1.276(3)	C14	C15	1.518(3)
O3	B2	1.549(3)	C15	C16	1.391(3)
O4	C21	1.265(3)	C15	C20	1.384(3)

O4	B1	1.563(3)		C16	C17	1.381(3)
O5	C21	1.269(3)		C17	C18	1.368(4)
O5	B2	1.584(3)		C18	C19	1.382(4)
C1	C2	1.396(3)		C19	C20	1.385(4)
C1	C6	1.401(3)		C21	C22	1.496(3)
C1	B1	1.591(3)		C22	C23	1.511(3)
C2	C3	1.385(3)		C23	C24	1.382(3)
C3	C4	1.380(4)		C23	C28	1.389(3)
C4	C5	1.381(4)		C24	C25	1.389(4)
C5	C6	1.386(3)		C25	C26	1.375(5)
C7	C8	1.397(3)		C26	C27	1.368(4)
C7	C12	1.406(3)		C27	C28	1.374(4)

Table 5 Bond Angles for 16srv431.								
Atom	Atom	Atom	Angle/°		Atom	Atom	Atom	Angle/°
B1	O1	B2	111.77(18)		C20	C15	C16	119.1(2)
C13	O2	B1	121.02(18)		C17	C16	C15	120.5(2)
C13	O3	B2	117.88(18)		C18	C17	C16	120.1(2)
C21	O4	B1	118.15(18)		C17	C18	C19	120.1(2)
C21	O5	B2	120.15(18)		C18	C19	C20	120.2(3)
C2	C1	C6	115.4(2)		C15	C20	C19	120.0(2)
C2	C1	B1	126.3(2)		O4	C21	O5	123.7(2)
C6	C1	B1	118.2(2)		O4	C21	C22	117.7(2)
C1	C2	I1	121.50(16)		O5	C21	C22	118.6(2)
C3	C2	I1	115.38(17)		C21	C22	C23	113.99(19)
C3	C2	C1	123.1(2)		C24	C23	C22	121.2(2)
C4	C3	C2	119.4(2)		C24	C23	C28	119.4(2)
C3	C4	C5	119.8(2)		C28	C23	C22	119.4(2)
C4	C5	C6	119.8(2)		C23	C24	C25	119.7(3)
C5	C6	C1	122.5(2)		C26	C25	C24	120.1(3)
C8	C7	C12	115.6(2)		C27	C26	C25	120.3(3)
C8	C7	B2	124.0(2)		C26	C27	C28	120.2(3)
C12	C7	B2	120.3(2)		C27	C28	C23	120.3(3)
C7	C8	I2	122.22(17)		O1	B1	O2	109.09(18)
C9	C8	I2	115.08(17)		O1	B1	O4	108.61(18)
C9	C8	C7	122.7(2)		O1	B1	C1	118.13(19)
C10	C9	C8	119.5(2)		O2	B1	C1	107.74(17)
C11	C10	C9	119.9(2)		O4	B1	O2	102.55(16)
C10	C11	C12	119.8(2)		O4	B1	C1	109.59(18)
C11	C12	C7	122.4(2)		O1	B2	O3	109.39(18)
O2	C13	O3	123.6(2)		O1	B2	O5	109.15(18)
O2	C13	C14	118.3(2)		O1	B2	C7	118.47(19)
O3	C13	C14	118.0(2)		O3	B2	O5	101.05(16)
C13	C14	C15	108.64(18)		O3	B2	C7	108.68(18)
C16	C15	C14	119.7(2)		O5	B2	C7	108.69(18)
C20	C15	C14	121.1(2)					

A	B	C	D	Angle/°	A	B	C	D	Angle/°
C1	B1	O2	C13	-145.81(19)	C15	C14	C13	O3	-86.1(2)
C1	B1	O4	C21	163.42(19)	C21	O4	B1	O1	33.0(3)
C2	C1	B1	O1	-177.2(2)	C21	O4	B1	O2	-82.3(2)
C2	C1	B1	O2	-53.1(3)	C21	O5	B2	O1	-12.9(3)
C2	C1	B1	O4	57.7(3)	C21	O5	B2	O3	102.3(2)
C6	C1	B1	O1	-0.8(3)	C21	C22	C23	C24	58.2(3)
C6	C1	B1	O2	123.3(2)	C21	C22	C23	C28	-124.5(2)
C6	C1	B1	O4	-125.9(2)	C23	C22	C21	O4	-130.9(2)
C7	B2	O3	C13	163.67(18)	C23	C22	C21	O5	49.9(3)
C7	B2	O5	C21	-143.4(2)	B1	O1	B2	O3	-59.2(2)
C8	C7	B2	O1	-61.7(3)	B1	O1	B2	O5	50.5(2)
C8	C7	B2	O3	172.74(19)	B1	O1	B2	C7	175.52(19)
C8	C7	B2	O5	63.6(3)	B1	O2	C13	O3	-9.8(3)
C12	C7	B2	O1	115.9(2)	B1	O2	C13	C14	173.48(18)
C12	C7	B2	O3	-9.7(3)	B1	O4	C21	O5	4.4(3)
C12	C7	B2	O5	-118.9(2)	B1	O4	C21	C22	-174.70(19)
C13	O2	B1	O1	-16.4(3)	B2	O1	B1	O2	50.8(2)
C13	O2	B1	O4	98.6(2)	B2	O1	B1	O4	-60.2(2)
C13	O3	B2	O1	32.9(3)	B2	O1	B1	C1	174.23(19)
C13	O3	B2	O5	-82.1(2)	B2	O3	C13	O2	1.4(3)
C13	C14	C15	C16	-86.1(3)	B2	O3	C13	C14	178.10(18)
C13	C14	C15	C20	93.5(3)	B2	O5	C21	O4	-14.7(3)
C15	C14	C13	O2	90.8(2)	B2	O5	C21	C22	164.4(2)

Atom	x	y	z	U(eq)
H3	15780	7927	2980	27
H4	15821	9875	2220	34
H5	13751	11633	1587	32
H6	11665	11440	1706	24
H9	4848	14419	1895	30
H10	3937	14358	220	32
H11	5042	12534	-735	27
H12	7063	10800	-39	22
H14A	11606	6878	185	24
H14B	10053	7582	-314	24
H16	12107	5283	1844	25
H17	11619	3659	2818	35
H18	9483	3629	2601	42
H19	7798	5249	1436	42
H20	8277	6876	446	32
H22A	8324	9772	5120	25
H22B	9765	8486	5268	25
H24	9569	6594	4166	34
H25	8353	5304	4413	47
H26	6219	6045	5319	48
H27	5241	8095	5915	44
H28	6407	9406	5646	29

Refinement model description

Number of restraints - 0, number of constraints - unknown.

Details:

1. Fixed Uiso

At 1.2 times of:

All C(H) groups, All C(H,H) groups

2.a Secondary CH₂ refined with riding coordinates:

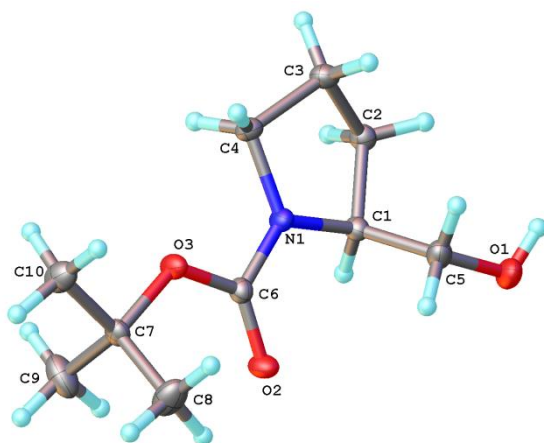
C14(H14A,H14B), C22(H22A,H22B)

2.b Aromatic/amide H refined with riding coordinates:

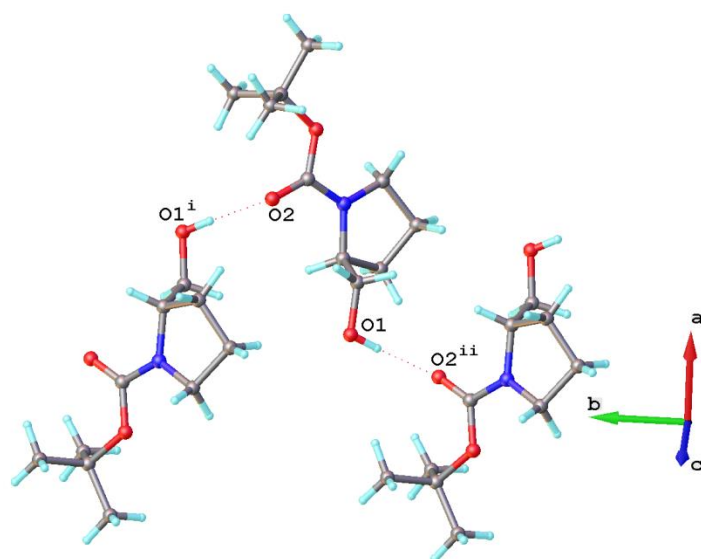
C3(H3), C4(H4), C5(H5), C6(H6), C9(H9), C10(H10), C11(H11), C12(H12),

C16(H16), C17(H17), C18(H18), C19(H19), C20(H20), C24(H24), C25(H25), C26(H26), C27(H27), C28(H28)

(S)-N-(*tert*-Butoxycarbonyl)-2-(hydroxymethyl)pyrrolidine 159:



Intermolecular hydrogen bonding:



5. Appendix 2

List of attended seminars

1. Prof Richard Layfield “Organo-Lanthanide Molecular Nanomagnets”
2. Prof Bob Tooze “Catalysis on the edge”
3. Prof Graham Sandford “Durham fluorine meets industry”
4. Dr Simon Beaumont “Nanoparticles and in situ spectroscopy for understanding syngas conversion catalysts”
5. Prof Michael Buchmeiser “Ionic Mo- and Ru-Based metathesis Catalysts”
6. Dr Juan Aguilar “Resolving $^1\text{H-NMR}$ signals beyond the limit dictated by your spectrometer: pure shift NMR”
7. Dr Jackie Mosely “Ion Mobility Mass Spectrometry - what it is and what it may be able to do for you”
8. Prof. Gabriel Lemcoff “Latent Olefin Metathesis”
9. Dr John Spencer “Design of New Chemical Tools for Cancer”
10. Dr Justin Hargreaves “Interstitial nitrides - reservoirs of activated nitrogen?”
11. Prof Declan Giheany “New Useful Reactions in Organophosphorus Chemistry”
12. Prof Stuart Conway “Chemistry Enabling Biology: The Synthesis of Chemical Probes for Biological Systems”
13. Prof. Christopher Hardacre “Development of in situ methods to study gas- and liquid-phase heterogeneously-catalysed reactions”
14. Prof Frank de Proft “Conceptual DFT: Theory and Applications in Organic and Inorganic Chemistry”
15. Prof John Blacker “What is Chemical Process Development?”
16. Dr Andy Beale “Chemical imaging of catalytic materials and beyond...”
17. Dr Tom Sheppard “Water Driven Chemistry: Activation and Formation of Carbon-Oxygen Bonds”
18. Prof Jacques Mortier “Directed ortho and remote metalation of arenes (DoM and DreM). Recent Advances”
19. Dr Stefan Mix “Biocatalysis Applications in the Pharmaceutical Industry”
20. Prof Roger Hunter “New Synthesis Methodology for Bioactive Motifs: Mysteries of and Applications to C-N and S-S bond Synthesis”
21. Prof Todd Marder “Transition Metal Catalyzed Borylation of C-H and C-X Bonds: Synthesis of Aryl and Alkyl Coronates”
22. Prof Robert Grubbs “Controlled polymer synthesis with olefin metathesis catalysts”
23. Prof Sir Fraser Stoddart “The Nature of the Mechanical Bond: From Molecules to Machines”

6. References.

1. T. M. Lowry, I. J. Faulkner, *J. Chem. Soc.* **1925**, 2883.
2. E. J. Corey, R. K. Bakshi, S. Shibata, *J. Am. Chem. Soc.* **1987**, *109*, 5551.
3. G. C. Welch, R. R. S. Juan, J. D. Masuda, D. W. Stephan, *Science*, **2006**, *314*, 1124.
4. D. W. Stephan, *Org. Biomol. Chem.* **2008**, *6*, 1535.
5. L. J. Hounjet, D. W. Stephan, *Org. Process Res. Dev.* **2014**, *18*, 385.
6. G. N. Lewis, *Valence and the Structure of Atoms and Molecules*, Chemical Catalogue Company, Inc., New York, **1923**.
7. a) H. C. Brown, H. I. Schlesinger, S. Z. Cardon, *J. Am. Chem. Soc.* **1942**, *64*, 325.
b) W. Tochtermann, *Angew. Chem. Int. Ed.* **1966**, *5*, 351.
8. P. Chase, T. Jurca, D. W. Stephan, *Chem. Commun.* **2008**, 1701.
9. D. W. Stephan, S. Greenberg, T. W. Graham, P. Chase, J. J. Hastie, S. J. Geier, J. M. Farrell, C. C. Brown, Z. M. Heiden, G. C. Welch, M. Ullrich, *Inorg. Chem.* **2011**, *50*, 12338; D. W. Stephan, *Org. Biomol. Chem.* **2012**, *10*, 5740.
10. G. C. Welch, D. W. Stephan, *J. Am. Chem. Soc.* **2007**, *129*, 1880; V. Sumerin, F. Schulz, M. Nieger, M. Leskelä, T. Repo, B. Rieger, *Angew. Chem. Int. Ed.* **2008**, *47*, 6001; M. Ullrich, A. J. Lough, D. W. Stephan, *J. Am. Chem. Soc.* **2009**, *131*, 52.
11. V. Sumerin, F. Schulz, M. Nieger, M. Atsumi, C. Wang, M. Leskela, P. Pyykko, T. Repo, B. J. Rieger, *J. Organomet. Chem.* **2009**, *694*, 2654.
12. P. A. Chase, G. C. Welch, T. Jurca, D. W. Stephan, *Angew. Chem. Int. Ed.* **2007**, *46*, 8050
13. V. Sumerin, F. Schulz, M. Atsumi, C. Wang, M. Nieger, M. Leskelä, T. Repo, P. Pyykkö, B. Rieger, *J. Am. Chem. Soc.* **2008**, *130*, 14117.
14. P. Spies, G. Erker, G. Kehr, K. Bergander, R. Fröhlich, S. Grimme, D. W. Stephan, *Chem. Commun.* **2007**, 5072; P. Spies, S. Schwendemann, S. Lange, G. Kehr, R. Fröhlich, G. Erker, *Angew. Chem. Int. Ed.* **2008**, *47*, 7543.
15. S. Schwendemann, T. A. Tumay, K. V. Axenov, I. Peuser, G. Kehr, R. Fröhlich, G. Erker, *Organometallics* **2010**, *29*, 1067.
16. D. J. Chen, J. Klankermayer, *Chem. Commun.* **2008**, 2130.
17. K. V. Axenov, G. Kehr, R. Fröhlich, G. Erker *J. Am. Chem. Soc.* **2009**, *131*, 3454.
18. T. Mahdi, Z. M. Heiden, S. Grimme, D. W. Stephan, *J. Am. Chem. Soc.* **2012**, *134*, 4088.
19. S. J. Geier, P. A. Chase, D. W. Stephan, *Chem. Commun.* **2010**, *46*, 4884.
20. T. Mahdi, J. N. del Castillo, D. W. Stephan, *Organometallics* **2013**, *32*, 1971.
21. Y. Liu, H. Du, *J. Am. Chem. Soc.* **2013**, *135*, 12968.
22. D. J. Chen, Y. T. Wang, J. Klankermayer, *Angew. Chem. Int. Ed.* **2010**, *49*, 9475.
23. G. Ghattas, D. Chen, F. Pan, J. Klankermayer, *Dalton Trans.* **2012**, *41*, 9026.
24. Y. Liu, H. Du, *J. Am. Chem. Soc.* **2013**, *135*, 6810.
25. C. Jiang, O. Blacque, H. Berke, *Chem. Commun.* **2009**, 5518.
26. H. Wang, R. Fröhlich, G. Kehr, G. Erker, *Chem. Commun.* **2008**, 5966.
27. L. Greb, P. Oña-Burgos, A. Kubas, F. C. Falk, F. Breher, K. Finkc, J. Paradies, *Dalton Trans.* **2012**, *41*, 9056.
28. G. Erös, H. Mehdi, I. Pápai, T. A. Rokob, P. Király, G. Tárkányi, T. Soós, *Angew. Chem. Int. Ed.* **2010**, *49*, 6559.
29. B. Inés, D. Palomas, S. Holle, S. Steinberg, J. A. Nicasio, M. Alcarazo, *Angew. Chem. Int. Ed.* **2012**, *51*, 12367.

-
30. L. Greb, C.-G. Daniliuc, K. Bergander, J. Paradies, *Angew. Chem. Int. Ed.* **2013**, *52*, 5876.
 31. Y. Segawa, D. W. Stephan, *Chem. Commun.* **2012**, *48*, 11963.
 32. L. Greb, P. Oña-Burgos, B. Schirmer, F. Breher, S. Grimme, D. W. Stephan, J. Paradies, *Angew. Chem. Int. Ed.* **2012**, *51*, 10164.
 33. K. Chernichenko, A. Madarász, I. Pápai, M. Nieger, M. Leskelä, T. Repo, *Nature Chemistry* **2013**, *5*, 718.
 34. G. D. Frey, V. Lavallo, B. Donnadiou, W. W. Schoeller, G. Bertrand, *Science*, **2007**, *316*, 439.
 35. D. W. Stephan, *Dalton Trans.* **2009**, 3129.
 36. P. A. Chase, D. W. Stephan, *Angew. Chem. Int. Ed.* **2008**, *47*, 7433.
 37. D. Holschumacher, T. Bannenberg, C. G. Hrib, P. G. Jones, M. Tamm, *Angew. Chem. Int. Ed.* **2008**, *47*, 7428.
 38. L. J. Hounjet, C. Bannwarth, C. N. Garon, C. B. Caputo, S. Grimme, D. W. Stephan, *Angew. Chem. Int. Ed.* **2013**, *52*, 7492.
 39. A. M. Chapman, D. F. Wass, *Dalton Trans.* **2012**, *41*, 9067.
 40. T. A. Rokob, A. Hamza, A. Stirling, T. Soós, I. Pápai, *Angew. Chem. Int. Ed.* **2008**, *47*, 2435.
 41. S. Grimme, H. Kruse, L. Goerigk, G. Erker, *Angew. Chem. Int. Ed.* **2010**, *49*, 1402.
 42. T. A. Rokob, I. Bakó, A. Stirling, A. Hamza, I. Pápai, *J. Am. Chem. Soc.* **2013**, *135*, 4425.
 43. L. Greb, S. Tussing, B. Schirmer, P. Oña-Burgos, K. Kaupmees, M. Lőkóv, I. Leito, S. Grimme, J. Paradies, *Chem. Sci.* **2013**, *4*, 2788.
 44. D. W. Stephan, G. Erker, *Angew. Chem. Int. Ed.* **2010**, *49*, 46; G. Erker, *C. R. Chimie* **2011**, *14*, 831.
 45. J. S. J. McCahill, G. C. Welch, D. W. Stephan, *Angew. Chem. Int. Ed.* **2007**, *46*, 4968.
 46. M. Ullrich, K. S.-H. Seto, A. J. Lough, D. W. Stephan, *Chem. Commun.* **2009**, 2335.
 47. C. M. Mömming, S. Frömel, G. Kehr, R. Fröhlich, S. Grimme, G. Erker, *J. Am. Chem. Soc.* **2009**, *131*, 12280.
 48. T. Voss, C. Chen, G. Kehr, E. Nauha, G. Erker, D. W. Stephan, *Chem. Eur. J.* **2010**, *16*, 3005.
 49. C. Rosorius, C. G. Daniliuc, R. Fröhlich, G. Kehr, G. Erker, *J. Organomet. Chem.* **2013**, *744*, 149.
 50. M. A. Dureen, D. W. Stephan, *J. Am. Chem. Soc.* **2009**, *131*, 8396.
 51. C. Jiang, O. Blacque, H. Berke, *Organometallics* **2010**, *29*, 125.
 52. a) M. A. Dureen, C. C. Brown, D. W. Stephan, *Organometallics* **2010**, *29*, 6594.
b) M. Alcarazo, C. Gomez, S. Holle, R. Goddard, *Angew. Chem. Int. Ed.* **2010**, *49*, 5788.
 53. C. M. Mömming, G. Kehr, B. Wibbeling, R. Fröhlich, B. Schirmer, S. Grimme, G. Erker, *Angew. Chem. Int. Ed.* **2010**, *49*, 2414.
 54. P. Feldhaus, B. Schirmer, B. Wibbeling, C. G. Daniliuc, R. Fröhlich, S. Grimme, G. Kehr, G. Erker, *Dalton Trans.* **2012**, *41*, 9135.
 55. C. Chen, R. Fröhlich, G. Kehr, G. Erker, *Chem. Commun.* **2010**, *46*, 3580.
 56. C. M. Mömming, G. Kehr, B. Wibbeling, R. Fröhlich, G. Erker, *Dalton Trans.* **2010**, *39*, 7556.

-
57. S. Moebs-Sanchez, G. Bouhadir, N. Saffon, L. Maron, D. Bourissou, *Chem. Commun.* **2008**, 3435.
58. Edwin Otten, Rebecca C. Neu, and Douglas W. Stephan, *J. Am. Chem. Soc.* **2009**, *131*, 9918.
59. C. M. Mömming, E. Otten, G. Kehr, R. Fröhlich, S. Grimme, D. W. Stephan, G. Erker, *Angew. Chem. Int. Ed.* **2009**, *48*, 6643.
60. a) G. Ménard, D. W. Stephan, *J. Am. Chem. Soc.* **2010**, *132*, 1796.
b) R. Dobrovetsky, D. W. Stephan, *Isr. J. Chem.* **2014**, *54*, 1.
61. A. E. Ashley, A. L. Thompson, D. O'Hare, *Angew. Chem. Int. Ed.* **2009**, *48*, 9839.
62. A. Berkefeld, W. E. Piers, M. Parvez, *J. Am. Chem. Soc.* **2010**, *132*, 10660.
63. X. Zhao, D. W. Stephan, *Chem. Commun.* **2011**, *47*, 1833.
64. S. D. Tran, T. A. Tronic, W. Kaminsky, D. M. Heinekey, J. M. Mayer, *Inorg. Chim. Acta* **2011**, *369*, 126.
65. E. Theuergarten, J. Schlösser, D. Schlüns, M. Freytag, C. G. Daniliuc, P. G. Jones, M. Tamm, *Dalton Trans.* **2012**, *41*, 9101.
66. B. Birkmann, T. Voss, S. J. Geier, M. Ullrich, G. Kehr, G. Erker, D. W. Stephan, *Organometallics* **2010**, *29*, 5310.
67. C. Kreitner, S. J. Geier, L. J. E. Stanlake, C. B. Caputo, D. W. Stephan, *Dalton Trans.* **2011**, *40*, 6771.
68. D. W. Stephan, *J. Am. Chem. Soc.* **2015**, *137*, 10018.
69. N. Yu. Adonin, V. V. Bardin, *Russian Chemical Reviews.* **2010**, *79* (9), 757.
70. A. G. Massey, A. J. Park, *J. Organomet. Chem.* **1964**, *2*, 245.
71. H. Nakatsuka, R. Fröhlich, M. Kitamura, G. Kehr, G. Erker, *Eur. J. Inorg. Chem.* **2012**, 1163.
72. B.-H. Xu, G. Kehr, R. Fröhlich, B. Wibbeling, B. Schirmer, S. Grimme, G. Erker, *Angew. Chem. Int. Ed.* **2011**, *50*, 7183.
73. M. M. Hansmann, R. L. Melen, F. Rominger, A. S. K. Hashmi, D. W. Stephan, *J. Am. Chem. Soc.* **2014**, *136*, 777.
74. C. Fan, L. G. Mercier, W. E. Piers, H. M. Tuononen, M. Parvez, *J. Am. Chem. Soc.* **2010**, *132*, 9604.
75. A. Y. Houghton, V. A. Karttunen, C. Fan, W. E. Piers, H. M. Tuononen, *J. Am. Chem. Soc.* **2013**, *135*, 941.
76. A. Y. Houghton, V. A. Karttunen, W. E. Piers, H. M. Tuononen, *Chem. Commun.* **2014**, *50*, 1295.
77. G. I. Nikonov, S. F. Vyboishchikov, O. G. Shirobokov, *J. Am. Chem. Soc.* **2012**, *134*, 5488.
78. Y. Wang, W. Chen, Zh. Lu, Zh. H. Li, H. Wang, *Angew. Chem. Int. Ed.* **2013**, *52*, 7496.
79. C.-H. Lim, A. M. Holder, J. T. Hynes, C. B. Musgrave, *Inorg. Chem.* **2013**, *52*, 10062.
80. F. Buß, P. Mehlmann, C. Mück-Lichtenfeld, K. Bergander, F. Dielmann, *J. Am. Chem. Soc.* **2016**, *138*, 1840.
81. Á. Gyömöre, M. Bakos, T. Földes, I. Pápai, A. Domján, T. Soós, *ACS Catal.* **2015**, *5*, 5366.
82. M. A. Dureen, A. Lough, T. M. Gilbert, D. W. Stephan, *Chem. Commun.* **2008**, 4303.
83. S. Schwendemann, S. Oishi, S. Saito, R. Fröhlich, G. Kehr, G. Erker, *Chem. Asian J.* **2013**, *8*, 212.
84. S. J. Geier, D. W. Stephan, *J. Am. Chem. Soc.* **2009**, *131*, 3476.

-
85. A. Karkamkar, K. Parab, D. M. Camaioni, D. Neiner, H. Cho, T. K. Nielsen, T. Autrey, *Dalton Trans.* **2013**, 42, 615.
 86. T. A. Rokob, A. Hamza, I. Pápai, *J. Am. Chem. Soc.* **2009**, 131, 10701.
 87. F. Bertini, V. Lyaskovskyy, B. J. J. Timmer, F. J. J. de Kanter, M. Lutz, A. W. Ehlers, J. C. Slootweg, K. Lammertsma, *J. Am. Chem. Soc.* **2012**, 134, 201.
 88. M. Ullrich, A. J. Lough, D. W. Stephan, *Organometallics* **2010**, 29, 3647.
 89. K. Chernichenko, M. Nieger, M. Leskelä, T. Repo, *Dalton Trans.* **2012**, 41, 9029.
 90. C. B. Caputo, S. J. Geier, E. Y. Ouyang, C. Kreitner, D. W. Stephan, *Dalton Trans.* **2012**, 41, 237.
 91. C. A. Tanur, D. W. Stephan, *Organometallics* **2011**, 30, 3652.
 92. J. Boudreau, M.-A. Courtemanche and F.-G. Fontaine, *Chem. Commun.* **2011**, 47, 11131.
 93. S. Roters, C. Appelt, H. Westenberg, A. Hepp, J. C. Slootweg, K. Lammertsma, W. Uhl, *Dalton Trans.* **2012**, 41, 9033.
 94. M. J. Sgro, J. Dömer, D. W. Stephan, *Chem. Commun.* **2012**, 48, 7253.
 95. L. M. Litvinenko, N. M. Oleinik, *Russian Chemical Reviews*, **1978**, 47 (5), 401.
 96. B.-H. Xu, K. Bussmann, R. Fröhlich, C. G. Daniliuc, J. G. Brandenburg, S. Grimme, G. Kehr, G. Erker, *Organometallics* **2013**, 32, 6745.
 97. G. C. Welch, R. Prieto, M. A. Dureen, A. J. Lough, O. A. Labeodan, T. Höltrichter-Rössmann, D. W. Stephan, *Dalton Trans.* **2009**, 1559.
 98. T. Voss, T. Mahdi, E. Otten, R. Fröhlich, G. Kehr, D. W. Stephan, G. Erker, *Organometallics* **2012**, 31, 2367.
 99. J.-B. Sortais, T. Voss, G. Kehr, R. Fröhlich, G. Erker, *Chem. Commun.* **2009**, 7417.
 100. T. Voss, J.-B. Sortais, R. Fröhlich, G. Kehr, G. Erker, *Organometallics* **2011**, 30, 584.
 101. Y. Zhang, G. M. Miyake, M. G. John, L. Falivene, L. Caporaso, L. Cavallo, E. Y.-X. Chen, *Dalton Trans.* **2012**, 41, 9119.
 102. T. Xu, E. Y.-X. Chen, *J. Am. Chem. Soc.* **2014**, 136, 1774.
 103. S. J. Geier, A. L. Gille, T. M. Gilbert, D. W. Stephan, *Inorg. Chem.* **2009**, 48, 10466.
 104. T. Setoyama, *Catalysis Today* **2006**, 116, 250.
 105. O. Ekkert, G. Kehr, C. G. Daniliuc, R. Fröhlich, B. Wibbeling, J. L. Petersen, G. Erker, *Z. Anorg. Allg. Chem.* **2013**, 639 (14), 2455.
 106. J. A. Nicasio, S. Steinberg, B. Inés, M. Alcarazo, *Chem. Eur. J.* **2013**, 19, 11016.
 107. D. J. Morrison, W. E. Piers, *Org. Lett.* **2003**, 5, 2857.
 108. X. Zhao, T. M. Gilbert, D. W. Stephan, *Chem. Eur. J.* **2010**, 16, 10304.
 109. A. K. Dash, R. F. Jordan, *Organometallics* **2002**, 21, 777.
 110. J. W. Thomson, J. A. Hatnean, J. J. Hastie, A. Pasternak, D. W. Stephan, P. A. Chase, *Org. Process Res. Dev.* **2013**, 17, 1287.
 111. S. W. Coghlan, R. L. Giles, J. A. K. Howard, L. G. F. Patrick, M. R. Probert, G. E. Smith, A. Whiting, *J. Organomet. Chem.* **2005**, 690, 4784.
 112. S. Liu, Y. Yang, X. Liu, F. K. Ferdousi, A. S. Batsanov, A. Whiting, *Eur. J. Org. Chem.* **2013**, 5692.
 113. C. Rosorius, G. Kehr, R. Fröhlich, S. Grimme, G. Erker, *Organometallics* **2011**, 30, 4211.
 114. H. Li, A. J. A. Aquino, D. B. Cordes, F. Hung-Low, W. L. Hase, C. Krempner, *J. Am. Chem. Soc.* **2013**, 135, 16066.

-
115. M.-A. Courtemanche, M.-A. Légaré, L. Maron, F.-G. Fontaine, *J. Am. Chem. Soc.* **2014**, *136*, 10708.
116. M.-A. Courtemanche, A. P. Pulis, É. Rochette, M.-A. Légaré, D. W. Stephan, F.-G. Fontaine, *Chem. Commun.* **2015**, *51*, 9797.
117. Y.-B. Jia, W.-M. Ren, S.-J. Liu, T. Xu, Y.-B. Wang, X.-B. Lu, *ACS Macro Lett.* **2014**, *3*, 896.
118. X. Zhao, D. W. Stephan, *J. Am. Chem. Soc.* **2011**, *133*, 12448.
119. T. M. Gilbert, *Dalton Trans.* **2012**, *41*, 9046.
120. J. Beckmann, E. Hupf, E. Lork, S. Mebs, *Inorg. Chem.* **2013**, *52*, 11881.
121. S. J. Geier, T. M. Gilbert, D. W. Stephan, *J. Am. Chem. Soc.* **2008**, *130*, 12632.
122. M. T. Whited, *Beilstein J. Org. Chem.* **2012**, *8*, 1554.
123. T. A. Rokob, A. Hamza, A. Stirling, I. Pápai, *J. Am. Chem. Soc.* **2009**, *131*, 2029.
124. C. Jiang, O. Blacque, T. Fox, H. Berke, *Organometallics* **2011**, *30*, 2117.
125. D. Palomas, S. Holle, B. Inés, H. Bruns, R. Goddard, M. Alcarazo, *Dalton Trans.* **2012**, *41*, 9073.
126. K. Matsuo, S. Saito, S. Yamaguchi, *J. Am. Chem. Soc.* **2014**, *136*, 12580.
127. R. G. Potter, M. Somayazulu, G. Cody, R. J. Hemley, *J. Phys. Chem. C* **2014**, *118*, 7280.
128. Y. Cao, J. K. Nagle, M. O. Wolf, B. O. Patrick, *J. Am. Chem. Soc.* **2015**, *137*, 4888.
129. S. Bhunya, A. Paul, *Chem. Eur. J.* **2013**, *19*, 11541.
130. P. Muller, *Pure and Applied Chemistry* **1994**, *66* (5), 1077.
131. A. S. Batsanov, I. Georgiou, P. R. Girling, L. Pommier, H. C. Shen, A. Whiting, *Asian J. Org. Chem.* **2014**, *3*, 470.
132. A. Stute, G. Kehr, C. G. Daniliuc, R. Fröhlich, G. Erker, *Dalton Trans.* **2013**, *42*, 4487.
133. X. Wang, G. Kehr, C. G. Daniliuc, G. Erker, *J. Am. Chem. Soc.* **2014**, *136*, 3293.
134. H. Charville, D. Jackson, G. Hodges, A. Whiting, *Chem. Commun.* **2010**, *46*, 1813.
135. T. Krause, S. Baader, B. Erb, L. J. Gooßen, *Nat. Commun.* **2016**, *7*, 11732; V. R. Pattabiraman, J. W. Bode, *Nature*, **2011**, *480*, 471; S. Ghosh, A. Bhaumik, J. Mondal, A. Mallik, S. Sengupta, C. Mukhopadhyay, *Green Chem.* **2012**, *14*, 3220.
136. I. Georgiou, G. Ilyashenko, A. Whiting, *Acc. Chem. Res.*, **2009**, *42*, 756
137. K. Arnold, A. S. Batsanov, B. Davies, C. Grosjean, T. Schütz, A. Whiting, K. Zawatsky, *Chem. Commun.* **2008**, 3879.
138. T. E. Cole, B.D. Haly, *Organometallics*, **1992**, *11*, 652
139. A. F. Burchat, J. M. Chong, *J. Organomet. Chem.* **1997**, *542*, 281.
140. K. L. Chan, S. E. Watkins, C. S. K. Mak, M. J. McKiernan, C. R. Towns, S. I. Pascu, A. B. Holmes, *Chem. Commun.* **2005**, 5766
141. R. Van Veen, F. Bickelhaupt, *J. Organomet. Chem.* **1972**, *43*, 241; T. Agou, M. Sekine, T. Kawashima, *Tetr. Lett.* **2010**, *51*, 5013; E. Januszewski, A. Lorbach, R. Grewal, M. Bolte, J. W. Bats, H.-W. Lerner, M. Wagner, *Chem. Eur. J.* **2011**, *17*, 12696.
142. P. M. Maitlis, *J. Chem. Soc.* **1961**, 425.

-
143. T. Agou, M. Sekine, J. Kobayashi, T. Kawashima, *Chem. Commun.* **2009**, 1894.
144. P. J. Grisdale, B. E. Babb, J. C. Doty, T. H. Regan, D. P. Maier, J. L. R. Williams, *J. Organomet. Chem.* **1968**, *14*, 63; A. Tsurusaki, T. Sasamori, A. Wakamiya, S. Yamaguchi, K. Nagura, S. Irle, N. Tokitoh, *Angew. Chem. Int. Ed.* **2011**, *50*, 10940.
145. J. Yoshino, N. Kano, T. Kawashima, *J. Org. Chem.* **2009**, *74*, 7496.
146. J. Yoshino, N. Kano, T. Kawashima, *Tetrahedron*, **2008**, *64*, 7774.
147. J. C. Thomas, J. C. Peters, *Inorganic Chemistry*, **2003**, *42*, 5055.
148. E. W. Abel, W. Gerrard, M.F. Lappert, *J. Chem. Soc.* **1957**, 3833.
149. a) S. Berger, S. Braun, H.-O. Kalinowski, *NMR spectroscopy of the non-metallic elements*, Wiley, Chichester, **1997**.
b) A. J. J. Lennox, G. C. Lloyd-Jones, *J. Am. Chem. Soc.* **2012**, *134*, 7431.
150. N. M. D. Brown, F. Davidson, R. McMullan, J. W. Wilson, *J. Organomet. Chem.* **1980**, *193*, 271.
151. a) Y. Basel, A. Hassner, *J. Org. Chem.* **2000**, *65*, 6368.
b) T. A. Johnson, D. O. Jang, B. W. Slafer, M. D. Curtis, P. Beak, *J. Am. Chem. Soc.* **2002**, *124*, 11689.
c) P. O'Brien, K. B. Wilberg, W. F. Bailey, J.-P. R. Hermet, M. J. McGrath, *J. Am. Chem. Soc.* **2004**, *126*, 15480.
152. P. Jacob, *J. Organomet. Chem.* **1978**, *156*, 101.
153. I. Georgiou, A. Whiting, *Eur. J. Org. Chem.* **2012**, 4110.
154. H. Ito, K. Kubota, *Org. Lett.* **2012**, *14*, 890.
155. A. Joshi-Pangu, X. Ma, M. Diane, S. Iqbal, R. J. Kribs, R. Huang, C.-Y. Wang, M. R. Biscoe, *J. Org. Chem.* **2012**, *77*, 6629.
156. D. S. Matteson, R. W. H. Mah, *J. Am. Chem. Soc.* **1963**, *85*, 2599.
157. J. Sun, M. T. Perfetti, W. L. Santos, *J. Org. Chem.* **2011**, *76*, 3571.
158. E. Vedejs, R. W. Chapman, S. C. Fields, S. Lin, M. R. Schrimpf, *J. Org. Chem.* **1995**, *60*, 3020.
159. A. J. J. Lennox, G. C. Lloyd-Jones, *Angew. Chem. Int. Ed.* **2012**, *51*, 9385.
160. S. C. Malhotra, *Inorg. Chem.* **1964**, *3* (6), 862.
161. J. E. Leffler, E. Dolan, T. Tanigaki, *J. Am. Chem. Soc.* **1965**, *87* (4), 927.
162. P. M. Nair, and J. D. Roberts, *J. Am. Chem. Soc.* **1957**, *79*, 4565.
163. G. P. Moss, *Pure & Appl. Chem.* **1996**, *68*, 2193.
164. W. P. Aue, J. Karhan, R. R. Ernst, *J. Chem. Phys.* **1976**, *64*, 4226.
165. J. A. Aguilar, S. Faulkner, M. Nilsson, G. A. Morris, *Angew. Chem. Int. Ed.* **2010**, *49*, 3901.
166. M. Foroozandeh, R. W. Adams, N. J. Meharry, D. Jeannerat, M. Nilsson, G. A. Morris, *Angew. Chem. Int. Ed.* **2014**, *53*, 6990.
167. Y. Kuwahara, A. Zhang, H. Soma, A. Tsuda, *Org. Lett.* **2012**, *14*, 3376.
168. a) K. Tanveer, K. Jarrah, M. S. Taylor, *Org. Lett.* **2015**, *17*, 3482.
b) K. A. D'Angelo, M. S. Taylor, *J. Am. Chem. Soc.* **2016**, *138*, 11058.
c) K. A. D'Angelo, M. S. Taylor, *Chem Commun.* **2017**, Advance article.
169. J. de M. Muñoz, J. Alcázar, A. de la Hoz, Á. Díaz-Ortiz, S.-A. Alonso de Diego, *Green Chem.* **2012**, *14*, 1335.
170. T. Gustafsson, F. Pontén, P. H. Seeberger, *Chem. Commun.* **2008**, 1100.
171. W. F. Slotema, G. Sandoval, D. Guieysse, A. J. J. Straathof, A. Marty, *Biotechnol. Bioeng.* **2003**, *82*, 664.

-
172. J. W. Comerford, T. J. Farmer, D. J. Macquarrie, S. W. Breeden, J. H. Clark, *Arkivoc*, **2012**, vii, 282.
173. F. K. Ferdousi, Doctoral thesis "Novel approaches for catalytic direct amide formation", **2015**.
174. A. Schäfer, W. Saak, D. Haase, T. Müller, *Angew. Chem. Int. Ed.* **2012**, 51, 2981.
175. S. W. Coghlan, R. L. Giles, J. A. K. Howard, L. G. F. Patrick, M. R. Probert, G. E. Smith, A. Whiting, *J. Organomet. Chem.* **2005**, 690, 4784.
176. J. A. Gonzales, O. M. Ogba, G. F. Morehouse, N. Rosson, K. N. Houk, A. G. Leach, P. H.-Y. Cheong, M. D. Burke, G. C. Lloyd-Jones, *Nature Chemistry*, **2016**, 8, 1067.
177. L. K. Mohler, A. W. Czarnik, *J. Am. Chem. Soc.* **1993**, 115, 7037.
178. T. M. El Dine, J. Rouden, J. Blanchet, *Chem. Commun.* **2015**, 51, 16084.
179. A. Kawachi, S. Nagae, Y. Onoue, O. Harada, Y. Yamamoto, *Chem. Eur. J.* **2001**, 17, 8005.
180. A. Leggio, R. D. Marco, F. Perri, M. Spinella, A. Liguori, *Eur. J. Org. Chem.* **2012**, 114.
181. T. Marcelli, *Angew. Chem. Int. Ed.* **2010**, 49, 6840.
182. K. Ishihara, S. Ohara, H. Yamamoto, *J. Org. Chem.* **1996**, 61, 4196.
183. K. L. Chan, S. E. Watkins, C. S. K. Mak, M. J. McKiernan, C. R. Towns, S. I. Pascu, A. B. Holmes, *Chem. Commun.* **2005**, 5766.
184. R. L. Letsinger, I. Skoog, *J. Am. Chem. Soc.* **1955**, 77, 2491.
185. E. Alonso, D. J. Ramón, M. Yus, *Tetrahedron*, **1998**, 54, 13629.
186. Lu, A.; Gao, P.; Wu, Y.; Wang, Y.; Zhou, Z.; Tang, C. *Org. Biomol. Chem.* **2009**, 7, 3141; L.-Y. Chen, S. Guillarme, A. Whiting, C. Saluzzo, *Arkivoc*, **2014**, iv, 215.